Enhanced Frequency Control for Greater Decentralisation and Distributed Operation of Power Systems: Design to Laboratory Validation

PhD Thesis

M. H. Syed

Dynamic Power Systems Laboratory
Institute for Energy and Environment
Electronic and Electrical Engineering Department
University of Strathclyde, Glasgow

August 13, 2018

This thesis is the result of the author's original research. It has been composed by the author and has not been previously submitted for examination which has led to the award of a degree.

Acknowledgements

First and foremost, I would like to thank my supervisor, Prof Graeme Burt for his continuous support and relentless motivation throughout the course of my PhD. He has been a true inspiration, not only for the duration of my PhD, but will continue to be, for any career I look forward to.

I owe a lot to the Dynamic Power Systems Laboratory team members: Efren Guillo-Sansano, Dr Steven M. Blair, Richard Munro, Paulius Dumbrauskas and Anthony Florida-James. I truly appreciate the great work environment they constitute.

I am immensely grateful to Dr. Andrew Roscoe and Prof Campbell Booth for their continuous support throughout my PhD.

I would also like to thank colleagues at TNO and ETP, especially Dr Koen Kok, for providing expert technical direction, training and financial support throughout my PhD.

ти си моја љубав. Не бих био без тебе

Last but not the least, I especially would like to thank my Father, Syed Kaleemuddin, for his belief, confidence and trust in me over the years.

Abstract

With the increasing penetration of renewable generation in power systems and the consequent fall in system inertia, frequency control using conventional mechanisms is proving to be a major challenge for network operators around the world. Alternative faster means to manage frequency of interconnected power systems are being actively sought. At the same time, the need to prioritise remedial frequency control measures electrically closer to the source of a disturbance, referred to herein as responsibilisation, is being realised. A frequency management approach that is fast acting and responsibilising, a necessity for future power systems, is fairly non-existent in literature and present day power systems.

This thesis works towards development of frequency control solutions that are fast acting and responsibilising, that is to ensure fast prioritisation of local response to a disturbance (electrically as close as possible), thereby driving towards a new paradigm of increased decentralisation and distributed operation of the power system. As responsibilisation is conventionally incorporated in secondary frequency control, its speed of response is improved. This is followed by introduction of responsibilisation within primary frequency control. The two proposed controls are enabled by effective event detection techniques developed. The efficacy of the two approaches is demonstrated and compared to that of present day control, by means of real-time simulation and small-signal analysis conducted on a reduced model of the Great Britain power system. The two control approaches ensure the prioritisation of local response to a local disturbance, reducing the divergence from planned system conditions, thereby minimising the operational implications of any system disturbance. In addition, they support enhanced scalability in the future grid given the relative autonomy of the approaches.

This development will lead to increased system resilience during imbalance events.

Demonstrating the feasibility of the proposed approaches in real-time simulations serves as a proof of concept, thereby appraising the solutions to technology readiness level (TRL) 3. The thesis continues to appraise the develop frequency control approaches to TRL 5, requiring high fidelity integration within a laboratory environment and a demonstration of its efficacy in relevant environment. In the process of appraising the developed frequency control approaches to TRL 5, this thesis presents the practical challenges of integrating novel control solutions within a laboratory environment for their validation. Using the smart grid architecture model (SGAM), a methodology to alleviate the presented challenges and facilitate the integration of radical control solutions within laboratory environments for their rigorous validation is proposed. Furthermore, in this thesis, the controller and power hardware in the loop validation of the developed secondary frequency control is shown to extend the traditional bounds of existing validation techniques.

Contents

Acknowledgements **ii**

Abstract **iii**

List of Figures **x**

List of Tables **xiv**

Glossary of Abbreviations **xvii**

1 Introduction **1**

1.1 Research Context 1

1.2 Research Contributions 3

1.3 Thesis Overview 5

1.4 Publications 7

1.4.1 Journal Articles 7

1.4.2 Conference Papers 8

2 Towards Decentralisation and Distributed Operation of Power Systems **13**

2.1 Introduction 13

2.2 Fundamentals of Frequency Stability and Control 14

2.2.1 Inertial Response 15

2.2.2 Primary Frequency Response 16

2.2.3 Secondary Frequency Response 17

2.2.4 Tertiary Frequency Response 17
2.3 Frequency Control of Synchronous (Interconnected or Islanded) Power Systems 17
2.3.1 Load Frequency Control Process 19
2.4 Frequency Control within the Great Britain Power System 22
2.4.1 Frequency Response Services 23
2.4.2 Reserve Services 24
2.5 Control Architectures 25
2.5.1 Centralised Architecture 26
2.5.2 Decentralised Architecture 27
2.5.3 Distributed Architecture 29
2.5.4 An Architectural Analysis of Present Day Frequency Control of Power Systems 30
2.6 Transformation of the Great Britain Power System 33
2.7 Analysing the Impact of Transformation 35
2.7.1 System Frequency Response 35
2.7.2 System Stability 39
2.7.3 System Controllability 41
2.8 The Research Objectives 44
2.9 Chapter Summary 45

3 Enhanced Load Frequency Control Framework for Future Power Systems 58

3.1 Introduction 58
3.2 Reference Power System and Imbalance Event 59
3.2.1 Great Britain Power System 59
3.2.2 Reference Imbalance Event- Frequency Disturbance 62
3.2.3 Quick Recap 64
3.3 Legacy Load Frequency Control Framework 65
3.3.1 Conventional LFC Framework Modeling 65

3.3.2 Incorporating Conventional LFC Framework within Reference Power System . . . 67
3.3.3 Baseline Simulation Results . . . 69
3.3.4 Quick Recap . . . 69
3.4 Analysis of Conventional LFC Framework . . . 71
3.5 Proposed Enhancements to LFC Framework . . . 74
3.5.1 EFC-FB Modelling . . . 75
3.5.2 Incorporating EFC-FB within Reference Power System . . . 77
3.5.3 Quick Recap . . . 78
3.6 Performance Evaluation . . . 78
3.6.1 Response to Reference Imbalance Event . . . 79
3.6.2 Sensitivity analysis . . . 80
3.6.3 Importance of ADO . . . 81
3.6.4 Choosing ΔP^{tie} over ACE . . . 83
3.7 Conclusions . . . 85

4 Novel Decentralised Primary Frequency Control: Introducing Responsibilisation within Primary Frequency Control 91
4.1 Introduction . . . 91
4.2 Conventional Primary Frequency Control . . . 92
4.2.1 Modelling of Conventional Primary Frequency Control . . . 92
4.2.2 Reference Power System Adaptation . . . 93
4.2.3 Analysis of Conventional Primary Frequency Control's Responsibilisation Capability . . . 94
4.3 Responsibilising Primary Frequency Control . . . 96
4.4 Proposed Novel Decentralised Responsibilising Primary Frequency Control 99
4.4.1 Fast Event Location Detection by Transient Phase Offset . . . 99
4.4.2 TPO based Responsibilisation . . . 101
4.4.3 Incorporating Novel Responsibilising Primary Enhanced Frequency Control within the Reference Power System . . . 103

4.5 Performance Evaluation of Proposed Novel Responsibilising Primary Enhanced Frequency Control . . . 106
4.5.1 Response to Imbalance Event . . . 107
4.5.2 Small Signal Analysis . . . 109
4.6 Conclusions . . . 112

5 Design to Validation: Using SGAM as a Tool to Facilitate Laboratory Validation of Control Solutions 116
5.1 Introduction . . . 116
5.2 Validation of Control Solutions . . . 117
5.2.1 Classification of Validation Approaches . . . 117
5.2.2 Validation Chain . . . 121
5.3 Challenges with Laboratory Validation of Control Solutions . . . 124
5.3.1 Single Laboratory Validation Challenges . . . 124
5.3.2 Multiple Laboratory Validation/ Round Robin Validation Challenges . . . 126
5.3.3 Analysing Laboratory Validation Challenges . . . 127
5.4 Exploring the Literature for a Methodology . . . 129
5.5 Appraisal of SGAM Methodology for Facilitating Laboratory Validation 132
5.5.1 Conventional SGAM Modelling Approach . . . 132
5.5.2 Assessment of Applicability of SGAM Methodology for Laboratory Validation . . . 133
5.6 Proposed SGAM Modelling Approach for Laboratory Validation . . . 136
5.6.1 Adapted SGAM Modelling Approach . . . 136
5.6.2 SGAM Zone Mapping Guidelines . . . 138
5.7 Applying the Proposed SGAM Methodology for Validation of the EFC Framework . . . 141
5.7.1 Stage I: Control Solution Description . . . 142
5.7.2 Stage II: Consolidated Function Mapping . . . 146
5.7.3 Stage III: Reference Power System Selection . . . 149
5.7.4 Stage IV: Experiment Specification . . . 149

5.8 Evaluation of the Proposed SGAM Modelling Approach 154
5.8.1 Transition from Control Solution Design to its Validation 154
5.8.2 Distributed Development and Implementation Workflow 155
5.8.3 Ensuring Repeatability and Extending Validation 156
5.8.4 Facilitation of Round Robin/Multi-Laboratory Validation 159
5.8.5 Adaptation to Non-Monolithic Test Setups 162
5.9 Conclusions 163

6 Appraisal of Fast Balancing Enhanced Frequency Control to TRL 5 173
6.1 Introduction 173
6.2 Validation Results 174
6.2.1 PoI-1 174
6.2.2 PoI-2 177
6.2.3 PoI-3 181
6.3 The P-HiL Setup 182
6.3.1 Components of the P-HiL Setup 182
6.3.2 Initialisation and Synchronisation of the P-HiL Setup 186
6.3.3 Accuracy of the P-HiL Setup 192
6.3.4 Initialisation and Synchronisation Results 193
6.4 Validation Results Continued 197
6.4.1 PoI-3 197
6.5 Conclusions 199

7 Conclusions and Future Work 205
7.1 Summary 205
7.2 Conclusions 206
7.2.1 Enhanced Frequency Control Approaches 206
7.2.2 Methodology to Facilitate Laboratory Validation of Complex Smart Grid Control Solutions 209
7.2.3 Extending the Boundaries of Real-Time Power Hardware-in-the-Loop Simulations 210

7.3 Future Work 210
7.3.1 Enhanced Frequency Control Architecture for Future Power Systems 211
7.3.2 Refinement of Laboratory Validation Approach 211
7.3.3 Improving Real-Time Simulations for Extending Laboratory Validations 212
7.3.4 Monetisation of Developed Frequency Control Approaches 212

Appendices **213**

A Reduced Dynamic Model Parameters **214**

List of Figures

2.1 Functional and temporal view of frequency control framework [10]. . . . 15
2.2 Example droop curve for primary frequency response [13]. 16
2.3 Example of secondary frequency control implementation [13]. 17
2.4 Functional and temporal view of load frequency control [22]. 19
2.5 Hierarchy and Obligations of operational areas [22]. 20
2.6 European Power System: Synchronous Areas, LFC Blocks and LFC Areas [22]. 21
2.7 A classification of ENTSO-E and GB balancing services in terms of conventional frequency control terminology. 22
2.8 A mapping of GB balancing services to ENTSO-E LFCR (by means of objective of service). 23
2.9 An illustration of control architectures within power systems domain [26]. 26
2.10 An illustration of distributed control architectures within power systems domain [26]. 28
2.11 Example implementations of primary frequency control. 31
2.12 Example hierarchical architectural representation of synchronous power system. 32
2.13 Impact of wind generation penetration, 30% (red), 60% (blue) and 90% (black) of system load, on system frequency excursions during power imbalance , [54]. 36
2.14 Angles of zones following a loss of line in transmission corridor [77]. . . . 39

2.15 Results from a study in [78] demonstrating the benefits of frequency response closer to the source of imbalance. 40
2.16 Advantage of fast acting devices for primary frequency control [53]. . . . 42

3.1 Reference power system. 59
3.2 Hour-to-hour wind fluctuation for year 2012 [7]. 63
3.3 Unplanned outages of England-France inter-connector for the reporting year 2016 [8]. 64
3.4 Load Frequency Control Framework. 65
3.5 Reference power system divided into six LFC areas. 68
3.6 AGC response to reference event. 70
3.7 System frequency response subject to reference imbalance event in Area 2 for different values of T_I. 71
3.8 LFC framework incorporating proposed SFC. 74
3.9 Response to disturbance 79
3.10 Sensitivity analysis 81
3.11 Eigenvalue analysis 83
3.12 AGC; system response to 1 GW generation loss in LFC 2. 84

4.1 Example conventional droop curve. 92
4.2 Modified reference power system representation. 93
4.3 System PFC response to 1000MW generation loss. 95
4.4 Individual LFC areas' contribution to PFC 96
4.5 Responsibilising PFC proposed in [3]. 98
4.6 System Response to 1000 MW Generation Loss. 100
4.7 Proposed droop curve for primary frequency control. 102
4.8 Calculation of RoCoF over different window lengths. 104
4.9 System Response to 1000MW Generation Loss. 108
4.10 Analysis of System Response to 1000 MW Generation Loss. 109
4.11 n-area interconnected power system frequency response model. 110
4.12 Pole zero map. 111

5.1 Classification of validation approaches. 118
5.2 Representation of C-Hil and P-Hil setup. 120
5.3 Validation chain proposed in [5]. 121
5.4 Validation chain to technology readiness level comparison. 123
5.5 The validation and verification model [33]. 129
5.6 SGAM domains, zones and layers [37]. 130
5.7 Conventional modelling approach. 133
5.8 Modelling approach for laboratory validation. 136
5.9 Enhanced Frequency Control Framework. 141
5.10 Simplified control representation of EFC-FB framework. 142
5.11 Identified functions under test. 143
5.12 SGAM function layer. 147
5.13 SGAM information layer: business context view. 148
5.14 Reference power system chosen for laboratory implementation. 148
5.15 SGAM component layer. 150
5.16 SGAM component layer process zone for LFC areas 1-6. 151
5.17 SGAM communication layer. 152
5.18 SGAM information layer canonical view. 153
5.19 SGAM component layer representation for demonstrating repeatability. 157
5.20 SGAM component layer representation incorporating responsibilising PFC, EFC framework. 158
5.21 SGAM information layer canonical view. 160
5.22 SGAM information layer canonical view. 161
5.23 An example SGAM communication layer for co-simulation setup. 162

6.1 Abstract representation of C-HiL setup 174
6.2 PoI-1: EFC-FB performance comparison, pure simulation vs C-HiL implementation. 175
6.3 Time delay distribution utilised for PoI-2 178
6.4 PoI-2: EFC-FB performance comparison with delays. 179
6.5 PoI-2: Further analysis of ELFC performance with delays. 180

6.6 Example P-HiL setup 182
6.7 Five area GB reference power system. 183
6.8 Dynamic Power Systems Laboratory Architecture 185
6.9 P-HiL initialisation and synchronisation. 190
6.10 Time delay compensation method employed [22]. 193
6.11 Time delay compensation 194
6.12 Initialisation and synchronisation results for GB reference power system 195
6.13 An abstract representation of control and power HiL setup 197
6.14 PoI-3: Frequency response in P-HiL implementation. 199

A.1 Single line diagram of the reduced Great Britain model 214

List of Tables

2.1 Overview of balancing services in GB [24] 24

4.1 Calculated TPOs and TPO Thresholds 105

5.1 Functions under Test: In Scope Functions 143
5.2 Functions under Test: Auxiliary Functions 144
5.3 Inputs, outputs for FuT with their required refresh rate 147
5.4 Identified laboratory components: UST 151
5.5 Functions under Test 157
5.6 Identified laboratory components: CRES 158

6.1 PoI-1: Test Metrics 176
6.2 PoI-2: Test Metrics 180
6.3 Bus wise Generation (MVA) 183
6.4 Bus wise Load: Active (MW) 183
6.5 Bus wise Load: Reactive (MVAR) 183
6.6 Inter-Area Power Flow: Active (MW) 184
6.7 Inter-Area Power Flow: Reactive (MVAR) 184

A.1 Generator Generic Parameters 215
A.2 Specific Generator Parameters 215
A.3 Governor Model Parameters 216
A.4 Excitation Model Parameters 216
A.5 Transformer Model Parameters 216

A.6 Load: Active (MW) 216
A.7 Load: Reactive (MVAr) 217
A.8 Line Parameters 217

Glossary of Abbreviations

4G	Fourth Generation
A/D	Analog to Digital
ACE	Area Control Error
ADI	Applied Dynamics International
ADO	Area Disturbance Observer
AEMC	Australian Energy Market Commission
AEMO	Australian Energy Market Operator
AGC	Automatic Generation Control
ARQ	Automatic Repeat reQuest
BCL	Balance Control Loop
BESS	Battery Energy Storage System
BM	Balancing Mechanisms
CCA	Clear Channel Assessment
CG	Conventional Generators
C-HiL	Controller Hardware-in-the-Loop
CRES	Center for Renewable Energy Sources and Saving

D/A Digital to Analog

DER Distributed Energy Resource

D-H Distributed Horizontal

D-H-C Distributed Horizontal Centralised

D-H-P Distributed Horizontal Peer to Peer

DISCERN Distributed Intelligence for Cost-Effective and Reliable Distribution Network Operation

DPSL Dynamic Power Systems Laboratory

DRTS Digital Real-Time Simulator

DSA Demand Side Aggregator

DSM Demand Side Management

DSO Distribution System Operator

D-V Distributed Vertical

D-V-D Distributed Vertical Determinate

D-V-I Distributed Vertical Iterative

EEGI European Electricity Grid Initiative

EFC Enhanced Frequency Control

EFC-FB Fast Balancing Enhanced Frequency Control

EFC-RP Responsibilising Primary Enhanced Frequency Control

EFCC Enhanced Frequency Control Capability

ELFC Enhanced Load Frequency Control

ENTSOE European Network of Transmission System Operators for Electricity

Glossary of Abbreviations

EPEC	Electrical Power and Energy Conference
ERCOT	Electric Reliability Council of Texas
ETYS	Electricity Ten Year Statement
FCDM	Frequency Control by Demand Management
FCR	Frequency Containment Reserves
FES	Future Energy Scenario
FFR	Firm Frequency Reserves
FOS	Frequency operating Standard
FRR	Frequency Restoration Reserves
FuT	Functions under Test
GB	Great Britain
GTS	Guaranteed Time Slots
HAN	Home Area Network
HiL	Hardware-in-Loop
HuT	Hardware under Test
ICT	Informations and Communications Technology
IED	Intelligent Electronic Devices
IEEE	Institute of Electrical and Electronics Engineers
IESO	Independent Electricity System Operator
IET	The Institution of Engineering and Technology
IPC	Inter Process Communications

Glossary of Abbreviations

ISM	Industrial, Scientific and Medical
ITM	Ideal Transformer Method
LFC	Load Frequency Control
LFCR	Load Frequency Control and Regulation
LTE	Long-Term Evolution
MAS	Multi-Agent Systems
NAN	Neighborhood Area Network
NERC	North American Electricity Reliability Council
NETS	National Electricity Transmission System
NGIC	National Grid Inter-connectors Limited
NIST	National Institute of Standards and Technology
OC-3c	Optical Carrier 3
P2P	Peer to Peer
PCC	Point of Common Coupling
PFC	Primary Frequency Control
P-HiL	Power Hardware-in-the-Loop
PI	Proportional Integral
PoI	Purpose of Investigation
RoCoF	Rate of Change of Frequency
RR	Replacement Reserves
RTE	Réseau de Transport d Electricité

SDH Synchronous Digital Hierarchy

SFC Secondary Frequency Control

SGAM Smart Grid Architecture Model

SGCG Smart Grid Coordination Group

SONET Synchronous Optical Networking

STM1 Synchronous Transport Module 1

TCR Test Criteria

TPO Transient Phase Offset

TRL Technology Readiness Level

TSO Transmission System Operator

UCTE Union for the Coordination of Transmission of Electricity

UDP User Datagram Protocol

UST University of Strathclyde

VSG Virtual Synchronous Generator

WAN Wide Area Network

Chapter 1

Introduction

1.1 Research Context

Power systems around the world are in a continuous process of growth, change and development. The electricity demand of the world has doubled over the past four decades [1], and this trend is expected to continue or even expedite [2]. The expedition can be attributed not only to the electrification of loads such as domestic heating and vehicles but also to their adoption by consumers [3], in addition to the other common factors such as growth in population [4] and increasing availability of electricity in developing countries [1]. Furthermore, to meet the global climate change targets of CO_2 emission reduction, penetration of renewable energy resources is rapidly increasing and is accommodated throughout the transmission and distribution network. Such developments have contributed to the increase in the diversity of electrical sources and loads, and future power systems design is driven to support the integration of diversity through increased progressive developmental strategies.

Power system frequency control refers to the process of maintaining equilibrium between the generation and load in steady state, while restoring the equilibrium following a disturbance with as little unintentional load loss as possible [5], and is the responsibility of the system operator. The emanating impact of the aforementioned developments on system control, response, and stability, especially during and following disturbances, is of growing concern to the system operators as they pose significant

challenges to power system frequency control [6]-[8]. Some such challenges are briefly described below:

- There will be a need to accommodate the fast variations and forecast errors introduced by highly intermittent renewable energy resources. This will prove to be a greater challenge with the falling number of conventional generators capable of participating in frequency control due to their decommissioning resulting from policy measures in support of decarbonisation. Consequently, there will be a need to increase the amount of regulation reserves within the network. In an investigation conducted by ERCOT [9], it was found that, on a capacity basis, the required percentage increase in regulation reserves is equal to the percentage of wind penetration.

- Synchronous machines inherently provide valuable damping torque in support of the system subject to any frequency excursion. A large amount of renewable generation integrated within the network is converter interfaced and is unable to deliver any inherent inertial support. In future, with fewer synchronous machines and the anticipation of reduced and variable system inertia, system frequency excursions will be further accelerated and magnified in comparison to present day power systems. Such excursions in frequency in a reduced inertia system can be mitigated by contracting much larger volume of conventional governor response from the remaining synchronous generation. The extra volume of reserves will help limit the frequency deviation but would have no meaningful impact on the larger initial rate of change of frequency (RoCoF). As the inertia of the network further declines, the slower response from synchronous generators would no longer be able to arrest the frequency deviation to an acceptable bound, regardless of the volume of additional reserves procured.

- To limit the initial RoCoF and the magnitude of frequency deviation within acceptable bounds, the speed of response of frequency services needs to improve. However, the fast release of large amount of power can impose greater stress on the angular stability of the network [10], especially in regions of constrained ca-

pacity exchange or weaker tie-lines. A potential solution identified is the release of the additional power in electrical proximity to the disturbance [11]. However, the location of the event is not known and the release of response in electrical proximity to the event is not incorporated in any frequency service market yet.

- A plethora of flexible devices are expected to be a part of the network on demand side in near future, with most capable of participating in frequency control services with fast response speeds. Some existing large scale demand side devices do participate in conventional frequency control mechanisms and the future participation of large number of distributed devices has been made possible by demand side aggregators. However, even with their fast response capability, their contribution to limiting RoCoF and magnitude of frequency deviation will be limited due to the nature of conventional services.

Therefore, the existing approaches to power system frequency control will no longer be capable of ensuring security of supply in future, with some power system operators around the world in the process of defining new frequency control services in anticipation. To this end, the work reported in this thesis complements the body of research related to development of improved power system frequency control services. This is achieved by analysing and identifying the barriers of present day approaches and proposing methods such that frequency control approaches are capable of ensuring security of supply in power systems of the future.

1.2 Research Contributions

This thesis provides the following contributions to knowledge:

- Establishment of the term **"responsibilisation"** to support the drive towards a new paradigm of increased decentralisation of power systems. **"The prioritisation of remedial control measures electrically closer to the source of the disturbance is referred to as responsibilisation"**

- Implementation of load frequency control within a reduced dynamic model of the Great Britain (GB) power system followed by an analysis and quantification of challenges associated with improving its speed of response and responsibilisation.

- Design, demonstration, analysis and validation of a novel secondary frequency control (SFC). The approach improves the speed of response of SFC while ensuring enhanced responsibilisation.

- Design, demonstration, and analysis of a novel decentralised responsibilising primary frequency control (PFC). The approach is fully decentralised as it relies on local measurement only, requiring no form of communication and supports enhanced scalability in the future grid given the relative autonomy of the approach.

- Design, application and qualitative analysis of a methodology that utilizes smart grid architecture model (SGAM) as a tool to facilitate the integration of radically new control solutions within a laboratory environment for their rigorous validation. The methodology is developed based on insights offered through the reporting of practical challenges that arise from the integration of control solutions within laboratory environments. The developed methodology (i) entails efficiency during the process of validation of control solutions, (ii) incorporates non-monolithic validation setups and (iii) reinforces repeatability and reproducibility of control solutions validation.

- Establishment and demonstration of a recommended initialisation and synchronisation process for power hardware-in-the-loop (P-HiL) simulations, wherein the hardware under test (HuT) represents a significant portion of the network compared to the rest of the system being simulated within the digital real-time simulator (DRTS). This process allows for safer and more stable P-HiL simulations, permitting validation of a wider range of realistic simulations through P-HiL to the betterment of new controllers and power components.

1.3 Thesis Overview

Chapter 2: This chapter begins with presenting the fundamentals of power system frequency control followed by frequency management within synchronous power system of Continental Europe and GB. This chapter further introduces the concepts of centralised, decentralised and distributed control architectures and presents an architectural analysis of present day frequency control of power systems. By presenting the expected transformations of GB power system in the near future, the impact of such system developments on system frequency response, stability and controllability are discussed. To support the drive towards increased decentralisation of power systems, a new term "responsibilisation" is introduced. Based on the discussion of the implications of the transformations, research questions for the thesis are set.

Chapter 3: With the research questions identified and the objectives of the thesis defined, this chapter focuses on the SFC of power system. The chapter begins with the presentation of the reference power system and the reference imbalance event that will be utilised throughout the thesis. By presenting the conventional SFC modelling and its incorporation within reference power system, an evaluation of its performance is undertaken while at the same time exploring the possibility of increasing its response speed and enhancing responsibilisation. A novel SFC, referred to as fast balancing enhanced frequency control (EFC-FB), is proposed and its performance is verified by real-time simulations and further corroborated by small-signal analysis.

Chapter 4: Having enhanced the responsibilisation within the SFC, this chapter explores achievement of responsibilisation within PFC. First, the conventional PFC modelling and its incorporation within reference power system is presented. This is followed by an evaluation of conventional PFC's responsibilisation capability. The approaches established in literature for responsibilisation within PFC are discussed and their potential disadvantages highlighted. To overcome the disadvantages, a novel PFC referred to as responsibilising primary enhanced frequency control (EFC-RP), where responsibilisation is achieved by means of measuring the transient phase offset (TPO)

within each of the LFC areas is proposed. Real-time simulation results verifying the performance of the proposed control are presented and further corroborated by small-signal analysis. The two novel controls developed, the EFC-FB and the EFC-RP, in conjunction constitute the Enhanced Frequency Control (EFC) framework.

Chapter 5: This chapter works towards development of a methodology to facilitate the system level validation of the EFC framework. The chapter begins with presenting a validation chain for smart grid control solutions and drawing a comparison with the well established technology readiness level (TRL) scale. Having the laboratory validation identified as the objective, this chapter continues to present the inappropriateness of laboratory validation approaches for system level validation given the increasing complexity of smart grids. Furthermore, new challenges with the integration of control solutions within laboratories, such as ensuring consistency in understanding, implementation, multi-domain user collaboration and the comparability of results after, are identified. Exploring the aforementioned challenges, an SGAM based methodology is proposed. Using the methodology, the objectives of the validations, a controller and power hardware in the loop validation environment for EFC (incorporating conventional PFC) are developed and its perceived advantages are brought forward.

Chapter 6: In this chapter, the EFC framework (incorporating conventional PFC) is appraised to TRL 5. In accordance with the objectives set forth in Chapter 5, first the results of controller hardware-in-the-loop implementation incorporating communications delays is presented. The setting up of P-HiL simulation is then presented, where a portion of the reference power system is represented by the hardware within the Dynamic Power Systems Laboratory. This is followed by appraising the performance of EFC under a realistic environment.

Chapter 7: This chapter summarizes the contributions of the research reported in this thesis and identifies issues worthy of being taken forward as future work. Focus is on the specific advances made towards achieving responsibilisation, in both primary and secondary frequency control, and towards the development of a robust methodology

for validation of control solutions. In addition, the challenge of P-HiL simulations of large synchronous power systems and the advances made towards addressing the challenge are reported. The identified future work focuses on the the development of an enhanced frequency control architecture and refining the proposed SGAM based validation methodology.

1.4 Publications

The work undertaken through the course of this PhD has contributed to the following publications :

1.4.1 Journal Articles

Published

- W. Yu, Y. Xu, T. Yi, K. Liao, **M. H. Syed**, E. Guillo-Sansano, and G. M. Burt, "Aggregated Energy Storage for Power System Frequency Control: A Finite-Time Consensus Approach", in *IEEE Trans. on Smart Grid*, April 2018.

- E. Guillo-Sansano, **M. H. Syed**, A. J. Roscoe, and G. M. Burt, "Initialization and Synchronization of Power Hardware-in-the-Loop Simulations: A Great Britain Network Case Study", in *Energies*, vol 11, no. 5, 1087, April 2018.

- **M. H. Syed**, E. Guillo-Sansano, S. M. Blair, A. J. Roscoe, , and G. M. Burt, "A Novel Decentralized Responsibilizing Primary Frequency Control", in *IEEE Trans. on Power Systems*, January 2018.

- A. M. Prostejovsky, M. Marinelli, M. Rezkalla, **M. H. Syed**, and E. Guillo-Sansano, "Tuningless Load Frequency Control through Active Engagement of Distributed Resources' in *IEEE Trans. on Power Systems*, September 2017.

- E. Rikos, C. Caerts, M. Cabiati, **M. H. Syed**, and G. M. Burt, "Adaptive Fuzzy Control for Power-Frequency Characteristic Regulation in High-RES Power Systems", in *Energies*, vol 10, no. 7, 982, July 2017.

Under Review

- W. Yu, **M. H. Syed**, E. Guillo-Sansano, Y. Xu, and G. M. Burt, "Inverter-Based Voltage Control of Distribution Networks: A New Distributed Hierarchical Method and Power Hardware-in-the-Loop Validation", in *IEEE Trans. on Industrial Informatics*, March 2018.

- W. Yu, Y. Xu, T. Yi, **M. H. Syed**, E. Guillo-Sansano, and G. M. Burt, "Inverter-based Hybrid Voltage Regulation of Power Distribution Networks", in *IET Generation, Transmission and Distribution*, February 2018.

1.4.2 Conference Papers

Published

- **M. H. Syed**, E. Guillo-Sansano, S. M. Blair, G. M. Burt, T. I. Strasser, H. Brunner, O. Gehrke, and J. E. Rodriguez-Seco, "Laboratory infrastructure driven key performance indicator development using the Smart Grid Architecture Model", in *proceedings of the* 24^{th} *International Conference and Exhibition on Electricity Distribution (CIRED)* Glasgow, United Kingdom, 2017.

- P. Dambrauskas, **M. H. Syed**, S. M. Blair, J. M. Irvine, I. F. Abdulhadi, G. M. Burt, and D. E. M. Bondy, "Impact of Realistic Communications for Fast-Acting Demand Side Management", in *proceedings of the* 24^{th} *International Conference and Exhibition on Electricity Distribution (CIRED)* Glasgow, United Kingdom, 2017.

- E. Rikos, **M. H. Syed**, C. Caerts, M. Rezkalla, M. Marinelli, and G. M. Burt, "Implementation of Fuzzy Logic for Mitigating Conflicts of Frequency Containment", in *proceedings of the* 24^{th} *International Conference and Exhibition on Electricity Distribution (CIRED)* Glasgow, United Kingdom, 2017.

- K. Johnstone, S. M. Blair, **M. H. Syed**, A. Emhemed, G. M. Burt, and T. I. Strasser, "A Co-Simulation Approach using Powerfactory and Matlab/Simulink

to Enable Validation of Distributed Control Concepts within Future Power Systems", in *proceedings of the* 24^{th} *International Conference and Exhibition on Electricity Distribution (CIRED)* Glasgow, United Kingdom, 2017.

- M. Chen, V. M. Catterson, **M. H. Syed**, S. D. J. McArthur, G. M. Burt, M. Marinelli, A. M. Prostejovsky, and K. Heussen, "Supporting Control Room Operators in Highly Automated Future Power Networks", in *proceedings of the* 24^{th} *International Conference and Exhibition on Electricity Distribution (CIRED)* Glasgow, United Kingdom, 2017.

- E. Guillo-Sansano, **M. H. Syed**, A. J. Roscoe, G. M. Burt, M. Stanovich, and K. Schoder, "Controller HIL Testing of Real-Time Distributed Frequency Control for Future Power Systems" in *proceedings of the 2016 IEEE PES Innovative Smart Grid Technologies (ISGT) Conference Europe*, Ljubljana, Slovenia, 2016.

- M. Chen, **M. H. Syed**, E. Guillo-Sansano, S. D. J. McArthur, G. M. Burt, and I. Kockar, "Distributed Negotiation in Future Power Networks: Rapid Prototyping using Multi-Agent System", in *proceedings of the 2016 IEEE PES Innovation Smart Grid Technologies (ISGT) Conference Europe*,Ljubljana, Slovenia, 2016.

- A. S. Zaher, V. M. Catterson, **M. H. Syed**, S. D. J. McArthur, G. M. Burt, M. Chen, M. Marinelli, and A. M. Prostejovsky, "Enhanced Situational Awareness and Decision Support for Operators of Future Distributed Power Network Architectures" in *proceedings of the 2016 IEEE Innovative Smart Grid Technologies (ISGT) Conference Europe*, Ljubljana, Slovenia, 2016.

- A. Chaichana, **M. H. Syed**, and G. M. Burt, "Vulnerability Mitigation of Transmission Line Outages using Demand Response Approach with Distribution Factors", in *proceedings of the 16 IEEE International Conference on Environment and Electrical Engineering*, Florence, Italy, 2016.

- E. Guillo-Sansano, **M. H. Syed**, P. Dambrauskas, M. Chen, G. M. Burt, S. D. J. McArthur, and T. I. Strasser, "Transitioning from Centralized to Distributed Control: Using SGAM to Support a Collaborative Development of Web of Cells

Architecture for Real Time Control", in *proceedings of the 2016 CIRED Workshop*, pp. 1-4, Helsinki, Finland, 2016.

- **M. H. Syed**, G. M. Burt, R. D'Hulst, and J. Verbeeck, "Experimental Validation of Flexibility Provision by Highly Distributed Demand Portfolio", in *proceedings of the 2016 CIRED Workshop*, pp. 1-4, Helsinki, Finland, 2016.

- **M. H. Syed**, P. Crolla, G. M. Burt, and J. K. Kok, "Ancillary Service Provision by Demand Side Management: A Real-Time Power Hardware-in-the-Loop Co-Simulation Demonstration", in *Proceedings of the 2015 International Symposium on Smart Electric Distribution Systems and Technologies (EDST)*, pp. 492-498, Vienna, Austria, Vienna, Austria, 2015.

- **M. H. Syed**, G. M. Burt, J. K. Kok, and R. D'Hulst, "Demand Side Participation for Frequency Containment in the Web of Cells Architecture", in *proceedings of the 2015 International Symposium on Smart Electric Distribution Systems and Technologies (EDST)*, pp. 588-592, Vienna, Austria, 2015.

- R. D'Hulst, J. Verbeeck, C. Caerts, **M. H. Syed**, A. S. Zaher, and G. M. Burt, "Frequency Restoration Reserves: Provision and Activation Using a Multi-Agent Demand Control System", in *proceedings of the 2015 International Symposium on Smart Electric Distribution Systems and Technologies (EDST)*, pp. 601-605, Vienna, Austria, 2015.

- **M. H. Syed**, P. Crolla, G. M. Burt, and J. K. Kok, "Development of an Assessment Framework for Supply/Demand Coordination Mechanisms based on Systems Engineering Approach' in *proceedings of the 2014 CIRED Workshop* pp. 1-5, Rome, Italy, 2014.

References

[1] "Key World Energy Statistics 2012", Technical report, International Energy Agency, 2012. [Online]. Available: http://www.iea.org/publications/freepublications/publication/kwes.pdf

[2] "Deciding the Future: Energy Policy Scenarios to 2050", Technical report, World Energy Council, 2007.

[3] J. Lassila, V. Tikka, J. Haakana, and J. Partanen, "Electric cars as part of electricity distribution - who pays, who benefits?", in *IET Electrical Systems in Transportation*, 2012.

[4] "World Population Prospects - The 2017 Revision", Technical report, United Nations, 2017.

[5] P. Kundur, J. Paserba, V. Ajjarapu, G. Andersson, A. Bose, C. Canizares, N. Hatziargyriou, D. Hill, A. Stankovic, C. Taylor, T. Van Cutsem, V. Vittal, "Definition and classification of power system stability IEEE/CIGRE joint task force on stability terms and definitions", in *IEEE Trans. on Power Systems*, vol. 19, no. 3, pp. 1387-1401, Aug. 2004.

[6] Ibraheem, P. Kumar and D. P. Kothari, "Recent philosophies of automatic generation control strategies in power systems", in *IEEE Trans. on Power Systems*, vol. 20, no. 1, pp. 346–357, 2005.

[7] D. Apostolopoulou, A. D. Domínguez-García and P. W. Sauer, "An Assessment of the Impact of Uncertainty on Automatic Generation Control Systems", in *IEEE Trans. on Power Systems*, vol 31, no. 4, pp. 2657-2665, 2016.

[8] J. Zhang, and A. Dominguez-Garcia, "On the Impact of Measurement Errors on Power System Automatic Generation Control",in *IEEE Trans. on Smart Grid*, vol. no.99, 2016.

[9] R. A. Walling, L. A. Freeman and W. P. Lasher, "Regulation requirements with high wind generation penetration in the ERCOT market", in *proceedings of the IEEE PES Power Systems Conference Expo*, Seattle, WA, USA, Mar. 2009.

[10] D. Wilson, S. Clark, S. Norris, J. Yu, P. Mohapatra, C. Grant, P. Ashton, P. Wall and V. Terzija, "Advances in wide area monitoring and control to address emerging requirements related to inertia, stability and power transfer in the GB power system", CIGRE, 2016.

[11] P. Wall, N. Shams, V. Terzija, V. Hamidi, C. Grant, D. Wilson, S. Norris, K. Maleka, C. Booth, Q. Hong, and A. Roscoe, "Smart frequency control for the future GB power system", in *proceedings of the IEEE PES Innovative Smart Grid Technology Conference (ISGT) Europe*, 2016.

Chapter 2

Towards Decentralisation and Distributed Operation of Power Systems

2.1 Introduction

Power system frequency is a continuous system-wide variable that reflects the instantaneous dynamic balance between system generation and demand. Maintaining this dynamic balance effectively to ensure the integrity and stability of power systems is highly dependent upon adequate procurement and prompt delivery of ancillary services. In this chapter, the fundamentals of power system frequency control will be presented followed by current practices of frequency management within synchronous power system of Continental Europe and Great Britain (GB). This chapter further introduces the concepts of centralised, decentralised and distributed control architectures and presents an architectural analysis of present day frequency control of power systems. By presenting the expected transformations of GB power system in the near future, the impact of such system developments on system frequency response, stability and controllability are discussed. Based on the discussion of the implications of the transformations, research questions for the thesis are derived.

2.2 Fundamentals of Frequency Stability and Control

Frequency stability is stated as: "the ability of a power system to maintain steady frequency following a severe system upset resulting in a significant imbalance between generation and load" [1]. Severe system imbalances lead to digression of system frequency, tie-line power flows and possibly voltage, requiring coordinated actions of a number of systems not accounted for in traditional transient or voltage stability analysis, therefore considered independently as frequency stability. Frequency instability presents itself in the form of sustained swings that can lead to generation or load trips. Such instabilities can be attributed to inadequate response from equipment, inadequate/insufficient procurement of reserves or a lack of adequate coordination of protection and control functions [2]-[5].

The objective of frequency control is to maintain frequency stability, i.e., to maintain equilibrium between generation and load in steady state, while restoring the equilibrium following a disturbance with as little unintentional load loss as possible [1]. The control actions are usually automated, or manual when automated actions are not capable to enforce frequency within statutory limits. To ensure quality of supply, operational policies have been drawn to regulate frequency response. These policies vary from interconnected grid to interconnected grid (not necessarily from country to country as a number of countries might be a part of an interconnected grid).

Frequency control framework can be broadly classified into four stages based on the operational timescales as identified below [6]-[10]:

- Inertial response, up to 10 seconds.
- Primary frequency response, from few seconds up to 30 seconds
- Secondary frequency response, from 30 seconds up to 30 minutes.
- Tertiary frequency response, from 15 minutes up to several hours.

The functional and temporal overview of the framework has been shown in Fig. 2.1 . For the GB power system, the operational bound for frequency is defined as 49.8-50.2

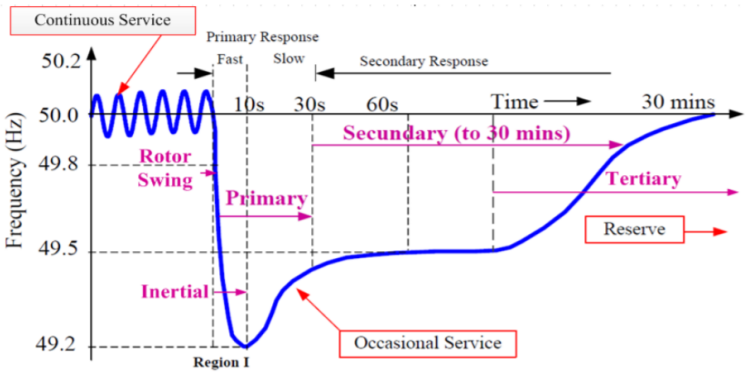

Figure 2.1: Functional and temporal view of frequency control framework [10].

Hz, with the statutory limit set at 49.5-50.5 Hz. The maximum instantaneous deviation in frequency from nominal is set at 0.8 Hz only for a duration of 60 s in response to loss of largest infeed (1800 MW for GB) [11].

2.2.1 Inertial Response

Inertial response is the inherent response of synchronous generators to any power imbalance, perceived as a change in frequency of the system. It is the release or the absorption of kinetic energy from/to the rotating mass of electrical machines connected to the grid. This release/absorption of kinetic energy contributes towards limiting the rate of change of frequency following an imbalance [12]. The kinetic energy stored in a rotating machine (and its ability to limit the rate of change of frequency) is determined by the inertia constant given by [13], [14]:

$$H = \frac{J\omega_0^2}{2S_n} \tag{2.1}$$

where H is the inertia constant, J is the moment of inertia, ω_0 is the rated angular velocity of the machine and S_n is the rated power of the machine. Typically a power system comprises a combination of generation units with different inertia constants owing to diversity in type of fuel and the size of individual units. The equivalent inertia constant (H_{eq}) of a power system with n machines can be calculated as [15],

[16]:

$$H_{eq} = \frac{\sum_{i=1}^{n} H_i \cdot S_i}{\sum_{i=1}^{n} S_i} \tag{2.2}$$

The values of the inertia constants of power systems are typically in the range of 2 s to 9 s [17].

2.2.2 Primary Frequency Response

The objective of primary frequency response is to contain the frequency to an acceptable value after an imbalance event. In addition, in synchronous power systems, the primary frequency response is crucial to ensure smooth operation of a system to cater for continuous load changes. In conventional power systems, such a response is regulated by the governors of synchronous machines operating upon a droop curve [18]. An example droop curve is presented in Fig. 2.2, where the change in power output (ΔP) is inversely proportional to the change in rotor speed ω or the deviation in system frequency (Δf).

In a multi-generator power system, droop additionally serves the purpose of load sharing, where the sum of the increase or decrease in power output of n machines is equal to the imbalance [19].

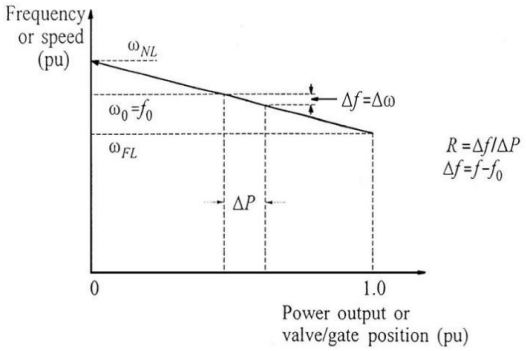

Figure 2.2: Example droop curve for primary frequency response [13].

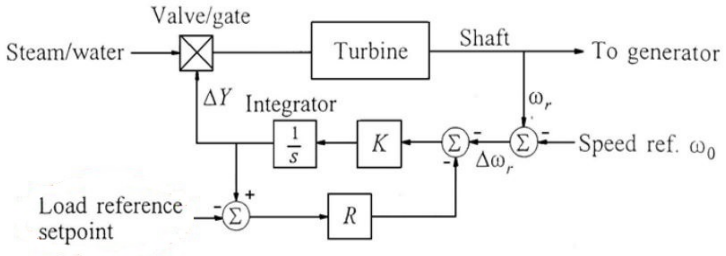

Figure 2.3: Example of secondary frequency control implementation [13].

2.2.3 Secondary Frequency Response

Once the frequency has been contained by the primary frequency response, it is the responsibility of the secondary frequency response to restore the frequency to its nominal value. Conventionally, secondary frequency response is a much slower control achieved by adjusting the load reference set-point of generation units as shown in Fig. 2.3. The change in load reference set-point in an interconnected synchronous power system is coordinated by the system operator.

2.2.4 Tertiary Frequency Response

The objective of tertiary frequency response is to alleviate the secondary frequency response reserves activated for restoring the frequency to its nominal value. Tertiary frequency response reserves are also referred to as replacement reserves, following an economic dispatch or optimal power flow [20]. On-line spinning reserves (hot reserves) capable of response within 15 minutes or off-line non-spinning reserves (cold reserves) for strategic replacement of hot reserves are generally contracted as tertiary reserves.

2.3 Frequency Control of Synchronous (Interconnected or Islanded) Power Systems

The synchronous grid of Continental Europe is the largest synchronous power network (power capacity) in the world. This grid spans across a number of countries with a number of transmission system operators (TSO). The Union for the Co-ordination of

Transmission of Electricity (UCTE) has coordinated the operation and development of the Continental Europe grid, ensuring reliable supply of electricity in Continental Europe. UCTE operated since 1951, redefined itself as an association of TSO's in 1999, and was wounded up in 2009 with its responsibilities handed over to European Network of Transmission System Operators for Electricity (ENTSO-E). ENTSO-E is responsible not only for the Continental Europe grid but harmonizes the operation of the European Grids representing 43 TSO's from 36 countries across Europe [21].

In a synchronous grid, the network frequency is a common physical parameter, observable throughout the network. On one hand, the frequency of the network impacts all the installations (generation and demand) of the network, while on the other hand, all installations impact the frequency. Therefore, although a TSO is responsible for its own region (the geographical region across which the transmission network is spread), ensuring a stable frequency control process is a common task of all operators within the synchronous grid and a precondition for secure operation of the network. This can be achieved if:

- A well defined and organised structure for load frequency control (LFC) is developed.
- TSO's are obliged to cooperate.

For this reason, ENTSO-E has drafted the Network Code for Load Frequency Control and Reserves (LFCR) to ensure frequency stability. Some of the key enabling features of the network code are [22]:

- harmonised quality targets
- harmonised operational procedures
- harmonised minimum requirements

This chapter provides a common European framework for the Load-Frequency Control processes by setting technical requirements for the technical control structure and the according responsibilities of the TSOs.

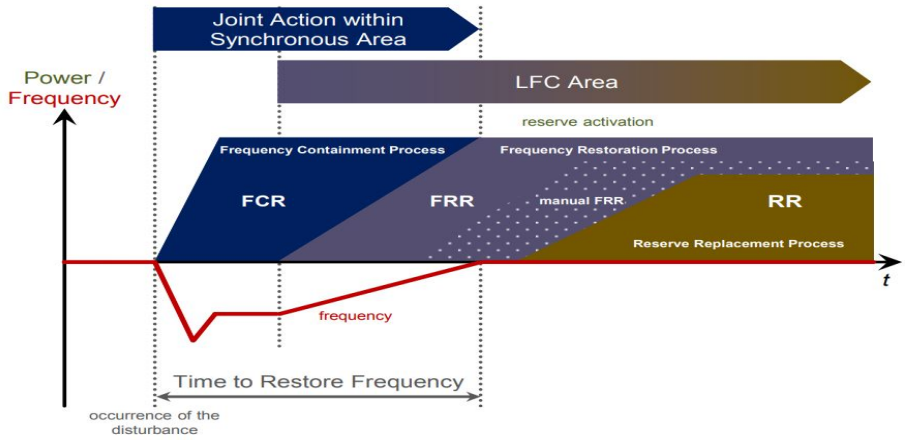

Figure 2.4: Functional and temporal view of load frequency control [22].

2.3.1 Load Frequency Control Process

To effectively coordinate the frequency of the European Grid and yet to be flexible (to be viable for all TSO's and Countries involved), the best practices in power system operation and control have been adopted within the framework of Load-Frequency Control and can be represented by the Fig. 2.4:

Frequency Containment Process: Equivalent to the primary frequency response, the frequency containment process stabilizes the frequency after an imbalance at a steady state value by joint action of Frequency Containment Reserves (FCR) within the entire synchronous area.

Frequency Restoration Process: Equivalent to the secondary frequency response, the frequency restoration process drives the frequency towards its nominal value by activation of Frequency Restoration Reserves (FRR). The frequency restoration process is initiated by the LFC area experiencing the imbalance.

Reserve Replacement Process: Equivalent to the tertiary frequency response, the reserve replacement process, as is suggested by its name, is responsible to replace the activated FRR, or in some cases assist the FRR by means of replacement reserves (RR). Similar to the frequency restoration process, the replacement reserves are activated by

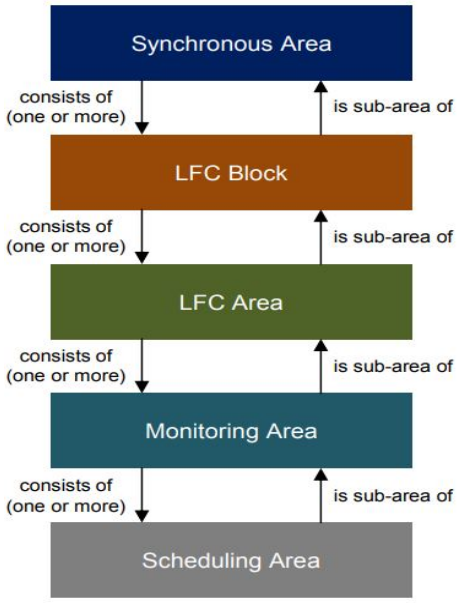

(a) Hierarchy of operational areas within LFCR framework [22].

Obligations	Scheduling Area	Monitoring Area	LFC Area	LFC Block	Synchronous Area
Scheduling	MANDATORY	MANDATORY	MANDATORY	MANDATORY	MANDATORY
online calculation and monitoring of actual power interchange	NA	MANDATORY	MANDATORY	MANDATORY	MANDATORY
calculation and monitoring of the Frequency Restoration Error	NA	NA	MANDATORY	MANDATORY	MANDATORY
Frequency Restoration Process	NA	NA	MANDATORY	MANDATORY	MANDATORY
Frequency Restoration Quality Target Parameters	NA	NA	MANDATORY	MANDATORY	MANDATORY
FRR/RR Dimensioning	NA	NA	NA	MANDATORY	MANDATORY
Frequency Containment Process	NA	NA	NA	NA	MANDATORY
Frequency Quality Target and FCR Dimensioning	NA	NA	NA	NA	MANDATORY
Reserve Replacement Process	NA	NA	OPTIONAL	NA	NA

(b) Obligations of operational areas within LFCR framework [22].

Figure 2.5: Hierarchy and Obligations of operational areas [22].

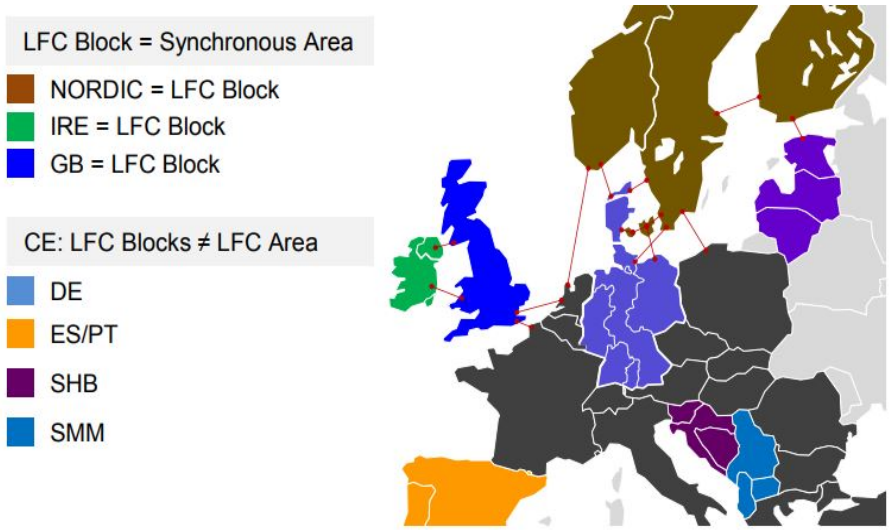

Figure 2.6: European Power System: Synchronous Areas, LFC Blocks and LFC Areas [22].

the LFC area experiencing the imbalance.

As can be observed from Fig. 2.4, the frequency control process is coordinated among different operational areas (synchronous area and LFC within example provided). In an effort to have a coordinated response, ENTSO-E operates a hierarchy of operational areas as shown in Fig. 2.5a. The responsibilities of each of the operational area are summarised in 2.5b.

With the hierarchy and obligations of operational areas presented, Fig. 2.6 presents the organisation of the European Grid. As can be observed, within Europe (under ENTSO-E), there are four synchronous areas, namely the Nordic, Ireland, Great Britain and the Continental Europe. Each of the synchronous areas are interconnected by means of high voltage direct current (HVDC) links. Within Continental Europe, there are four LFC blocks which are further subdivided into LFC areas (not shown in figure).

As has been mentioned earlier, each synchronous area is solely responsible for maintaining its frequency (occupying the top spot among operational areas hierarchy). Although, all the synchronous areas are obliged under the common framework defined by ENTSO-E, each of the synchronous areas operate independently. The synchronous

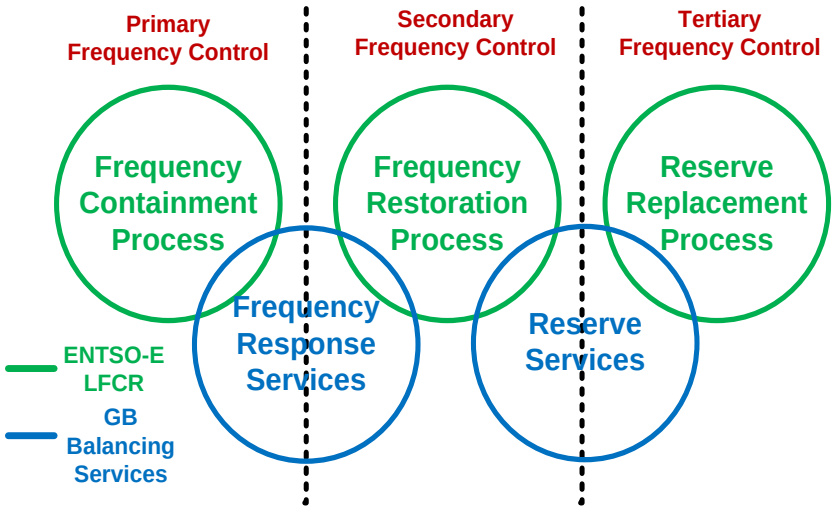

Figure 2.7: A classification of ENTSO-E and GB balancing services in terms of conventional frequency control terminology.

areas are at will to decide upon their respective operational and threshold margins as is evident from [23].

2.4 Frequency Control within the Great Britain Power System

Maintaining the frequency of GB power system is the responsibility of National Grid, the TSO. The frequency is managed by means of procuring services referred to as the balancing services [23]. This section aims to bring a common understanding of these services in context with the fundamentals of frequency control and frequency management as defined by ENTSO-E.

Under the umbrella of balancing services, National Grid operates two services (as shown in Fig. 2.7) and the main difference between the two is highlighted below:

- Frequency Response Services [24]: By definition, frequency response services are automatic services that respond based on measuring local frequency.
- Reserve Services [25]: Reserve services are activated by the operator by means of a dispatch signal. This signal can be automatically generated or by means of

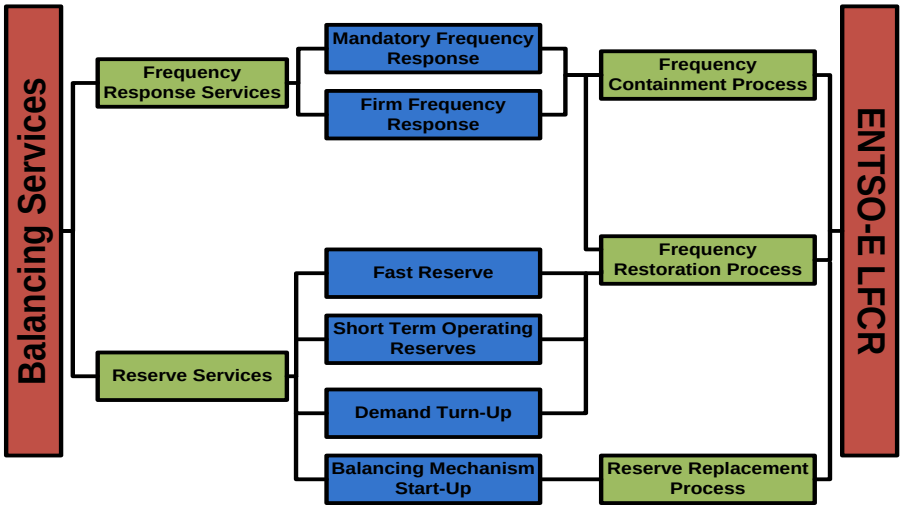

Figure 2.8: A mapping of GB balancing services to ENTSO-E LFCR (by means of objective of service).

manual intervention.

In Fig. 2.8, the frequency control objectives towards which the above services contribute to are represented. As can be observed, the frequency response services contribute to the objectives of frequency containment process and frequency restoration process while the reserve services contribute to the objectives of frequency restoration process and reserve replacement process. The following two sub-sections present the two services briefly with the technical requirements summarised in Table 2.1.

2.4.1 Frequency Response Services

As explained earlier, frequency response services contribute towards the objective of frequency containment (including regulation) and restoration by means of a set of two services as explained below:

Mandatory Frequency Response

The automatic change in active power in response to change in frequency is referred to as the mandatory frequency response. This is a requirement by the grid code for generators (usually greater than 30 MW).

Table 2.1: Overview of balancing services in GB [24]

Service	Response Speed seconds (s) minutes (m) hours (h)	Response Magnitude (Minimum)	Response Time seconds (s) minutes (m) hours (h)
Frequency Response Services			
Mandatory Frequency Response	Primary- within 10 s Secondary-within 30 s	3-5%	Primary- 20 s Secondary- 30 m
Firm Frequency Response	Primary-within 10 s Secondary-within 30 s	1 MW	Primary- 20 s Secondary- 30 m
Reserve Services			
Fast Reserve	within 2 m	50 MW	15 m
Short Term Operating Reserve	under 20 m preferable, maximum 240 m	3 MW	2 h
Demand Turn-Up	customer dependent 7 h 20 m (average 2017)	1 MW	varies
Balancing Mechanism Start-Up	varies	Any balancing mechanism participant	varies

Firm Frequency Response

To allow for smaller devices (generators or load, individual or aggregated) to participate within balancing service markets, firm frequency response (FFR) was introduced. Apart from providing a pathway for smaller participants, FFR ensures a degree of stability against price uncertainty in mandatory service arrangements.

2.4.2 Reserve Services

Reserve services contribute towards the objective of frequency restoration and replacement by means of a set of four services as explained below:

Fast Reserve

The rapid and reliable delivery of active power by means of increasing output from generating devices or reducing consumption from demand sources is referred to as Fast Reserve service.

Short Term Operating Reserves

The delivery of active power by means of increasing output from generating devices or reducing consumption from demand sources only at certain times of the day is referred to as short term operating reserve. This service is intended to cater for forecast errors and unforeseen generation unavailability.

Demand Turn-Up

The demand turn up service encourages large customers (load or generation) to either increase demand or reduce generation at times of high renewable output and low national demand. This service is usually requested overnight and during weekend afternoons in summer.

Balancing Mechanism (BM) Start-Up

This service can be regarded as the precautionary (or anticipatory) service and is made up of two elements: (i) BM start up where generation units are brought to a state at which they will be able to synchronize to the network within 89 minutes, and (ii) hot standby where the generation unit is capable to synchronize with the grid.

2.5 Control Architectures

The spatial distribution and function of the entities, such as the control elements and instrumentation, within a control system and the relations between those entities can be referred to as the control architecture [26]. The control architectures within power systems domain can be classified into three:

- centralised architecture

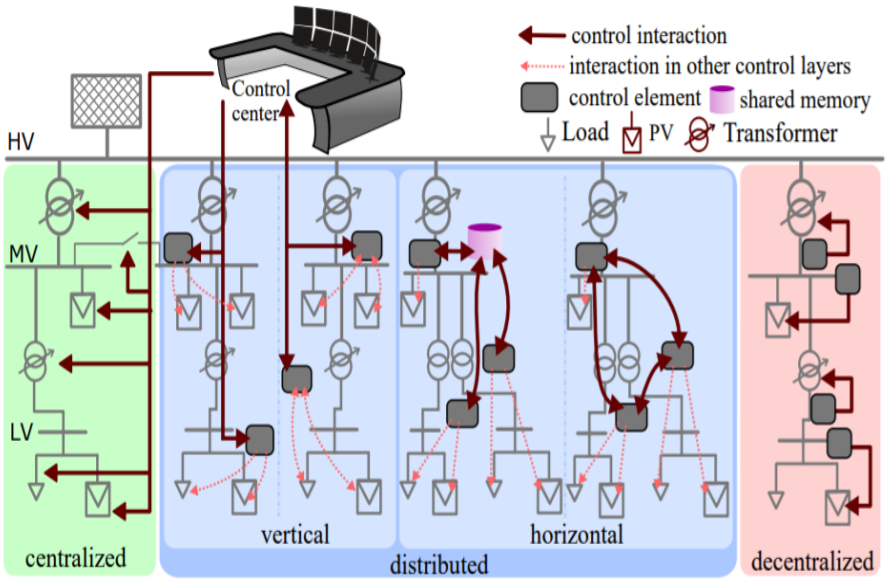

Figure 2.9: An illustration of control architectures within power systems domain [26].

- decentralised architecture
- distributed architecture

An illustration of the control architectures is presented in Fig. 2.9 and discussed in detail in the following sub-sections.

2.5.1 Centralised Architecture

In a centralised architecture, a single control entity relies on gathering information from a number of remote locations to take decisive actions such as determining a set-point for remote actuation [26]. This single control entity, also referred to as the control centre, is responsible for data collection and analysis, and is therefore subject to certain requirement of computation and communication resources.

Examples of centralised control architecture employment within power systems are abundant with examples including unit commitment, active network management, frequency and voltage control [27]-[33]. The commonly identified advantages of centralised control architecture are [34]:

- A centralised control architecture is simple to implement, comprehend and therefore also easy to maintain.
- A centralised control architecture enables complete observability, i.e. ensures the availability of overall system state or overall system knowledge.
- Owing to the comprehensive knowledge of the system, a centralised control architecture enables implementation of controls that guarantee fairness and optimality.

On the other hand, the disadvantages of a centralised control architecture can be summarised as [34]:

- As all the intelligent computation is at one location within one entity (control centre), centralised control architectures are susceptible to single point of failure.
- The responsiveness, in other words the performance, of a centralised control architecture is highly dependent upon the computational resources and communication architecture employed.
- The scalability of centralised control architectures are limited by the computational resources and communication architecture employed.

2.5.2 Decentralised Architecture

In a decentralised architecture, multiple control entities are jointly responsible for a common objective, intended to take decisive actions independently of each other based on local observables only [26]. The most common decentralised control for power system is the primary frequency control via active power/frequency droop [35] or the local voltage control via reactive power/voltage droop [36].

The reliance of decentralised control on local observables voids any need for communication, thereby offering a form of resilience. This resilience is the reason for decentralised control often being employed for system critical services such as primary frequency control, the first line of defence in case of large system contingencies, and over current protection against faults within the network.

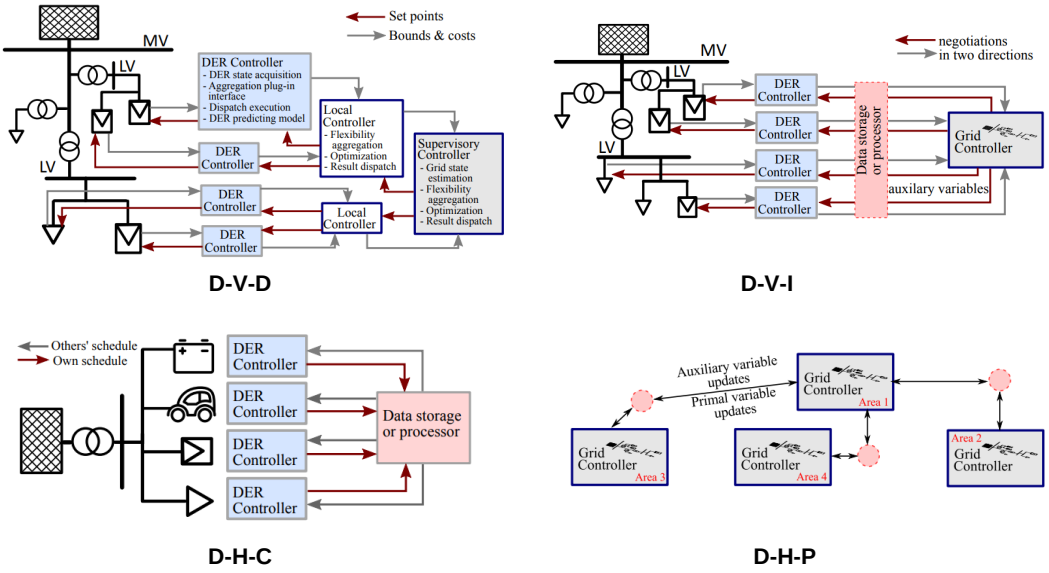

Figure 2.10: An illustration of distributed control architectures within power systems domain [26].

Coordination within decentralised control algorithms is difficult due to the lack of interaction among the entities involved. A system level coordination in primary frequency control is achieved due to the physical property of the controlled process, i.e., the steady-state frequency is same irrespective of where it is measured within a network and therefore acting as means of information. As the decisions taken by decentralised control are under partial knowledge of the system, it is also difficult to achieve optimality and to ensure fairness. An attempt to improve optimality in decentralised controls by means of local signal processing and employment of improved process models is reported in [37], while parametrisation of local control parameters by addition of topological information to achieve fairness is reported in [38].

Although the mass deployment of such control is easy, owing to dependence on local observables only, design and maintenance of such control algorithms are often more challenging.

2.5.3 Distributed Architecture

A distributed control architecture can be observed as a hybrid (some form of combination of centralised and decentralised) where a common control objective is decomposed and delegated to independent control elements. Depending upon how the common control objective is decomposed and delegated, the distributed architectures can be classified into two [26]:

Distributed Vertical (D-V): When the common control objective is decomposed and delegated in a way such that the decision of one control element is imposed on the other, the architecture is referred to as D-V. The D-V architecture imposes a level of hierarchy among the participating control elements. In such an architecture, the low level controllers (decentralised controllers) do lose a degree of freedom, however, owing to the characteristics of hierarchy (a form of centralisation), more optimal solutions are feasible. Examples are [39]-[42].

Distributed Horizontal (D-H): When the control responsibilities of all the control elements involved are symmetrical such that there is no hierarchy among them, the control architecture is referred to as D-H. A system level coordination with such an architecture is difficult and although the controllers have a higher degree of freedom, the solutions are not necessarily optimal. Examples are [43]-[46].

Based on the type of information exchange between the control elements, each of the two distributed architectures can be further sub-classified into two:

Distributed Vertical Determinate (D-V-D): An example representation of D-V-D architecture is presented in Fig. 2.10. As can be observed, in a D-V-D architecture, there is a hierarchical information collection and a centralised decision making. The lower-level control elements do not have a say in the deterministic decision taken at the higher level control. Examples are [41] and [42].

Distributed Vertical Iterative (D-V-I): Similar to the D-V-D architecture, in a D-V-I architecture, the information gathering is hierarchical; however, the lower-level controllers can negotiate the decision brought by the higher-level controller, and therefore incorporating the term iterative in its name. The negotiation between the different control levels is captured by bi-directional arrows in 2.10. Examples are [39], [40] and [47].

Distributed Horizontal Centralised (D-H-C): With the control responsibility of all control elements involved being symmetrical, if an additional centralised entity exists that coordinates the information exchange between the control elements, the architecture is referred to as D-H-C (as shown in Fig 2.10). While the existence of a centralised entity makes the architecture more susceptible to a single point of failure, it reduces the burden on communications infrastructure, making it more scalable. Examples are [43] and [44].

Distributed Horizontal Peer to Peer (D-H-P): The final architecture is the D-H-P, a fully distributed architecture, where the information exchange is wholly between the controllers, peer to peer (P2P). Examples are [45] and [46]. The burden imposed on communications infrastructure by the P2P information exchange can limit the scalability of such architectures. In recent literature, graph theory has been utilised to enforce sparse communication within a set of controllers, while ensuring that the control objective is achieved.

2.5.4 An Architectural Analysis of Present Day Frequency Control of Power Systems

Generally in power systems, any control problem is mathematically decomposed into three time-dependent cascaded layers referred to as the primary, secondary, and tertiary control layers [48]. More often, the following architectural view is widely assumed for the three layers:

- Primary ⇒ Decentralised

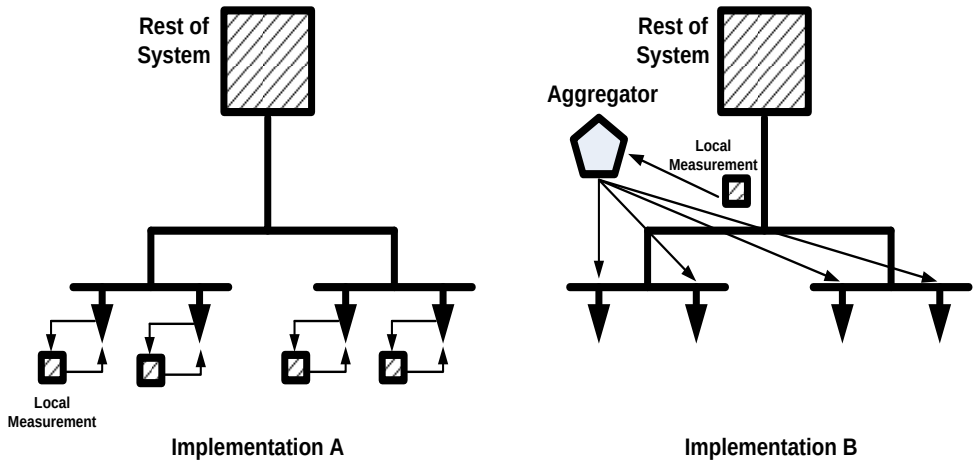

Figure 2.11: Example implementations of primary frequency control.

- Secondary ⇒ Centralised
- Tertiary ⇒ Centralised

In literature, many alternative architectural realisations have been proposed [34]. Moreover, the control architecture adopted depends upon the hierarchical level from which the analysis is undertaken. To explain this better, in this section, an architectural analysis of the conventional frequency control is presented.

Primary Frequency Control: It is well known that the primary frequency response needs to be coordinated throughout the entire synchronous power system. However, as there is no real-time communication during the operation of this control scheme, i.e., the response is based on local measurements only (as shown in Fig. 2.11, Implementation A), primary frequency control is a purely decentralised control. An alternative implementation of primary frequency control is presented in Fig. 2.11 (Implementation B). When observed from a system level, the primary frequency response from the aggregator is decentralised, no real-time communication between the system and the aggregator (the aggregator responds based on local measurement). When observed from the aggregator it can be discerned that the aggregator employs D-V-D architecture.

Secondary Frequency Control: An example hierarchical representation of synchronous power system is presented in Fig. 2.12. As has been explained earlier, the

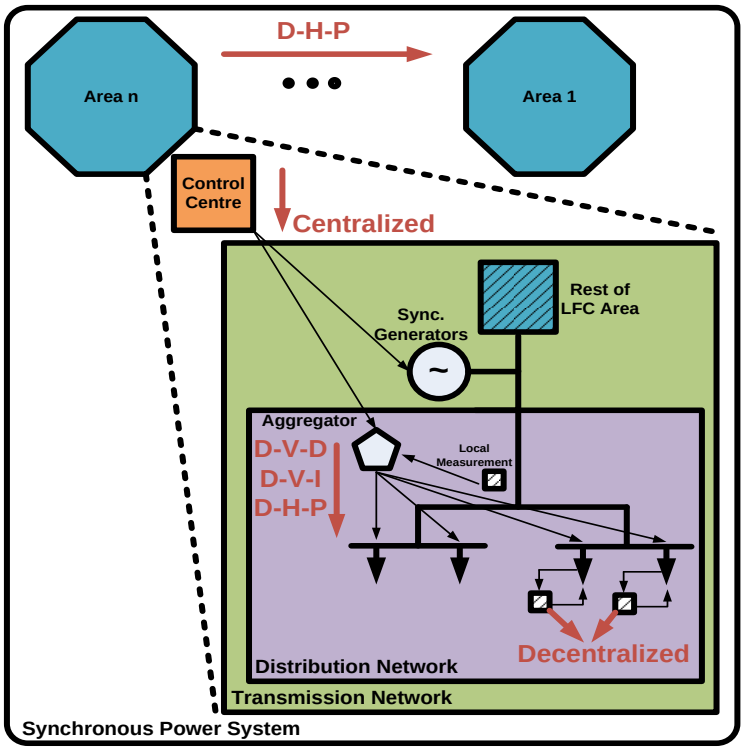

Figure 2.12: Example hierarchical architectural representation of synchronous power system.

area that initiates an imbalance is responsible to restore the frequency to its nominal value. Assuming a control centre within each LFC area, the secondary frequency control is centralised within an LFC area. In real-time, the control commands (set-points) are sent to participating resources (such as aggregators and synchronous machines as depicted in figure) while the participation factor is pre-determined. As can be observed from Fig. 2.12, when aggregators participate in secondary frequency control, the aggregators can adopt either D-V-D, D-V-I or D-H-P control architecture. When the control effort within an LFC area is not sufficient, an LFC area can collaborate with another LFC area to restore the frequency. Under such circumstance, the control architecture at an LFC area level is D-H-P, as each of the areas can be observed as equal peers.

Tertiary Frequency Control: Similar to secondary frequency control, if replacement reserves chosen are from within the LFC area, then the tertiary frequency control is centralised within an areas. In the circumstance that there are insufficient econom-

ical replacement reserves within an area, the D-H-P architecture is adopted between the LFC areas.

2.6 Transformation of the Great Britain Power System

For the past several decades, power systems have been characterised as "unidirectional", with a small number of relatively large power plants feeding power to end consumers. End consumers remained fairly passive with no interaction with power delivery mechanism. In the recent years, power systems have been experiencing a number of changes in generation and consumption that have begun to set a trend internationally and present a challenge to the traditional "unidirectional" view of the power system. In this section, these changes will be presented for the GB power system categorically, summarising views and foresights from the Institution of Engineering Technology (IET) reported in a position statement towards a 2030 GB power system [49] and by National Grid reported in the Future Energy Scenarios (FES) towards a 2050 power system [50]. These categories presented below are considered as the challenges power networks face in the circumstance of the transition.

Increasing Renewable Generation Penetration: About 34% (34GW) of the installed capacity (100GW) within the GB grid is renewable generation (as of 2016) and is expected to grow rapidly with increasing pressure to meet the climate change objectives. Based on the two degree scenario of the FES, it is expected that there will be 223% increase in capacity of renewable generation. This increased capacity will represent 60% (110GW) of the total generation capacity ($\sim$ 184GW) in 2050. Among the different types of renewable resources, wind is expected to dominate in terms of the magnitude of installation (50 GW of wind installation compared to 44 GW of solar installation) however solar is expected to see the highest percentage (400%) increase.

Increasing Distributed Generation Penetration: In 2016, the reported installed capacity from distributed generation (generation installed at distribution level rather than transmission level) was 27% ($\sim$ 26GW) of total installed capacity. In 2050, an

increase to a total of 93 GW is expected, representing 50% of the total installed capacity. This expected increase will be from a mix of generation sources. Interestingly, 24GW of small-scale thermal generation is expected to be distributed within the grid. The majority of the 44 GW solar penetration mentioned earlier will also be at the distribution level. Energy storage (larger dedicated storage units or the battery within an electric vehicle) is expected to be part of the distributed generation.

Changing Demand Profile: In 2050, electricity peak demand can be expected to increase to 85GW from around 60GW in 2016. Electric vehicles are expected to see a steady growth, owing to increasing customer acceptance and technology improvements, with about one million cars in 2020 and more than nine million by 2030+. As per estimation, without coordinated smart charging mechanism, this increasing penetration could directly translate to an increase in 8 GW of demand at peak times. With changing weather patterns, it is further anticipated that with an increase in temperature, peak demand in summer could raise to levels as seen in winter due to increase in air conditioning load. The increase in peak demand is not the only expected change, a change in peak period is anticipated with increasing penetration of distributed generation. For example, in a future scenario with large percentage of residential consumers with photovoltaic (PV) rooftops, sun shining in a summer month can lead to significant reduction in transmission demand. This would set a new trend of noon time being considered as the time with least demand (as compared to early mornings today).

Demand Side Management: In the present day power system, although there is an increasing interest in utilising demand side to assist the network, this has been limited to larger industrial demand. This is evident from the preference of 100kW or greater capacity participants by the twenty three aggregators within the GB network. Effectively, there is 0% penetration of home energy management in broad terms, i.e. all the domestic residential demand is passive. With the mass roll-out of smart meters, 95% of UK homes are expected to be capable of providing real-time information for active demand response by 2020. It is estimated that with only half of the installed smart meters linked to an energy management system, there will be about 15 million

units available for utilisation by 2030.

Modern Control and Automation: The advancements in information and communication technologies (ICT) and automation technologies will bring more opportunities (and challenges at the same time) to the traditional controls employed within the present day power system. For example, in present day GB network 10-15 large generating units connected at transmission level operate in frequency control mode, maintaining the frequency of the network. In the future, most electrical devices are expected to be interconnected and controllable via a phone or an aggregator. Although the extent to how much flexibility this can deliver is unclear, an example representation is the availability of 600,000 units available for assisting in frequency control if only 10% of interconnected devices are utilised. In a similar manner, about 10,000 devices are responsible for voltage regulation within the present day distribution network under the umbrella of distribution network automation. In the future, there will be 900,000 units capable of participation in voltage regulation within the distribution network, a 90% increase.

2.7 Analysing the Impact of Transformation

In this section, the impact of the transformations of GB power system summarised in the previous section will be analysed with respect to the following three categories:

- System Frequency Response
- System Stability
- System Controllability

2.7.1 System Frequency Response

A majority of the renewable generation resources, such as PV and wind, are interconnected to the grid through power electronics. As inertia of a system is derived from energy stored in rotating masses within the network, the renewable resources effectively

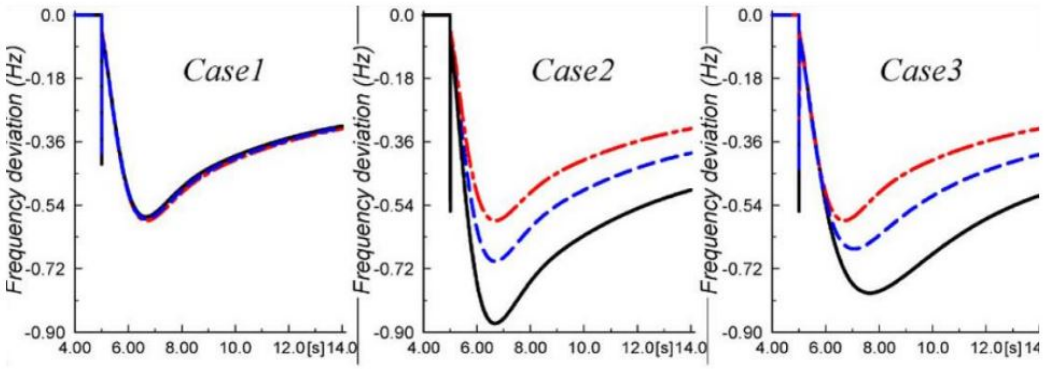

Figure 2.13: Impact of wind generation penetration, 30% (red), 60% (blue) and 90% (black) of system load, on system frequency excursions during power imbalance , [54].

decoupled from the grid by power electronics inherently do not contribute to the system inertia [51]. Therefore, with an increase in penetration of renewable resources, the inertia of the system will decline as is evident from the concerns raised by National Grid in [52]. In this sub-section, an example of the impact of increasing penetration of wind generation on system frequency response, from a study undertaken in [53] as per [54], is presented. For a thorough analysis, the following three case studies were undertaken:

- Case 1: Wind generation penetration of 30%, 60% and 90% of the demand with no change to system synchronous generation capacity i.e., no change in system inertia.
- Case 2: Wind generation penetration of 30%, 60% and 90% of the demand with equal reduction in system synchronous generation capacity i.e., system inertia is reduced.
- Case 3: Wind generation penetration of 30%, 60% and 90% of the demand with equal reduction in system synchronous generation capacity but with same level of inertia. This is achieved by means of adjusting the inertia constants of existing synchronous generators.

The results of the analysis are presented in Fig. 2.13. Case 1 provides evidence that the system frequency response with high penetration of renewable energy resources would

be unaffected if the capacity of synchronous generation within the system remains unchanged. Case 2 provides the evidence of the impact of reduction of inertia of the network on the system frequency response. The reduction in synchronous generation capacity does not only impact the rate of change of frequency but also the frequency nadir. Case 3 provides evidence that the increasing penetration of renewable generation and simultaneous reduction of synchronous generation capacity, even without decreasing the system inertia, degrades the frequency response of the system (in terms of frequency nadir).

From the above study it becomes clear that increasing penetration of renewable generation sources, the decreasing penetration of synchronous generation and the consequent decrease in system inertia deteriorates the system frequency response. This deterioration in frequency response represents an emerging frequency control challenge faced by system operators around the world. For example, in a study undertaken by Australian Energy Market Operator (AEMO), the RoCoF level is expected to increase with the expected change in generation mix (i.e., with rapid uptake of non-synchronous generation) [55]. With the new expected levels of RoCoF in 2021-2022, it is anticipated that there would be less than two seconds for primary frequency control actions to arrest the frequency before it declines below the containment band defined by Frequency Operating Standard (FOS) [56]. The two seconds range is much faster than the typically observed response time of synchronous generators. Therefore, it can be said that, the decreasing inertia in the network imposes new time restrictions (or requirements) on existing services. As existing services are basically classified in terms of time of response, the previous statement can be rephrased as: the decreasing inertia in the network imposes new time restrictions (or requirements) therefore requiring new services to be defined.

The need to reduce the RoCoF has motivated the development of virtual synchronous generators (VSGs). The term VSG refers to a converter control approach that enables emulation of inertial response of synchronous machines over short periods of time, often referred to as virtual, synthetic or emulated inertia [57]-[59]. Typically, any power electronic interfaced distributed generation with appropriate control

can help improve the dynamic response of the system (i.e., help improve RoCoF). Although in recent literature a number of works have proposed novel synthetic-inertial control approaches [60]-[65], in practice synthetic inertia is commercially unavailable [66]. Furthermore, as reported in [66], virtual inertia emulation is feasible within power networks with high inertia, but it becomes increasingly challenging to obtain an appropriate transient response in low inertia circumstances. In addition, system operators realize the adaptable nature of power electronic interfaced devices can yield a wider range of responses and enforcing only inertial response from such devices can be limiting and can curb further developments.

Therefore the need for faster acting service provision has been realised by the system operators. In this context, the inertial response from power electronic interfaced devices is encompassed within the umbrella of fast acting service provision but not limited to it. In essence, system operators are looking for fast response in the entire spectrum of frequency control mechanisms as is evident from the pilots and plans of some international system operators summarised below [67]:

- In Canada, Hydro-Quebec has mandated all wind generation connecting to its network to provide inertial response [68]. Ontario and Brazil have more recently introduced similar mandatory requirements[69], [70].

- In GB, National Grid has planned to pilot one second Enhanced Frequency Response service to be delivered by batteries [71]. This service is based on droop but with a narrow dead band, similar to primary frequency response delivered by synchronous governors.

- In the USA, PJM has employed batteries and flywheels for dynamic regulation services, responding to SFC signals. Participants are paid a price proportional to their speed of response, encouraging faster response [72].

- In New Zealand, a one second service is already delivered by demand response towards objective of primary frequency control [73].

- In Texas, Electric Reliability Council of Texas (ERCOT) proposed a half second

response from demand to contribute towards objective of primary frequency control but was rejected (deemed unnecessary at time) by stakeholders [74]. also has a fast demand response service. It might be given consideration in near future.

- In Ireland, EirGrid has proposed the introduction of a one to two second response service, incentivising faster response [75].

From the above discussion, the following can be concluded: Although system operators around the world utilize different terminology, they share a common concern of declining system inertia and its effect on system frequency and the challenges brought forwards towards frequency control. In general, each system operator is working towards better understanding and integrating faster response within their frequency control mechanisms. It is important to note that the service towards which the fast response will contribute to remains flexible. i.e., whether it will be part of existing mechanisms (as in New Zealand) or new services will be defined (as in Great Britain).

2.7.2 System Stability

Frequency stability refers to the ability of a power system to maintain steady frequency following a significant imbalance between generation and load while angle stability refers to the ability of synchronous machines of an interconnected power system to remain in synchronism after being subjected to a disturbance [1]. Frequency stability following a disturbance is ensured by response from governors of synchronous machines (primary

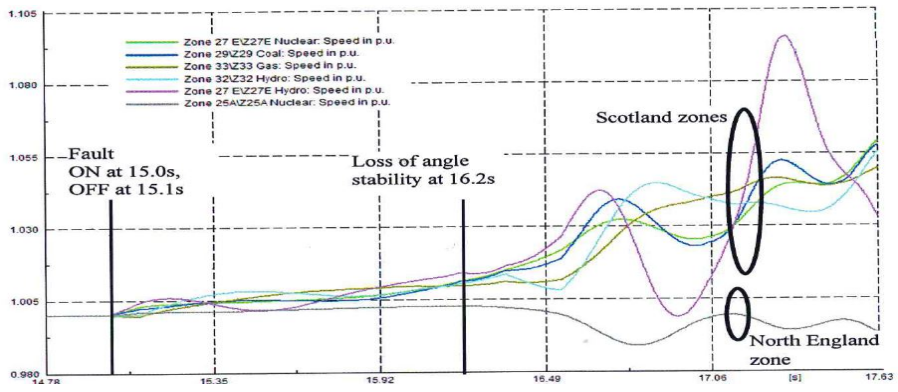

Figure 2.14: Angles of zones following a loss of line in transmission corridor [77].

frequency response) within 10s of the disturbance. Angle stability involves the first swing response of the power system for which the first second after the disturbance is of particular importance. Conventionally, the different timescale of frequency stability and angle stability has allowed for the two to be dealt with separately.

It is known that the angular separation of areas linked by a transmission corridor impacts the power transfer capability of the corridor [76]. In a similar manner, a sudden change in power flow through the corridor due to imbalance between the

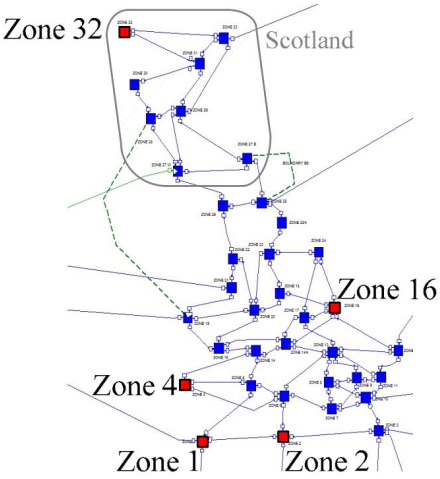

(a) A representation of 36 zone GB power system

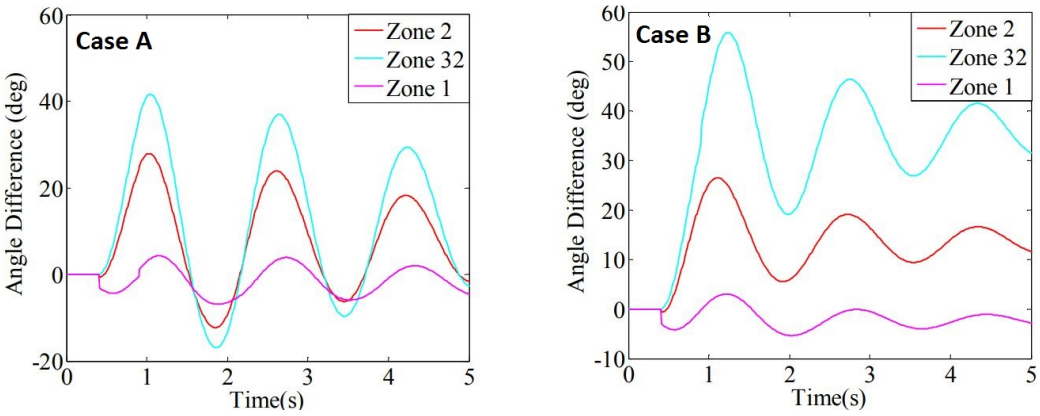

(b) The angle difference of three zones for a disturbance in zone 1

Figure 2.15: Results from a study in [78] demonstrating the benefits of frequency response closer to the source of imbalance.

generation and load impacts the angular separation of areas and therefore the angular stability. This has been shown for the GB power system in which the transmission corridor between Scotland and England is stability limited. The loss of one line of the transmission corridor due to a fault lead to loss of synchronism in 1.3 seconds as shown by simulations of a simplified GB network model presented in Fig. 2.14 [77]. In another study undertaken on a 36 zone GB power system (developed by National Grid shown in Fig. 2.15a), the relationship between the frequency stability and angle stability was demonstrated [78]. The angle difference of three chosen zones (1,2 and 32) for a disturbance in zone 1 is presented in Fig. 2.15b. Case A (left) represents the angles when the frequency support action was taken at zone 1 while Case B (right) represents the angles when the frequency support action was taken at zone 32. The above two studies provide evidence of the interaction of the frequency response and angular stability. For example, if a large generation trip in Scotland is compensated for by a resource in England, the angular separation over the transmission corridor might increase and lead to system separation. In contrast if the large trip is compensated for by a resource close to the trip, the stability of the transmission corridor would be improved.

It can therefore be said that if frequency response is prioritised close to the source of the disturbance, the angular separation of interconnected power system can be improved. National Grid has pre-emptively realised the importance of prioritising response closer to source of imbalance evident from the Enhanced Frequency Control Capability (EFCC) project [1] [79], where achieving a targeted response close to the source of disturbance within a second is being explored.

2.7.3 System Controllability

Conventionally the need for faster acting frequency services can be resolved by the use of fast acting gas turbines as the regulation providing units; however, their availability

[1]The project was near completion at the time of this thesis and only preliminary controller details had been made available. No field trials were planned during the course of the project. It is interesting to note that the service (primary or secondary) within which such a response would be utilised is not yet clear.

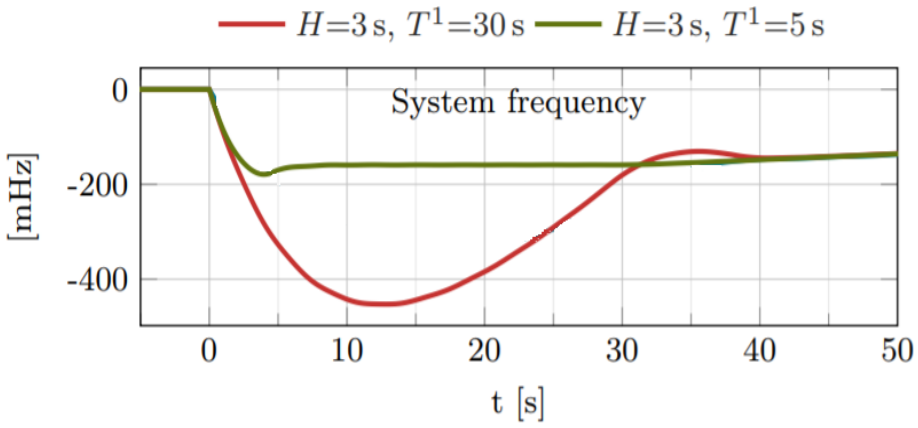

Figure 2.16: Advantage of fast acting devices for primary frequency control [53].

and cost of operation can restrict their implementation [80]. An alternative to the conventional approach is the use of flexible demand available within the network. The use of flexible demand does not only offer an alternative source of reserve to be utilised by the operators but the fast acting nature of these devices (such as batteries and heat-pumps) can be beneficial to the frequency response of the system. Consider the example result of a study undertaken in [53] presented in Fig. 2.16. The responses of a system subject to a disturbance with only primary frequency control is presented. As can be observed, the response of the system with fast acting devices (green, fast acting behaviour emulated by means of resource response time, T=5s in this case) shows an improved frequency response compared to the response with slower devices (red, T=30s). In another study undertaken in [81], the aggregated response from flexible load participating in frequency control based on local measurements has been proven to be close to that of a synchronous generator in behaviour. Transitioning towards more flexible and efficient power system operation does not only involve incorporating the diversity of energy resources but also the incorporation of intelligent control strategies. A number of works in literature have proposed the use of demand side devices for primary frequency control [82]-[87].

The use of fast acting demand side devices is not limited to primary frequency control. A number of works in literature have incorporated demand side devices for

secondary frequency control and have brought forwards the advantages of the fast acting nature of such devices. For example, in [88] and [89], it has been shown that the utilisation of a utility scale battery energy storage system (BESS) in conjunction with conventional generators (CG) improves the AGC performance of the CGs. In a study that characterizes the effectiveness of utilising BESS for AGC compared to CGs, it has been claimed that the utilisation of BESS reduces the regulation requirement even when BESS constitute a small portion of total capacity [90]. This has also been confirmed in studies conducted by [91]. Although the performance of AGC is improved by utilising fast acting devices, the slow nature of AGC, due to ramp rate constraints on CGs, does not allow for exploitation of the true potential of such devices.

An approach, already in use in the GB power system and referred to as frequency control by demand management (FCDM) [92], provides an alternative means to exploit the power ramping potential of fast acting devices. This approach is based on determining a frequency threshold for participating fast acting devices [93]. The amount of reserves activated by such means is subtracted from the AGC regulation command. In [94], it was shown that such an approach alleviates the burden on AGC and provides a better frequency response. Bringing EFCC in context, it can be said that EFCC is an improvement to the existing FCDM, extended to utilize faster responding devices with responsibilisation. At present, only relatively large commercial customers participate in FCDM and are activated by means of under-frequency relays while the market structure for EFCC remains unclear. The dimensioning of FCDM reserves and the thresholds for activation of FCDM reserves are carefully determined based on the system power frequency characteristics. In the future, with high penetration of intermittent renewable energy resources within the grid, the dimensioning of FCDM reserves and calculation of thresholds for their activation will prove to be even more challenging as highly variable system power frequency characteristics are anticipated. The opportunity of participating in FCDM will be extended to the large amount of flexibility foreseen to be available within the grid (including domestic devices such as electric vehicles and heat pumps). Devices interfaced by power electronics will have no difficulty in participating through local measurements, however, some devices that inherently do not incorporate local

observables may not be able to participate even with large amount of such devices may be ICT enabled.

In other words, the large amount of distributed domestic flexibility within the network will be available to participate through the traditional AGC (as it does not require local measurements but requires ICT enabled devices). In [95]-[97], alternative structures for AGC and controls for fast acting devices to participate in such structures have been proposed. This does play into the idea of utilising fast acting devices for a wide spectrum of services (not just primary but secondary as well), however, as the nature of AGC is centralised, the approach may not be able to operate under increased number of participating units. This may be either due to the requirement of complex communications network with two-way communication links or the requirement of a powerful central controller to process large amount of data, both of which reduce overall system reliability and increases its sensitivity to failures [34]. The establishment of the concept of demand side aggregators has facilitated the transition of AGC from a centralised control approach to a distributed approach. In the process it has also facilitated the participation of fast acting devices within AGC structures.

2.8 The Research Objectives

The analysis undertaken in the previous section affirms the challenges posed to conventional approaches to frequency management under the certainty of changes expected within the power systems around the world. To ensure the security of supply, following requirements can be established:

- Frequency control approaches need to be faster acting.
- Frequency control approaches need to be locationally targeted.
- Frequency control approaches need to be able to incorporate the variety of devices available within the network effectively.

Out of the three requirements identified, the most recently identified concept is the need for incorporating locational information. Acknowledging this emerging need to

incorporate locational information for a targeted response to a power system imbalance, this thesis introduces the term "responsibilisation":

"The prioritisation of remedial control measures electrically closer to the source of the disturbance is referred to as responsibilisation".

The introduction of the term is aimed at filling a gap in referring to an important concept thereby supporting the drive towards the new paradigm of greater decentralisation of power systems. With the review of fundamentals and practices of frequency control presented, the requirements for frequency control approaches derived, and the introduction of the term "responsibilisation", the research questions to be addressed by this thesis can be formulated as:

- Observing from a synchronous power system perspective, as every LFC area is responsible to cater for its own imbalance, it can be said that responsibilisation is incorporated within secondary frequency control implemented within the number of LFC areas of the synchronous region. However, can its speed of response be improved without jeopardising system stability?
- Primary frequency control's operation at a much faster timescale than secondary frequency control, where responsibilisation is conventionally in place, presents a challenge for responsibilisation. Can effective decentralised method for responsibilisation be developed for primary frequency control?
- The participation of demand side management in ancillary service provision is proven in a number of energy markets, yet its full potential to benefit frequency management, including the exploitation of fast power ramping capability of some devices, is still undergoing research. Can the fast power ramping capability of demand side devices be effectively harnessed?

2.9 Chapter Summary

In this chapter, the fundamentals of power system frequency control were presented followed by frequency management within synchronous power system of Continental Eu-

rope and GB. This chapter further introduced the concepts of centralised, decentralised and distributed control architectures and presented an architectural analysis of present day frequency control of power systems. By presenting the expected transformations of GB power system in the near future, the impact of such system developments on system frequency response, stability and controllability were discussed. From the analysis of the impact, the emerging need to prioritize control measures close to the source of imbalance events is acknowledged and the term responsibilisation is introduced. With the discussion of the implications of the transformations, research questions for the thesis were derived.

References

[1] P. Kundur, J. Paserba, V. Ajjarapu, G. Andersson, A. Bose, C. Canizares, N. Hatziargyriou, D. Hill, A. Stankovic, C. Taylor, T. Van Cutsem, V. Vittal, "Definition and classification of power system stability IEEE/CIGRE joint task force on stability terms and definitions", in *IEEE Trans. on Power Systems*, vol. 19, no. 3, pp. 1387-1401, Aug. 2004.

[2] "Analysis and Modeling Needs of Power Systems Under Major Frequency Disturbances", CIGRE Task Force 38.02.14 Rep., Jan. 1999.

[3] P. Kundur, D. C. Lee, J. P. Bayne, and P. L. Dandeno, "Impact of turbine generator controls on unit performance under system disturbance conditions", in *IEEE Trans. Power Apparatus and Systems*, vol. PAS-104, pp. 1262-1267, June 1985.

[4] Q. B. Chow, P. Kundur, P. N. Acchione, and B. Lautsch, "Improving nuclear generating station response for electrical grid islanding", in *IEEE Trans. Energy Conversion*, vol. EC-4, pp. 406–413, Sept. 1989.

[5] P. Kundur, "A survey of utility experiences with power plant response during partial load rejections and system disturbances", in *IEEE Trans. Power Apparatus and Systems*, vol. PAS-100, pp. 2471–2475, May 1981.

[6] F. Gonzalez-Longatt, E. Chikuni, and E. Rashayi, "Effects of the Synthetic Inertia from wind power on the total system inertia after a frequency disturbance", in *proceedings of the 2013 IEEE International Conference on Industrial Technology (ICIT)*, 2013, pp. 826-832.

[7] J. Machowski, J. W. Bialek, and J. R. Bumby, Power System Dynamics - Stability and Control, Second ed.: John Wiley & Sons, Ltd, 2008.

[8] "The Grid Code Issue 5 Revision 14", National Grid, 26 August 2015.

[9] "Policy P1: Load-Frequency Control and Performance", in Continental Europe Operation Handbook, ENTSO-E, 2016. [Online]. Avail-

able: https://www.entsoe.eu/publications/system-operations-reports/operation-handbook/Pages/default.aspx

[10] R. S. Pearmine, "Review of primary frequency control requirements on the GB power system against a background of increasing renewable generation", Brunel University 2006.

[11] "NETS Security and Quality of Supply Standard", National Grid, 05 March 2012.

[12] "Frequency Response Standard Background Document", North American Electric Reliability Corporation (NERC), Nov. 2012.

[13] P. Kundur, Power System Stability and Control: McGraw-Hill Inc., 1993.

[14] G. Shrinivasan, Power System Analysis: Technical Publications, 2009.

[15] P. Tielens and D. Van Hertem, "Grid Inertia and Frequency Control in Power Systems with High Penetration of Renewables", status: published, 2012.

[16] U. Rudez and R. Mihalic, "Analysis of Underfrequency Load Shedding Using a Frequency Gradient", in *IEEE Trans. on Power Delivery*, vol. 26, pp. 565-575, 2011.

[17] J. Grainger and W. Stevenson, Power System Analysis: New York, 1994.

[18] J. Undrill, "Power and Frequency Control as it Relates to Wind-Powered Generation", Dec. 2010.

[19] M. Peydayesh and R. Baldick, "The Effects of Very Fast Response to Frequency Fluctuation", in *proceedings of the USAEE/IAEE North American Conference*, Taxes, 2012.

[20] B. H. Chowdhury and S. Rahman, "A review of recent advances in economic dispatch", in *IEEE Trans. on Power Systems*, vol. 5, pp. 1248-1259, 1990.

[21] "Who is ENTSO-E", European Network of Transmission System Operators for Electricity, Website: https://www.entsoe.eu/about-entso-e/Pages/default.aspx

[22] "Supporting Document for the Network Code on Load-Frequency Control and Reserves", European Network of Transmission System Operators for Electricity. [Online]. Available: https://www.acer.europa.eu/Official_documents/Acts_of_the_Agency/Annexes/ENTSO-E%E2%80%99s%20supporting%20document%20to%20the%20submitted%20Network%20Code%20on%20Load-Frequency%20Control%20and%20Reserves.pdf

[23] "Balancing Services", National Grid, Website: https://www.nationalgrid.com/uk/electricity/balancing-services

[24] "Frequency Response Services", National Grid, Website: https://www.nationalgrid.com/uk/electricity/balancing-services/frequency-response-services

[25] "Reserve Services", National Grid, Website: https://www.nationalgrid.com/uk/electricity/balancing-services/reserve-services

[26] X. Han, K. Heussen, O. Gehrke, H. W. Bindner and B. Kroposki, "Taxonomy for Evaluation of Distributed Control Strategies for Distributed Energy Resources", in *IEEE Trans. on Smart Grid*, vol. PP, no. 99, pp. 1-1.

[27] M. Juelsgaard, P. Andersen, and R. Wisniewski, "Distribution loss reduction by household consumption coordination in smart grids", in *IEEE Trans. Smart Grid*, vol. 5, no. 4, pp. 2133-2144, 2014.

[28] I.-K. Song, W.-W. Jung, J.-Y. Kim, S.-Y. Yun, J.-H. Choi, and S.-J. Ahn, "Operation schemes of smart distribution networks with distributed energy resources for loss reduction and service restoration", in *IEEE Trans. Smart Grid*, vol. 4, no. 1, pp. 367-374, 2013.

[29] C. Zhao, J. Wang, J.-P. Watson, and Y. Guan, "Multi-stage robust unit commitment considering wind and demand response uncertainties", in *IEEE Trans. Power Systems*, vol. 28, no. 3, pp. 2708-2717, 2013.

[30] S. Han, S. Han, and K. Sezaki, "Development of an optimal vehicleto-grid aggregator for frequency regulation", in *IEEE Trans. on Smart Grid*, vol. 1, no. 1,

pp. 65-72, 2010.

[31] A. Keane, L. F. Ochoa, E. Vittal, C. J. Dent, and G. P. Harrison, "Enhanced utilization of voltage control resources with distributed generation", in *IEEE Trans. on Power Systems*, vol. 26, no. 1, pp. 252-260, 2011.

[32] N. Rotering and M. Ilic, "Optimal charge control of plug-in hybrid electric vehicles in deregulated electricity markets", in *IEEE Trans. on Power Systems*, vol. 26, no. 3, pp. 1021-1029, 2011.

[33] L. H. Macedo, J. F. Franco, M. J. Rider, and R. Romero, "Optimal operation of distribution networks considering energy storage devices", in *IEEE Trans. on Smart Grid*, vol. 6, no. 6, pp. 2825-2836, 2015.

[34] M. Yazdanian and A. Mehrizi-Sani, "Distributed control techniques in microgrids", in *IEEE Trans. on Smart Grid*, vol. 5, no. 6, pp. 2901-2909, Nov. 2014.

[35] S. Steffel and A. Dinkel, "Absorbing the rays: Advanced inverters help integrate PV into electric utility distribution systems", in *IEEE Power Energy Magazine*, vol. 11, no. 2, pp. 45-54, 2013.

[36] T. Fawzy, D. Premm, B. Bletterie, and A. Gorsek, "Active contribution of PV inverters to voltage control–from a smart grid vision to fullscale implementation", in *Elektrotechnik und Informationstechnik*, vol. 128, no. 4, pp. 110-115, 2011.

[37] B. B. Johnson, S. V. Dhople, A. O. Hamadeh, and P. T. Krein, "Synchronization of parallel single-phase inverters with virtual oscillator control", in *IEEE Trans. on Power Electronics*, vol. 29, no. 11, pp. 6124-6138, 2014.

[38] P. J. Douglass, R. Garcia-Valle, J. Ostergaard, and O. C. Tudora, "Voltage-sensitive load controllers for voltage regulation and increased load factor in distribution systems", in *IEEE Trans. on Smart Grid*, vol. 5, no. 5, 2014.

[39] D. Papadaskalopoulos, D. Pudjianto, and G. Strbac, "Decentralized coordination of microgrids with flexible demand and energy storage", in *IEEE Trans. on Sustainable Energy*, vol. 5, no. 4, pp. 1406-1414, 2014.

[40] E. Dallr'Anese, S. V. Dhople, B. B. Johnson, and G. B. Giannakis, "Decentralized optimal dispatch of photovoltaic inverters in residential distribution systems", in *IEEE Trans. on Energy Conversion*, vol. 29, no. 4, pp. 957-967, 2014.

[41] F. Delfino, R. Minciardi, F. Pampararo, and M. Robba, "A multilevel approach for the optimal control of distributed energy resources and storage", in *IEEE Trans. on Smart Grid*, vol. 5, no. 4, pp. 2155-2162, 2014.

[42] A. A. Aquino-Lugo, R. Klump, and T. J. Overbye, "A control framework for the smart grid for voltage support using agent-based technologies", in *IEEE Trans. on Smart Grid*, vol. 2, no. 1, pp. 173-180, 2011.

[43] A. Barbato, A. Capone, L. Chen, F. Martignon, and S. Paris, "A distributed demand-side management framework for the smart grid", in *Computer Communications*, vol. 57, pp. 13-24, 2014.

[44] N. Forouzandehmehr, M. Esmalifalak, H. Mohsenian-Rad, and Z. Han, "Autonomous demand response using stochastic differential games", in *IEEE Trans. on Smart Grid*, vol. 6, no. 1, pp. 291-300, 2015.

[45] L. Xiao and S. Boyd, "Optimal scaling of a gradient method for distributed resource allocation", in *Journal of optimization theory and applications*, vol. 129, no. 3, pp. 469-488, 2006.

[46] B. Zhang, A. Y. Lam, A. D. Domınguez-Garcıa, and D. Tse, "An optimal and distributed method for voltage regulation in power distribution systems", in *IEEE Trans. on Power Systems*, vol. 30, no. 4, pp. 1714-1726, 2015.

[47] O. Ardakanian, S. Keshav, and C. Rosenberg, "Real-time distributed control for smart electric vehicle chargers: From a static to a dynamic study", in *IEEE Trans. on Smart Grid*, vol. 5, no. 5, pp. 2295-2305, 2014.

[48] K. Heussen, A. Saleem, and M. Lind, "Control architecture of power systems: Modeling of purpose and function," in *proceedings of the IEEE Power and Energy Society General Meeting*, 2009.

[49] "Electricity networks - handling a shock to the system", The Institution for Engineering and Technology (IET), 2013. [Online]. Available: https://www.theiet.org/factfiles/energy/elec-shock-page.cfm

[50] "Future Energy Scenarios 2017", National Grid, 2017. [Online]. Available: http://fes.nationalgrid.com/media/1253/final-fes-2017-updated-interactive-pdf-44-amended.pdf

[51] E. Loukarakis, I. Margaris, and P. Moutis, "Frequency control support and participation methods provided by wind generation", in *proceedings of the 2009 IEEE Electrical Power & Energy Conference (EPEC)*, 2009, pp. 1-6.

[52] "GC022 - Frequency Response", National Grid Frequency Response Workgroup, 2013.

[53] X. Cao, "A novel zonal adaptive DG antiislanding protection scheme to enhance future system stability using real-time inertia estimates", PhD thesis, University of Strathclyde, 2016.

[54] M. Kayikci and J.V.Milanovic, "Dynamic Contribution of DFIG-Based Wind Plants to System Frequency Disturbances", in *IEEE Trans. on Power Systems*, vol. 24, pp. 859-867, 2009.

[55] "National Transmission Network Development Plan", Australian Energy Market Operator (AEMO), 2016. [Online]. Available: http://aemo.com.au/-/media/Files/Electricity/NEM/Planning_and_Forecasting/NTNDP/2016/Dec/2016-NATIONAL-TRANSMISSION-NETWORK-DEVELOPMENTPLAN.pdf

[56] "Frequency Operating Standards", Australian Energy Market Commission (AEMC), 2017. [Online]. Available: https://www.aemc.gov.au/markets-reviews-advice/review-of-the-frequency-operating-standard

[57] "J. Driesen and K. Visscher, "Virtual synchronous generators", in *proceedings of the 2008 IEEE Power and Energy Society General Meeting-Conversion and Delivery of Electrical Energy in the 21st Century*, pp. 1-3, 2008.

[58] Q.-C. Zhong and G. Weiss, "Synchronverters: Inverters that mimic synchronous generators", in *IEEE Trans. on Industrial Electronics*, vol. 58, no. 4, pp. 1259-1267, 2011.

[59] H. Bevrani, T. Ise, and Y. Miura, "Virtual synchronous generators: a survey and new perspectives", in *International Journal of Electrical Power & Energy Systems*, vol. 54, pp. 244-254, 2014.

[60] M. Torres, L. Lopes, L. Moran, and J. Espinoza, "Self-tuning virtual synchronous machine: a control strategy for energy storage systems to support dynamic frequency control", in *IEEE Trans. on Energy Conversion*, vol. 29, no. 4, pp. 833-840, 2014.

[61] M. Torres and L. A. Lopes, "An optimal virtual inertia controller to support frequency regulation in autonomous diesel power systems with high penetration of renewables", in *proceedings of the International Conference on Renewable Energies and Power Quality (ICREPQ11)*, Las Palmas de Gran Canaria, Spain, 2011.

[62] E. Rakhshani, D. Remon, A. M. Cantarellas, and P. Rodriguez, "Analysis of derivative control based virtual inertia in multi-area high-voltage direct current interconnected power systems", in *IET Generation, Transmission and Distribution*, vol. 10, no. 6, pp. 1458-1469, 2016.

[63] N. Soni, S. Doolla, and M. C. Chandorkar, "Improvement of transient response in microgrids using virtual inertia", in *IEEE Trans. on Power Delivery*, vol. 28, no. 3, pp. 1830-1838, 2013.

[64] J. Alipoor, Y. Miura, and T. Ise, "Stability assessment and optimization methods for microgrid with multiple vsg units", in *IEEE Trans. on Smart Grid*, 2016.

[65] J. Alipoor, Y. Miura, and T. Ise, "Power system stabilization using virtual synchronous generator with alternating moment of inertia", in *IEEE Journal of Emerging and Selected Topics in Power Electronics*, vol. 3, no. 2, pp. 451-458, 2015.

[66] "Fast Frequency Response in the NEM- Working Paper", Australian Energy Market Operator (AEMO), 2017. [Online]. Available: https://www.aemo.com.au/-/media/Files/Electricity/NEM/Security_and_Reliability/Reports/2017/FFR-Working-Paper---Final.pdf

[67] "International Review of Frequency Control Adaptation", DGA Consulting report to AEMO, 2016. [Online]. Available: https://www.aemo.com.au/-/media/Files/Electricity/NEM/Security_and_Reliability/Reports/FPSS---International-Review-of-FrequencyControl.pdf

[68] M. Asmine and C.-E. Langlois, "Field measurements for the assessment of inertial response for wind power plants based on Hydro-Quebec TransEnergie requirements," in *IET Renewable Power Generation*, vol. 10, no. 1, pp. 25-32, 2016.

[69] "LRP I RFP Backgrounder - Connection," Independent Electricity System Operator (IESO), 10 March 2015.

[70] D. Caldas, M. Fischer and S. Engelken, "Inertial Response Provided by Full Converter Wind Turbines", in *proceedings of the Brazil Wind Power Conference & Exhibition*, Rio de Janeiro, Brazil, 3 September 2015.

[71] "Enhanced Frequency Control Capability (EFCC) - Battery Storage Investigation Report", National Grid, June 2015.

[72] "Case Study - PJM Interconnection (PA, US) - Regulation Services", Ecoult Energy Storage Solutions.

[73] "System Operator TASC - TASC 033 Report," Transpower New Zealand Ltd - The National Grid, July 2014.

[74] "ERCOT Concept Paper - Future Ancillary Services in ERCOT", ERCOT, Electric Reliability Council of Texas, 27 September 2013.

[75] "DS3 RoCoF Alternative Solutions Project Phase 1 Summary Report", EirGrid/SONI, 25 June 2015.

[76] D. Wang, D. H. Wilson, and S. Clark, "Defining constant thresholds by angles in a stability constrained corridor with high wind", in *proceedings of the IEEE T&D*, Chicago, April, 2014.

[77] D. Wilson, S. Clark, S. Norris, J. Yu, P. Mohapatra, C. Grant, P. Ashton, P. Wall and V. Terzija, "Advances in wide area monitoring and control to address emerging requirements related to inertia, stability and power transfer in the GB power system", CIGRE, 2016.

[78] P. Wall, N. Shams, V. Terzija, V. Hamidi, C. Grant, D. Wilson, S. Norris, K. Maleka, C. Booth, Q. Hong, and A. Roscoe, "Smart frequency control for the future GB power system", in *proceedings of the IEEE PES Innovative Smart Grid Technology Conference (ISGT) Europe*, 2016.

[79] "Smart Frequency Control Project - The balance of power", National Grid, [Online]. Available: http://www.nationalgridconnecting.com/The˙balance˙of˙power/.

[80] C. Jin, et al., "A coordinating algorithm for dispatching regulation services between slow and fast power regulating resources", in *IEEE Trans. on Smart Grid*, vol. 5, no. 2, pp. 1043-1050, Oct. 2013.

[81] A. Molina-Garcia, F. Bouffard and D. S. Kirschen, "Decentralized demand-side contribution to primary frequency control", in *IEEE Trans. on Power Systems*, vol. 26, 2011.

[82] A. Molina-Garcia, I. Munoz-Benavente, A. D. Hansen and E. Gomez-Lazaro, "Demand-Side Contribution to Primary Frequency Control With Wind Farm

Auxiliary Control", in *IEEE Trans. on Power Systems*, vol. 29, no. 5, pp. 2391-2399, Sept. 2014.

[83] A. Delavari and I. Kamwa, "Sparse and Resilient Hierarchical Direct Load Control for Primary Frequency Response Improvement and Inter-Area Oscillations Damping," in *IEEE Trans. on Power Systems*, vol. PP, no. 99, pp. 1-1.

[84] Q. Shi, H. Cui, F. Li, Y. Liu, W. Ju and Y. Sun, "A hybrid dynamic demand control strategy for power system frequency regulation", in *CSEE Journal of Power and Energy Systems*, vol. 3, no. 2, pp. 176-185, June 2017.

[85] A. Kasis, E. Devane, C. Spanias and I. Lestas, "Primary Frequency Regulation With Load-Side Participation—Part I: Stability and Optimality", in *IEEE Trans. on Power Systems*, vol. 32, no. 5, pp. 3505-3518, Sept. 2017.

[86] E. Devane, A. Kasis, M. Antoniou and I. Lestas, "Primary Frequency Regulation With Load-Side Participation—Part II: Beyond Passivity Approaches", in *IEEE Trans. on Power Systems*, vol. 32, no. 5, pp. 3519-3528, Sept. 2017.

[87] V. Trovato, I. M. Sanz, B. Chaudhuri and G. Strbac, "Advanced Control of Thermostatic Loads for Rapid Frequency Response in Great Britain", in *IEEE Trans. on Power Systems*, vol. 32, no. 3, pp. 2106-2117, May 2017.

[88] Y. Guo et al., "Improving AGC performance of a coal-fueled generators with MW-level BESS", in *proceedings of 2016 IEEE PES Innovative Smart Grid Technology Conference (ISGT)*, Minneapolis, pp. 1-5, 2016.

[89] X. Xie, Y. Guo, B. Wang, Y. Dong, L. Mou and F. Xue, "Improving AGC Performance of Coal-fueled Thermal Generators using Multi-MW Scale BESS: a Practical Application", in *IEEE Trans. Smart Grid*, vol. no.99, 2016.

[90] F. Zhang, Z. Hu, X. Xie, J. Zhang and Y. Song, "Assessment of the effectiveness of energy storage resources in the frequency regulation of a single-area power system", in *IEEE Trans. on Power Systems*, vol. no.99, 2016.

[91] M. Kintner-Meyer, "Regulatory Policy and Markets for Energy Storage in North America", in *Proceedings of the IEEE*, vol. 102, no. 7, 2014.

[92] "Frequency Control by Demand Management (FCDM)", National Grid. [Online]. Available:http://www2.nationalgrid.com/WorkArea/DownloadAsset.aspx?id=41294

[93] J. A. Short, D. G. Infield and L. L. Freris, "Stabilization of grid frequency through dynamic demand control", in *IEEE Trans. on Power Systems*, vol. 22, no. 3, Aug. 2007.

[94] J. Hu, J. Cao, J. M. Guerrero, T. Yong and J. Yu, "Improving Frequency Stability Based on Distributed Control of Multiple Load Aggregators", in *IEEE Trans. on Smart Grid*, vol. no.99, pp.1-15, 2016.

[95] A. Keyhani and A. Chatterjee, "Automatic Generation Control Structure for Smart Power Grids", in *IEEE Trans. on Smart Grid*, Sept. 2012.

[96] M. H. Variani and K. Tomsovic, "Distributed Automatic Generation Control Using Flatness-Based Approach for High Penetration of Wind Generation", in *IEEE Trans. on Power Systems*, vol. 28, no. 3, Aug. 2013

[97] P. Xie, Y. Li, L. Zhu, D. Shi and X. Duan, "Supplementary automatic generation control using controllable energy storage in electric vehicle battery swapping stations", in *IET Generation, Transmission and Distribution*, vol. 10, no. 4, pp. 1107-1116, 2016.

Chapter 3

Enhanced Load Frequency Control Framework for Future Power Systems

3.1 Introduction

Having the research questions defined in Chapter 2, this chapter begins to work towards exploring the objective of improving the speed of response of frequency ancillary services while at the same time observing opportunities to enhance responsibilisation, aimed at supporting decentralised and distributed operation of power system.

This chapter will focus on the secondary frequency control of power system and is organised as follows: The reference power system and the reference imbalance event that will be utilised throughout this thesis are presented in Section 3.2. Section 3.3 presents the conventional secondary frequency control (SFC) modelling and its incorporation within reference power system. This is followed by an evaluation of its performance while exploring the possibility of increasing its response speed and enhancing responsibilisation. A novel SFC is proposed in Section 3.5. The performance of the proposed control is verified by real-time simulations and corroborated by small-signal analysis in Section 3.6. Section 3.7 concludes the chapter.

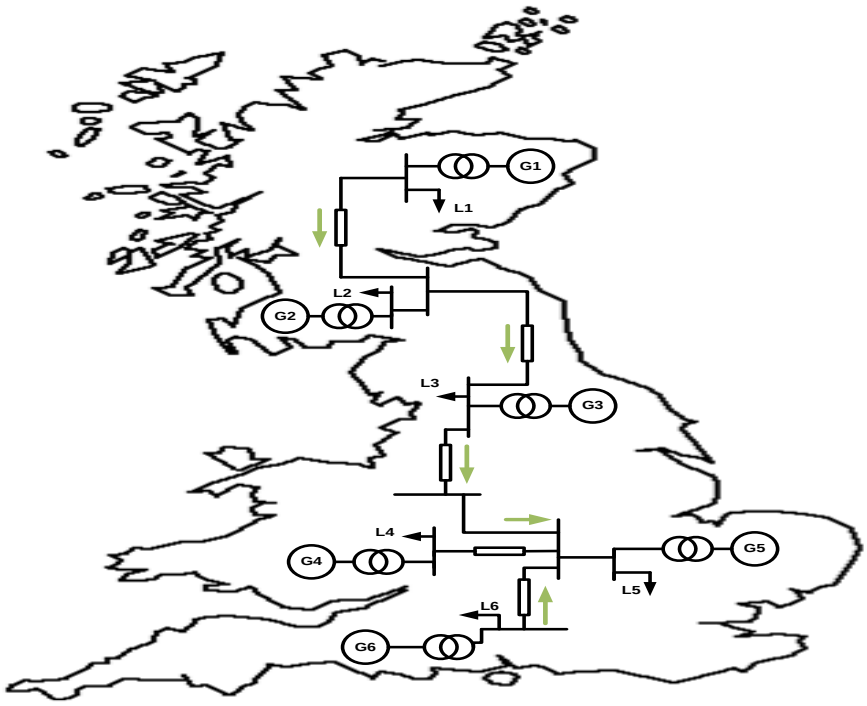

Figure 3.1: Reference power system.

3.2 Reference Power System and Imbalance Event

In this section, first, the power system chosen as the reference for implementation of frequency control frameworks is presented. This includes the validity of the model and its validation. This is followed by defining a reference imbalance event that will serve as the basis for evaluation of frequency control frameworks throughout this work.

3.2.1 Great Britain Power System

For analysing frequency control frameworks, in this work a reduced six-machine dynamic model of the Great Britain (GB) power system as shown in Fig. 3.1 has been chosen as the reference power system. Each bus of the reduced model, comprised of an aggregated load and an aggregated generator, represents one of the six regions identified in the GB National Electricity Transmission System (NETS) boundary map presented in the Electricity Ten Year Statement (ETYS) of National Grid (NG), the Transmission

System Operator (TSO) of GB [1]. The six regions have been identified around major generation sources, power flow corridors and load centres [1].

Model Validity

From the discussion presented in Chapter 2, it is clear that the GB grid is inevitably moving towards a drastic change over the next decade. Considering these changes, the GB grid offers to be a suitable test bed due to the following:

- The future GB network will encompass all the major challenges expected within power networks across the world in the coming decades- to name a few, the uncertainty of secure operation with increasing penetration of intermittent sources of energy, reducing system inertia and increasing profile of demand side participation. Interestingly, some of these challenges have begun to present themselves within the present day GB network.

- As the GB grid has primarily been operated in a centralised manner, with no elements of decentralised operation as inherent within the larger synchronous grid of Continental Europe (although limited), the advantages of more decentralised and distributed operation are expected to be more perceptible and apparent within the GB grid.

Therefore, the implementation of decentralised/distributed frequency control frameworks within the GB grid and assessment of its performance, does not only form a basis for this work but also holds the potential to offer interesting insights to the wider community including the system operators of GB.

Model Validation

The six-machine model has been developed in RSCAD and simulated in real-time using a Real Time Digital Simulator from RTDS Technologies, with each area comprising an aggregated generator and an aggregated load. Each aggregated generator is modelled as a large synchronous machine connected to the transmission system via a step-up

transformer (13.8/400kV). The rating of each generator is set according to the predicted GB 2017 load flow [1]. Each generator is controlled by the widely used IEEE type 1 static excitation system. A gas turbine and speed governor control the speed and input torque of each machine. The synchronous machine, excitation system and gas turbine parameters have been obtained from [2], while the governor speed control parameters are tuned against real recorded events as will be explained in the following paragraph. The transmission lines are modelled using Pi-sections with lumped resistance, capacitance, and inductance parameters calculated from the power flow data provided by the NG ETYS for 2017 [1] as per the methodology presented in [3].
The model has been validated by means of two tests in [4] :

1. Load flow analysis: This test is to evaluate the steady-state performance of the model. The load flow simulation data of the six-machine test system closely matches (average error $< 3.24\%$, maximum error $< 8.69\%$) the predicted data obtained from ETYS, for the winter peak of 2017 [1]. This includes the generation and demand data at each region and the power flow across the boundaries of the regions.

2. Dynamic frequency response evaluation: The dynamic response of the six-machine reference power system model is benchmarked against a number of real historic frequency deviation events data recorded by phasor measurement units (PMU) located at various points of the GB power transmission network. In [4], the event chosen was the trip of the England-France HVDC inter-connector on 11th of January 2016 leading to a power loss of 900MW. In other words, the model represents the real-world GB network on the 11th of January, 2016. The total generation and demand of the model is adjusted to match the values on the day of the event (total demand=59.56GW). The inertia constant, the governor time constant, the droop percentage, and the load reference set-point parameters are tuned to ensure the model frequency response matches the frequency response (pre-disturbance, rate of change of frequency and frequency nadir) obtained from the PMUs.

The model parameters can be found in [4], and in Appendix A of the thesis.

Model Adaptation

The model initial frequency in [4] was adjusted to match that of the real GB power network on the 11th of January 2016. However, as this work analyses frequency control frameworks including primary and secondary control, the load reference of the model was modified such that in steady state the model frequency is 50 Hz.

3.2.2 Reference Imbalance Event- Frequency Disturbance

In this sub-section, the frequency disturbance against which the performance of frequency control frameworks will be assessed is quantified. In addition, justification for the size of the disturbance is presented, considering the power system of 2030+.

Frequency control should cover the single biggest credible net generation loss (N-1 criteria) that ensures restoration of frequency within acceptable limits should the loss occur. The biggest credible generation in the GB grid is 1800MW, up from 1320MW in 2014. As per ENTSO-E guidelines, performance of any frequency control should be assessed for net generation loss of 1000MW or greater [5]. For the present day power system, where large synchronous generation still dominate the generation mix, the assessment of performance of any frequency control against a net generation loss of 1000 MW is credible. The question that arises is whether this magnitude of disturbance remains to be credible for a 2030+ power system. The remainder of this sub-section, presents a discussion on the security of supply of the GB grid with respect to wind energy penetration and HVDC inter-connectors, establishing the credibility of the magnitude of imbalance event.

Security of supply with high penetration of wind energy: With the decommissioning of Longannet power station (capacity 2400MW) in 2016, the commitment of GB to end the era of reliance on fossil fuel based generation units has been reaffirmed, with plans to decommission the last coal fired power plant in 2025. Moving forward, large penetration of smaller sized distributed generation are set to take over the gener-

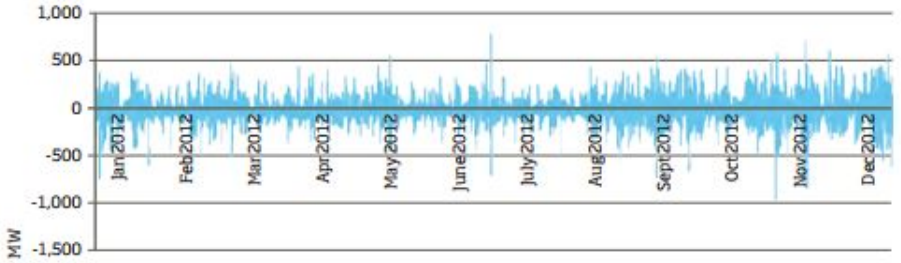

Figure 3.2: Hour-to-hour wind fluctuation for year 2012 [7].

ation capacity of GB. A significant portion of this capacity mix is expected to be wind. In such a scenario, defining the largest credible net generation loss becomes difficult. The power system should be able to cope with periods of low wind but high demand, and periods of high wind but low demand. Up to 2020, the level of wind penetration is not expected to present major difficulties but by 2030, at times, generation mix almost totally of nuclear and renewables can be expected. Therefore, three main events pose a major challenge to security of supply- low wind events, high wind events and rapid fluctuations in wind. It is a standard practice to calculate capacity margin (headroom to ensure demand can be met) based on de-rating factor of generation technology. The de-rating factor of wind is in the order of 0.17-0.24 [6]. With wind penetration of 26GW (as expected in 2020), on occasions of low wind (negligible output from wind), this translates to a shortfall of 4.4GW expected to double to 8.8GW with wind penetration of 50GW suggested for 2030. Furthermore, based on the hour-to-hour wind output data from 2012 (shown in Fig. 3.2) [7], random fluctuations of up to 700MW have been observed. This magnitude can be higher than reported as only transmission connected wind capacity is reported.

Security of supply with HVDC inter-connectors: As per NETS, the GB transmission system currently operates two inter-connectors: (i) England-France inter-connector and (ii) England-Netherlands inter-connector. The England-France inter-connector is jointly owned by National Grid Inter-connectors Limited (NGIC) and Réseau de Transport d Electricité (RTE-French TSO), has a total capability of 2000MW, made up of four circuits of 500 MW each. The England-Netherlands inter-connector is jointly

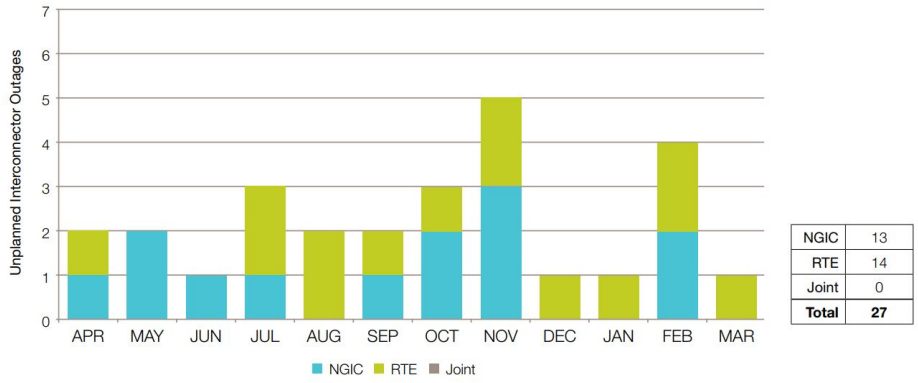

Figure 3.3: Unplanned outages of England-France inter-connector for the reporting year 2016 [8].

owned by National Grid and TenneT (Dutch TSO), has a capability of 1000MW, made of two poles of 500 MW each. There is no redundancy of the major components making up each of the above mentioned circuits and poles, and therefore all outages affect real time capability. The performance of the England-France inter-connectors in terms of the number of unplanned outages for the reporting year 2016 has been presented in Fig. 3.3 [8]. As can be observed from the figure, there were 27 unplanned outages, each of which led to a deviation in frequency. In addition to the two currently active inter-connectors, the following inter-connectors are planned: (i) England-Ireland 500MW, (ii) England-Belgium 1000MW, (iii) England-Norway 1400MW and (iv) England-France.

From the above presented scenarios, it becomes clear that even with decommissioning of large power stations and increased penetration of smaller sized distributed generation, net-generation losses in magnitude of 1000MW remain plausible. Therefore, for this work, a net generation loss of 1000MW has been chosen as the reference imbalance event.

3.2.3 Quick Recap

In this section, first the reference power system that will be utilised throughout this work was introduced. The validity of the model for frequency control frameworks evaluation was discussed. The validation of the model established the credibility of the

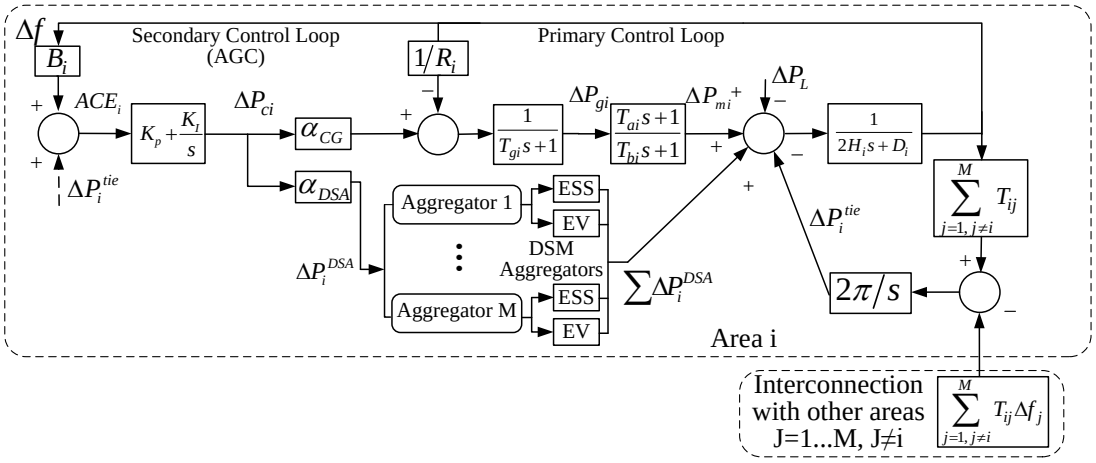

Figure 3.4: Load Frequency Control Framework.

developed model. Furthermore, the magnitude of the imbalance event was quantified and justified.

3.3 Legacy Load Frequency Control Framework

A synchronous power system is divided into a number of LFC areas, each responsible to maintain the frequency of the system by means of maintaining its own scheduled power flows. The frequency is restored to its nominal value by means of changing the set-point of certain conventional generators (CG) chosen to participate in the restoration process [5], [9].

3.3.1 Conventional LFC Framework Modeling

Consider an interconnected power system with M control areas indexed by $i = 1, \cdots, M$. The LFC model of the i^{th} control area is presented in Fig. 3.4. As shown, the LFC comprises a primary control loop and a secondary control loop, where the aim of primary control is to contain the frequency deviation caused by power imbalance in any control area, while the secondary control, i.e. automatic generation control (AGC), is responsible to recover the frequency back to its nominal value [5]. The system dynamics of the i^{th} area can be represented by the following differential equations

$$\Delta \dot{f}_i(t) = -\frac{D}{2H}\Delta f_i(t) + \frac{1}{2H_i}\left(\Delta P_{mi}(t) - \Delta P_{L,i}(t)\right) - \Delta P_{tie,i}(t) + \Delta P_{DSA,i}(t)) \quad (3.1)$$

$$\Delta \dot{P}_{mi}(t) = -\frac{1}{T_{bi}}\Delta P_{mi}(t) + \frac{1}{T_{bi}}\Delta P_{gi(t)} + \frac{T_{ai}}{T_{bi}}\Delta \dot{P}_{gi}(t) \tag{3.2}$$

$$\Delta \dot{P}_{gi}(t) = -\frac{1}{T_{gi}}\Delta P_{gi}(t) + \frac{1}{T_{gi}}\Delta P_{ci}(t) - \frac{1}{R_i T_{gi}}\Delta f_i(t) \tag{3.3}$$

where Δf_i is the change in system frequency, ΔP_{ci} denotes control effort of secondary control, ΔP_{mi} and ΔP_{gi} are the deviations of generator mechanical output and valve position, for area i respectively. H_i, D_i, R_i, T_{gi} T_{ai} and T_{bi} are the inertia constant , load damping coefficient, speed droop, governor and turbine time constants, for area i respectively. $\Delta P_{L,i}$, $\Delta P_{tie,i}$ and $\Delta P_{DSA,i}$ are power variations of loads, tie-line and demand side aggregators (DSA), respectively, which can be viewed as external disturbances to the system. The secondary control input is a signal referred to as the area control error (ACE) defined as

$$ACE_i(t) = \beta_i \Delta f_i(t) + \Delta P_{tie,i}(t) \tag{3.4}$$

where β_i is the frequency bias factor expressed mathematically as

$$\beta_i = \frac{1}{R_i} + D_i \tag{3.5}$$

where, R_i is the representative droop of area i and D_i is the load damping characteristic of area i. The value of β is calculated by most of the area operators based on their experience of areas frequency characteristics, i.e. based on historical behaviour of their system to frequency deviations. Therefore, the ACE represents the cumulative deviation of the area from its scheduled net import or export of power flow over all tie-lines. Upon occurrence of an event that leads to a deviation in frequency and ACE beyond a set threshold, a proportional integral (PI) control is employed to force the ACE to zero and can be represented as

$$\Delta P_{ci}(t) = -K_P ACE_i(t) - \frac{1}{T_I}\int ACE_i(t) \tag{3.6}$$

where K_P and T_I are the proportional gain and integral time constant, respectively. The required regulation power ΔP_{ci} calculated is then distributed among the units of the area chosen to participate in frequency restoration. Broadly classifying the

participating units into two categories- CGs and DSAs, the regulation commands for the units can be represented as

$$\Delta P_{CGs}(t) = \alpha_{CGs} \Delta P_{ci}(t) \tag{3.7}$$

$$\Delta P_{DSAs}(t) = \alpha_{DSAs} \Delta P_{ci}(t) \tag{3.8}$$

where, ΔP_{CGs} is the regulation power command to the CGs, ΔP_{DSAs} is the regulation power command to the DSAs, α_{CGs} and α_{DSAs} are the participation factors of CGs and DSAs respectively. It is a common practice to allocate participation factors on a pro-rata basis in practical implementations of conventional LFC framework. The restoration control only responds to deviations beyond a frequency dead-band, (f_{db}) such that for measured frequency $f = f_{nom} \pm f_{db}$, no frequency control measure is employed. Although the restoration control only responds to deviations beyond f_{db}, once activated it restores the frequency to its nominal value f_{nom}.

3.3.2 Incorporating Conventional LFC Framework within Reference Power System

As has been mentioned earlier in Chapter 2, the GB power network is operated as an independent LFC block. In this sub-section, first the adaptation of the reference power system to incorporate the conventional LFC is presented followed by the details of control implementation.

Reference Power System Adaptation

The incorporation of conventional LFC framework requires the division of the power network into a number of smaller areas. As National Grid has identified six major power flow corridors within the GB grid, the division of the network into areas around the major power flow corridors offers the most plausible implementation. The representation of the GB power system divided into six areas is presented in Fig 3.5

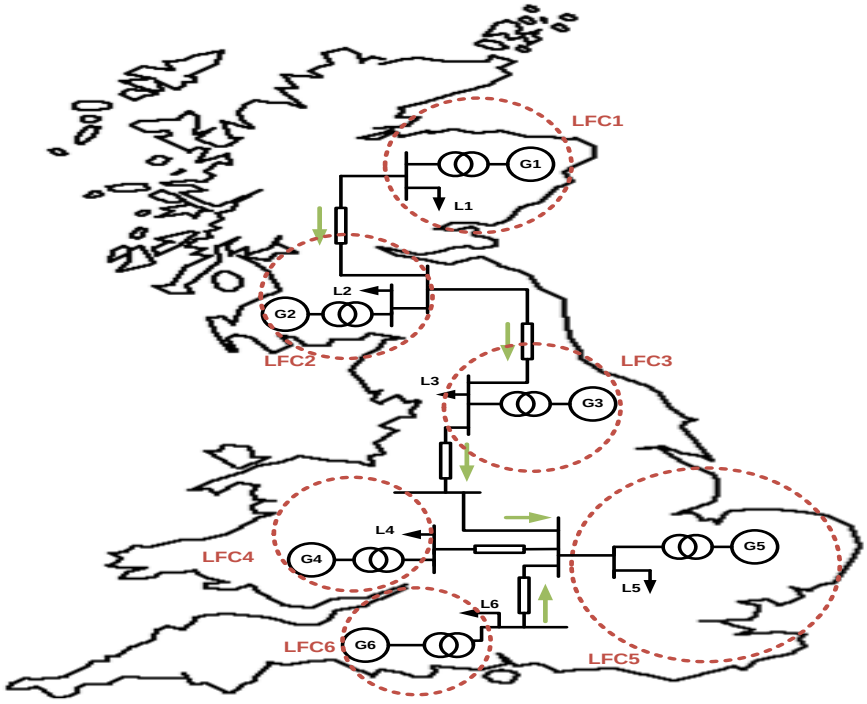

Figure 3.5: Reference power system divided into six LFC areas.

Control Implementation

The control framework is implemented in each of the six areas of the GB power system with nominal frequency of the network as $f_{nom} = 50$Hz. The system inertia is 4.456s and the value of D is chosen as 0.3. The parameters utilised are presented below.

Primary Control Loop: The synchronous generators in each of the areas participate proportionally to their capacity to contain the frequency with a droop setting of 13%.

Secondary Control Loop: The typical values of K_P and T_I are in the range of $0.1 - 1.0$ and $50 - 200$s respectively [5], [9]. The best (fastest) value of $T_I = 50$s has been chosen. The value of K_P has been chosen as 0.1 [9]. f_{db} is selected as 0.1Hz [10]. Both the synchronous generator and aggregated load constitute the secondary reserves with $\alpha_{CG} = 0.25$ and $\alpha_{DSA} = 0.75$. This ratio has been chosen based on the assumption that there will be a large amount of economically feasible flexibility

available within the network in the near future [11]. The accurate determination of this ratio is an important research question to be considered for future, as it can play a role in determining the performance of any control.

Delays: The measurement and communication delays are incorporated within the secondary control loop, i.e., the values of ACE are updated every 2s representing the measurement delay [12] while the outputs of the secondary control loop, ΔP_{ci}, is delayed by 1s representing communications delay [13].

DSA Response Dynamics: The DSAs respond to the control command immediately with no turn on/off delays considered for this work. This is to explore the full potential of fast acting devices as also utilised in [14].

3.3.3 Baseline Simulation Results

In this sub-section, the performance of the conventional LFC framework is presented. It is assumed that sufficient amount of restoration reserves are procured by each of the areas. The results of conventional LFC framework subject to reference imbalance event within area 2 at $t = 10$s are presented in Fig. 3.6. As can be observed in Fig. 3.6a, after the event, the frequency is gradually restored to its nominal value of 50Hz. The ACE for all areas and the amount of regulation reserves contributed by each areas to restore the frequency is presented in Fig. 3.6b and 3.6c. As had been discussed earlier, the ACE helps identification of an external disturbance from an internal one and therefore the regulation power to restore the frequency is predominantly only provided by the LFC area within which the imbalance event had initiated.

3.3.4 Quick Recap

In this section, the conventional LFC framework was detailed followed by its incorporation within the reference power system. The baseline simulation results presented in this section reveal a satisfactory frequency response and confirm an appropriate implementation of the conventional LFC framework. To the best of author's knowledge, this

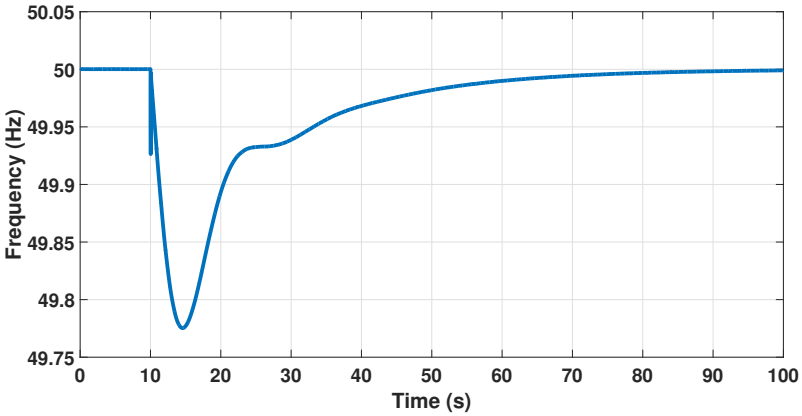

(a) Frequency

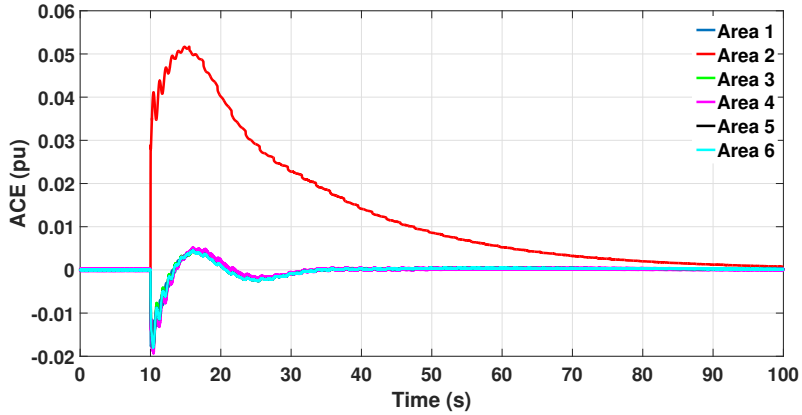

(b) ACE

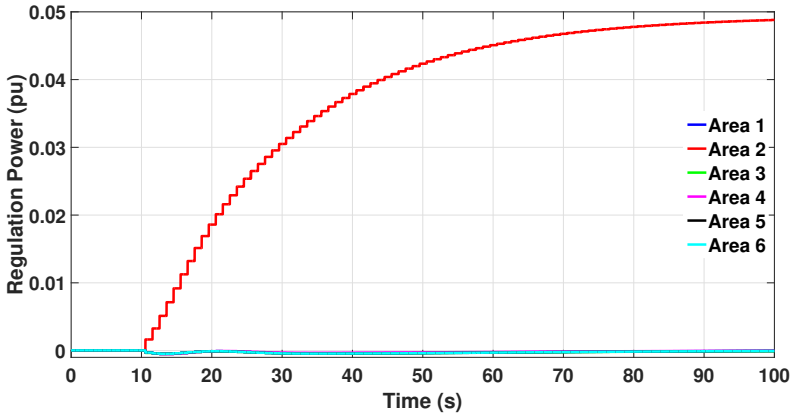

(c) Regulation Power

Figure 3.6: AGC response to reference event.

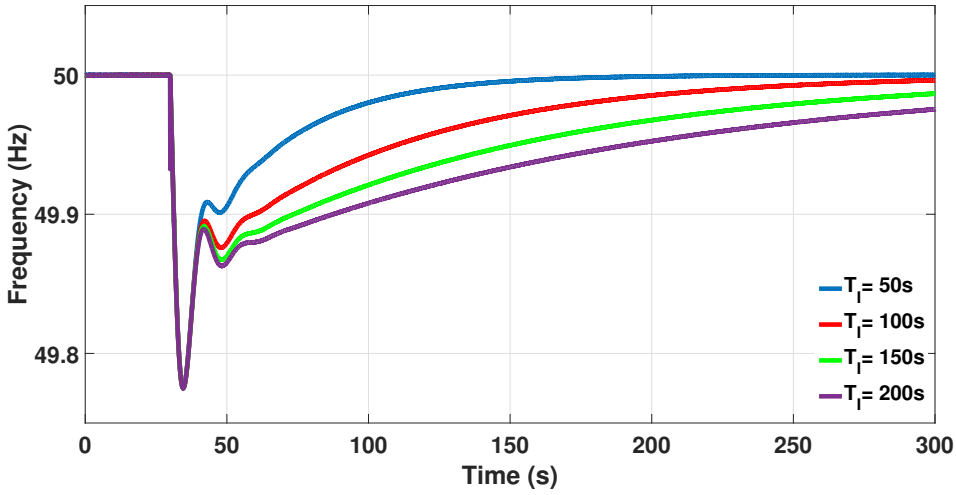

Figure 3.7: System frequency response subject to reference imbalance event in Area 2 for different values of T_I.

is the first implementation where the conventional LFC framework has been incorporated within the GB grid. The incorporation of conventional LFC framework within the GB grid begins to introduce a degree of decentralisation and responsibilisation. Remedial measures are taken closer to the location of the imbalance event, i.e. within the area of the disturbance as opposed to the current practice within GB grid where the response is from across GB.

3.4 Analysis of Conventional LFC Framework

Having incorporated the conventional LFC framework within the reference power system and establishing a baseline response, in this section, the performance of the conventional framework is analysed. The analysis takes into consideration the changes expected within the near future, aimed at identifying issues that might need to be addressed or areas where the performance of the conventional LFC can be further improved.

For the baseline simulation results presented in Section 3.3.3, although 75% of the regulation power is from DSAs (based on the participation factor chosen) that utilize fast acting demand side resources with no turn on/off delays, the effect of their fast

response is not apparent in the frequency response. This is due to the fact that the regulation command to DSAs and the CGs is from a common PI controller. As can be observed from Fig. 3.7, the time it takes for the frequency to be restored to its nominal value is dominated by the value of T_I chosen. It is inversely proportional to T_I, i.e., the smaller the value of T_I, the faster is the frequency restored. A question that arises is: why is the secondary frequency control slow? Why cannot a smaller value of T_I be utilised?

Theoretically, the distinction between primary and secondary frequency control is their control objective, i.e., primary contains frequency deviations and secondary restores the frequency to its nominal value. Practically a time scale of operation is also associated with the two controls, i.e. the primary response is expected within ten seconds of the observed imbalance event while secondary response can vary from thirty seconds to minutes. This is, in general, observed as the secondary control intentionally being designed for much slower operation than primary control. However, this association of time with control objective is due to practical limitations as identified below:

Disturbance location identification: Within the conventional framework, although the entire synchronous area observes the disturbance as a change in frequency, only the area with the disturbance is responsible to restore the frequency. This decentralised operation is achieved by means of ACE, i.e., assuming appropriate calculation of β, the ACE distinguishes an internal disturbance (within the area) from an external one (outside the area), as has been explained earlier. With the ACE, there is no definitive identification of the disturbance, rather only an indication based on whether the ACE is zero or non-zero.

Primary and secondary control interaction: A satisfactory performance of the secondary control is very much dependent upon the primary control. The response of secondary control is driven by ACE, that is a combination of the actual power interchange over the tie-lines and a function of the frequency deviation. Immediately after the disturbance, every area observes a non-zero ACE due to the areas participation in

primary frequency control. This transient non-zero ACE observed by non-disturbance areas slowly converges to zero as the primary frequency response stabilizes. Therefore, to avoid the participation of non disturbance areas in frequency restoration while the transient ACE converges to zero, the secondary frequency control is time delayed. This ensures minimal participation of non disturbance areas in frequency restoration while their ACE is converging to zero. If the speed of response of secondary control is increased, the transient non-zero ACE can enforce secondary participation from non disturbance areas. This can further be exacerbated when β is miscalculated.

Ramp-rate constraint of CGs: Large CGs constitute a majority of the secondary reserves today. The power ramp rate constraint of these participating generators further limits the speed of response of secondary control. The power ramp-rate effectively acts as a delay and increasing the speed of response would cause sympathetic activations, i.e., more activations than are necessary but only for a short duration of time. This can further deteriorate the frequency response of the system.

In a future power system, although a large volume of fast acting demand side resources might be available within the network, their participation within LFC framework will be limited to secondary control as had been identified in Chapter 2. With the decreasing inertia, along with the increasing RoCoF, lower frequency nadirs can be expected. If the limitations of conventional LFC framework can be overcome to increase the speed of response, the potential of fast acting devices can be effectively utilised to contribute to the objectives of both, primary and secondary frequency control.

Considering the limitations identified above, the following can be hypothesised:

- If the identification of the location of the disturbance can be definitive, the speed of response of conventional LFC can be improved, with no risk of non-disturbance area participating in secondary control.

- It is important that the definitive location identification is autonomous, fully decentralised, and fast. It needs to be faster than the convergence of non-disturbance areas transient ACE to zero as in the conventional LFC framework.

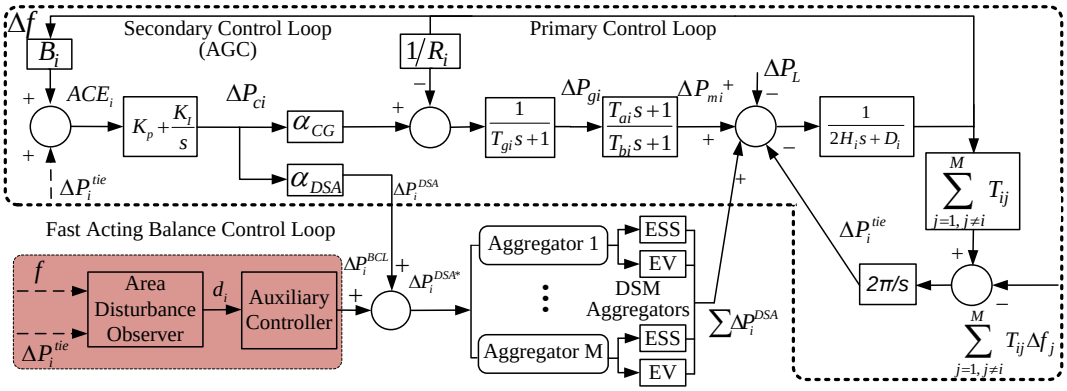

Figure 3.8: LFC framework incorporating proposed SFC.

- There is no effective power ramp-rate restriction on the response of DSAs, therefore, if the control effort of CGs can be decoupled from that of the control effort of DSAs, the overall response speed of conventional LFC can be improved.

3.5 Proposed Enhancements to LFC Framework

To overcome the limitations of the conventional approach, a novel SFC is proposed. The LFC framework incorporating the proposed SFC is illustrated in Fig. 3.8. As can be observed, the proposed SFC consolidates a fast acting balance control loop (BCL), in addition to the secondary control loop. The key features of the proposed control are as follows:

- The BCL comprises an area disturbance observer, capable of fast and autonomous identification of disturbance location in a completely decentralised manner. This ensures activation of reserves unilaterally only within the area that has initiated the disturbance, allowing for faster response speeds.

- The area power imbalance observed over tie-lines is the control input as opposed to the conventionally utilised ACE. The non dependence of control input on frequency eliminates deteriorating interaction with primary control and avoids sympathetic activations.

- The BCL employs only fast acting demand side devices through DSAs as regulation providing reserves, eliminating any restriction on speed of response due to ramp-rate constraints. Therefore, the power regulation command of the DSAs comprises two parts: (i) regulation command from AGC with predefined participation factor α_{DSA} and (ii) regulation command from the BCL.

The fast acting nature of the BCL enables active contribution to objectives of both, primary and secondary control, hence justifying its existence as an independent loop. With the two attributes of the proposed SFC, i.e., the fast acting nature and its use of power imbalance as control input, it will be referred to as the fast balancing enhanced frequency control (EFC-FB) henceforth. The description of the fast acting BCL is presented in the following section.

3.5.1 EFC-FB Modelling

In this section, the operation of the fast acting BCL is explained.

Area Disturbance Observer

The objective of the area disturbance observer (ADO) is to autonomously, quickly and unambiguously distinguish between disturbances originating within the area from those originating elsewhere in the synchronous region.The operating principle of the ADO is presented below.

Any sudden imbalance between generator input mechanical power and load will lead to a deviation in system frequency, the dynamics of which can be represented by the swing equation as [2]:

$$\Delta P = \frac{2H}{f_{nom}} \frac{df}{dt} \tag{3.9}$$

where ΔP is the power imbalance in the system, H is the inertia constant of the system, f_{nom} is the nominal frequency and $\frac{df}{dt}$ is the rate of change of frequency (RoCoF). RoCoF at a specific time instant t_k can be estimated as [15]:

$$\frac{df}{dt} = \frac{f_{t_k} - f_{t_k,T_n}}{T_n} \tag{3.10}$$

where T_n is the length of the measuring window.Within a synchronous area $\mathcal{A}$ and for area under consideration i, the neighborhood can be defined as $\mathcal{NH}_i = \{i, \mathcal{AN}_i\} \subseteq \mathcal{A}$. With $j \in \mathcal{AN}_i$ as adjacent areas coupled over tie-lines with breaker state δ_{ij}, the change in tie-line power flow for area i, subject to the imbalance, can be calculated as

$$\Delta P_i^{tie} = \sum_{j \in \mathcal{AN}_i} \delta_{ij} P_{0,i}^{tie} - \sum_{j \in \mathcal{AN}_i} \delta_{ij} P_{meas,i}^{tie} \tag{3.11}$$

where $P_{0,i}^{tie}$ and $P_{meas,i}^{tie}$ are the scheduled and measured tie-line power flow respectively. As the change in electric power flow is immediate, upon occurrence of an imbalance such that $\Delta P_i^{tie} \geq \Delta P_{Th,i}^{tie}$, measuring the extremum of $\frac{df}{dt}$ as $\frac{df}{dt}^*$, for ΔP_i^{tie}, $\frac{df}{dt}^* \neq 0$, the disturbance is classified as originating within the area if

$$\text{floor}\left(\frac{\frac{df}{dt}^*}{\left|\frac{df}{dt}^*\right| + 1}\right) - \text{floor}\left(\frac{-\frac{df}{dt}^*}{\left|\frac{df}{dt}^*\right| + 1}\right) \neq \text{floor}\left(\frac{\Delta P_i^{tie}}{\left|\Delta P_i^{tie}\right| + 1}\right) - \text{floor}\left(\frac{-\Delta P_i^{tie}}{\left|\Delta P_i^{tie}\right| + 1}\right) \tag{3.12}$$

where floor represents the flooring function, $\Delta P_{Th,i}^{tie}$ is the threshold of change in tie-line power flow set based on largest expected load variation in area i. Upon satisfying equation (3.12), the output of the disturbance observer is $d_i = \Delta P_i^{tie}$, else $d_i = 0$. Therefore, each area of $\mathcal{A}$ can identify disturbances originating within themselves based on local measurements in a decentralised manner within 200ms. Although the identification is fast, there might be a frequency dead-band, (f_{db}) such that for measured frequency $f = f_{nom} \pm f_{db}$, no frequency control measure is employed.

Auxiliary Controller

The output of ADO is an input to the auxiliary controller, and for when equation (3.12) is true, d_i should be controlled to zero. Employing a PI control, the control effort can be represented as

$$\Delta P_i^{BCL}(t) = -K_{P,aux} di(t) - \frac{1}{T_{I,aux}} \int d_i(t) \tag{3.13}$$

where $K_{p,aux}$ and $T_{I,aux}$ are the proportional gain and integral time constant of the auxiliary control. Contrary to the secondary control loop, where smaller values of T_I

are limited by ramp rate constraints of CGs, $T_{I,aux}$ can be chosen for faster response. The use of PI control for BCL is not mandatory and the output of ADO can be an auxiliary hook for direct load frequency control [16]. The effective power regulation command issued to the DSAs can be represented as

$$\Delta P_i^{DSA^*}(t) = \Delta P_i^{DSA}(t) + \Delta P_i^{BCL}(t) \tag{3.14}$$

Low Pass Filtering

To suppress the measurement noise and to smoothen the response of BCL, a low pass filter is utilised for ΔP_i^{tie} and $\frac{df}{dt}$. The filtered signals at time instant t_k can be represented as

$$\Delta P_i^{tie,*}(t_k) = (1-a)\,\Delta P_i^{tie,*}(t_k - 1) + a\Delta P_i^{tie}(t_k) \tag{3.15}$$

$$\frac{df}{dt}^*(t_k) = (1-a)\,\frac{df}{dt}^*(t_k - 1) + a\frac{df}{dt}(t_k) \tag{3.16}$$

where $a = \frac{t_h}{T_f + t_h}$, with t_h as the time step of control implementation and T_f as the filter time constant. It is important to choose filter time constant such that it renders satisfactory quality of input while attributing least delay.

3.5.2 Incorporating EFC-FB within Reference Power System

The incorporation of the proposed EFC-FB does not require any further adaptation of the reference power system. The EFC-FB is incorporated within the LFC framework implemented in each of the six areas of the GB power system similar to the incorporation of the conventional LFC framework. The parameters of primary control loop and secondary control loop are same as utilised for conventional LFC framework. The additional parameters chosen for implementation of the proposed EFC-FB are presented below.

Balance Control Loop: With aggregated loads participating as reserves, the values of $K_{P,aux}$ and $T_{I,aux}$ are selected as 0.1 and 5s respectively. With no ramp-rate constraints, a smaller value of $T_{I,aux}$ has been chosen to demonstrate the effectiveness

of BCL. For the ADO, the values of $\Delta P^{tie}_{Th,i} = 50$MW, $T_n = 0.02$s and $T_f = 0.02$s are selected.

Delays: The measurement and communication delays are incorporated within the balance control loop similar to as incorporated within secondary control loop , i.e., the values of ACE are updated every 2s representing the measurement delay while the outputs of the BCL, ΔP^{BCL}_i are delayed by 1s representing communications delay.

3.5.3 Quick Recap

In this section, a novel SFC referred to as EFC-FB is introduced and its modelling presented. The design of EFC-FB overcomes the limitations set upon the conventional LFC framework, as had been identified in Section 3.4. The incorporation of EFC-FB within the reference power system with necessary parameters is presented.

3.6 Performance Evaluation

In this section, the applicability of the proposed EFC-FB is validated by means of real-time simulations.

Methodology: The performance of LFC framework with EFC-FB is compared to that of conventional LFC framework by means of the following two defined scenarios

1. **Response to Reference Imbalance Event:** The system is subject to two disturbances, loss of generation and loss of load.
2. **Sensitivity Analysis:** A sensitivity analysis by varying the inertia of the system and the size of disturbance is undertaken.

To aid the assessment, two key indicators are defined as:

- **Frequency Restoration Time** (T^{Rest})**:** To asses the T^{rest} of the controllers, an error margin $\epsilon = 0.01$ is defined such that T^{rest} is the time interval between the initiation of disturbance to the point when $|\Delta f| = |f - f_{nom}| < \epsilon$, and can be represented as $T^{rest} = \{T^{rest} \in \mathcal{R} : \forall\ t > T^{rest}, |\Delta f| \leq \epsilon\}$.

- **Relative Frequency Overshoot** (Δf^{ovr})**:** Defining the minimum and maximum frequency after a disturbance as f_{max} and f_{min} respectively, the relative overshoot is calculated as $\Delta f^{ovr} = \left|\frac{f_{max}-f_{nom}}{f_{nom}-f_{min}}\right| \cdot 100\%$.

In addition to the evaluation of EFC-FBs performance, this section further justifies the following design choices:

1. **Importance of ADO:** The importance of ADO is demonstrated by means of small-signal stability analysis, comparing the EFC-FB with and without the ADO. Note that EFC-FB without ADO is equivalent to an additional PI controller within the conventional LFC for decoupling of regulation power of CGs and DSAs.

2. **Choosing ΔP^{tie} over ACE:** The benefit of choosing ΔP^{tie} over conventionally utilised ACE is justified by presenting some further simulation analysis.

3.6.1 Response to Reference Imbalance Event

The system frequency response subject to generation loss at $t = 10$s and a load loss at $t = 110$s for both LFC frameworks is presented in Fig. 3.9. The restoration time for conventional LFC framework is 61.67s with no overshoot. The LFC framework with

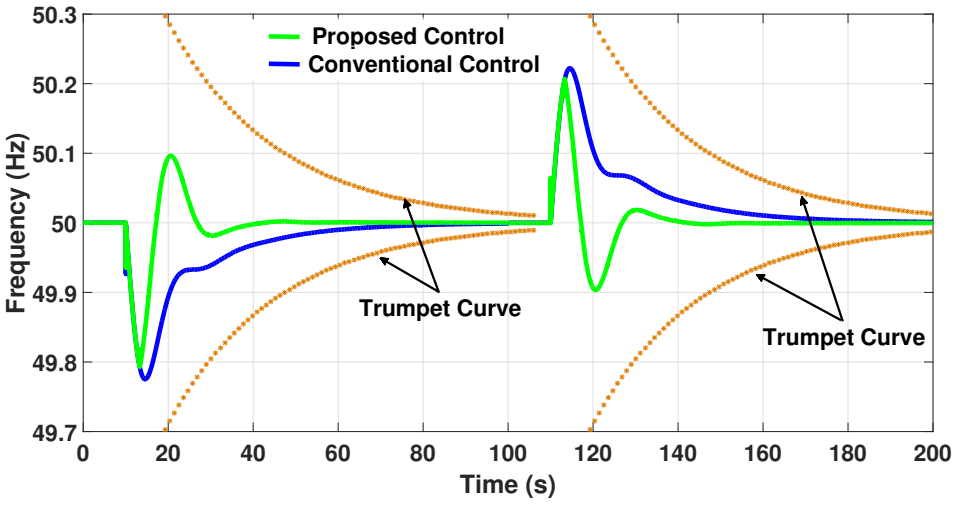

Figure 3.9: Response to disturbance

EFC-FB, by means of fast and accurate detection of disturbance location, contributes to improving frequency nadir (frequency zenith for load loss) and leads to a faster restoration time. With a restoration time of 27.6s, the EFC-FB is twice as fast but presents an overshoot of 42.5%. An acceptable frequency response of a system subject to a disturbance is defined by an exponentially decaying function $H(s) = f_{nom} \pm Ae^{-\frac{1}{T}t}$ referred to as trumpet curve, set as a requirement by ENTSO-E [5]. Considering the response of conventional control as reference, trumpet curve parameters are calculated as $A = 0.31$Hz and $T = 11$s. As can be observed from Fig. 3.9, the response of LFC framework with EFC-FB, with a 42.5% overshoot, is well within the bound set by the trumpet curve.

The overshoot observed is due to the slower dynamics of the governor implementing the PFC response. The proposed control will benefit, in terms of its overshoot response, when faster acting devices overtake the PFC responsibility. In addition, at the same time, alternative ways such as adapting the droops for PFC can be explored to improve the performance of the proposed control.

In addition to the reference power system, the performance of the proposed control subject to a step change in load or generation has been verified in a number pure simulation validation environments within the ELECTRA IRP consortium's work package 7- Integration and Lab Testing for Proof of Concept as reported in [17].

3.6.2 Sensitivity analysis

To further evaluate the performance of the EFC-FB, a sensitivity analysis for variation in size of disturbance and system inertia is undertaken. The size of disturbance (P^{step}) is varied by means of a multiplier μ_{step} such that $P^{step} = \mu_{step} P_0^{step}$, where P_0^{step} is the reference disturbance magnitude. In a similar manner, a multiplier $\mu_{inertia}$, scales the system inertia constant (H) such that $H = \mu_{inertia} H_0$, where $H_0 = 4.68$s. The results of the analysis for conventional LFC framework and LFC framework with EFC-FB are presented in Fig. 3.10. As can be observed, the restoration time for conventional LFC framework increases with increase in disturbance size but the decrease in system inertia does not have a significant impact. On the other hand, the performance of LFC

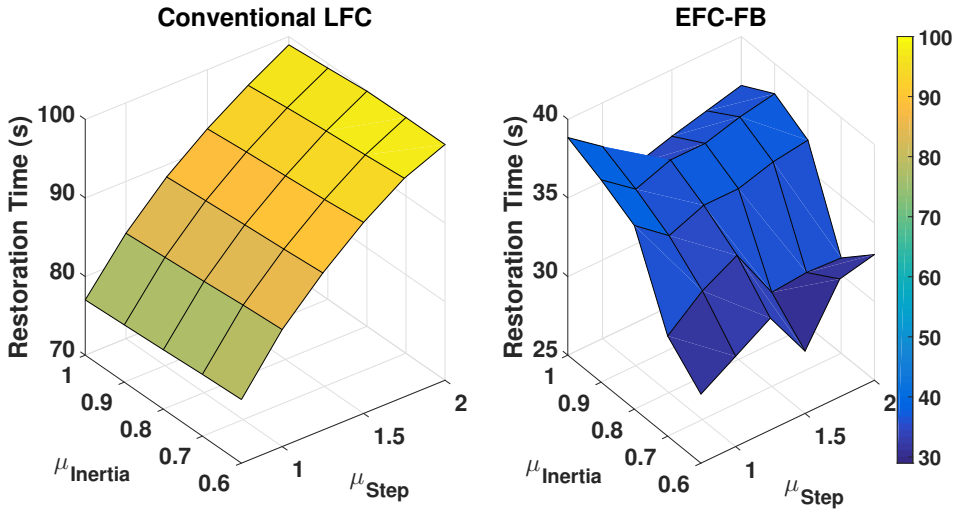

Figure 3.10: Sensitivity analysis

framework with EFC-FB is significantly different, the restoration time of which is not effected by the increase in disturbance size while at the same time, a decrease in system inertia leads to faster restoration times. Therefore, the LFC framework with EFC-FB is more robust to varying disturbance sizes and system characteristics, a necessity for future power systems.

With variations in disturbance size and system inertia, the relative overshoot for the proposed control is always under 45% and within the bounds set by the respective trumpet curve. While the conventional framework exhibits no overshooting characteristic, with decreasing system inertia, the frequency nadir significantly decreases. The LFC framework with EFC-FB improves the frequency nadir for all the cases assessed.

3.6.3 Importance of ADO

In this sub-section, the importance of ADO is demonstrated by means of conducting small-signal stability analysis on the test power system. The two cases for comparison are: (i) the LFC framework with EFC-FB and (ii) the conventional LFC framework incorporating the auxiliary controller only. The state-space model of M-area intercon-

nected power system with BCL (as shown in Fig. 3.8) can be represented as [18]

$$\begin{cases} \dot{x} = Ax + Bu + Fw \\ y = Cx \end{cases} \tag{3.17}$$

where the state vector

$$x = [x_1, x_2, x_3, x_4, x_5]^T \tag{3.18}$$

the control vector

$$u = [u_1, u_2]^T \tag{3.19}$$

the disturbance vector

$$w = [\Delta P_{L_1}, \ldots, \Delta P_{L_M}]^T \tag{3.20}$$

The internal states can be represented as

$$x_1 = [\Delta f_1, \ldots, \Delta f_M] \tag{3.21}$$

$$x_2 = [\Delta P_{m_1}, \ldots, \Delta P_{m_M}] \tag{3.22}$$

$$x_3 = \left[\Delta P_1^{tie}, \ldots, \Delta P_M^{tie}\right] \tag{3.23}$$

$$x_4 = \left[\int ACE_1, \ldots, \int ACE_M\right] \tag{3.24}$$

$$x_5 = \left[\int d_1, \ldots, \int d_M\right] \tag{3.25}$$

The internal inputs can be represented as

$$u_1 = [\Delta P_{c_1}, \ldots, \Delta P_{c_M}] \tag{3.26}$$

$$u_2 = \left[\Delta P_1^{DSA}, \ldots, \Delta P_M^{DSA}\right] \tag{3.27}$$

The coefficient matrices A, B, and C can be found in [18]. The system is linearised around f_{nom} in steady-state. The input to the system is a disturbance in area 2 and

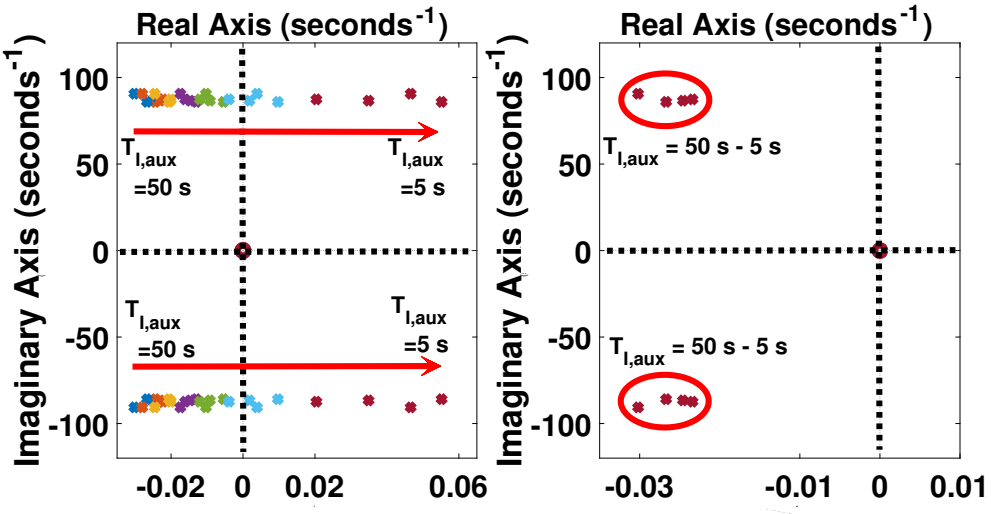

Figure 3.11: Eigenvalue analysis

the output is the system frequency. The Eigenvalues for the two cases are obtained by varying the $T_{I,aux}$ from 50s to 20s in steps of 10s and then to 5s in steps of 5s. In Fig. 3.11, the pole-zero map for the conventional LFC framework (left) and the LFC framework with EFC-FB (right) have been presented. Only the states that are impacted by $T_{I,aux}$ are shown for clearer representation. As can be observed from Fig. 3.11, for conventional LFC framework, as the value of $T_{I,aux}$ is reduced, the poles move towards the imaginary axis. For $T_{I,aux}$ = 10s, the poles cross the imaginary axis representing an unstable system. However, for the LFC framework with EFC-FB, where the ADO ensures unilateral reserve activations only within the area where the disturbance has occurred, the poles are very slightly impacted by the reduction in $T_{I,aux}$, which therefore does not deteriorate the stability of the system.

3.6.4 Choosing ΔP^{tie} over ACE

This sub-section presents a justification for the use of ΔP^{tie} within BCL as opposed to the conventionally used ACE. Consider the frequency responses presented in Fig. 3.12a, with β miscalculation of 5% for both the conventional LFC framework and LFC framework with EFC-FB. As can be observed, a 5% miscalculation of β results in a $\pm$17s variation in T^{set} for the conventional LFC framework while has no significant

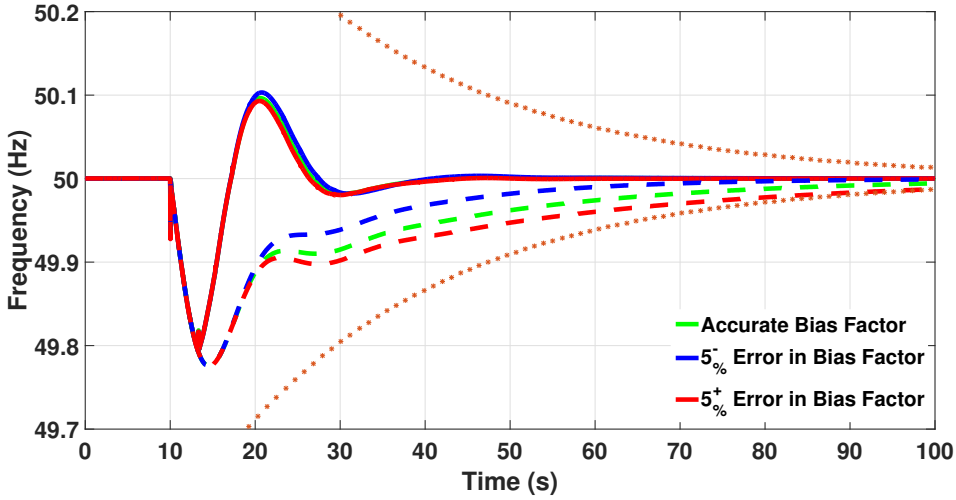

(a) Frequency

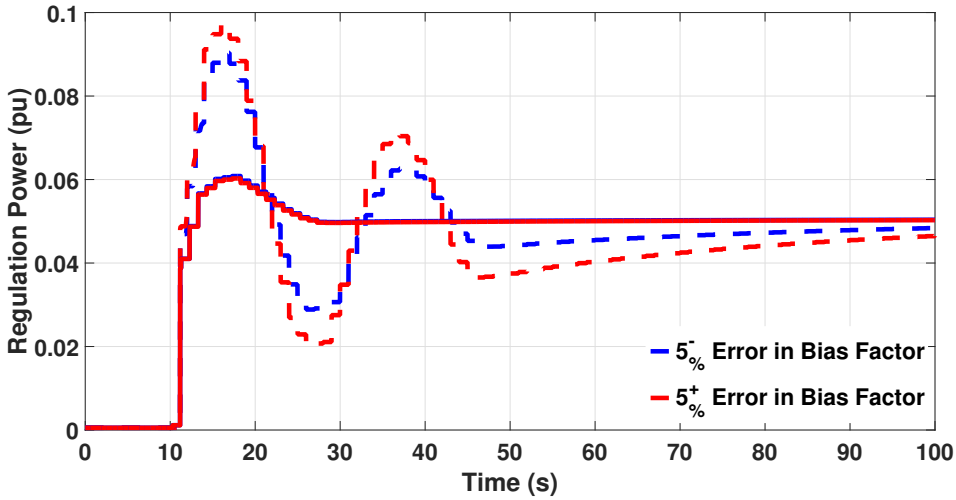

(b) Regulation power

Figure 3.12: AGC; system response to 1 GW generation loss in LFC 2.

impact within the proposed control. β is a combination of the droop set for the area and the damping offered by the load within the area; and it is not uncommon for errors in its calculation. Larger generating units within the network are bound by the grid code to provide a set percentage response to a variation in frequency. However, if the units do not abide by the set droop, this will lead to miscalculation of β. Furthermore, presently it is normal practice to determine β on a yearly basis [10]. In future systems, it is expected that the characteristics of the network (e.g. system inertia) will vary

vastly within a single day. It is also expected that the difference between the peak load and the base load will increase significantly [19], thereby resulting in the load offering a different damping effect at different times. Therefore, the proposed control utilising ΔP^{tie} is more resilient to changes expected within the future power system.

Furthermore, if ACE is utilised within the BCL of the proposed framework, although the activations of reserves are guaranteed to be unilateral within the area where disturbance has been detected, the miscalculation of β leads to nuisance activations as shown in Fig. 3.12b. It should be noted that utilising ΔP^{tie} avoids any nuisance activations.

3.7 Conclusions

In response to the research questions set forth in Chapter 2, this chapter investigates enhanced responsibilisation for secondary frequency control. To this end, the approach, key conclusions and findings are summarised below:

- The modeling of conventional LFC framework was presented, followed by its incorporation within the validated reduced dynamic model of GB reference power system. The baseline simulation results revealed a satisfactory frequency response. The incorporation of conventional LFC framework within the GB grid begins to introduce a degree of decentralisation and responsibilisation. Remedial measures are taken closer to the location of the imbalance event, i.e., within the area of the disturbance as opposed to the current practice within GB grid where the response is from across GB. To the best of authors knowledge, this is the first implementation where the conventional LFC framework has been incorporated within the GB grid.

- An analysis of the conventional LFC framework response revealed that the two objectives set in Chapter 2, i.e., improved responsibilisation and improved response speed, were contradictory to each other. An increase in response speed of conventional LFC would lead to degrading responsibilisation. Furthermore, in regards to the third objective of effective utilisation of fast acting demand side

devices within the network, it was found that although a large proportion of activated secondary reserves were fast acting, the speed of response of such devices did not contribute to frequency restoration speed. Further analysis identified practical limitations that lead to conflicting objectives. These limitations are:

  - Lack of fast and definitive identification of the location of imbalance.
  - A common control effort for both CGs, that may have a ramp-rate constraint and fast acting resources with no ramp-rate constraint.

- To overcome the limitations of the conventional approach, a novel SFC (EFC-FB) is proposed. The control incorporates a fast acting balance control loop (BCL), in addition to the secondary control loop. The key features of the proposed framework are:

  - It incorporates an area disturbance observer capable of fast, autonomous and definitive identification of location of the imbalance.
  - The impact of definitive identification of location of imbalance is two-fold: (i) it ensures unilateral activation of reserves only within the LFC area where the imbalance initiated, allowing faster response speed, and (ii) enables use of area power imbalance observed over tie-lines as control input as opposed to conventionally utilised area control error, avoiding sympathetic activations due to faster response speeds.
  - Decouples the control effort of fast acting resources from that of CGs. The control effort to fast acting resources is a combination of effort from BCL and secondary control loop, while the control effort to CGs is from secondary control loop only.

- The results of real-time simulations and small-signal analysis conducted on the reduced dynamic model of GB presented within this chapter provides a high degree of confidence in the performance of the proposed control. This chapter further presents a justification, informed by simulation and small-signal analysis results, of design choices of the proposed control. It should be noted that al-

though no offline simulations have been undertaken in this work, they serve an important role in large scale representative studies of the power system for both theoretical and practical applications. One such example is the determination of accurate/realistic value of load damping characteristic D under varying load composition. Detailed modelling of a power system is made possible by offline simulation tools that do not have restrictions such as the computational effort in clock time imposed on real-time simulators.

- The work presented in this chapter effectively works towards addressing the research questions and objectives set in Chapter 2. The proposed control enables fast response speeds while at the same time ensuring effective, improved responsibilisation. In addition, the EFC-FB enables effective utilisation of fast acting devices, allowing for their fast response speed to contribute to frequency restoration time.

REFERENCES

[1] "Electricity Ten Year Statement 2016", National Grid, 2016. [Online]. Available: http://www2.nationalgrid.com/UK/Industry-information/Future-of-Energy/Electricity-ten-year-statement

[2] P. Kundur, "Control of Active Power and Reactive Power", in Power System Stability and Control, McGraw-Hill, Inc., ch. 11, sec. 11.1.6, pp. 617-623.

[3] X. Jun and A. Dysko,"UK transmission system modelling and validation for dynamic studies", in *proceedings of 4ˆth IEEE PES Innovative Smart Grid Technologies (ISGT Europe)*, Lyngby, Denmark, pp. 1-5, 2013.

[4] A. Emhemed, et al., "Studies of dynamic interactions in hybrid ac-dc grid under different fault conditions using real time digital simulation", in *proceedings of the 13ˆth IET International conference on AC and DC Power Transmission*, Manchester, pp. 1-5, 2017.

[5] "Policy P1: Load-Frequency Control and Performance", in Continental Europe Operation Handbook, ENTSO-E, 2016. [Online]. Available:https://www.entsoe.eu/publications/system-operations-reports/operation-handbook/Pages/default.aspx

[6] "Electricity Capacity Assessment Report", ofgem, 2013. [Online]. Available:https://www.ofgem.gov.uk/ofgem-publications/75232/electricity-capacity-assessment-report-2013-pdf

[7] "Wind energy implications of large scale deployment", Royal Academy of Engineering, 2014. [Online]. Available:https://www.raeng.org.uk/publications/reports/wind-energy-implications-of-large-scale-deployment

[8] "National Electricity Transmission System Performance Report 2015-2016 – Report to the Gas and Electricity Markets Authority", National Grid, 2016. [Online]. Available:http://www2.nationalgrid.com/WorkArea/DownloadAsset.aspx?id=8589936830

[9] "Appendix 1: Load-Frequency Control and Performance", in Continental Europe Operation Handbook, ENTSO-E, 2016. [Online]. Available: https://www.entsoe.eu/publications/system-operations-reports/operation-handbook/Pages/default.aspx

[10] "Balancing and Frequency Control", NERC, 2011. [Online]. Available: http://www.nerc.com/docs/oc/rs/NERC%20Balancing%20and%20Frequency%20Control%20040520111.pdf

[11] "The Power of Transformation – Wind, Sun and the Economics of Flexible Power Systems", International Energy Agency, 2014. [Online]. Available: https://www.iea.org/publications/freepublications/publication/The_power_of_Transformation.pdf

[12] C. K. Zhang, L. Jiang, Q. H. Wu, Y. He and M. Wu,"Delay-Dependent Robust Load Frequency Control for Time Delay Power Systems", in *IEEE Trans. on Power Systems*, vol. 28, no. 3, pp. 2192-2201, Aug. 2013.

[13] K. S. Ko and D. K. Sung, "The Effect of Cellular Network-based Communication Delays in an EV Aggregator's Domain on Frequency Regulation Service", in *IEEE Trans. on Smart Grid*, vol. PP, no. 99, pp. 1-1.

[14] N. Lu et al, "Design Considerations of a Centralized Load Controller Using Thermostatically Controlled Appliances for Continuous Regulation Reserves", in *IEEE Trans. on Smart Grid*, vol. 4, no. 2, June 2013.

[15] F. Ding, et. al, "Peak-ratio analysis method for enhancement of LOM protection using M class PMUs", in *IEEE Trans. on Smart Grid*, 2016, pp. 291-299.

[16] A. M. Prostejovsky, M. Marinelli, M. Rezkalla, M. H. Syed, and E. Guillo Sansano, "Tuningless Load Frequency Control through Active Engagement of Distributed Resources' in *IEEE Trans. on Power Systems*, September 2017.

[17] "Report on the evaluation and validation of the ELECTRA WoC control concept" ELECTRA IRP consortium, Deliverable D7.1, 2018.

[18] N. V. Ramana, "Two-Area Load Frequency Control", in Power System Operation and Control, Pearson Education India, ch. 6, pp. 115-131.

[19] "System Operability Framework 2016", National Grid, 2016. [Online]. Available: http://www2.nationalgrid.com/UK/Industry-information/Future-of-Energy/System-Operability-Framework

Chapter 4

Novel Decentralised Primary Frequency Control: Introducing Responsibilisation within Primary Frequency Control

4.1 Introduction

Having improved the response speed of secondary frequency control (SFC) by means of introducing enhanced responsibilisation in Chapter 3, this chapter works towards achieving responsibilisation within primary frequency control (PFC).

This chapter is organised as follows: Section 4.2 presents the conventional PFC modelling and its incorporation within reference power system. This is followed by an evaluation of its responsibilisation capability. Section 4.3 discusses the approaches established in literature for PFC responsibilisation. A novel decentralised PFC, where responsibilisation is achieved by means of measuring the transient phase offset (TPO) within each of the load frequency control (LFC) areas is proposed in Section 4.4. The performance of the proposed control is verified by real-time simulations and corroborated by small-signal analysis in Section 4.5. Section 4.6 concludes the chapter.

4.2 Conventional Primary Frequency Control

In this section, the fundamentals of PFC operation are established followed by presenting the adaptation of the reference power system for its incorporation. This allows for the performance of conventional PFC, in terms of its responsibilisation capability, to be evaluated.

4.2.1 Modelling of Conventional Primary Frequency Control

The objective of PFC is to contain the frequency upon occurrence of load-generation imbalance. PFC response is provided in the first few seconds following a frequency change and is maintained until it is replaced by SFC action. PFC operates based on a droop curve (as shown in Fig. 4.1) that defines the relation between the measured frequency and the power output of resources participating in PFC. The fall or rise in frequency is arrested by means of increasing or decreasing the active power output of resources participating in PFC. This change in active power is based on defined droop characteristic represented as

$$P_{out} = P_0 + \frac{1}{R}(f_0 - f_{meas}) \tag{4.1}$$

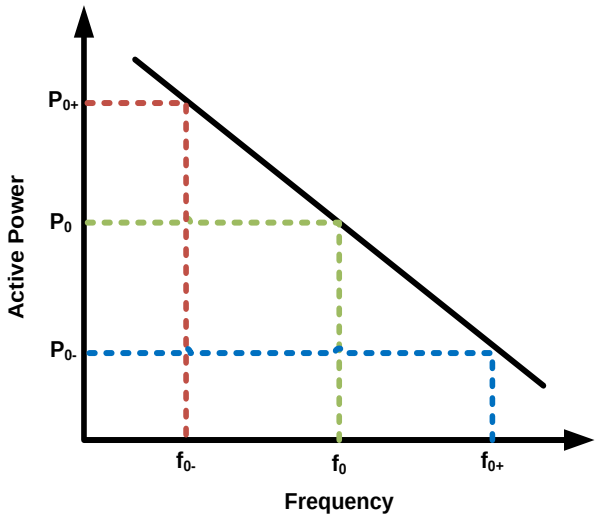

Figure 4.1: Example conventional droop curve.

where P_{out} is the active power output set-point of the participating resource, P_0 is the power set-point at nominal frequency f_0, f_{meas} is the measured frequency and R is the droop gain. In synchronous power systems, PFC is designed such that each Load Frequency Control (LFC) area responds proportionally to its capacity based on the droop slope set by the system operator. As can be observed from Fig. 4.1, when there is a decrease in system frequency from f_0 to f_{0-}, the power output set-point of the LFC areas increases from P_0 to P_{0+}. Similarly when the system frequency increases from f_0 to f_{0+}, the power output set-point of the LFC areas decreases from P_0 to P_{0-}.

4.2.2 Reference Power System Adaptation

The reference power system utilised in this work thus far comprised of six LFC areas as presented in Chapter 3. The reference power system model developed is a detailed model running in real-time at a time-step of 50μs. The model is computationally very expensive requiring 1 $PB5$ processing card and 3 GPC processing cards. Incorporation of any further control or component within the model leads to computational time-step

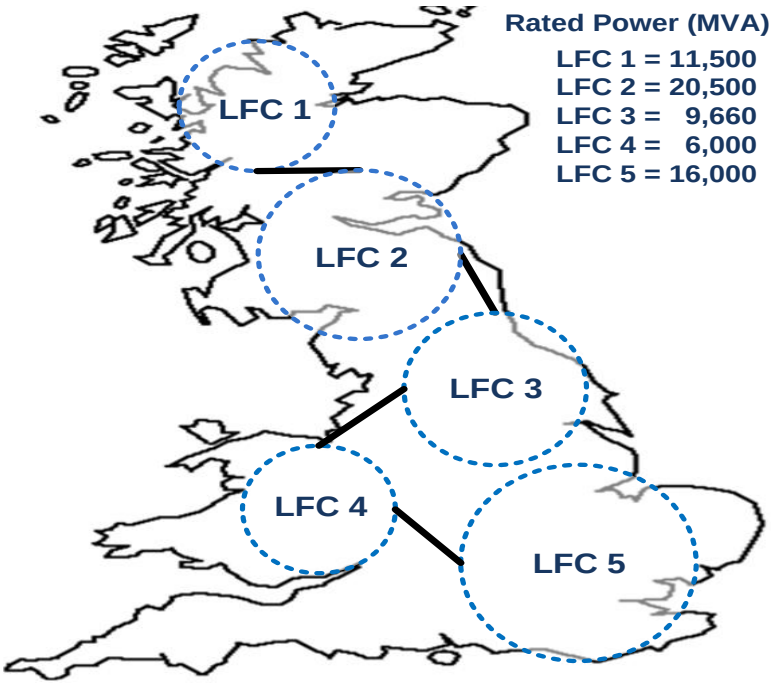

Figure 4.2: Modified reference power system representation.

over flow. As this work requires incorporation of further controls and components (such as breakers), two options available are:

1. To increase the time-step of simulation.

2. To reduce the number of nodes available within the model.

To ensure high fidelity simulation, it was decided not to increase the time-step of simulation but to reduce the number of nodes within the model. This was achieved by means of reducing the number of LFC areas of the model to five, i.e., to combine area 4 and area 6 of the reference power system. It should be noted that the computational effort gained by combining the two areas is higher than computational effort gained by increasing the time-step from 50μs to 60μs. This was an observation and no calculations to determine the computational effort were undertaken. Furthermore, changing the time step to 60μs would present difficulties.

It was further found that the synchronous generators utilised within the model were sized for a minimum droop value of 13% (the tuning of the governor during the dynamic validation of the reference power system yielded a droop value of 13%) . To allow for exploring the performance of the system with lower droop percentages, the ratings of the synchronous generators were increased by 500MW.

The aforementioned adaptations to the model might impact the dynamic response of the model slightly, however, would not impact the integrity of the model as all other critical parameters such as inter-area power flows, system inertia and system loading remain same. The modified reference power system representation with the rated capacity of each LFC is shown in Fig. 4.2.

4.2.3 Analysis of Conventional Primary Frequency Control's Responsibilisation Capability

To analyze the responsibilisation capability of conventional PFC, consider the response of the system to reference magnitude imbalance (net generation loss) within LFC area 2 for two values of droop gain: 5% and 13%, shown in Fig. 4.3. As can be observed from Fig. 4.3a, with no SFC response, the frequency settles at a new steady state value

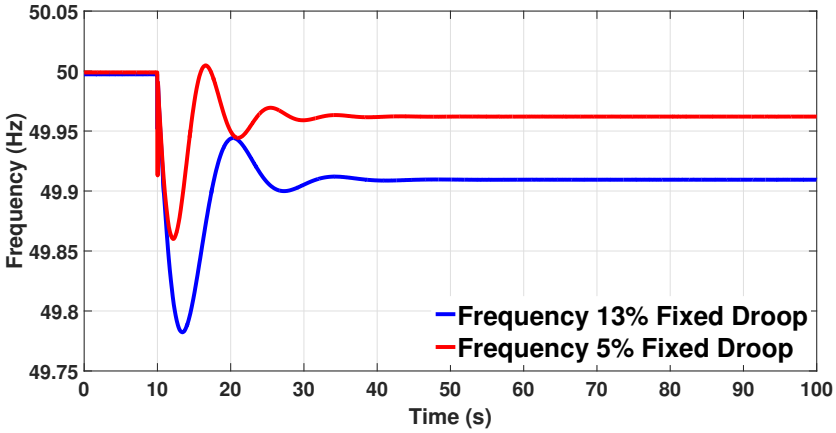

(a) Frequency.

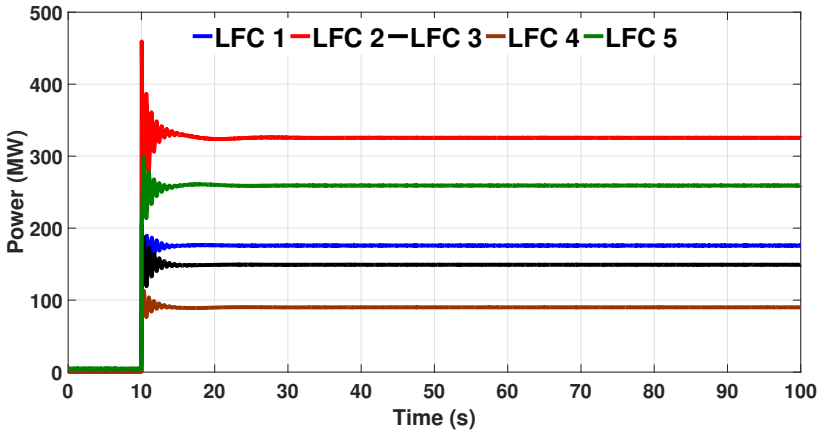

(b) PFC response.

Figure 4.3: System PFC response to 1000MW generation loss.

after the imbalance. In accordance with droop response, the frequency settles at two different values for the two different droop gains utilised. A 5% droop gain corresponds to a higher PFC response and therefore the frequency settles at a higher value than compared to with droop gain of 13%. However, it should be noted that although two different values of droop gains have been utilised, for a disturbance of reference magnitude, the contribution of active power from each of the LFC area remains same and proportional to the capacity of individual LFC area as shown in Fig. 4.3b. For further evaluation, reference magnitude imbalance is emulated in each of the LFC areas individually with a variation in droop gain from 13% to 5%. The droop is varied in

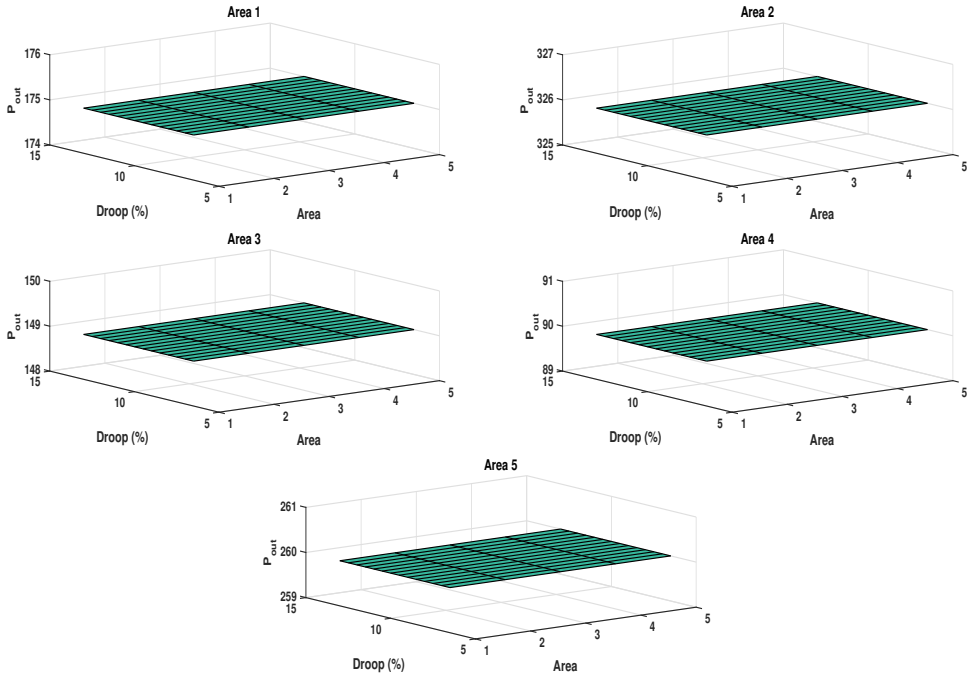

Figure 4.4: Individual LFC areas' contribution to PFC

steps of 1% for all the LFC areas, i.e, if the droop value is 6%, it is 6% for all the LFC areas. The increase in power output of individual LFC area, i.e., the PFC response of each LFC area, is presented in Fig. 4.4. As can be observed, irrespective of the location of the imbalance event or the value of droop gain chosen (as long as it is same for each area), the PFC response of each LFC area remains same, i.e., proportional to the capacity of the LFC area.

From the analysis presented above, it can therefore be inferred that there is no inherent responsibilisation within the conventional PFC as there is in conventional SFC.

4.3 Responsibilising Primary Frequency Control

Introducing responsibilisation within PFC of synchronous power systems refers to enforcing the LFC area with an imbalance event to contribute more PFC response to the

event. PFC's operation at a much faster timescale than SFC, presents a challenge for responsibilisation to be incorporated and there have been no satisfactory decentralised alternatives available. Responsibilisation can be achieved by means of adapting the droop slopes of the LFC areas in real-time, i.e., allocation of a higher active-power response contribution (lower frequency droop percentage) to the area with the imbalance event. The droops can be adapted if the location of the event can be detected within the timescale of PFC. A number of works in literature discuss adaptive droops for microgrids [1], [2], but only [3] introduces the concept for PFC of LFC areas.

In [3], adaptive droops for PFC of LFC areas is introduced (as shown in Fig. 4.5), where the droop slope of the areas is adapted by a fuzzy controller incorporating an event detection technique. The scope of the adaptation is to reduce PFC response when the imbalance event is outwith the area, i.e., somewhere else in the power system, while for the case when the imbalance event is within the area, the droop slope remains unchanged. The fuzzy controller relies on two input functions, namely the deviation in frequency and the deviation in tie-line power flow, for event detection and the droop contributions are adapted by means of a set of defined logic membership functions (as shown in Fig. 4.5b). Although the approach presents successful adaptation of droops for PFC, it does not introduce responsibilisation. This is due to the fact that the PFC response of area with the imbalance event remains unchanged. It should be noted that the approach does not restrict increasing the contribution from the area with the imbalance, but has been identified to be out of scope of the study presented in [3].

The area disturbance observer (ADO) designed and developed for fast balancing enhanced frequency control (EFC-FB) in Chapter 3 can be utilised for the purpose of incorporating responsibilisation within PFC. The ADO is capable of event detection within 100ms of its occurrence, well suitable for PFC timescale. In addition, the ADO approach for event detection is much more robust than the fuzzy controller based approach as the ADO based event detection is definitive while the fuzzy controller based event detection is only indicative. Nonetheless, the ADO and fuzzy controller based event detection can be utilised for introducing responsibilisation within PFC, however, the following potential drawbacks should be noted:

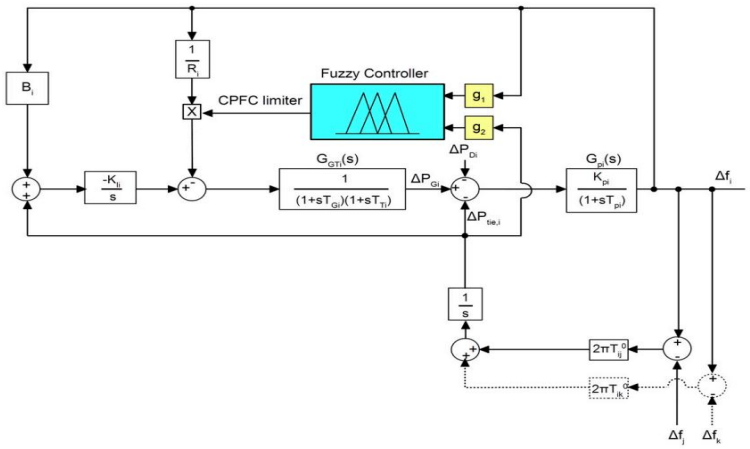

(a) Block diagram of responsibilising PFC implementation.

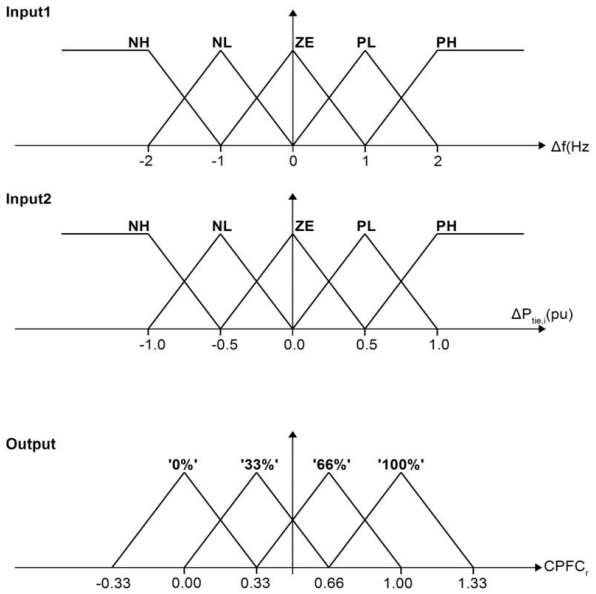

(b) Fuzzy logic membership functions.

Figure 4.5: Responsibilising PFC proposed in [3].

- The event detection in both the aforementioned approaches is centralised within the LFC area. This is acceptable for SFC where the conventional approach is either centralised at a synchronous system level or at the LFC area level. However, conventional PFC is fully decentralised. Proposing a centralised control would be taking a step back from the objective of greater decentralisation and distributed operation of power systems.

- Although the event detection by fuzzy based control is only indicative, its performance for PFC has been shown to be satisfactory in [3]. However, the appraisal of the approach does not incorporate communication delays. It is important to note that once the event has been identified, the new values of droop percentages do need to be communicated to the resources participating in PFC. Therefore, the performance of the approach relies extensively on communication infrastructure.
- The above approaches require more observables than that utilised by present day PFC, and therefore would be subject to higher measurement uncertainty.

4.4 Proposed Novel Decentralised Responsibilising Primary Frequency Control

This work proposes an alternative novel decentralised PFC, referred to as the responsibilising primary enhanced frequency control (EFC-RP), where responsibilisation is achieved by means of measuring the TPO within each of the LFC areas. The proposed approach is fully decentralised as it relies on a single local measurement only and requires no form of communication. In the following sub-sections, the TPO based method of responsibilisation is presented.

4.4.1 Fast Event Location Detection by Transient Phase Offset

Any sudden imbalance between generator mechanical power and load leads to a perceived change in frequency, in high or low inertia systems, due to the changing phase angles across network impedances, as active power flows change. The local Rate of Change of Frequency ($RoCoF$) in response to sudden imbalance can be approximated as [4]:

$$RoCoF = \frac{\Delta P \cdot f}{2 \cdot G \cdot H} \text{ Hz/s} \tag{4.2}$$

where ΔP is the change in active power output, f is the system frequency, G is the nominal generator rating of the area under consideration and H is the inertia constant

of the generator of the area under consideration. The local $RoCoF$ at time instant k can then be measured as [4]:

$$RoCoF = \frac{f_k - f_{(k-T)}}{T} \text{ Hz/s} \tag{4.3}$$

where T represents the measurement window length. Essentially, $RoCoF$ is an estimate of local double derivative of the phase angle ϕ over the window T, obtainable by:

$$f = \frac{d\phi}{dt} \tag{4.4}$$

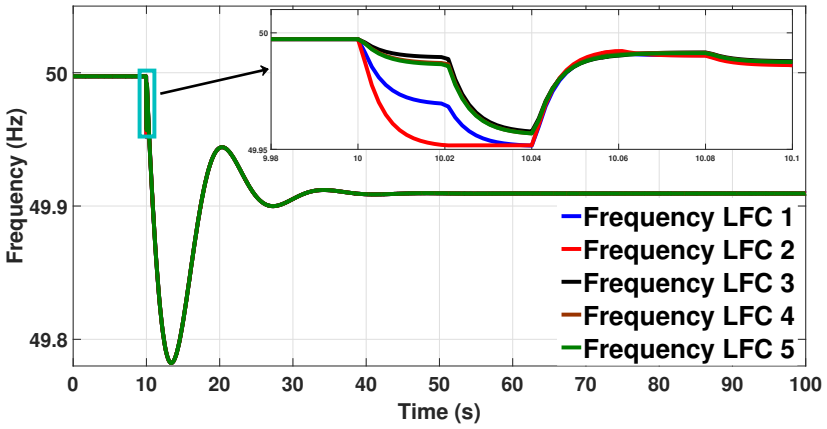

(a) Frequency.

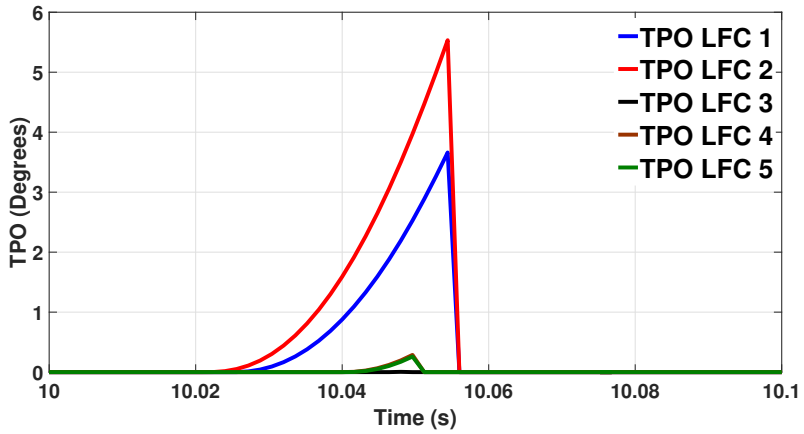

(b) TPO.

Figure 4.6: System Response to 1000 MW Generation Loss.

$$RoCoF = \frac{df}{dt} = \frac{1}{360}\left(\frac{d}{dt}\left(\frac{d\phi}{dt}\right)\right) = \frac{1}{360}\left(\frac{d^2\phi}{dt^2}\right), \phi \text{ in degrees} \tag{4.5}$$

or

$$RoCoF = \frac{df}{dt} = \frac{1}{2\pi}\left(\frac{d}{dt}\left(\frac{d\phi}{dt}\right)\right) = \frac{1}{2\pi}\left(\frac{d^2\phi}{dt^2}\right), \phi \text{ in radians} \tag{4.6}$$

The TPO of a system relative to a stable frequency can be estimated as [5]:

$$\phi_o = 360 \int \left(\int (RoCoF \cdot dt)\right) \cdot dt, \phi \text{ in degrees} \tag{4.7}$$

or

$$\phi_o = 2\pi \int \left(\int (RoCoF \cdot dt)\right) \cdot dt, \phi \text{ in radians} \tag{4.8}$$

Equations (4.7) and (4.8), estimate local deviations of phase, from a linear phase ramp extrapolated from pre-event conditions. The pre-event non-zero values of phase and frequency are removed via the double differentiation, allowing local phase deviation to be reconstructed via double integration.

Upon occurrence of an event, the TPO is larger when measured geographically closer to the event than further away. Therefore, in a synchronous power system that is divided into a number of LFC areas, a local TPO measurement can be utilised to quickly and autonomously detect if an area should contribute more to PFC than other areas. To illustrate this further, consider the response of reference power system, to reference magnitude loss of generation in LFC 2 presented in Fig. 4.6. One frequency measurement is taken in each of the LFC areas, and Fig.4.6b shows that the observed TPO is the largest in LFC 2. In a similar manner, the next largest observed TPO is for LFC 1 that is next closest to the event (Fig. 4.2).

4.4.2 TPO based Responsibilisation

Having the event detection explained, it is important to design a droop curve that would work based on TPO and introduces responsibilisation. The droop curve for the proposed control is presented in Fig. 4.7 and is designed as follows:

1. the lower and higher frequency thresholds beyond which the droop is adaptive

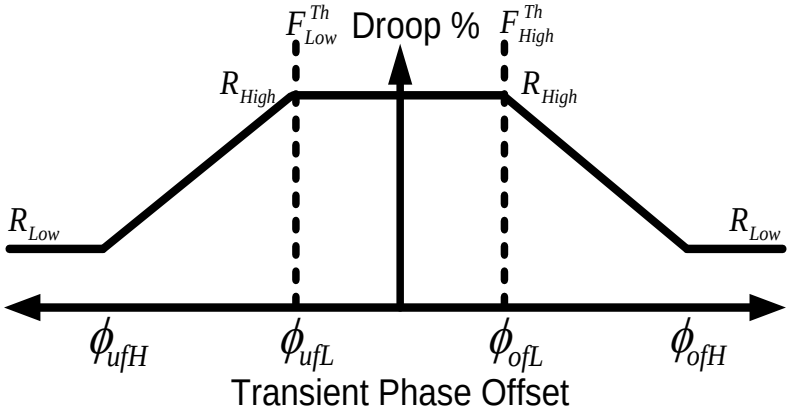

Figure 4.7: Proposed droop curve for primary frequency control.

are defined as F^{Th}_{Low} and F^{Th}_{High} respectively

2. the lower and the higher droop percentages are defined as R_{Low} and R_{High} respectively

3. the smallest and largest event size accommodated within this design are defined as P_{Low} and P_{High} respectively

4. the TPO thresholds (ϕ^{Th}_{Uf} for under frequency events and ϕ^{Th}_{Of} for over frequency events) are then determined as:

$$\phi^{Th}_{Uf} = \begin{cases} \phi_{ufL} = \dfrac{\sum_{i=1}^{n} \phi^i_o}{n} & , \quad P^+_{Low} \\ \phi_{ufH} = \dfrac{\sum_{i=1}^{n} \phi^i_o}{n} & , \quad P^+_{High} \end{cases} \tag{4.9}$$

$$\phi^{Th}_{Of} = \begin{cases} \phi_{ofL} = \dfrac{\sum_{i=1}^{n} \phi^i_o}{n} & , \quad P^-_{Low} \\ \phi_{ofH} = \dfrac{\sum_{i=1}^{n} \phi^i_o}{n} & , \quad P^-_{High} \end{cases} \tag{4.10}$$

where n is the total number of LFC areas, ϕ^i_o is the TPO observed in LFC area i with an event of defined size. P^+ indicates an increase in net load and P^- a decrease. Therefore, the TPO is continuously monitored within all the LFC areas and upon occurrence of an event that causes a deviation in frequency beyond F^{Th}_{Low} or F^{Th}_{High}, the droop value based

on the observed TPO is utilised. This value of droop is latched until the frequency of the system is restored within the error margin (ε) defined. An increase in droop percentage corresponds to a decrease in response. It should be noted that the values of droop are a design choice, and the applicability of the proposed approach remains the same for any value R_{High} and R_{Low} satisfying: $R_{High}, R_{low} \in R_{(>0)}, \forall R_{High} > R_{Low}$.

4.4.3 Incorporating Novel Responsibilising Primary Enhanced Frequency Control within the Reference Power System

The proposed novel EFC-RP is implemented in each of the five areas of the reference power system. One frequency measurement is present within each of the LFC areas. Some of the parameters for the proposed control are chosen while others are obtained as per the design procedure.

Frequency Thresholds: The lower and higher frequency thresholds beyond which the droop is adaptive are chosen as $F_{Low}^{Th} = 49.9$Hz and $F_{High}^{Th} = 50.1$Hz.

Measuring TPO

The implementation of the TPO measurement algorithm is detailed here. The real implementation is digital in discrete time steps. The steps involved in measurement of TPO are shown below:

1. Measure frequency f. Measurement using the zero crossing detection method has been utilised for this work.

2. Calculate $RoCoF$. The window length T over which the $RoCoF$ is calculated plays an important role for the calculation of TPO. Consider the frequency response of the reference power system for reference magnitude generation loss in LFC area 2 in Fig. 4.8a. The $RoCoF$ calculated using three different window lengths ($T = 0.01$s, 0.02s, and 0.04s) in response is presented in Fig. 4.8b. The essential information that can be utilised for determining the location of the event is within a duration of 40ms. It was found that a window length of 20ms was

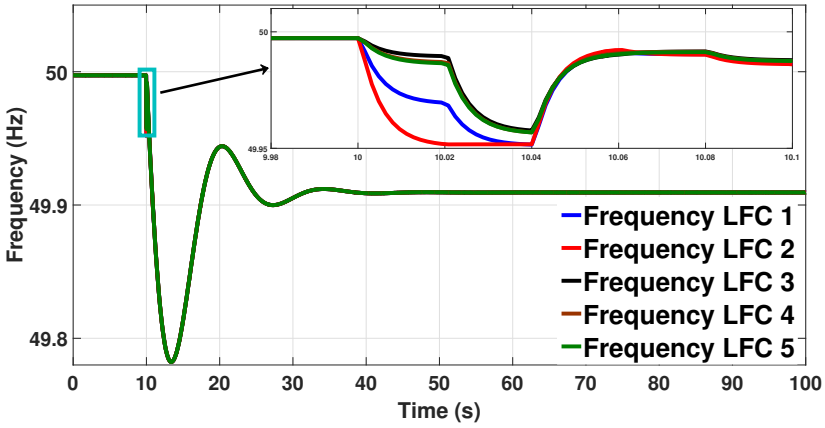

(a) Frequency.

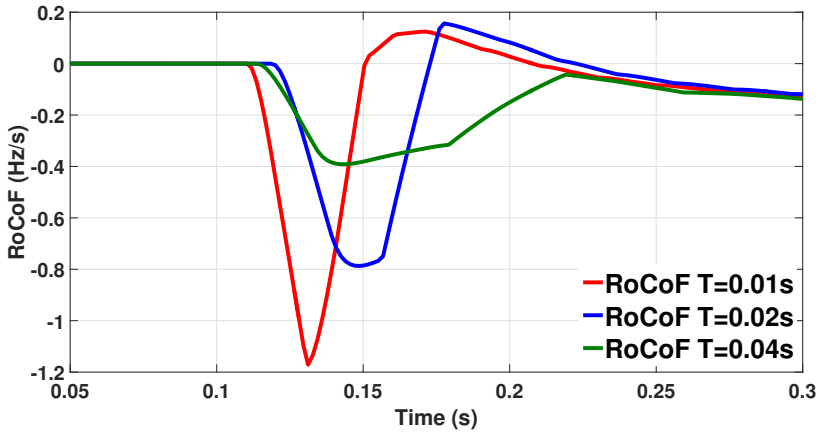

(b) Rate of change of frequency LFC area 2.

Figure 4.8: Calculation of RoCoF over different window lengths.

acceptable. Furthermore, noise and/or spikes on this signal are acceptable as it will be averaged out by two cascaded integration steps.

3. Calculate frequency offset $f_o = \int_{t_t}^{t} RoCoF \cdot dt$ where t_t is the time at which the integration is triggered.

4. Calculate phase offset $\phi_o = 360 \int_{t_t}^{t} f_o \cdot dt$ where t_t is the time at which the integration is triggered, and ϕ_o is the phase offset in degrees.

As can be inferred from the steps above, an algorithm to trigger the start of integration is also required; in the absence of which the integrals above would lead to frequency

and phase accumulation for normal small fluctuations in frequency which occur in all power networks. Therefore, a value of $RoCoF$ threshold $R_{Trigger}$ is utilised, set by the expected $RoCoF$ during normal network operation.

In addition to triggering the main integrations, the algorithm also has the ability to reset the integrators. This is required when sometimes the integrators may be triggered (the main integrators of steps 3 and 4 begin to accumulate frequency and phase offset), but the frequency may not exceed the defined thresholds. In the given algorithm, the integrators are reset when the $RoCoF$ passes through a zero-crossing. Alternative approaches such as observing the frequency offset and phase offset zero crossing can also be employed, however, they have not been explored for this work.

It should be noted that the measurement of frequency incorporates noise and the differentiation of frequency to obtain $RoCoF$ leads to an even noisier measurement as is well recognised within the research community. On the other hand, TPO obtained by the double-integration of $RoCoF$, is much more immune to noise as the double-integration effectively acts as double averaging, canceling out the noise in the process.

TPO Thresholds

The TPO thresholds are obtained by means of the design step 4 presented in Section 4.4.2. Imbalance events, both net generation loss (P^+) and net load loss (P^-), of defined size P_{Low} and P_{High} are emulated within each of the LFC areas individually

Table 4.1: Calculated TPOs and TPO Thresholds

Area	ϕ_o,P^+_{Low}	ϕ_o,P^+_{High}	ϕ_o,P^-_{Low}	ϕ_o,P^-_{High}
Area 1	2.104	8.783	2.213	8.942
Area 2	2.035	9.14	1.981	9.087
Area 3	1.876	9.045	2.064	9.115
Area 4	1.934	8.967	1.804	9.1
Area 5	1.96	8.5	1.95	8.99
ϕ_{ufL}		1.9818		
ϕ_{ufH}		8.887		
ϕ_{ofL}		2.0024		
ϕ_{ofH}		9.0468		

and the TPO is calculated. The TPO of each LFC for P^{+}_{Low}, P^{+}_{High}i and P^{-}_{Low} , P^{-}_{High} are tabulated in Table: 4.1. As per the design procedure, averaging the calculated TPOs of all areas, the TPO thresholds are obtained as ϕ_{ufL}= 2, ϕ_{ufH}= 9, ϕ_{ofL}= 2 and ϕ_{ofH}= 9 (rounded to nearest integer).

Droop Range: In the validation of the reference power system, the droop value was observed as 13% [6]. In general, ENTSO-E recommends a droop value in the range of 2-12% [7]. Assuming that 13% would be the maximum value of droop within the reference power system and the typical value of droop identified as 5% in [8], the droop values were chosen as $R_{Low} = 5\%$ and $R_{High} = 13\%$.

Event Size: The smallest and the largest event size need to be defined for obtaining the TPO thresholds. The smallest event size is chosen as three times the expected load change while the largest event size is according to N-1 contingency planning. For the given study, the values are chosen as $P_{Low} = 500$MW and $P_{High} = 1800$MW. To be consistent with the remainder of the thesis, in this chapter the performance of the proposed control will be evaluated for the reference event, i.e., 1000MW in size.

4.5 Performance Evaluation of Proposed Novel Responsibilising Primary Enhanced Frequency Control

In this section, the applicability of the proposed novel EFC-RP is validated by means of real-time simulations.

Methodology: The performance of the proposed novel EFC-RP is compared to that of conventional PFC by means of the following defined scenario:
Response to Reference Imbalance Event: The system is subject to one disturbance, net loss of generation of reference magnitude.
To aid the assessment, one key indicator is defined as:

- **Percentage Change in Primary Frequency Control Response** (ΔP^{C}_{PFC})**:** ΔP^{C}_{PFC} is defined as the percentage change (increase or decrease) in PFC re-

sponse of individual LFC area subject to an imbalance event compared to that of conventional PFC approach where fixed droops for all LFC areas are utilised and can be calculated as :

$$\Delta P_{PFC}^{C} = \frac{\Delta P_{PFC}^{PPFC} - \Delta P_{PFC}^{CPFC}}{\Delta P_{PFC}^{CPFC}} 100\% \tag{4.11}$$

where ΔP_{PFC}^{PPFC} is the PFC response with proposed PFC and ΔP_{PFC}^{CPFC} is the PFC response with conventional PFC.

In addition to the evaluation of proposed EFC-RP performance, this section further presents a small-signal stability analysis to affirm the applicability of the approach in conjunction with SFC.

4.5.1 Response to Imbalance Event

The system response subject to reference magnitude generation loss at $t = 10$s is presented in Fig. 4.9. The system frequency response is shown in Fig. 4.9a to be stable and between fixed droop response of R_{Low} and R_{High}. The PFC response, i.e., the active power contribution of each LFC, and change in droop of each LFC are presented in Fig. 4.9b and Fig. 4.9c. As can be observed, the change in droop is within 1s of the occurrence of the event. The solid line represents the system response with fixed droop and the dotted line represents system response with the proposed control. LFC area 2 increases its PFC response contribution to the event, demonstrating greater responsibilisation. In a similar manner, LFC area 1 (that is next closest to the imbalance event) increases its PFC response while all the other LFC areas decrease their PFC response. The percentage change in PFC response of all the areas is shown in Fig. 4.10a

To further evaluate the performance of the proposed control and to demonstrate its applicability, the imbalance event is emulated in each of the LFC areas individually. The change in PFC response of each LFC area for the above scenarios are shown in Fig. 4.10b. Within a synchronous area $\mathcal{A}$ and for area under consideration i, defining the neighborhood as $\mathcal{NH}_i = \{i, \mathcal{AN}_i\} \subseteq \mathcal{A}$, with $j \in \mathcal{AN}_i$ as adjacent areas coupled over

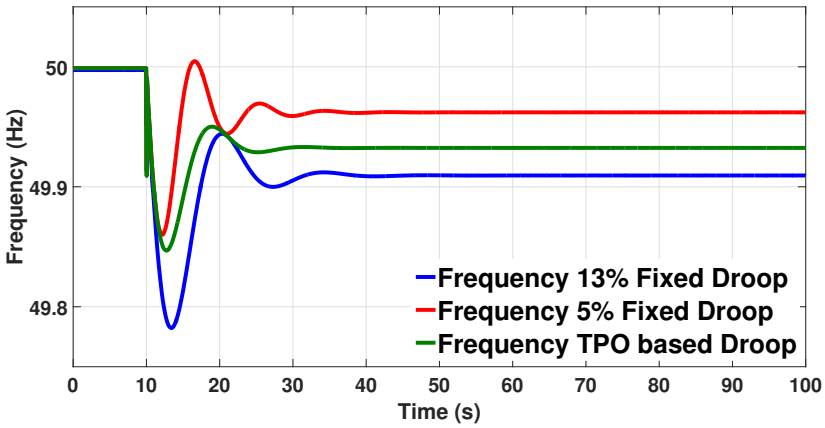

(a) Frequency response.

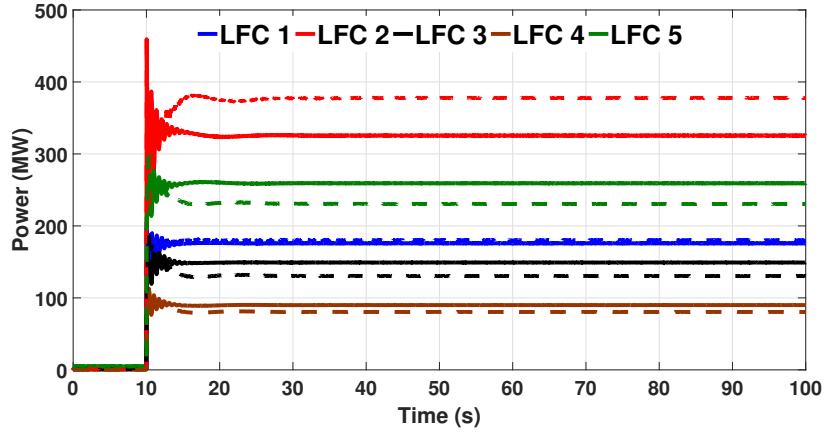

(b) PFC response comparison.

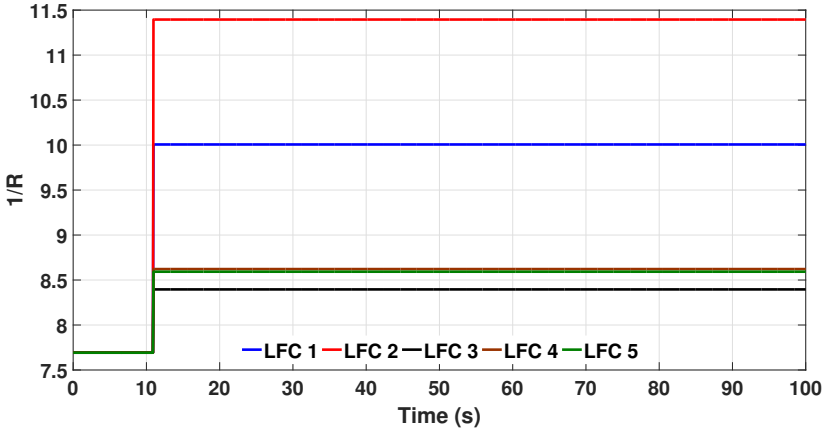

(c) Change in droop.

Figure 4.9: System Response to 1000MW Generation Loss.

tie-lines with breaker state δ_{ij}, it can be observed that for an event in area i, in most cases there is increase in PFC response from $\{i, j\}$ and a decrease from $\{\mathcal{A} - \mathcal{NH}_i\}$.

This study therefore demonstrates the ability of the proposed control to introduce responsibilisation within PFC and serves as a proof of concept.

4.5.2 Small Signal Analysis

It is essential to assess the stability of a system with the proposed EFC-RP operating in conjunction with SFC. In this sub-section, the stability is assessed by means of a

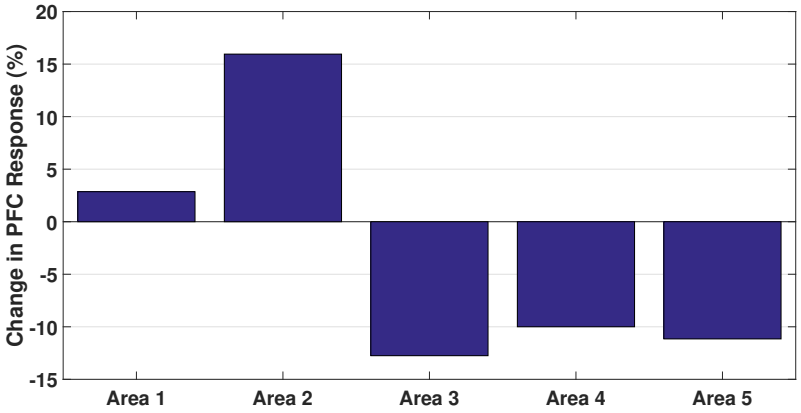

(a) Percentage change in PFC response.

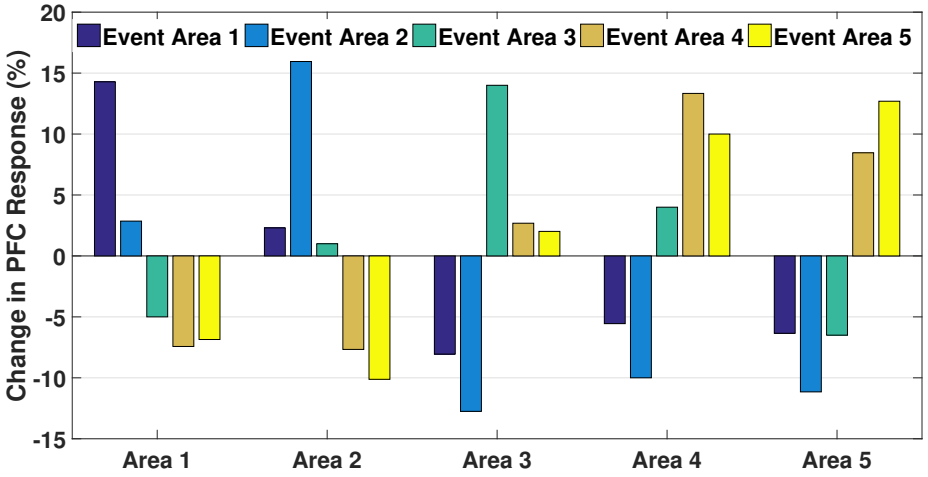

(b) A snapshot of change in PFC response for events in individual LFC areas

Figure 4.10: Analysis of System Response to 1000 MW Generation Loss.

small-signal analysis. Small-signal analysis affirms the soundness and feasibility of the approach. As highlighted by [9], small-signal analysis is a pragmatic approach, results of which are of great practical relevance.

The system frequency response model of an n-area interconnected power system is presented in Fig. 4.11. It should be noted that the model is similar to the model utilised for small-signal analysis in the previous chapter, but not the same. For the purpose of simplicity, only the conventional SFC is considered. The state-space model of n-area system can be represented as [10]:

$$\begin{cases} \dot{x} = Ax + Bu + Fw \\ y = Cx \end{cases} \tag{4.12}$$

where the state vector

$$x = [x_1, x_2, x_3, x_4]^T \tag{4.13}$$

the control vector

$$u = [\delta P^r_{CGs1}, \ldots, \delta P^r_{CGsn}]^T \tag{4.14}$$

the disturbance vector

$$w = [\Delta P_{D1}, \ldots, \Delta P_{Dn}]^T \tag{4.15}$$

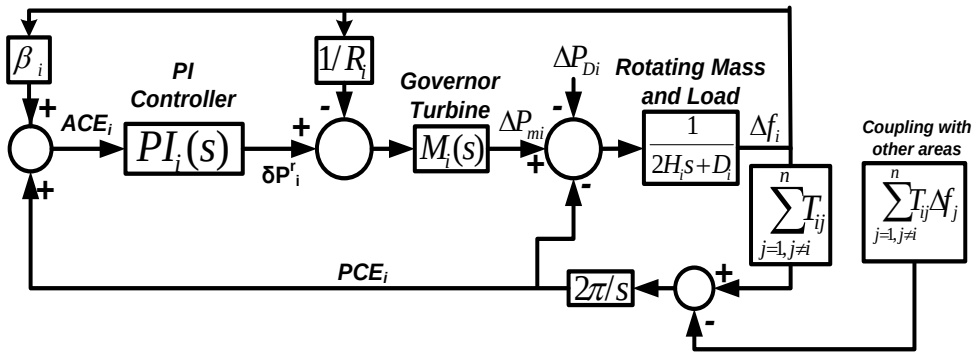

Figure 4.11: n-area interconnected power system frequency response model.

The internal states can be represented as

$$x_1 = [\Delta f_1, \ldots, \Delta f_n] \tag{4.16}$$

$$x_2 = [\Delta P_{m1}, \ldots, \Delta P_{mn}] \tag{4.17}$$

$$x_3 = [PCE_1, \ldots, PCE_n] \tag{4.18}$$

$$x_4 = \left[\int ACE_1, \ldots, \int ACE_n\right] \tag{4.19}$$

ACE_i is the area control error, PCE_i is the power control error, δP_i^r is the regulation power output from the PI controller, ΔP_{mi} is the governor power output, and ΔP_{Di} is the power disturbance within LFC area i. The coefficient matrices A, B, and C can be found in [10]. Based on the model presented above, small-signal analysis has been conducted on the five area power system with the reference imbalance event in LFC area 2 as input disturbance and system frequency as output. The system is linearised around f_0 in steady-state. The control parameters remain same as in the previous study.

For the given disturbance, the droop value of LFC area 2, where the imbalance event takes place, is decreased in steps of 0.5% from R_{High} to R_{Low}, representable as

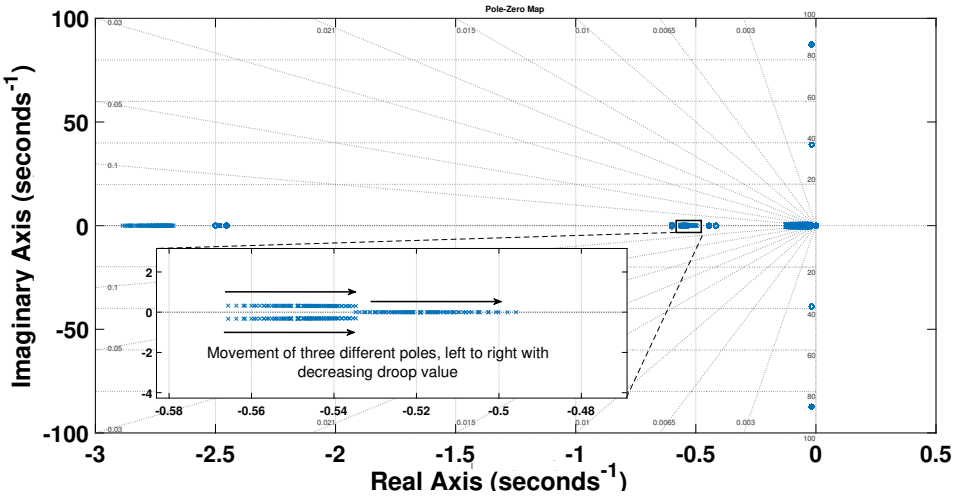

Figure 4.12: Pole zero map.

$R_{LFC}^{event} = \{R_{High} : -0.5 : R_{Low}\}$. For each aforementioned step reduction, the non-event LFC areas droop values are changed by parametric sweep in steps of 0.5% from R_{High} to R_{Low}, representable as $R_{LFC}^{non-event} = \{R_{High} : -0.5 : R_{Low}\} \forall R \in R_{LFC}^{event}$. For all of the above defined cases, it can be observed that the non-zero eigenvalues lie on the left half plane (as shown in Fig. 4.12). This demonstrates stable operation of the system with proposed EFC-RP operating in conjunction with SFC for the chosen design parameters.

4.6 Conclusions

This chapter has worked towards introducing responsibilisation within PFC. The key conclusions are summarised below:

- A novel decentralised responsibilising PFC, referred to as the responsibilising primary enhanced frequency control, has been proposed. The control achieves responsibilisation by means of fast and autonomous event detection and droop adaptation of LFC areas in real-time.

- The fast and autonomous event detection is achieved by means of calculating the TPO locally at every resource participating in PFC. Simulation results have shown that an event can effectively be identified within 100ms of its occurrence.

- Although $RoCoF$ can also be utilised for achieving responsibilisation, the TPO algorithm is robust for real-time implementation and more immune to noise and interference effects than $RoCoF$. TPO is calculated by double integration of $RoCoF$, effectively equivalent to two stages of averaging, and therefore offering good rejection of noise on a frequency/$RoCoF$ measurement.

- The droops of LFC areas are adapted based on the droop curve proposed. Simulation results show that the droop curve enables effective responsibilisation, where the PFC response of areas closer to the imbalance event is increased.

- The linear droop curve proposed in this work serves as a proof of concept. More

sophisticated droop curves can be designed to achieve more effective responsibilisation. This has not been explored within this work.

- It should be noted that the window length utilised for the measurement of TPO could also play a role in adaptation of droops, in addition to the droop curve. This has not been explored in this work but will be considered for expansion of the work.

- The applicability and soundness of the proposed approach to be operated in conjunction with SFC has been demonstrated by means of small-signal analysis.

- In contrast to the only approach in literature for achieving responsibilisation within PFC of synchronous areas, the proposed approach is fully decentralised as it relies on local measurement only and requires no form of communication.

REFERENCES

[1] Y. Han, H. Li, P. Shen, E. A. A. Coelho, and J. M. Guerrero "Review of Active and Reactive Power Sharing Strategies in Hierarchical Controlled Microgrids", in *IEEE Trans. on Power Electronics*, 2017, pp. 2427-2451.

[2] S. M. Malik, X. Ai, Y. Sun, C. Zhenqgi and Z. Shupeng, "Voltage and frequency control strategies of hybrid AC/DC microgrid: a review", in *IET Generation, Transmission and Distribution*, 2017, pp. 303-313.

[3] E. Rikos, et al., "Adaptive Fuzzy Control for Power-Frequency Characteristic Regulation in High-RES Power Systems", Energies, 2017, pp. 1-14.

[4] F. Ding, C. D. Booth, and A. J. Roscoe, "Peak-ratio analysis method for enhancement of LOM protection using M class PMUs", in *IEEE Trans. on Smart Grid*, 2016, pp. 291-299.

[5] A. J. Roscoe, "Measurement, control and protection of microgrids at low frame rates supporting security of supply", Ch. 6. PhD thesis, University of Strathclyde, 2009, pp. 262-329.

[6] A. Emhemed, G. Adam, Q. Hong, and G. M. Burt, "Studies of dynamic interactions in hybrid ac-dc grid under different fault conditions using real time digital simulation", in *proceedings of the 13ˆth IET International conference on AC and DC Power Transmission*, Manchester, pp. 1-5, 2017.

[7] "Policy P1: Load-Frequency Control and Performance", in Continental Europe Operation Handbook, ENTSO-E, 2016. [Online]. Available:https://www.entsoe.eu/publications/system-operations-reports/operation-handbook/Pages/default.aspx

[8] "International Review of Frequency Control Adaptation", Australian Energy Market Operator (AEMO). [Online]. Available: https://www.aemo.com.au/-/media/Files/Electricity/NEM/Security_and_Reliability/Reports/FPSS---International-Review-of-Frequency-Control.pdf

[9] P. Kundur, J. Paserba, V. Ajjarapu, G. Andersson, A. Bose, C. Canizares, N. Hatziargyriou, D. Hill, A. Stankovic, C. Taylor, T. Van Cutsem, V. Vittal, "Definition and classification of power system stability IEEE/CIGRE joint task force on stability terms and definitions", in *IEEE Trans. on Power Systems*, vol. 19, no. 3, pp. 1387-1401, Aug. 2004.

[10] N. V. Ramana, "Two-Area Load Frequency Control", in Power System Operation and Control, Pearson Education India, ch. 6, pp. 115-131.

Chapter 5

Design to Validation: Using SGAM as a Tool to Facilitate Laboratory Validation of Control Solutions

5.1 Introduction

The evolution of power systems into a more complex cyber-physical system has been facilitated by the integration of advanced automation and communication technologies [1]. The benefits of intelligent smart grid control solutions developed within this realm have already been brought forward by means of a number of research and demonstration projects [2]. It is now more probable that such control solutions will make their way to the market either as a product, solution or a service. Validation plays a pivotal role in the roll-out, wide scale deployment and acceptance of any such control solution and this aspect has been identified as a major European infrastructure priority [3, 4].

In a validation chain proposed for smart grid control solutions [5], the necessity for laboratory validation before field implementation has been brought out. Laboratory validation is not uncommon within the power systems domain and is sometimes also

undertaken across multiple laboratories [6], referred to as round robin testing, where the objective is to compare the results of tests undertaken at independent laboratories using same test method, same equipment under test, but different auxiliary test equipment. Round robin tests confirm the applicability of developed control solutions under diverse implementation environments.

The increasing complexity of smart grids presents a challenge for a system level validation that is necessary to ensure secure supply of electricity. Laboratory validation approaches so far have been device/component oriented [7], focusing on type/conformance testing, and therefore are not appropriate for systems level validation of smart grid control solutions. Furthermore, the integration of control solutions within laboratories presents new challenges such as ensuring consistency in understanding, implementation, multi-domain user collaboration and the comparability of results after.

Exploring the aforementioned challenges, this chapter works towards development of a methodology to facilitate the system level validation of the enhanced frequency control (EFC) framework, i.e. the combination of two proposed controls, the fast balancing EFC (EFC-FB) proposed in Chapter 3 and the responsibilising primary EFC (EFC-RP) proposed in Chapter 4.

5.2 Validation of Control Solutions

In this section, the established validation approaches for control solutions are presented followed by a validation chain.

5.2.1 Classification of Validation Approaches

In this sub-section, the validation approaches for power system controls reported in literature are summarised. This section aims to establish the terminology while the details can be found in [8].

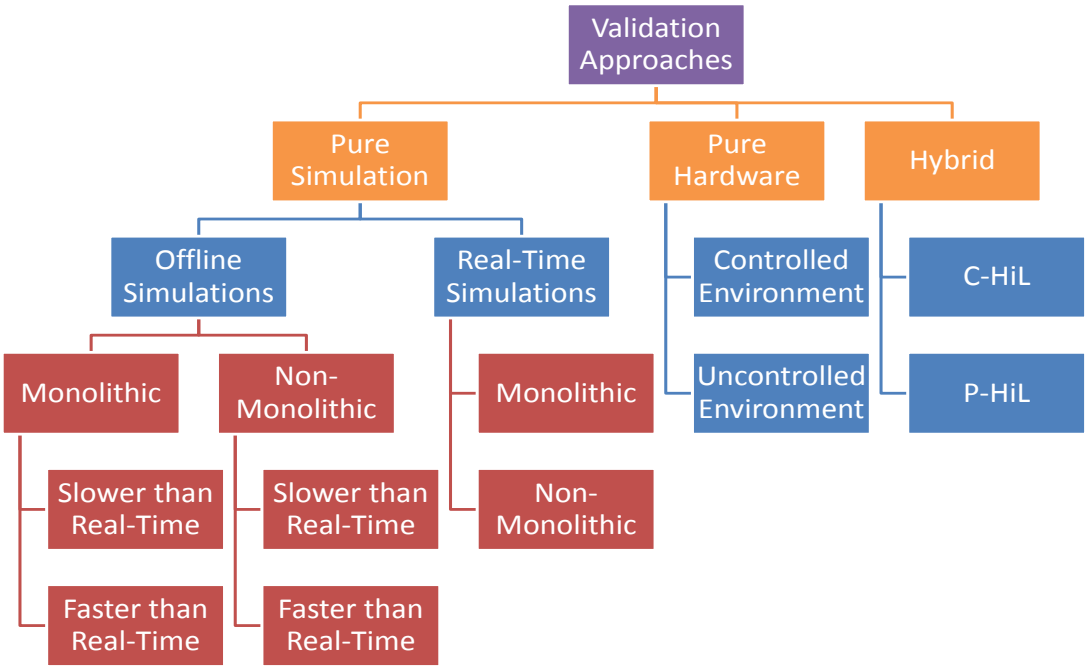

Figure 5.1: Classification of validation approaches.

Pure Simulation Approaches

Pure simulation based approaches can be broadly classified into two: (i) off-line simulations and (ii) real-time simulations. To define and distinguish between the two, first let us define execution time (τ_{ex}) as the time taken by a processor to integrate given set of equations for the defined time step (τ_s). The two types of pure simulations can now be defined as:

Off-line Simulations: Simulations where $\tau_{ex} \neq \tau_s$ are referred to as off-line simulations.

Real-Time Simulations: Simulations where $\tau_{ex} = \tau_s$ is guaranteed, are referred to as real-time simulations.

Off-line simulations with $\tau_{ex} > \tau_s$ are referred to as slower than real-time and $\tau_{ex} < \tau_s$ as faster than real-time. Typically the execution time is always greater than the step time for off-line simulations. With increase in size and complexity of the system under simulation, the execution time increases significantly.

Pure simulation approaches (both off-line and real-time) can further be classified into two:

Monolithic: Simulation setup where only one simulation tool is employed.

Non-monolithic: Simulation setup where more than one simulation tool is employed. Non-monolithic pure simulations can be observed as co-simulation and are also referred to as software-in-the-loop in literature [9], [10].

Off-line simulations can be considered as the cheapest, easiest, and safest option available for validation while real-time simulations, with their ability to recreate power system dynamics at the natural time-scale of their occurrence, are being increasingly employed to obtain results closer to the real-world.

Pure Hardware Approaches

Validation approach where only actual power system components are utilised is referred to as pure hardware validation. They can be broadly classified into two depending upon the environment within which they are undertaken as:

Controlled Environment: Validation undertaken in a controlled environment such as a laboratory falls under this category. It offers more flexibility in terms of validation under extreme conditions and is less expensive compared to its alternative.

Uncontrolled Environment: Validation undertaken in the field falls under this category, often referred to as field trials. Field trials are expensive and limited to steady-state validation.

Both the above approaches are undertaken in real-world conditions, offering a higher degree of confidence. Typically, pure hardware validations are in real-time and often comprise more than one equipment constituting a real-time non-monolithic setup by nature.

Hybrid Approaches

Validation approaches that combine simulations and hardware in some form are referred to as hybrid approaches. They are commonly referred to as Hardware-in-the-Loop (HiL) simulations, involving a part of the simulated system to be present physically, i.e., as

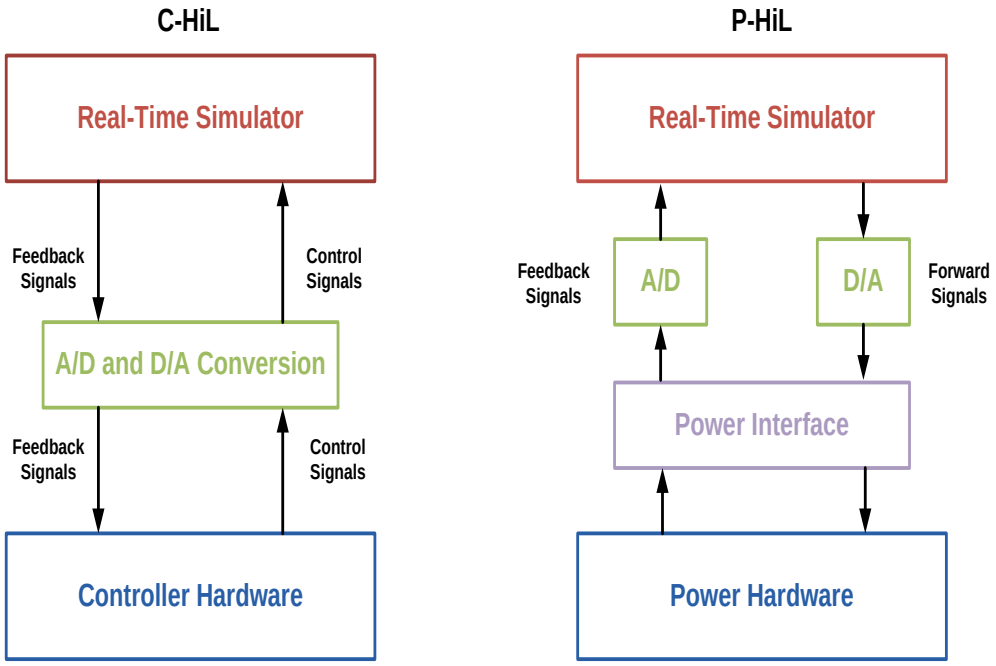

Figure 5.2: Representation of C-Hil and P-Hil setup.

hardware. The hardware in such a setup is referred to as the hardware under test (HuT), and is connected to the simulation platform through input/output interfaces, such as filters, analog-to-digital (A/D) and digital-to-analog (D/A) converters, amplifiers, signal conditioners, etc. The interaction between hardware and software brings it more closer to the actual real world system. HiL simulations can be broadly categorised in two:

Controller Hardware-in-the-Loop (C-HiL): C-HiL involves the separation of control and its implementation within a hardware controller board coupled to a real-time simulation of the power system.

Power Hardware-in-the-Loop (P-HiL): P-HiL involves the coupling of an actual power hardware to a real-time simulation of the power system.

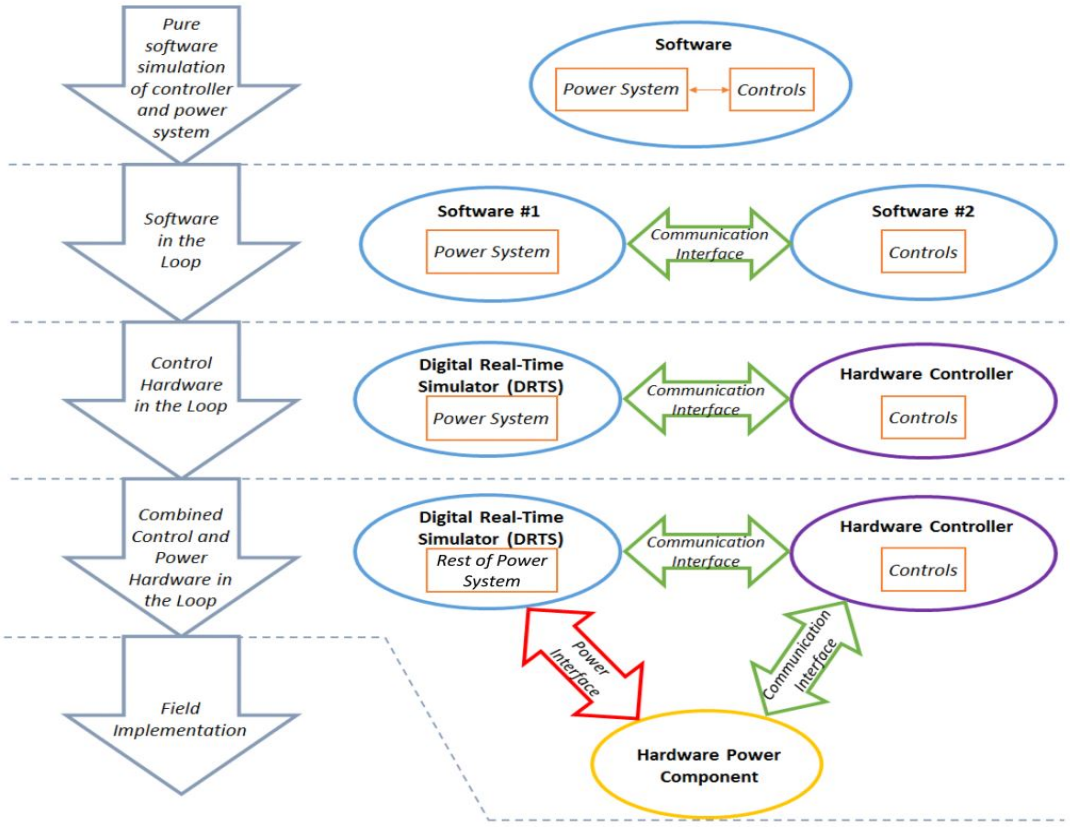

Figure 5.3: Validation chain proposed in [5].

The difference essentially lies in the levels (magnitude) of interface signals exchanged between the hardware and real-time simulation as shown in Fig. 5.2. C-HiL involves exchange of control signals (usually in the order of $\pm$10V) while P-HiL involves exchange of real power across the interface thus requiring an amplifier as the interface (in addition to the A/D, D/A cards).

5.2.2 Validation Chain

Having the terminologies of validation approaches established, this sub-section presents the validation chain for power system controls as proposed in [5], shown in Fig. 5.3. As can be observed from the figure, the validation chain comprises of five phases.

Phase I: First stage to validation is a pure software simulation approach wherein the power network and control are developed within one simulation platform. A plethora of

commercially available simulation tools can be utilised, some designed for steady state analysis (for example PSSE [11-13]) and some more specifically for transient analysis (for example PSCAD [14-16]).

Phase II: To adequately capture the interface between power and control systems, a natural progression is the use of two dedicated software simulation tools, one for power system and one for control system in closed loop configuration. In other words, phase II is a co-simulation or SiL approach [17-19].

Phase III: The next phase involves testing of the control in a C-HiL setup [20-22]. The advantages offered by C-HiL include: (i) the ability to reveal hidden issues of the control solution (often in terms of its implementation and real-time run capability) and (ii) allows for control solutions performance to be evaluated under realistic conditions.

Phase IV: The penultimate phase of the validation chain is the combination of C-HiL and P-HiL techniques in one simulation/experimental setup [23-25]. Such a setup enables validation of controls under a wide range of scenarios, which can be difficult, risky, expensive, and even impossible to perform in real life systems.

Phase V: The final phase of validation is by means of its implementation within the field.

The validation chain presented above is intended to be carried out serially for rigorous validation of a control solution developed for power systems. It should however be noted that phase I/II is/are often the only validation undertaken by researchers. This can be associated to the lack of availability of equipment required for the consequent phases of validation chain. It is also important to note that each phase of the validation chain offers significant advances in terms of the readiness of the proposed control solution. To illustrate this better, consider the relation drawn between each phase of the validation chain and technology readiness level (TRL) [26] in Fig. 5.4.

Phase I and II effectively establish the feasibility and soundness of the developed

control, providing a proof of concept, enhancing the control to TRL 3. Following a successful proof of concept, the implementation of the developed control on a hardware controller board in phase III, capable of running in real-time, offers validation with increased fidelity. This can be related to the control achieving TRL 4. The combined C-HiL and P-HiL experimental setup of phase IV offers validation with highest fidelity, capturing interactions between integrated control and power components, not as a single or separate entity, but as part of the whole system. This therefore enables a system level validation as required to achieve TRL 5. Field trials can be viewed as demonstration of the developed control and hence mapped to TRL 6.

The EFC-FB framework developed within this work has been through the phase I/II of the validation chain, where the feasibility and soundness of the approach has been demonstrated. As laboratory facilities are available at University of Strathclyde and accessible to the author, this thesis will work towards appraising the EFC-FB to TRL 5.

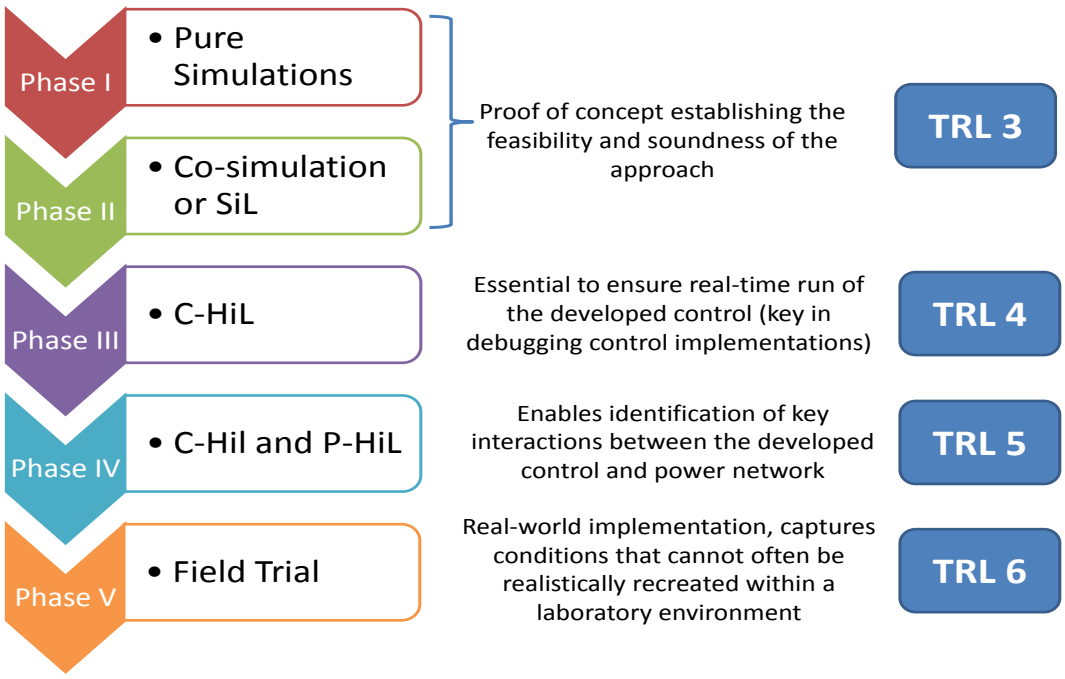

Figure 5.4: Validation chain to technology readiness level comparison.

5.3 Challenges with Laboratory Validation of Control Solutions

Challenges faced by laboratory users can be classified into two: (i) technical challenges and (ii) practical challenges. Technical challenges are often associated with capabilities of a laboratory. A good example is the stability and accuracy of a P-HiL setup, where ensuring a stable and accurate P-HiL setup for experimental validation is challenging and offers excellent research opportunities that are continuously addressed and reported by the research community. On the other hand, the practical challenges associated with laboratory validations have not been given much importance to date, although they are often time consuming and well recognised as an issue within the laboratory user community.

With increasing significance of laboratory validations, practical challenges are now being acknowledged as an important research direction. This section works towards establishing a set of practical challenges, derived by a discussion between dynamic power systems laboratory (DPSL) users, in consultation with users of three laboratories across Europe, and further developed through thought experiments. In addition, this section aims to deduce the root causes of these challenges.
The practical challenges with laboratory validations can be classified into two categories:

1. Single laboratory validation challenges
2. Multiple laboratory validation challenges

The following two sub-sections present each category in detail.

5.3.1 Single Laboratory Validation Challenges

Real-Time Implementation

Laboratory validations are expensive and control solution developers visit the laboratories for a short duration of time in order to validate their control solutions. As is usually the case, the control solutions are developed independently of the laboratory

within which they will be validated. Furthermore, the control solution developers are used to monolithic implementation (i.e. within a simulation tool) and do not necessarily understand the real-time requirements of laboratory implementation. The control solutions developed and brought to the laboratory for their validation by the control solution developers often require changes to enable the developed control to run in real-time. These changes may involve minor modifications to the control or sometimes complete re-development from scratch on a different platform. Therefore, it has been observed that usually more than one visit is required to carry out validation of control solutions, where the first visit is spent in understanding the implementation environment and the required control changes, and the second where the validation takes place.

Multi-Domain User Collaboration

Similar to the evolution of smart grids, the smart grid laboratories are in the process of continuous evolution and development. This development involves not only the addition of new equipment but also incorporation of new domains within the laboratories. This although enhances the capabilities of a laboratory, brings forth challenges in terms of multi-domain user collaboration. The process of validation of control solutions within a laboratory is adhoc, and with multiple users and multiple domains, this becomes even more challenging. Although the adhoc process of validation suits the dynamic nature of research work undertaken, it is not efficient and may lead to serialisation of tasks.

Repeatability

Generally speaking, users of the laboratories have a particular expertise they develop over time. The expertise may be (i) domain specific, such as communications, multi-agent systems, or power systems, (ii) research area specific, such as protection, frequency control or wide area monitoring and control, (iii) kit specific or (iv) technique specific such as real-time power hardware in the loop. Upon the departure of the users either due to graduation, or change in position, the transfer of knowledge is not always an easy process. This leads to uncertainty in terms of repeatability of experiments. Furthermore, when a particular control solution is enhanced after its initial validation and

brought for re-validation, not only is repeatability uncertain, often the whole process of implementing the control from scratch is chosen, i.e. there is little or no provision of extending the previously done experiments.

5.3.2 Multiple Laboratory Validation/ Round Robin Validation Challenges

Round robin testing refers to an inter-laboratory test undertaken independently a number of times. This involves testing by independent laboratories using same method and same or different equipment. Within power systems domain, round robin tests are generally undertaken on equipment, where the objective is to compare the results of tests undertaken at independent laboratories using same test method, same equipment under test, but different auxiliary test equipment. Development of round robin test procedures is an active area of research where the objective is to ensure the reproducibility of such procedures and is often undertaken by standardisation bodies [27]. In terms of validation of novel control solutions for smart grids, round robin tests can be undertaken to ensure the applicability of the developed control solution under diverse implementation environments. However, contrary to the testing of equipment where standard testing procedures can be developed, the nature of validation of control solutions is more dynamic. An important aspect to ensure while undertaking multiple laboratory testing is the comparability of results and the following challenges can be observed:

Consistency in Implementation

An important aspect to understand is that no two smart grid laboratories are the same. It is not uncommon that when a control solution is presented to two different laboratory user groups, the understanding in implementation of the two user group varies. This difference in understanding might be infrastructure driven or convenience driven. Most of the smart grid laboratories are designed to be flexible, and there is often more than one way in which a particular control solution can be implemented, unless otherwise restricted by infrastructure availability. Therefore, if results of validation

carried out independently at two laboratories are to be compared, the consistency in its implementation needs to be maintained.

Consistency in Recording and Reporting

To elaborate on the differences between two smart grid laboratories, the practices of recording and reporting experimentation results is a good example. In order for the results of two laboratories to be compared, consistency in terms of data recording and reporting needs to be maintained. Although a lot of work in this area is being undertaken in terms of developing standards such as IEC 61850 [28] and Common Information Model [29], not all laboratories have these standards incorporated and much effort is required to do so.

5.3.3 Analysing Laboratory Validation Challenges

Having the challenges associated with laboratory validation described, this sub-section presents some of the underlying causes deduced.

Limited Laboratory Engagement

It can be said that if laboratory validation of a control solution is the goal, as would be in the case when appraisal of a proposed control solution to TRL 5 is desired, involving the laboratory (or laboratory user group) in earlier stages of design and development of control solution would be beneficial. Consulting with targeted laboratory user groups during the developmental stages of a control solution can save valuable time.

Laboratory Infrastructure Bias

When control solutions are presented to multiple laboratory user groups, their understanding of its implementation is biased towards their individual laboratory infrastructure. This is not uncommon and is definitely not wrong. However, if the control solution is presented in a format that would enable the laboratory user groups to unambiguously identify the infrastructure needs to validate the solution, this can lead to more consistent implementation.

Multi-Domain Interoperability

Incorporating more than one domain in laboratory validation, in some simple form, has existed for a while. For example, communication delay being incorporated within laboratory validation in the form of a simple delay block (readily available in most commercial simulation tools). However, laboratories have witnessed inclusion of more sophisticated, dedicated, domain specific equipments and simulation tools. With these changes, it is important to develop a multi-domain approach to validation.

Lack of an Integrated Methodology

It is recognised that development of standard procedures for validation of novel control solutions is difficult owing to the the dynamic nature of validation (different control solutions would entail different validation objectives and approaches). However, a more holistic approach to deriving an integrated methodology can be undertaken. The need for such integrated methodology has also been acknowledged by the European Commission as is evident from the scope of the ERIGrid project [30]. It can also be inferred that some of the aforementioned challenges with laboratory validation can be attributed to lack of an integrated approach to validation.

Therefore, some of the challenges associated with laboratory validation of control solutions can be overcome if an integrated methodology is developed that incorporates the following features:

- Involves active engagement of laboratory (or laboratory user group) during the design and development of control solution.
- Defines a common unambiguous template for control solution description.
- Incorporates multiple domains and allows for interoperability to be captured.
- Defines a common template for documenting validation approach undertaken.

Such a methodology would facilitate the transition of control solution from its design to its validation. The emphasis on consistent implementations across multiple laboratories

increases the comparability of the results of validation. Documentation of validation approach enhances repeatability and reproducibility thereby supporting round robin validation.

5.4 Exploring the Literature for a Methodology

As has been emphasised so far, there is no standard methodology available in power systems literature that can be readily adopted for the purpose of facilitating laboratory validations. However, having the desired features of an integrated methodology at hand, the next step was to expand the literature search and explore if there are any similar approaches that can serve as a basis for development of an integrated methodology. This section summarizes the findings of the literature review undertaken.

An extensive survey on "validation of systems" and "systems testing" lead to the systems engineering approach referred to as the "V-Model" [31-33]. The V-model, also referred to as the Verification and Validation model, is a representation of a "systems" development life-cycle, and is primarily widely employed for project management. A

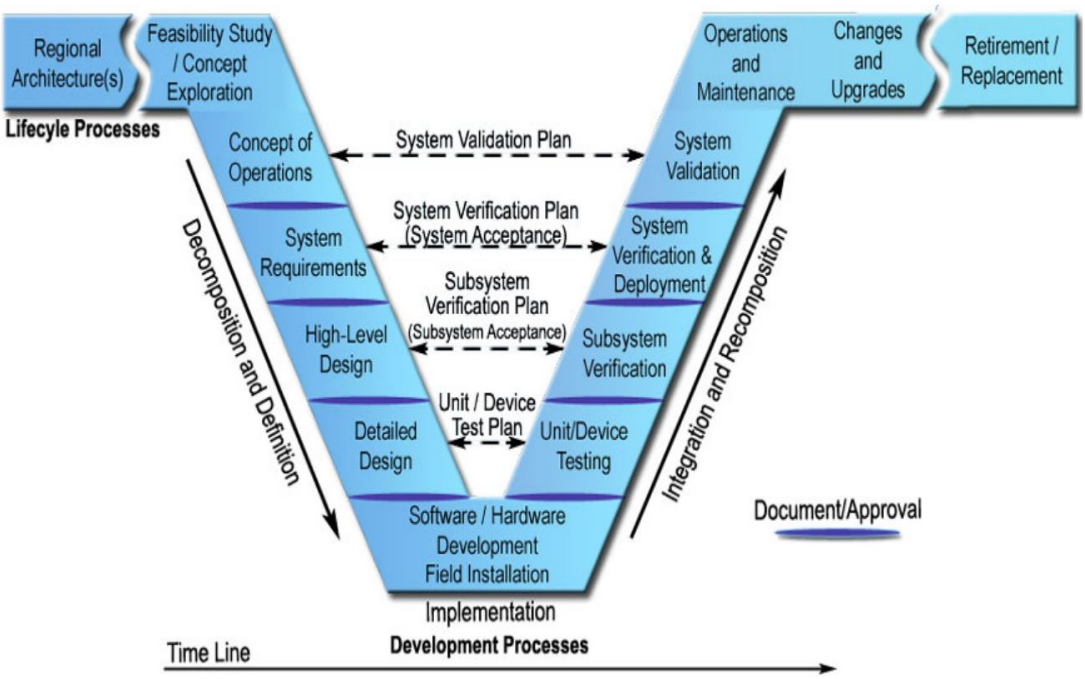

Figure 5.5: The validation and verification model [33].

graphical representation of V-model is depicted in Fig. 5.5. As can be observed, the left side of the "V" represents the decomposition of requirements, definition of system specifications while the right side represents integration of the parts and their validation. Validation is an integral part of the process since the beginning, evident from its planning in parallel with the corresponding phase of development in V-model. This attribute of V-model is of relevance and interest, drawing comparison to involving laboratories through the process of control solution development.

Like any other systems engineering approach, it does bring in a level of structuralism to any process it is incorporated within, however, it has very little in common with power systems domain or the smart-grids domain. Examples of use of V-model for project management and software development are in abundance in literature [34-36], but not many applications were found for power systems.

An extensive survey on "consistent power system/smart grid control solutions description" lead to the "Smart Grid Architecture Model" (SGAM) . SGAM is an outcome of the EU Mandate M/490's Reference Architecture working group [37]. SGAM is a

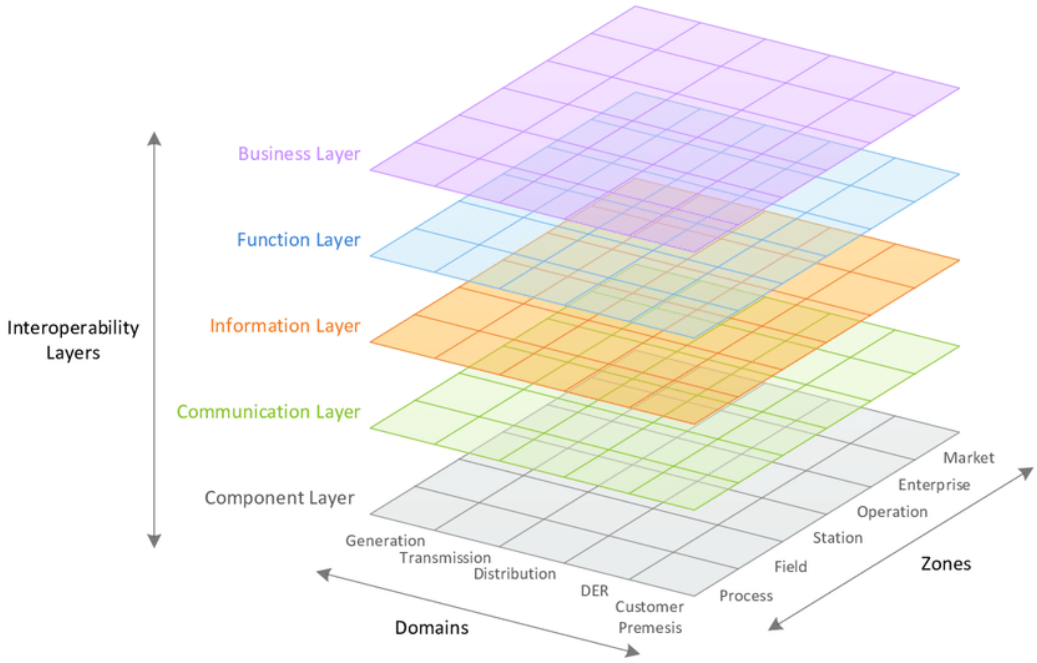

Figure 5.6: SGAM domains, zones and layers [37].

reference model intended to analyse and visualize smart grid use cases in a technology-neutral manner. It provides a systematic approach to cope with the complexity of smart grids, allowing representation of control solutions in the current state of the electrical grid as well as the ability to capture their evolution and integration within future smart grid scenarios.

The three dimensional representation of SGAM spans six hierarchical power system zones (Process, Field, Station, Operation, Enterprise and Market) and five domains encompassing complete electrical energy conversion chain (Generation, Transmission, Distribution, Distributed Energy Resources and Customer Premise) as shown in Fig. 5.6. Five superimposed layers (Business, Function, Information, Communication and Component Layer) allow for the interoperability of multiple functions in the power system to be depicted. Such a representation enables different smart grid control solutions to be visualised and compared.

The SGAM combines effective approaches of systems engineering with power systems in a simple yet comprehensive manner. SGAM builds upon significant existing work such as the National Institute of Standards and Technology (NIST) Conceptual Model [38], the GridWise Architecture Council Stack interoperability categories [39], the IntelliGrid Methodology [40], the European Conceptual Model and architecture standards like The Open Group Architecture Framework (TOGAF) and Archimate [41].

The use of SGAM in literature has been limited so far. One of the first reported use of SGAM was by standardisation bodies to identify standardisation gaps [42]. The capabilities of SGAM were then further enhanced by development of a methodology that allowed for smart grid control solutions to be represented within the three dimensions of SGAM (referred to as SGAM mappings henceforth) and analysed [43]. This was undertaken as part of the DISCERN project [44], where the participating Distribution System Operators (DSO) produced SGAM mappings for a control solutions deployed within their network [45]. The SGAM mappings of each DSO were then independently analysed by other participating DSOs. The objective was to allow DSOs to exchange information on smart grid realisation options from their experience of smart

grid technology deployment in a clear, consistent and unambiguous manner.

From the above discussion, the following can be observed:

- The SGAM modelling approach allows for control solutions to be represented in an unambiguous manner as is evident from DSOs exchanging experiences and implementation practices through representing solutions on SGAM.
- It incorporates multiple domains as is evident from the existence of five superimposed interoperability layers in SGAM.
- The SGAM modelling approach requires for the five layers to be filled (with relevant information as per the modelling approach), which also ensures consistent documentation.

It can therefore be inferred that the SGAM and SGAM modelling approach comprises three of the four identified features desired within a methodology to facilitate laboratory validation. The SGAM modelling approach serves as a perfect basis for development of a methodology for facilitating laboratory validations.

5.5 Appraisal of SGAM Methodology for Facilitating Laboratory Validation

In this section, the methodology for representing control solutions using SGAM proposed in [43], is assessed for its appropriateness to facilitate laboratory validations. This is done by presenting the description of the conventional SGAM modelling approach followed by its appraisal for laboratory validation.

5.5.1 Conventional SGAM Modelling Approach

As per the resources available in the literature [43], [46-48], the procedure of developing an SGAM representation of a control solution is as follows (shown in Fig. 5.7):

1. The control solution that is to be represented using SGAM is first described using the IEC 62559-2 template [49].

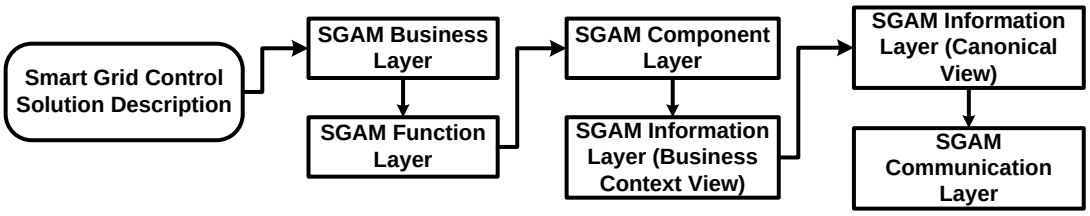

Figure 5.7: Conventional modelling approach.

2. The control solution associated business processes, services and organisations are mapped to the business layer.

3. The functionalities of the control solution are identified and mapped across the domains and zones of the function layer.

4. Next, components are associated to each functionality identified in the previous step and are populated on the component layer.

5. The information layer in SGAM has two views. In one of the views, referred to as the business context view, the information that is exchanged between the components is identified and mapped.

6. The second view is called the canonical view of information layer, upon which the data format for the information exchanged between the components is mapped.

7. The final layer of SGAM is the communication layer in which the technology used for exchanging information between components is mapped.

The hierarchical essence of SGAM and the modelling approach described above, allow for representation of the majority of the solutions for present day power systems.

5.5.2 Assessment of Applicability of SGAM Methodology for Laboratory Validation

The conventional SGAM modelling approach presented in the previous sub-section can be readily utilised when:

- Solutions already implemented in the field are to be visualised.
- Novel solutions are to be implemented within the installed utility equipment.

However, for the purpose of laboratory validation of novel control solutions, shortcomings within the conventional SGAM modelling approach have been identified and listed below:

S1. Missing Validation Objectives: The IEC 62559-2 template is aimed at deriving a technical requirement specification for implementation of a control solution in the field (i.e., within the installed utility equipment). This is not directly of relevance to laboratory validation. In contrast, for laboratory validation, deriving the objectives of validation is of more importance.

S2. Redundant Layer: SGAM is multi-faceted, allowing not only for technical implementation details of control solution to be depicted but also incorporating the business, organisational and regulatory aspects associated with the control solution. Although, this depiction within the business layer of SGAM does have an practical relevance to DSOs, it is not of relevance for laboratory validation of any given control solution.

S3. Inadequate Sequence of Layer Mapping: Within the conventional approach, after functionalities of a control solution are identified, the next step is to identify components that can be associated to the functionalities. As mentioned earlier, this is practical for control solutions that are already implemented within the field, or when a control solution has to be implemented within a given set of utility equipment. However, this transition from function layer to component layer is not appropriate for laboratory validation. Consider the following example: a simple control function, moving average filter, is to be implemented within laboratory. Within the DPSL, there are five implementation platforms (equipment) that can be utilised for this purpose. Without any additional information, the choice of equipment would be based on ease of implementation. However, this might not be an appropriate choice. On the other

hand, if the information that the control function is required to exchange is known, the frequency of information exchange is known, a more informed decision on the choice of implementation platform can be made.

S4. No Demarcation of Responsibility: The present methodology does not explicitly demarcate the responsibilities of the control solution developers and the laboratory users, although the involvement of the two is implicit.

S5. Unambiguous Guidance on Zone Mapping: The mapping of a function to an SGAM domain and zone is an integral step of the SGAM modelling approach. There is no formal guidance available on how a function is to be mapped on to a corresponding domain and zone. The formal description of the SGAM domains and zones, in addition to a limited number of example mappings in literature, serve as the only guidelines for prospective SGAM users. When novel control solutions are to be mapped on to SGAM, these guidelines may not be directly applicable. For a given control function, it is quite clear to which domain (generation, transmission, distribution, distributed energy resource (DER) or customer) it belongs to, however the description of zones is ambiguous and generally leads to users choosing a zone based on their understanding. As the objective of utilising SGAM is consistency, a clear set of unambiguous guidelines to choose a zone for control function are required.

S6. Limited to Representation of Control Solutions within a Single Entity: Due to the hierarchical nature of SGAM, solutions that can be represented using SGAM correspond to one single entity, such as a Transmission System Operator (TSO) or a Distribution Network Operator (DNO). If a control solution involves two TSOs, two SGAM representations are required, one for each TSO.

Therefore, the conventional SGAM methodology, presented in this section, requires adaptation to enable its effective utilisation to facilitate the laboratory validation of novel control solutions.

5.6 Proposed SGAM Modelling Approach for Laboratory Validation

In this section, the shortfalls identified within the conventional SGAM modelling approach will be addressed. First, an adapted SGAM modelling approach is proposed, followed by formalisation of guidelines for mapping functions on zones of SGAM plane.

5.6.1 Adapted SGAM Modelling Approach

The proposed SGAM modelling approach is presented in Fig. 5.8. As can be seen from the figure, the modelling approach is structured in four stages. The following subsections will present each of the stages in detail.

Stage I: Control Solution Description

For control solutions to be validated within a laboratory, it is essential to formulate clear validation objectives. In the conventional modelling procedure, the use case is described using the IEC 62559 template. However, as the IEC 62559 template is not intended to be utilised for the purpose of laboratory validation, a template specific to laboratory testing should be utilised, such as that presented in [50]. The test case specification template of [50] aims to clarify the "why, what and how" of the validation that is intended to be carried out. The template comprises a narrative, identification

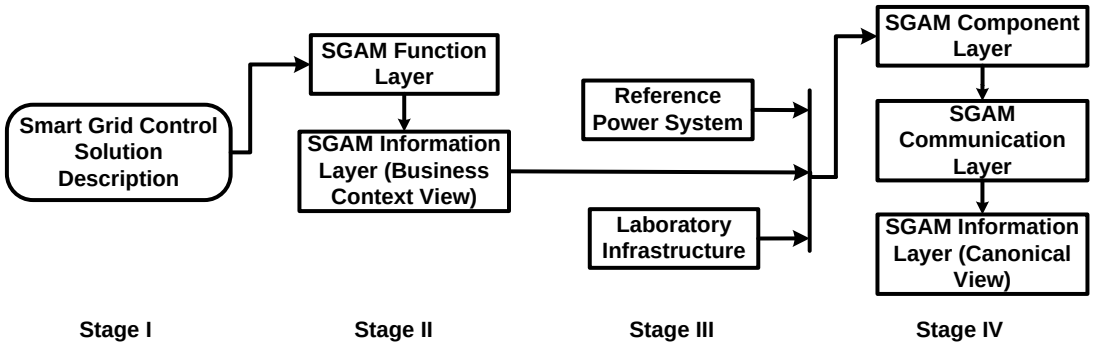

Figure 5.8: Modelling approach for laboratory validation.

of functions under test (FuT), establishing the purpose of investigation (PoI) and the test criteria (TCR). The narrative is a storyline summarising the motivation and scope of the test to be undertaken, FuT is a list of all functions required for the test. PoI formulates purpose of test in terms of characterisation, verification or validation while TCR enlists the measures to be quantified and evaluated for each PoI. This effectively addresses the shortcoming S1.

Stage II: Consolidated Function Mapping

As the business processes, services and organisations are not of interest for laboratory validation, the business layer can be omitted from the process. Similar to the conventional process, once the use case is described using the test case specification, the functions identified are mapped on to the function layer. However, after defining the function layer, in contrast to the conventional process, the information that is exchanged between the different functions is identified and the business context view of the SGAM information layer is developed. The next step is to establish the data transfer requirements (e.g. periodic refresh rate) for the information that is exchanged between the functions. This depends upon the application of the control solution and is usually determined by the control solution developers. The population of functional layer and the business context view of information layer completes the second stage of the methodology. The omission of business layer from the modelling process and the transition from function layer to business context view of information layer addresses the shortcomings S2 and S3. The process until now, stages I and II, is to be carried out by the control developers who wish for their developed solution to be tested within a laboratory.

Stage III: Reference Power System Selection

The remainder of the modelling process is to be undertaken by the laboratory that is to carry out the intended validation. In order to test and validate the smart grid control solution in the laboratory, a reference power network is required. In most laboratories, the reference power network is the power network available within the

laboratory. However, in laboratories capable of conducting power hardware-in-the-loop simulations (P-HiL), a larger power network can be simulated, with the laboratory network being a small part of the larger virtually simulated network. In such cases, a reference power system is chosen based on the individual laboratory capabilities. Furthermore, the objectives of the validation also influence the choice of reference power network. The clear assignment of responsibility to control solution developers and laboratory users and the a clear demarcation in the process addresses shortcoming S4.

Stage IV: Experiment Specification

Depending upon the data transfer requirements established in Stage II, the components – i.e. the intelligent electronic devices (IEDs) – in the laboratory that can be utilised for the implementation of the functions are identified. Once the components have been identified, the communication protocols and data formats supported by these components are summarised in a table. This enables the population of the component layer, communication layer and canonical view of information layer of SGAM. Having all the layers of SGAM populated provides a full view of the laboratory testing environment.

5.6.2 SGAM Zone Mapping Guidelines

In this section, guidelines for the zone mapping of a control solution functions are established by means of presenting the formal descriptions of zones and contrasting the changes and enhancements required, thereby addressing shortfall S5.

Process Zone

Definition: This zone is utilised to represent physical, chemical or spatial transformation of energy (such as power generation itself) and any equipment involved (such as generator).

Remark 1: *From the above description, it is clear that the process zone involves the elementary devices of the power system*

Guideline 1: For the purpose of representation of control solution functions, the process zone is not utilised. However, physical power system components expected to be part of the validation are represented on the process zone.

Field Zone

Definition: Any equipment to protect, control and monitor the process of power system is attributed to the field zone. Examples include protection relays, bay controllers and any IED that acquires data from power system.

Remark 2: *The formal description of field zone refers to equipment only, although it might be intuitive to map control functions associated with such equipment, it may constitute to confusion.*

Guideline 2: Any control function that is implemented at a device level is attributed to the field zone. Examples of such controls include speed governing control of synchronous machines and local power controller of domestic heater.

Station Zone

Definition: Aggregation of field zone functions or equipment are represented on the station zone. Data concentrators, substation automation and SCADA systems are some examples presented in literature.

Guideline 3: Any control function that operates at an aggregated level is attributed to station zone. This includes any function that relies on aggregated data or controls an aggregation of devices. Demand side aggregators form a good example of functions to be mapped on to the station zone.

Operation Zone

Definition: This zone hosts power system control operations. This includes distribution management systems, micro-grid management systems, etc.

Remark 3: *From the above description of operation zone, it may appear that all control operations of the power system are to be attributed to the operation zone. However, as is evident, the guidelines being proposed in this work have already attributed control functions to field and station zone of SGAM. This is another reason why a clear set of guidelines for consistent SGAM modelling is required.*

Guideline 4: A control function that is unique within the entity being represented on SGAM should be attributed to the operation zone. The word unique here points to the uniqueness of the objective of the function. If only one function with a particular objective exists, it should be represented on the operation zone. If more than one control function with a similar objective might exist, such control functions should be attributed to the station zone.

Enterprise Zone

Definition: Includes commercial and organisational processes, services and infrastructures for enterprises. Examples are asset management, logistics, staff training etc.

Remark 4: *The description of enterprise zone renders it irrelevant for laboratory validation of novel control solutions. However, as has been mentioned earlier, only a control solution implemented within an entity can be represented using SGAM. If a control solution within an entity relies on information exchange from another entity, there is no guidance available on how this interaction can be captured.*

Guideline 5: Any control function within an entity that relies on information from another entity is attributed to the enterprise zone.

Remark 5: *Being able to capture the interaction between two entities renders the capability of representing distributed control solutions that are implemented at different entity levels thereby addressing shortfall S6.*

Market Zone

Definition: Incorporates market operations such as energy trading, mass market and retail markets.

Guideline 6: For laboratory validations, it is rare that the interactions with markets are required. Nevertheless, the markets that the entity participates in can be represented within the market zone. These markets are the wholesale or mass markets within which multiple entities such as the one being represented using SGAM can participate. If there is a market existing within the entity itself, following the previous guidelines, such market functions can be represented within the operation zone if the market function is unique (such as the conceptual BidLadder platform [51] developed for the Belgian TSO) or within the station zone if multiple markets with the same objective exist.

5.7 Applying the Proposed SGAM Methodology for Validation of the EFC Framework

In this work, two novel approaches to frequency control have been proposed, a PFC referred to as the EFC-RP and a SFC referred to as the EFC-FB. The combination of the two responsibilising controls will henceforth be referred to as the enhanced frequency

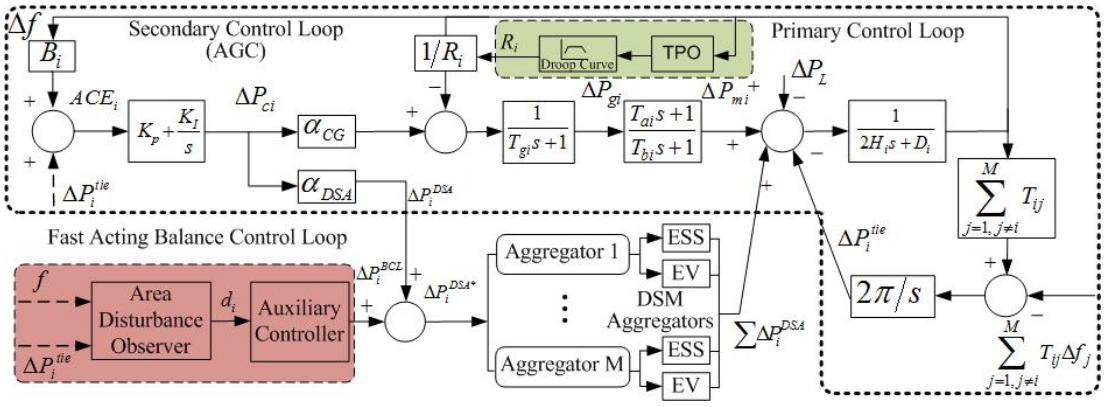

Figure 5.9: Enhanced Frequency Control Framework.

control framework as illustrated in Fig. 5.9. In this section, the proposed SGAM modelling approach will be utilised to facilitate the validation of the EFC framework. This serves dual purpose: (i) it allows for the applicability of the proposed SGAM modelling approach for validation of novel control solutions to be analysed, and (ii) enables transition of EFC-FB to laboratory for its appraisal to TRL 5.

In the following sub-sections, the four stages of the proposed SGAM modelling approach will be undertaken for the chosen control solution.

5.7.1 Stage I: Control Solution Description

The test case specification template presented in [50], comprises a narrative, identification of FuT, establishing the PoI and the TCR. The four parts of the test specification template for the chosen controller are presented in the following sub-sections.

Narrative

In Chapter 3, by means of simulations, limitations of conventional load frequency control (LFC) framework were identified. To overcome the limitations of the conventional approach, a novel EFC-FB is proposed. A simplified control diagram of the EFC-FB is shown in Fig. 5.10. The control incorporates a fast acting balance control loop (BCL),

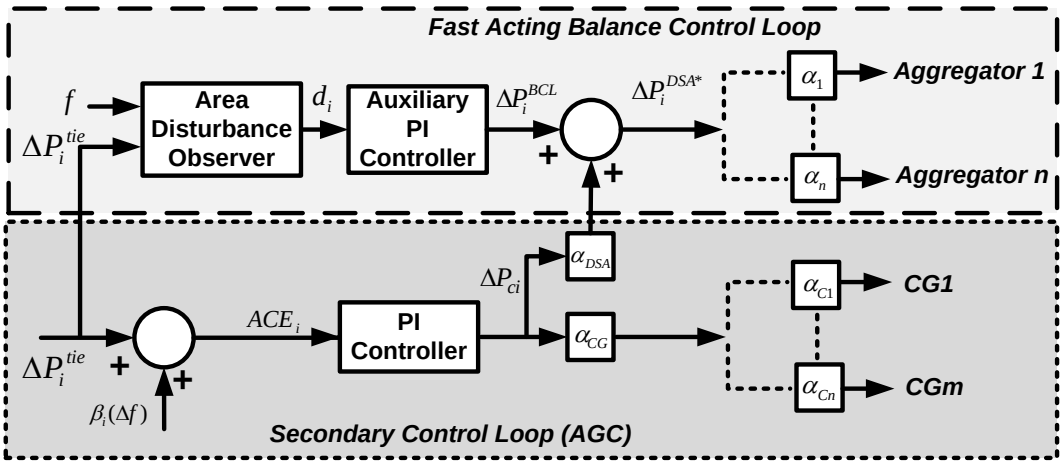

Figure 5.10: Simplified control representation of EFC-FB framework.

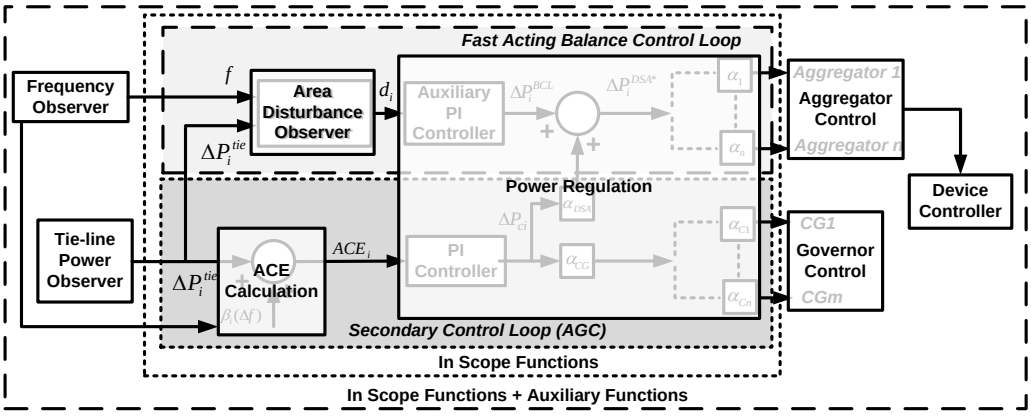

Figure 5.11: Identified functions under test.

in addition to the secondary control loop. The feasibility of the proposed EFC-FB has been verified by means of real-time simulations. The performance of the control in a realistic environment based on real measurements, for its appraisal to TRL 5, is to be assessed.

Table 5.1: Functions under Test: In Scope Functions

Function	Description
Area Control Error (ACE) Calculation	It is the error signal that represents the cumulative deviation of the area from its scheduled net import or export of power flow over all tie-lines. It is the sum of ΔP^{tie} and a function of frequency deviation. It is important to mention that the ΔP^{tie} calculation involves the power flow over a virtual tie-line. Virtual tie-line power flow is incorporated when an AGC participating unit of LFC area A is within the physical boundary of LFC area B.
Power Regulation	The conventional LFC framework relies on a proportional-integral (PI) controller to force the ACE to zero. The output of this function is power regulation command (the amount of power to be increased or decreased) that will be sent to aggregators and conventional generators (CGs).
Area Disturbance Observer	Based on the ΔP^{tie} and the $RoCoF$, this function identifies if the event is within the LFC area. The output of the function is normally zero, but replaced with ΔP^{tie} when event is within the LFC area.

Table 5.2: Functions under Test: Auxiliary Functions

Function	Description
Device Controller	Each flexible device within the network is associated with a controller. The controller has two objectives: (i) to formulate a bid for aggregator based on device flexibility and (ii) turns the device on or off based on the command signal received from the aggregator.
Frequency Observer	Frequency measurements required for calculation of ACE provided by this observer.
Tie-line Power Observer	The power measurement at the tie-lines required for ACE calculation is provided by this observer.
Aggregator Control	The aggregator central control has two functionalities: (i) to receive the flexibility bids from the flexible devices within its portfolio and formulate a cumulative bid for participation in the ancillary service market and (ii) formulate a command signal to be sent to the flexible devices upon receiving the regulation command from AGC.
Governor Control	The governor is responsible to maintain the speed of CGs and ensure requested primary frequency support. The regulation command from the AGC is received by the governor to enforce the change in power requested

Functions under Test

FuT are classified into two: in scope functions and auxiliary functions. The in scope functions are the functions derived directly from the controller and the auxiliary functions are the additional functions identified for the validation of the controller. FuT identified for the EFC-FB are shown in Fig. 5.11. A brief description of these functions is presented in Tables 5.1 and 5.2 to help readers better understand the domain-zone mapping (and the use of guidelines established) through the presented study.

Purpose of Investigation

PoI formulates the test objectives, stating whether it relates to characterisation, validation or verification objectives. The following PoIs have been formulated for the validation of the chosen control solution.

PoI-1: The performance of the EFC-FB has been verified by means of real-time simulations. To ensure its deployment in a real-world, a controller hardware in the loop implementation (C-HiL), where the EFC-FB will be prototyped within a hardware controller is required. Therefore, the first PoI is formulated as the characterisation of system frequency response with and without EFC-FB under pure real-time implementation compared to C-HiL implementation.

PoI-2: A detailed study on experimental validation of ancillary service provision capability of aggregators controlling a portfolio of highly distributed demand side devices has been under taken by the author [52]. The study identifies that validation of any control relying on demand side aggregators for provision of time critical ancillary services, should incorporate the communication delays to demonstrate robustness. The results presented earlier in the thesis assumes a fixed communications delay. However, the communication delay referred to in here is the time it takes for a control command from the aggregator to reach the participating device and is highly dependent upon the communication architecture used by the potential demand side aggregator. Therefore, the second PoI has been formulated as the the characterisation of system frequency response with EFC-FB incorporating no communication delays compared to implementation incorporating realistic delays in a C-HiL implementation. As this work does not consider any specific aggregator, the common communication architecture for aggregators defined in [53] will be utilised.

PoI-3: The performance improvement of EFC-FB over present day control has been achieved by means of incorporation of BCL that relies on area disturbance observer for a faster disturbance detection. The disturbance detection utilizes RoCoF, that is regarded as a very noisy measurement. Any control that relies on RoCoF should therefore be validated by means of real measurements enabled by power hardware-in-the-loop implementation. Therefore, the final PoI is to validate the disturbance detection function of the proposed control in P-HiL implementation.

Test Criteria

In the previous three sub-sections, the "what and why" of the case study have been detailed. It is important to understand the "how", i.e. how this is intended to be achieved. This will be achieved in a similar manner as undertaken for simulation based analysis in Chapter 3. To reiterate, a generation loss will be emulated at steady state to cause a deviation in frequency and the validity of the control will be evaluated. Three test metrics have been formulated as:

- **Frequency Restoration Time** (T^{Rest})**:** To asses the T^{rest} of the controllers, an error margin $\epsilon = 0.01$ is defined such that T^{rest} is the time interval between the initiation of disturbance to the point when $|\Delta f| = |f - f_{nom}| < \epsilon$, and can be represented as $T^{rest} = \{T^{rest} \in \mathcal{R} : \forall\ t > T^{rest}, |\Delta f| \leq \epsilon\}$.

- **Maximum Frequency Deviation** (f^{dev}_{max})**:** Defining the minimum and maximum frequency after a disturbance as f_{max} and f_{min} respectively, the maximum frequency deviation is calculated as $f^{dev}_{max} = max\left(|f_{max}|, |f_{min}|\right)$.

- **Relative Frequency Overshoot** (Δf^{ovr})**:** Defining the minimum and maximum frequency after a disturbance as f_{max} and f_{min} respectively, the relative overshoot is calculated as $\Delta f^{ovr} = \left|\frac{f_{max} - f_{nom}}{f_{nom} - f_{min}}\right| \cdot 100\%$.

5.7.2 Stage II: Consolidated Function Mapping

As per the methodology, from the functions that have been identified within the test case specification, the function layer is populated as shown in Fig. 5.12. Table 5.3 is tabulated comprising the inputs and outputs of all the functions with their required refresh rates. Based on the information in Table 5.3, the information layer is obtained as shown in Fig.5.13. As can be observed from the two figures (Fig.5.12 and 5.13), the process zone is populated with physical components expected to be part of the test. This allows for information exchange of device level functions such as the governor control to be represented. The process until now is to be carried out by the control developers who wish for their developed solution to be tested within a laboratory.

Table 5.3: Inputs, outputs for FuT with their required refresh rate

Function	*Inputs* (*In*)	*In Refresh Rate*	*Outputs* (*Out*)	*Out Refresh Rate*
ACE Calculation	P^{tie}_{meas} f $P^{tie}_{virtual}$	100 Hz 100 Hz 100 Hz	ACE_i ΔP^{tie}_i	100 Hz 100 Hz
Power Regulation	ACE_i ΔP^{tie}_i	100 Hz 100 Hz	$\alpha_{CG}\Delta P_{ci}$ ΔP^{DSA*}_i	1 Hz 1 Hz
ADO	ΔP^{tie}_i f	100 Hz 100 Hz	ΔP^{tie}_i	100 Hz
Aggregator Control	δP^{r}_{DSM}	1 Hz	Activation Signal	1 Hz
Device Controller	Activation Signal	1 Hz	On/Off	1 Hz
Governor Control	$\alpha_{CG}\Delta P_{ci}$	1 Hz	P_{SP}	Continuous
Frequency Observer	Raw Measurement	Analog	Frequency	100 Hz
Tie-line Power Observer	Raw Measurement	Analog	P^{Tie}_{meas}	100 Hz

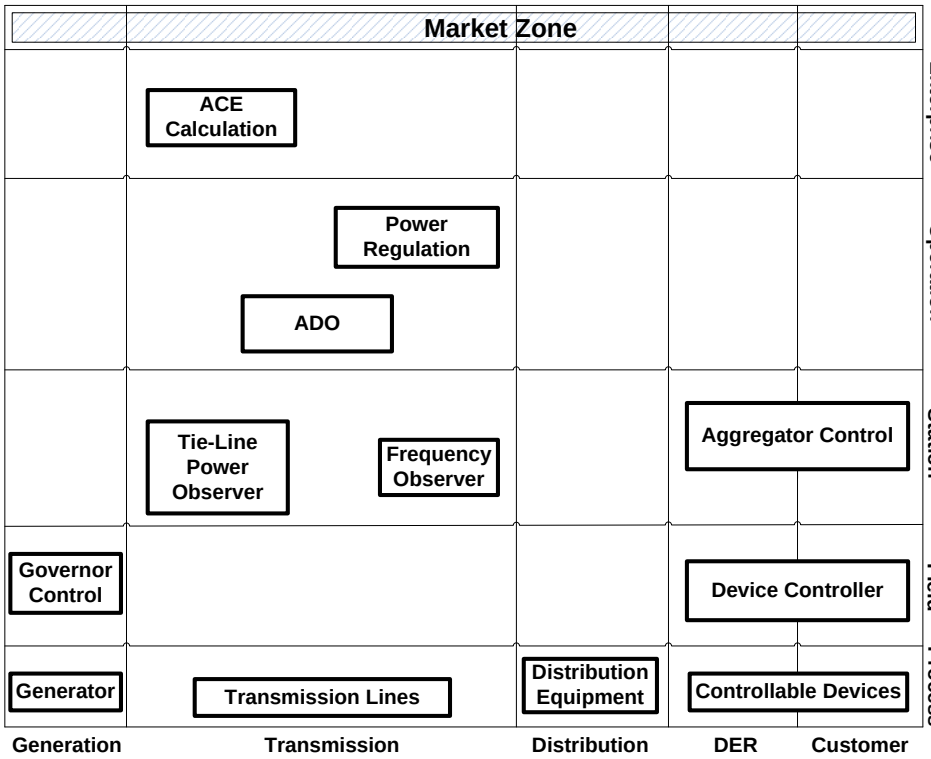

Figure 5.12: SGAM function layer.

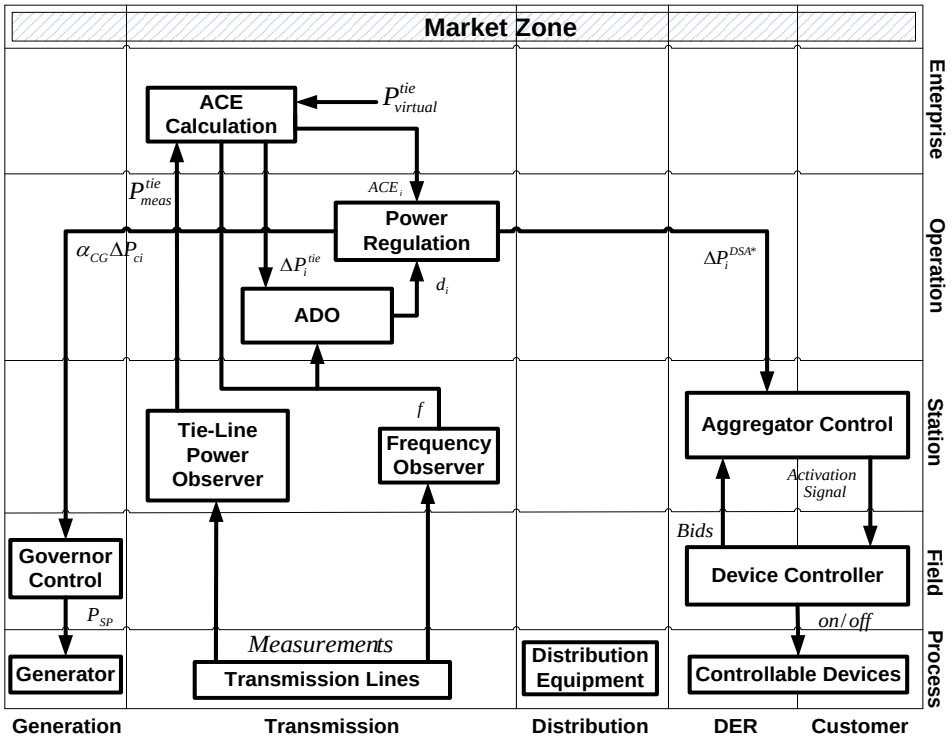

Figure 5.13: SGAM information layer: business context view.

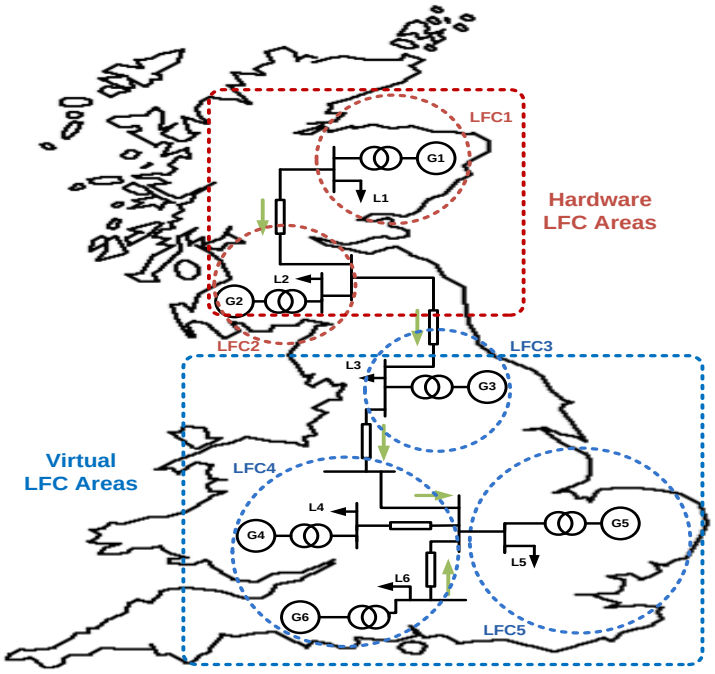

Figure 5.14: Reference power system chosen for laboratory implementation.

5.7.3 Stage III: Reference Power System Selection

For the presented study, Dynamic Power Systems Laboratory (DPSL) at University of Strathclyde (UST) is chosen for validating the EFC framework. As the capabilities at DPSL allow for C-HiL and P-HiL experiments to be conducted, the five-area reduced power system of Great Britain (GB) has been chosen as the reference power network (as in Chapter 4). The five-area GB power system is presented in Fig. 5.14. As can be observed from the figure, in P-HiL implementation two of the LFC areas will be represented by the physical micro-grid of the DPSL and the remaining three LFC areas will be simulated virtually in real-time using real time digital simulator from RTDS technologies. Apart from the reference power system, it is also essential to choose a reference event for validating the controller against. The test metrics chosen for validation of the controller specify generation loss as the event, and therefore a generation loss of 1GW in LFC area 2 (similar as in Chapter 3) is defined as reference event for chosen reference power system. It is important for the reference event to be emulated in LFC area represented by hardware so as to evaluate the ability of the control with real measurements.

5.7.4 Stage IV: Experiment Specification

The next step involves the selection of two types of components: (i) the IED that will host the control functions and (ii) the power components that will be utilised to test the control solution. As has been mentioned earlier, it is only possible to create an SGAM representation of a solution within one entity. As the proposed ELFC framework is implemented within each of the LFC areas, and more than one LFC areas are required to test the appropriateness of the solution, an SGAM representation for each LFC area is required. From the presented study, it can be said that, for the given solution, the function layer and the information layer will remain the same. However, different representations are required from component layer onwards. Based on the business context view of the information layer and the information presented in Table 5.3, the IEDs that will be utilised are identified. This allows for the component layer to populated, one component layer for each physical and virtual LFC areas is shown in

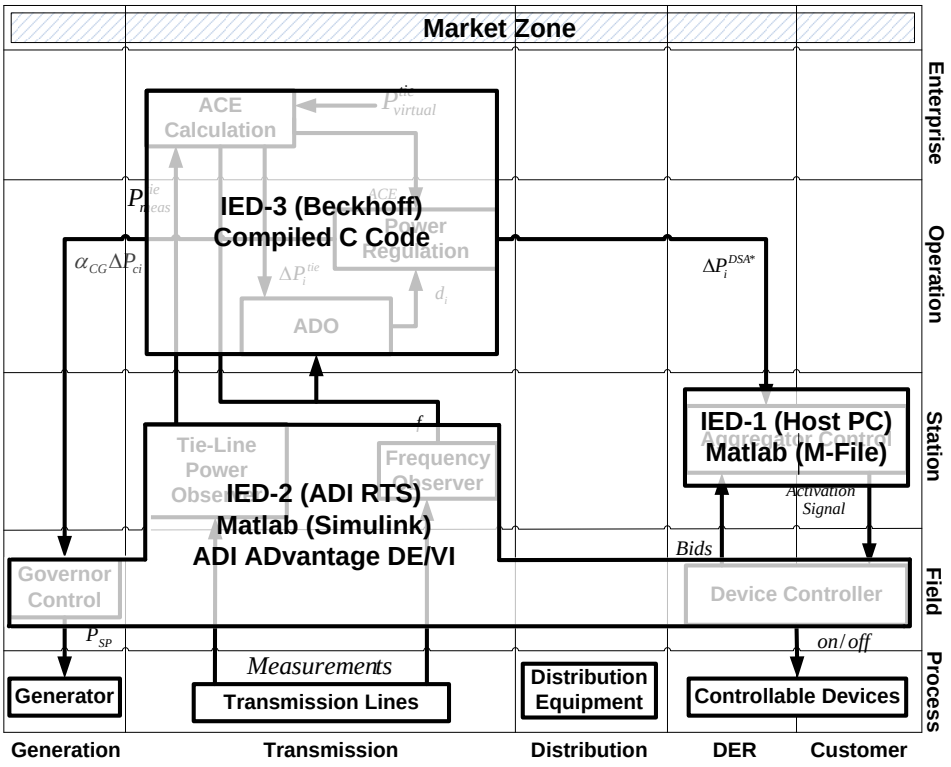

(a) SGAM component layer for physical LFC areas 1-2.

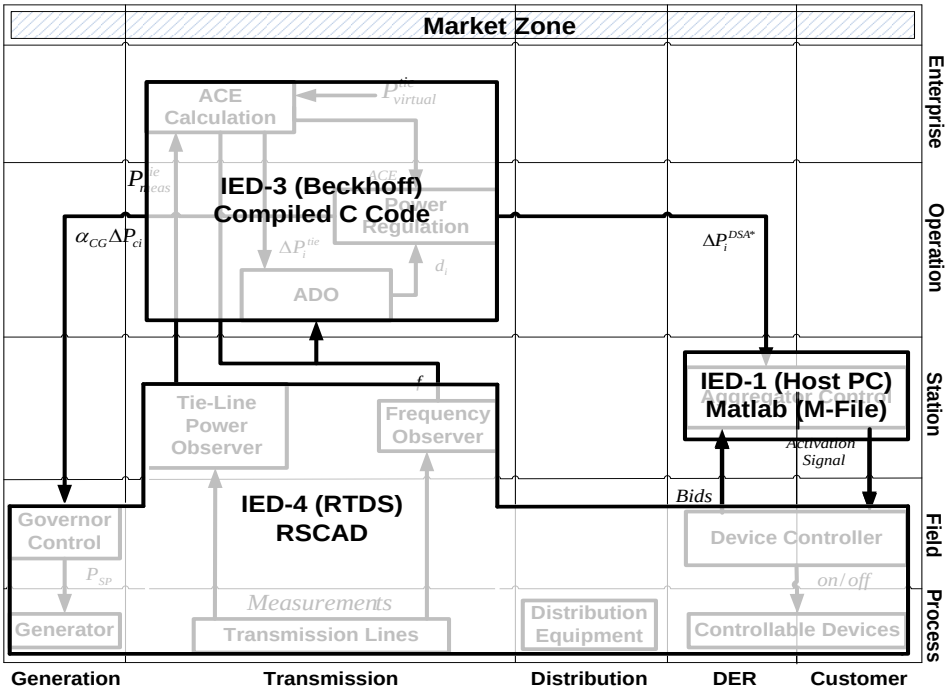

(b) SGAM component layer for virtual LFC areas 3-5.

Figure 5.15: SGAM component layer.

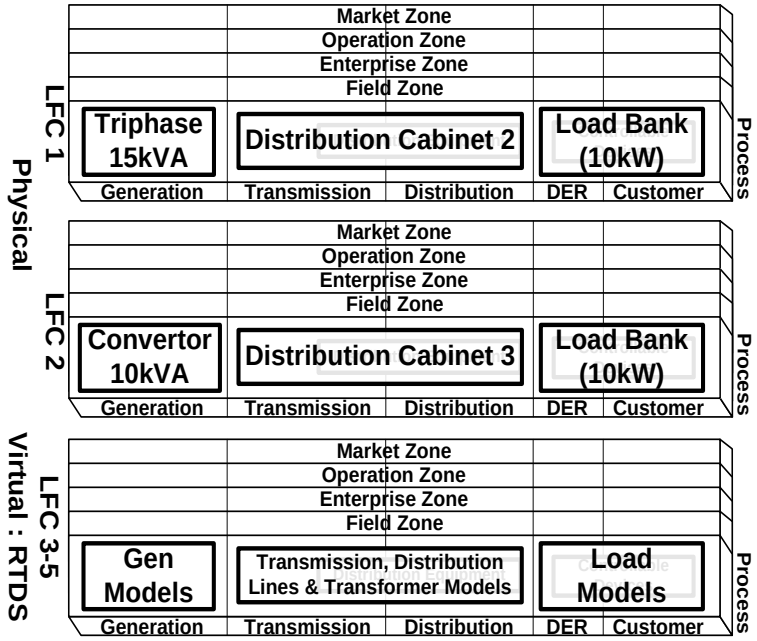

Figure 5.16: SGAM component layer process zone for LFC areas 1-6.

Fig. 5.15a and 5.15b respectively. Within DPSL, some of the control functions for all the areas (LFC 1-LFC 5) are implemented within the same IEDs (for example, the

Table 5.4: Identified laboratory components: UST

Lab Component	Functions	Environment	Communications Protocol	Data Format
IED-1 (Host PC)	Aggregator Control	MATLAB (M-File)	UDP	Custom
IED-2 (ADI RTS [54])	Governor Control Frequency Observer Tie-Line Observer Device Controller	MATLAB (Simulink)	UDP	Custom
IED-3 (Beckhoff [55])	ACE Calculation Power Regulation ADO	C	UDP	Custom
IED-4 (RTDS)	Governor Control Frequency Observer Tie-Line Observer Device Controller	Control	UDP	Custom

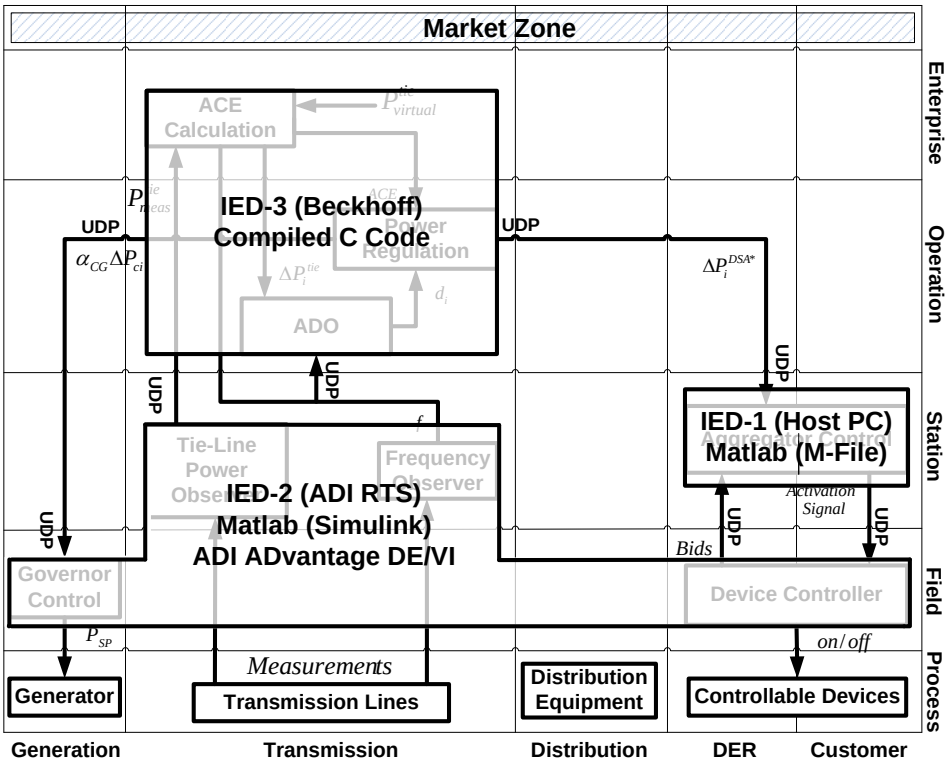

(a) SGAM communication layer for physical LFC areas 1-2.

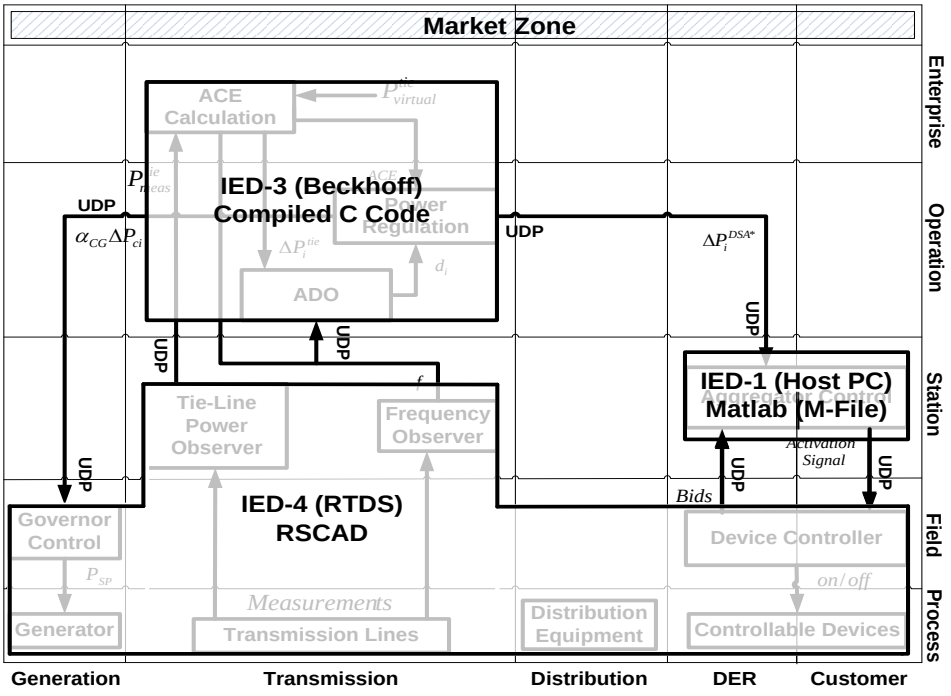

(b) SGAM communication layer for virtual LFC areas 3-5.

Figure 5.17: SGAM communication layer.

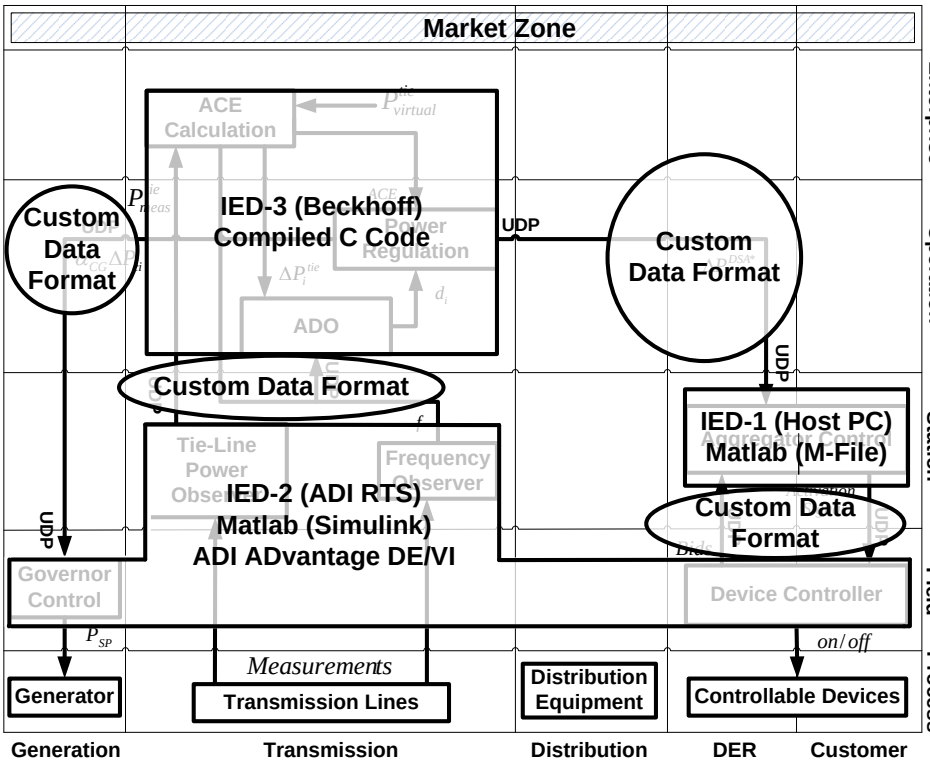

(a) SGAM information layer canonical view for physical LFC areas 1-2.

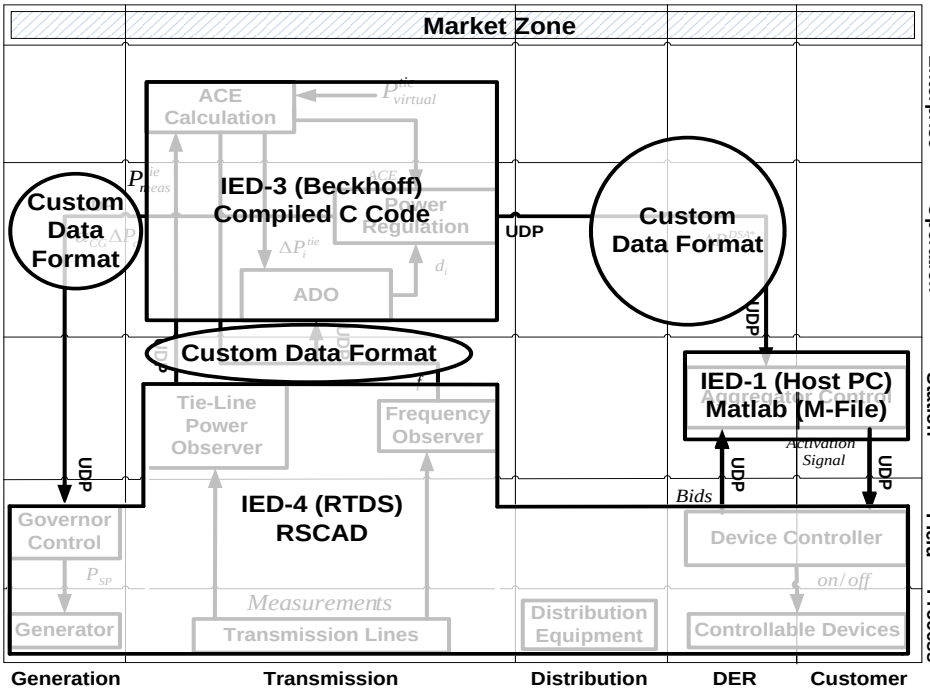

(b) SGAM information layer canonical view for virtual LFC areas 3-5.

Figure 5.18: SGAM information layer canonical view.

ACE calculation function for all the LFC areas is implemented within IED-3, but as individual task to maintain the distributed nature of implementation). As the power components for each of the LFC are unique, the process zones of all the LFC areas have been represented in Fig. 5.16. This completes the component layer.

After the component layer has been obtained, Table 5.4 is tabulated. Table 5.4 identifies the implementation platform, the communication protocols and the data format/model that will be utilised. This allows for the communication and the canonical view of information layer to be populated as shown in Fig. 5.17, and 5.18 respectively.

5.8 Evaluation of the Proposed SGAM Modelling Approach

In this section, the proposed SGAM modelling approach is analysed to evaluate its effectiveness to address or alleviate the identified challenges when moving from the design of a control solution to its laboratory validation. The discussion presented in the following sub-sections is from the experience gained by the use of the approach for the EFC framework. Reflecting on the experiences, best practices are drawn and recommendations offered.

5.8.1 Transition from Control Solution Design to its Validation

One of the challenges identified earlier is the development of control solutions independently of the laboratory within which they will be validated. Once developed and brought to the laboratory for validation, often changes are required to enable the developed control to run in real-time. This may involve minor modifications to the control or sometimes complete re-development from scratch on a different platform. A lot of time can therefore be saved if the control solution is developed in conjunction with the laboratory where it will be validated.

The SGAM modelling approach presented in this chapter requires the involvement of both, the control solution developers and the laboratory chosen for its validation. Although the proposed approach does support the transition of a control after its design

is complete, it has been experienced that utilising the approach during the development of the control can save time. The control solutions can be adapted during its development stage to allow it to run in real-time or the platform for control design can be chosen based on the capabilities of the laboratory. For example, for the ELFC framework study presented in this chapter, MATLAB Simulink was chosen as the platform for development of ACE calculation function, power regulation function and the area disturbance observer function based on feedback from the laboratory users. This is because MATLAB allows for exporting control blocks as a compiled C code that can be imported within the Beckhoff platform [56].

Therefore, an iterative process where the control solution developers complete Stage I of the proposed modelling approach during the control design and provide it to the laboratory for Stage II and gather their feedback before implementing the control is recommended.

5.8.2 Distributed Development and Implementation Workflow

Pure simulation based validation of control solutions typically involves one user and one simulation platform. Contrary to the workflow in simulation analysis of control solutions, the validation of such solutions within a laboratory involves multiple users with distinct expertise and multiple platforms. Any validation may require multiple users to collaborate, and the effective coordination among the users was identified as a challenge. For example, within the DPSL, for the presented study, five individual users were identified and allocated distinct tasks. The five tasks were: (i) installation of a new frequency measurement within distribution cabinet 3 (individual expertise: metrology), (ii) integration of aggregator control within IED-1 (individual expertise: demand side management), (iii) modification of the five area GB model for P-HiL simulations (individual expertise: P-HiL simulations), (iv) communications emulation between IEDs (individual expertise: communications for power systems) and (v) making the required measurements available through user datagram protocol (UDP) from IED-2 (kit specific). The use of the proposed approach allowed for clear task identification, allowing for the users to individually undertake the developmental work. In other words, it

can be said that the proposed approach enables modular development and integration testing, i.e., the breakdown of the implementation into simpler modules, where the individual users can identify their tasks and their dependencies, and work together with dependent user to complete their module integration. If a methodological approach, such as the one presented in this chapter, is not followed, a risk of serialisation of tasks arises. Following the presented approach, therefore, enables effective multi-domain user collaboration and distributed workflow within the laboratory.

5.8.3 Ensuring Repeatability and Extending Validation

In this sub-section, the following two aspects of the proposed approach will be explored: (i) repeatability of experiments when minor control modifications or implementation modifications have been identified, and (ii) the extension of validation when additional control solutions are introduced.

Repeatability

Recalling PoI-2, the EFC-FB validation needs to incorporate communications emulation, especially between the aggregator and its resources. Throughout the process of transitioning the EFC-FB to laboratory for its validation through the development of SGAM layers, it was inherently assumed that the communication between each of the IEDs would be emulated. However, due to unavailability of the communications emulation at time, it was decided that the communications delay from and to IED-4 would be emulated by means of delay block. The availability of the SGAM layers enabled quick identification of the modifications required to incorporate the delay block, and the updated component layer is presented in Fig. 5.19.

Extending Validation

In this work, the objective is to appraise the proposed EFC-FB to TRL 5, through laboratory validation. The responsibilising primary frequency control (PFC) proposed in Chapter 4, will not be appraised to TRL 5 at this stage. However, the ability of the proposed approach to support extended validations was evaluated by undertaking an

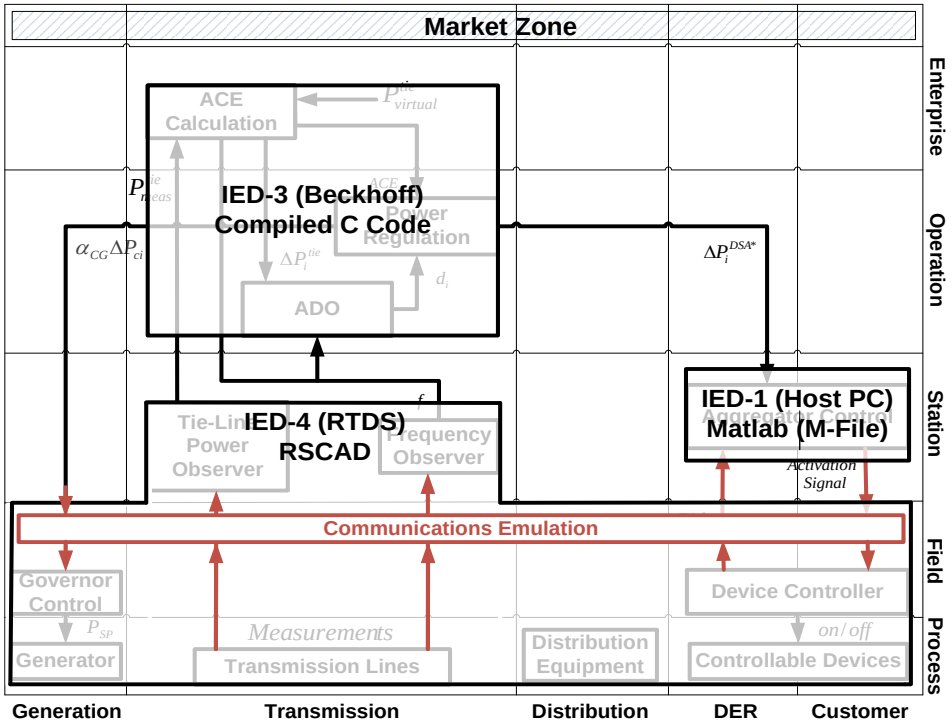

Figure 5.19: SGAM component layer representation for demonstrating repeatability.

exercise to incorporate the PFC within the validation. The proposed responsibilising PFC is an adaptive control that modifies the droop contribution of an LFC area based transient phase offset (TPO) measurement. In accordance with the proposed modelling approach, using the test specification template, the functions involved are identified and Table 5.5 is tabulated. It was identified that only one additional function (TPO) needed to be implemented whereas one other function (governor control) needed to be slightly modified. Furthermore, IED-2 was recognised as the best fit platform for the

Table 5.5: Functions under Test

Function	Description
TPO	The TPO at the participating PFC resource is calculated by this observer.
Governor Control	The governor is responsible to maintain the speed of CGs and ensure requested primary frequency support. In addition, based on the TPO measurement, this adapts the droop contribution of the participating PFC resource.

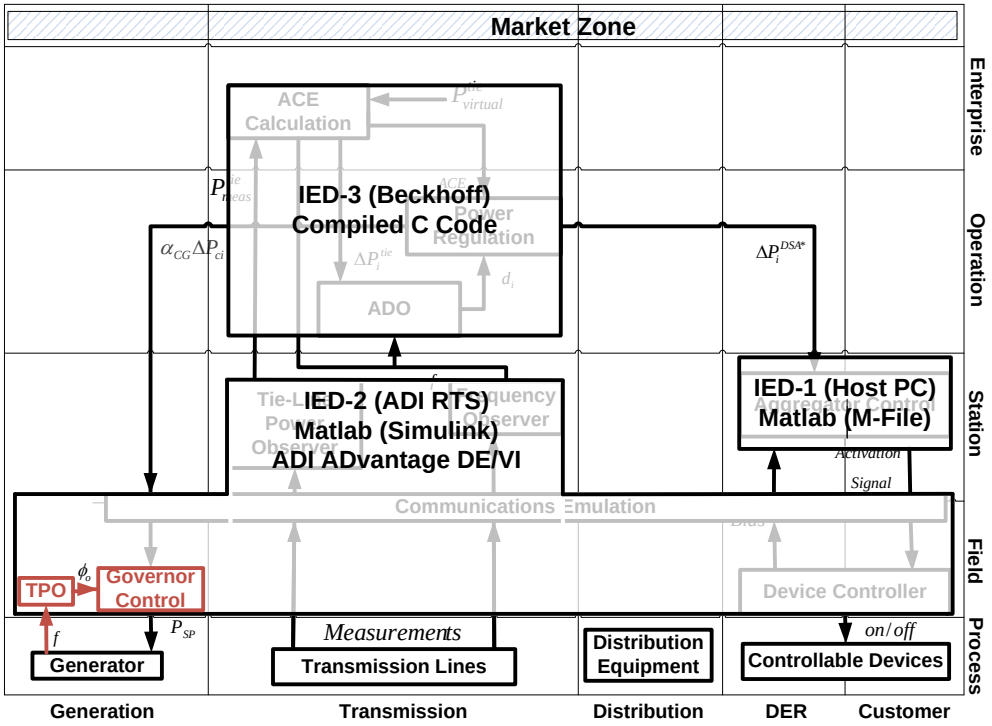

Figure 5.20: SGAM component layer representation incorporating responsibilising PFC, EFC framework.

implementation of the function as has been depicted in Fig. 5.20.

Therefore, the approach allowed for easy incorporation of additional control functions. It enabled identification of dependencies, avoiding any potential duplication, and allowed for appropriate platform selection for implementation. This further entails efficiency in extended validation scenarios.

Table 5.6: Identified laboratory components: CRES

Lab Component	*Implementation Environment*	*Communication Protocol*	*Data Format/Model*
IED−1 (Host PC)	*MATLAB (Simulink)*	*OPC*	*Custom Data Format*
IED−2 (Host PC)	*MATLAB (Simulink)*	*OPC*	*Custom Data Format*

5.8.4 Facilitation of Round Robin/Multi-Laboratory Validation

To evaluate the use of the proposed approach for the purpose of round robin validation, the EFC-FB was requested to be validated in an additional laboratory facility: the Centre for Renewable and Energy Sources and Savings (CRES). All the SGAM layers from the four stages of the approach along with the chosen reference power system from USTs validation were provided to CRES laboratory user group. With the implementation from UST at hand, the user group at CRES was able to confirm their laboratory's ability to validate the controller. The modelling approach was then followed by CRES, and only the chosen reference power system and selected SGAM layers have been presented in Fig. 5.21a, 5.21b, 5.22a and 5.22b. The identified laboratory components can be found in Table 5.6.

Undertaking the exercise of adopting the proposed SGAM approach within an independent laboratory (not involved in development of the approach), the following can be surmised:

1. As the first two stages of the approach are undertaken by control solution developers, depicting the control solution in a standardised template (SGAM function and information layers), any inconsistencies in terms of understanding of control solution are reduced if not eliminated. This allows for laboratories to assess their capabilities for validating the proposed control solution, enabling them to take an informed decision on agreeing to validate the control solution.

2. Once one laboratory has undertaken the final two stages of the approach, the full set of SGAM layers should be passed to any other laboratory intending to validate the control solution. This further ensures consistency in control implementation within laboratory equipment.

3. While ensuring consistency in understanding, the approach enables the differences in implementation to be easily captured. This helps any potential stakeholders to compare and understand the results with more confidence. To summarize the difference in implementation, the user group at CRES chose for a pure hardware setup for the purpose of validation and their laboratory network was chosen as

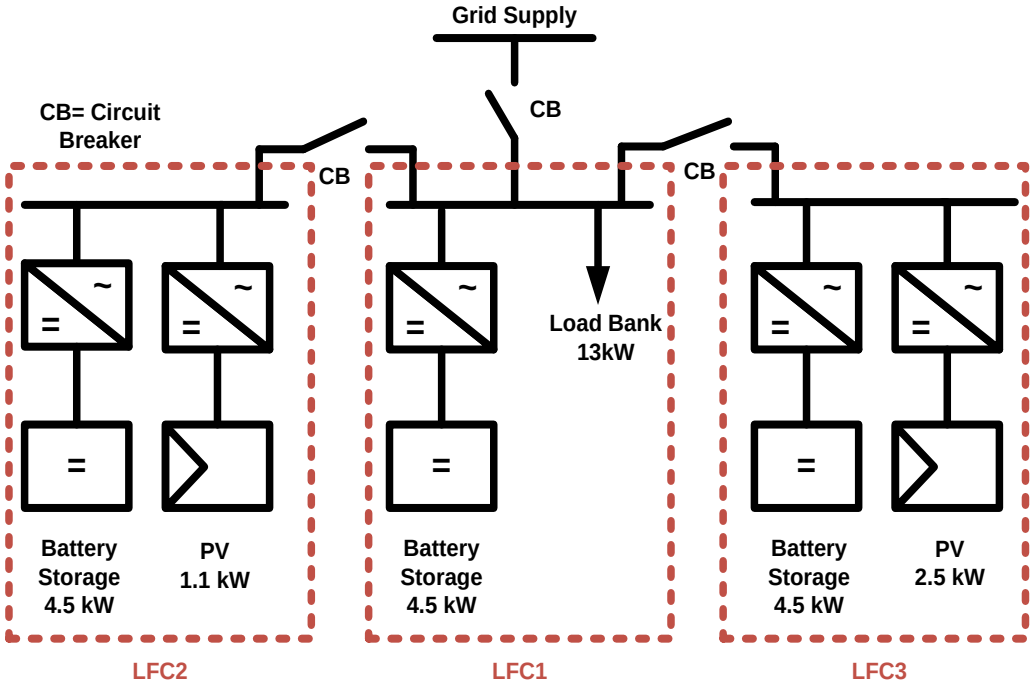

(a) CRES reference power system [57].

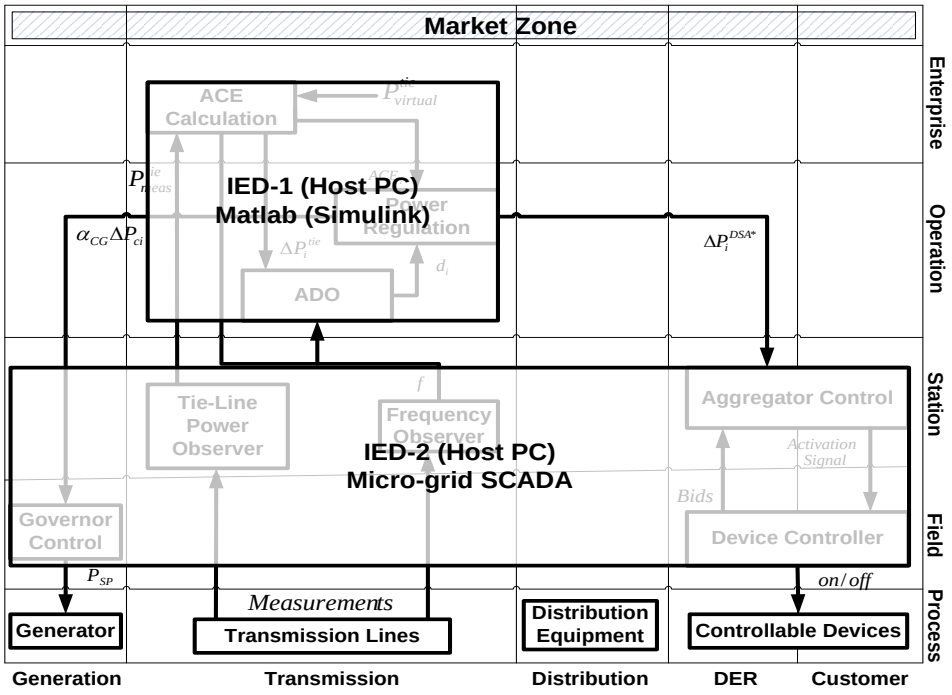

(b) CRES SGAM component layer.

Figure 5.21: SGAM information layer canonical view.

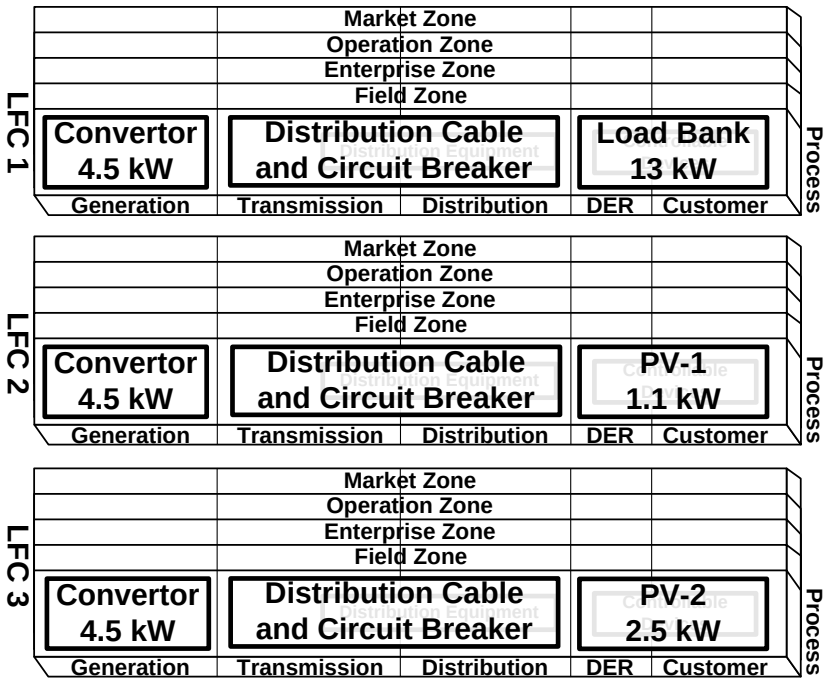

(a) CRES SGAM component layer process zones for all LFCs.

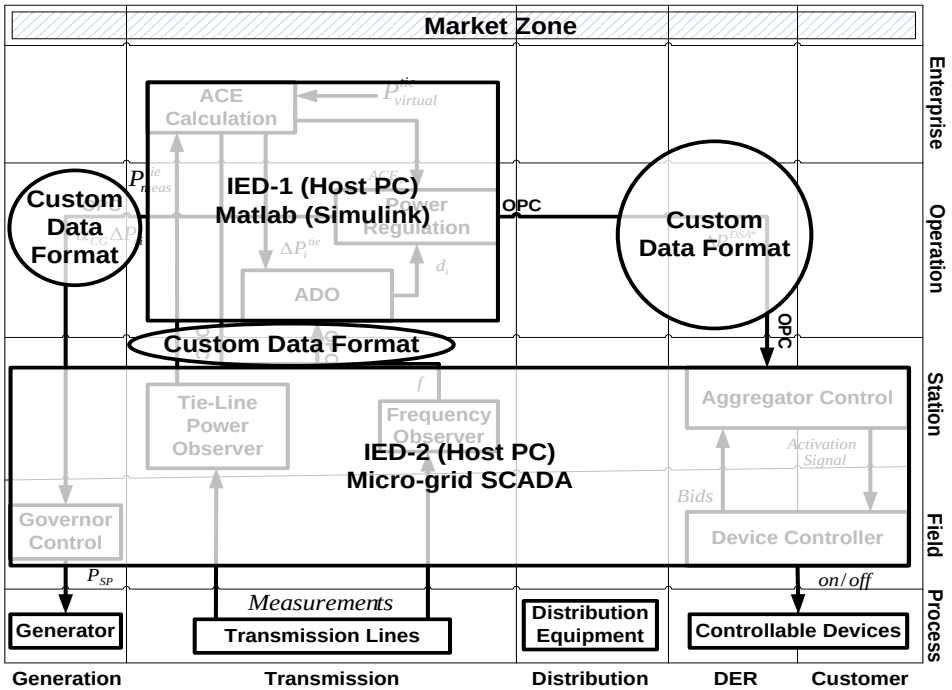

(b) CRES SGAM information layer canonical view for all LFCs.

Figure 5.22: SGAM information layer canonical view.

the reference power system (Fig. 5.21a). This further demonstrates the ability of the proposed approach to incorporate diverse implementation environments (its applicability not being limited by its development at UST).

Although it is difficult to develop standard validation process, following a structured modelling approach such as the proposed SGAM approach, supports round robin validation objectives as discussed above. At the time of reporting, experimental results from CRES were unavailable, and therefore an analysis on comparison of the results obtained was not undertaken.

5.8.5 Adaptation to Non-Monolithic Test Setups

The SGAM modelling approach presented in this work is intended for facilitating laboratory validation of novel control solutions. The methodology can accommodate a wide variety of laboratory experimental setups such as pure hardware, HiL, C-HiL and P-HiL, as demonstrated within this chapter. In addition, the approach can readily

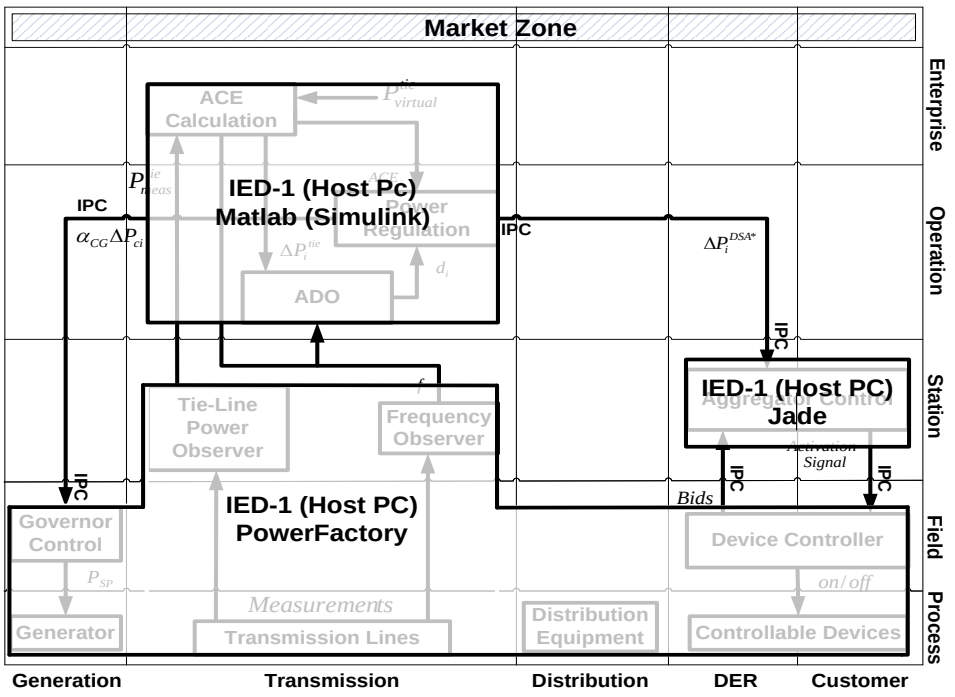

Figure 5.23: An example SGAM communication layer for co-simulation setup.

be adapted and utilised for the purpose facilitating validation by any non-monolithic setups such as those utilised within the paradigm of co-simulation. Although several multi-domain simulators such as MATLAB Simulink and OpenModelica are available to validate smart grid control solutions in a monolithic way, co-simulation is utilised when more accurate validation by means of utilising domain specific simulation tools is desired. For example, for the study presented in this chapter, three distinct domains can be identified: (i) power systems, (ii) controls and (iii) multi-agent system (MAS). For monolithic validation MATLAB Simulink can readily be utilised, however, more domain specific simulation tools exist for a thorough evaluation and can be utilised within a co-simulation setup. In Fig. 5.23, an example mapping for co-simulation setup is presented. As can be observed from the figure, three distinct simulation tools for each domain have been utilised, namely, PowerFactory for power systems, MATLAB Simulink for controls and Jade for MAS. As is common for co-simulation validation, all the three simulation tools are within the same IED and Inter Process Communication (IPC) is referred to as the common communication standard. When multiple IEDs are utilised, this can be easily captured within the mappings as earlier presented.

5.9 Conclusions

In this chapter, the transition of a control from its design to its validation is discussed. The key conclusions of the chapter are summarised below:

- The practical challenges that arise from the integration of control solutions within laboratory environments, for their validation, are identified. These practical challenges have been given little or no importance in the past, however, with increasing recognition of laboratory validations, to the best of authors knowledge, this is the first attempt at reporting these challenges.
- The challenges identified were correlated to a lack of an integrated methodology. To address this issue of lack of an integrated methodology, a structured approach that utilizes SGAM as a tool to facilitate laboratory validations is proposed.

- As per the proposed SGAM modelling approach, any control solution to be validated is first represented using the SGAM followed by adding the representation of the laboratory infrastructure which will validate the control solution. The structured approach that leads to combined representation of control solutions and laboratory infrastructure, in other words a validation environment, using the SGAM facilitates the transition from the design of radical grid control solutions, to their rigorous validation.

- The proposed SGAM modelling approach is applied to transition the EFC framework to laboratory for its validation. This served two purposes: (i) it allowed for developing the validation environment for the EFC-FB as is required for its appraisal to TRL 5, and (ii) served as a basis for evaluating the proposed SGAM modelling approach.

- An evaluation of the proposed SGAM modelling approach, apprised by the exercise of its application to EFC framework, is presented. The key findings can be summarised as:

  - The proposed SGAM modelling approach encourages cooperation of control solution developers and laboratory user groups from the design stage, entailing efficiency to the process.
  - The proposed SGAM modelling approach is laboratory independent, i.e., it supports representation of any non-monolithic validation setups, evident from its adoption in an independent smart grid laboratory (apart from DPSL where the approach was developed) and its adoption for example representation of a co-simulation setup.
  - The proposed SGAM modelling approach enhances: (i) repeatability after modification to a control solution or its implementation, or when additional control functions are incorporated, extending the scope of validation, and (ii) reproducibility, enabling independent laboratories to develop tailored validation environments for control solutions based on an example provided.

In essence, by enhancing repeatability and reproducibility of control solution validation, the proposed approach supports round robin validations.

- The conventional SGAM modelling approach is limited to representation of control solutions implemented within a single entity (for example, one DSO, one TSO, one LFC area, etc.). For the first time in this chapter, a concept to represent a control solution implemented within more than one entity is introduced. The concept still requires two individual SGAM representations, one for each entity, but enables capturing the information exchange between the two entities. This extends the ability of SGAM to represent distributed control solutions implemented between the entities.

- Consequently, for the first time, two state-of-the-art smart grid laboratories have been represented using the SGAM. The proposed SGAM modelling approach presents an effective way to communicate research infrastructure features for integration and validation of control solutions.

REFERENCES

[1] E. Widl, P. Palensky, P. Siano, C. Rehtanz, "Guest editorial modeling, simulation, and application of cyber-physical energy systems", in *IEEE Trans. Industrial Informatics*, Volume10, issue4, pp-2244-2246, 2014.

[2] T. I. Strasser, F. Andren, G. Lauss, R. Bründlinger, H. Brunner, C. Moyo, C. Seitl, S. Rohjans, S. Lehnhoff, P. Palensky, P. Kotsampopoulos N. Hatziargyriou, G. Arnold, W. Heckmann, E. Jong, M. Verga, G. Franchioni, L. Martini, A. Kosek, O. Gehrke, H. Bindner, F. Coffele, G. Burt, M. Calin, E. Rodriguez-Seco "Towards holistic power distribution system validation and testing—an overview and discussion of different possibilities", in *e & I Elektrotechnik und Informationstechnik*, pp. 71-77, 2017.

[3] "Smart Grids: from innovation to deployment", European Commission, Communication from the Commission to the European Parliament, the Council, the European Economic and Social Committee and the Committee of the Regions, 2011.

[4] "Roadmap 2010-18 and detailed implementation plan 2010-12", European Electricity Grid Initiative (EEGI), 2010.

[5] M. Maniatopoulos, D. Lagos, P. Kotsampopoulos, and N. Hatziargyriou, "Combined control and power hardware in-the-loop simulation for testing smart grid control algorithms", in*IET Generation, Transmission and Distribution*, vol. 11, no. 12, pp. 3009-3018, 2017.

[6] A. Gil de Muro, J. E. Rodriguez-Seco, E. Zabala, C. Mayr, R. Brundlinger, G. Romanovsky, O. Gehrke, and F. Isleifsson, "Inverter interconnection tests performed in the LABEIN-Tecnalia microgrid involved in the DERlab round-robin testing activity", in *proceedings of the International Conference Electrical Power Quality and Utilisation*, Lodz, pp. 1-5, 2009.

[7] R. Bründlinger, T. I. Strasser, G. Lauss, A. Hoke, S. Chakraborty, G. Martin, B.

Kroposki, J. Johnson, and E. Jong, "Lab tests: verifying that Smart Grid power converters are truly smart", in *IEEE Power Energy Magazine*, pp. 30-42, 2015.

[8] J. Belanger, P. Venne, J.-N, Paquin, "The what, where, and why of real-time simulation", Planet RT. 37-49, 2010.

[9] M. Muresan, D. Pitica, "Software in the loop environment reliability for testing embedded code", in *proceedings of IEEE 18th International Symposium for Design and Technology in Electronic Packaging*, Alba Iulia, Romania, pp. 325-328, October 2012.

[10] S. Werner, L. Masing, F. Lesniak, and J. Becker, "Software-in-the-loop simulation of embedded control applications based on virtual platforms", in *proceedings of 25th International Conference on Field Programmable Logic Applications*, London, England, pp. 1-8, September 2015.

[11] "PSSE User Manual v30.2, Siemens Power Transmission & Distribution", Siemens Power Technologies International Inc., 2005.

[12] M. Perron, E. Ghahremani, A. Heniche, I. Kamwa, C. Lafond, M. Racine, H. Akremi, P. Cadieux, S. Lebeau, and S. Landry, "Wide-area voltage control system of flexible AC transmission system devices to prevent voltage collapse", in *IET Generation, Transmission and Distribution*, vol. 11, no. 18, pp. 4556-4564, 2017.

[13] J. Coser, A. S. Costa and J. G. Rolim,"Metering Scheme Optimization With Emphasis on Ensuring Bad-Data Processing Capability", in *IEEE Trans. on Power Systems*, vol. 21, no. 4, pp. 1903-1911, Nov. 2006.

[14] J. Xu, C. Zhao, W. Liu and C. Guo, "Accelerated Model of Modular Multilevel Converters in PSCAD/EMTDC", in *IEEE Trans. on Power Delivery*, vol. 28, no. 1, pp. 129-136, Jan. 2013.

[15] X. Wu, V. Simha, Y. Xue and R. Wellman, "Substation Grounding Studies with More Accurate Fault Simulation Strategy and SI / MI Method", in *IEEE Trans. on Power Delivery*, vol. PP no. 99, pp. 1-1, 2018.

[16] J. Tant and J. Driesen, "On the Numerical Accuracy of Electromagnetic Transient Simulation with Power Electronics," in *IEEE Trans. on Power Delivery*, vol. PP no. 99, pp. 1-1, 2018.

[17] K. Johnstone, S. M. Blair, M. H. Syed, A. Emhemed, G. M. Burt and T. I. Strasser, "Co-simulation approach using PowerFactory and MATLAB/Simulink to enable validation of distributed control concepts within future power systems," in *CIRED - Open Access Proceedings Journal*, vol. 2017, no. 1, pp. 2192-2196, 10 2017.

[18] T. I. Strasser, M. Stifter, F. Andrén, and P. Palensky, "Co-simulation training platform for smart grids", in *IEEE Trans. on Power Systems*, 1989-1997, 2014.

[19] C. Steinbrink, S. Lehnhoff, S. Rohjans, T. I. Strasser, E. Widl, C. Moyo, G. Lauss, F. Lehfuss, M. Faschang, P. Palensky, A. A. van der Meer, K. Heussen, O. Gehrke, E. Guillo-Sansano, M. H. Syed, A. Emhemed, R. Brandl, V. H. Nguyen, A. Khavari, Q. T. Tran, P. Kotsampopoulos, N. Hatziargyriou, N. Akroud, E. Rikos, and M. Z. Degefa "Simulation-based validation of smart grids - status quo and future research trends", in *Proc. Int. Conf. on Ind. Appl. of Holonic and Multi-Agent Syst.*, Lyon, pp. 171-185, 2017.

[20] J. Jeon, J. Kim, H. Kim, S. Kim, C. Cho, J. Kim, J. Ahn, and K. Nam "Development of hardware in-the-loop simulation system for testing operation and control functions of microgrid", in *IEEE Trans. on Power Electronics*, 25, (12), pp. 2919-2929, 2010.

[21] M. O. Faruque, and V. Dinavahi, "Hardware-in-the-loop simulation of power electronic system using adaptive discretization",in *IEEE Trans. on Industrial Electronics*, pp. 1146-1158, 2010.

[22] J. Wang, Y. Song, W. Li, J. Guo, and A. Monti, "Development of a universal platform for hardware in-the-loop testing of microgrids",in *IEEE Trans. on Industrial Informatics*, pp. 2154-2165, 2014.

[23] P. Kotsampopoulos, F. Lehfuss, G. Lauss, B. Bletterie, and N. D. Hatziargyriou, "The limitations of digital simulation and the advantages of PHIL testing in studying distributed generation provision of ancillary services", in I*EEE Trans. on Industrial Electronics*, 62, (9), pp. 5502-5515, 2015.

[24] M. Steurer, C. S. Edrington, M. Sloderbeck, W. Ren, and J. Langston, "A megawatt-scale power hardware-in-the-loop simulation setup for motor drives", in*IEEE Trans. on Industrial Electronics*, 57, (4), pp. 1254-1260, 2010.

[25] G. F. Lauss, M. O. Faruque, K. Schoder, C. Dufour, A. Viehweider, and J. Langston, "Characteristics and design of power hardware-in-the-loop simulations for electrical power systems", in *IEEE Trans. on Industrial Electronics*, 63, (1), pp. 406-417, 2015.

[26] M. Heder, "From NASA to EU: the evolution of the TRL scale in Public Sector Innovation", in *The Innovation Journal*, pp. 1-23, 2017.

[27] "Test protocols for advances inverter interoperability functions", Sandia National Laboratories, Sandia Corporation, pp 1-22, 2013.

[28] IEC/TR 61850 (2003-04), Communication networks and systems in substations.

[29] CIM Users Group's Home Page, http://cimug.ucaiug.org/default.aspx

[30] "The Project", https://erigrid.eu/the-project/

[31] B. Marick, "New Models for Test Development", http://www.exampler.com/testing-com/writings/new-models.pdf

[32] C. Bucanac, "The V-Model", Quality Management, University of Karlskrona/Ronneby.

[33] T. Weilkiens, J. G. Lamm, S. Roth, and M. Walker, "Model based system architecture", John Wiley and Sons.

[34] "What is V-model- advantages, disadvantages and when to use it?", http://istqbexamcertification.com/what-is-v-model-advantages-disadvantages-and-when-to-use-it/

[35] R. S. Pressman, "Software Engineering: A Practitioner's Approach", The McGraw-Hill Companies.

[36] M. Hoffman, and B. Beaumont, "Application Development: Managing the Project Life Cycle", Mc Press.

[37] "Standardization Mandate to European Standardisation Organisations (ESOs) to support European Smart Grid deployment", European Commission. [Online]. Available: https://ec.europa.eu/energy/sites/ener/files/documents/2011_03_01_mandate_m490_en.pdf

[38] "NIST Framework and Roadmap for Smart Grid Interoperability, Interoperability Standards Release 1.0", Office of the National Coordinator for Smart Grid Interoperability, National Institute of Standards and Technology, U.S. Department of Commerce, 2009.

[39] "GridWise Interoperability Context-Setting Framework", 2008, GridWise Architecture Council, www.gridwiseac.org.

[40] "IntelliGrid Methodology for Developing Requirements for Energy Systems", IEC/PAS 62559. [Online]. Available: https://webstore.iec.ch/preview/info_iecpas62559%7Bed1.0%7Den.pdf

[41] "TOGAF 9 and ArchiMate 1.0 White paper", The Open Group 2010, [Online]. Available: http://pubs.opengroup.org/architecture/togaf9-doc/arch/ and http://pubs.opengroup.org/architecture/archimate2-doc/

[42] "Smart Grid Coordination Group (SGCG) First Set of Standards", CEN, CENELEC, and ETSI, Nov. 2012.

[43] R. Santodomingo, M. Uslar, A. Goring, M. Gottschalk, L. Nordstrom, A. Saleem, and M. Chenine, "SGAM-based methodology to analyse Smart Grid solutions in

DISCERN European research project", in *proceedings of 2014 IEEE International Energy Conference (ENERGYCON)*, Cavtat, pp. 751-758, 2014.

[44] "Annex I: Description of the Work", Distributed Intelligence for Cost-Effective and Reliable Distribution Network Operation (DISCERN) EU project, September 2012, http://www.discern.eu/

[45] "Deliverable D4.2: New system functionality", Distributed Intelligence for Cost-Effective and Reliable Distribution Network Operation (DISCERN), Jan. 2014.

[46] "Smart Grid Coordination Group (SGCG) Reference Architecture Smart Grid", CEN, CENELEC, and ETSI, Nov. 2012.

[47] "Smart Grid Coordination Group (SGCG) Methodology and New Applications", CEN, CENELEC, and ETSI, Dec. 2014.

[48] "Deliverable D1.3: Architecture templates and guidelines", Distributed Intelligence for Cost-Effective and Reliable Distribution Network Operation (DISCERN), Nov. 2013.

[49] "Draft IEC 62559: Use Case Methodology – Part 2: Definition of the templates for use cases, actor list and requirements list", IEC TC8 Standard, Jun. 2013.

[50] Blank, S. Lehnhoff, K. Heussen, D. E. M. Bondy, C. Moyo, and T. Strasser, "Towards a foundation for holistic power system validation and testing", in *proceedings of 2016 IEEE 21st International Conference on Emerging Technologies and Factory Automation (ETFA)*, 2016.

[51] "Proposal for the bidding and activation process and balancing energy products for the bid ladder platform", Elia. [online] Available: http://www.elia.be/en/users-group/ad-hoc-taskforce-balancing/Bid-ladder-platform.

[52] M. H. Syed, G.M. Burt, R. D'Hulst, and J. Verbeeck,"Experimental Validation of Flexibility Provision by Highly Distributed Demand Portfolio", in *proceedings of the 2016 CIRED Workshop*, pp. 1-4, Helsinki, Finland, 2016.

[53] P. Dambrauskas, M. H. Syed, S. M. Blair, J. M. Irvine, I. F. Abdulhadi, G. M. Burt, and D. E. M. Bondy "Impact of realistic communications for fast-acting demand side management," *in CIRED - Open Access Proceedings Journal*, vol. 2017, no. 1, pp. 1813-1817, 10 2017.

[54] T. Magisos, "Real-time Simulation and Model-Based-Systems Engineering using Commercial-Off-The-Shelf (COTS) Computer Equipment", Applied Dynamics International (ADI). [Online]. Available: https://www.adi.com/wp-content/uploads/2016/06/Real-time_COTS_Paper_v1.7.pdf

[55] S. M. Blair, "Beckhoff and TwinCAT 3 System Development Guide" Report. [Online]. Available https://strathprints.strath.ac.uk/55254/

[56] "Simulink Coder - Generate C and C++ code from Simulink and Stateflow models", MathWorks, 2012. [Online]. Available: http://www.mathworks.co.uk/products/simulinkcoder/.

[57] A. Neris, S. Tselepis, and C. Protogeropoulos, "Description of a Simulated Microgrid Test Field Facility and Results from System Testing under Different Load Control Strategies", in *proceedings of CIGRE Symposium, Power Systems with Dispersed Generation*, Athens, Greece, 13-16 April 2005.

Chapter 6

Appraisal of Fast Balancing Enhanced Frequency Control to TRL 5

6.1 Introduction

The validation of the fast balancing enhanced frequency control (EFC-FB) in real-time has demonstrated the feasibility and soundness of the approach effectively appraising it to technology readiness level (TRL) 3. With the three purpose of investigations (PoI) set in Chapter 5, in this chapter, the EFC-FB is appraised to TRL 5. In accordance with the PoI's, first the results of controller hardware-in-the-loop (C-HiL) implementation are presented. This involves the prototypical implementation of the EFC-FB within a controller hardware. This is followed by results from a C-HiL implementation incorporating realistic communications delays. With the C-HiL validation, EFC-FB is appraised to TRL 4. The incorporation of the reference power system, the five area Great Britain (GB) power system, in a power hardware-in-the-loop (P-HiL) setup is presented. This complex setup presented a challenge in terms of initialisation and synchronisation, for which a range of alternatives are investigated and recommended approach identified. This is followed by appraising the performance of EFC-FB under

a realistic environment to TRL 5.

6.2 Validation Results

In this section, the validation results for each of the PoI identified in Chapter 5 are presented.

6.2.1 PoI-1

The PoI-1 can be reiterated as follows:

PoI-1: The performance of the EFC-FB has been verified by means of real-time simulations. To ensure its deployment in a real-world, a C-HiL, where the EFC-FB will be prototyped within a hardware controller is required. Therefore, the first PoI is formulated as the characterisation of system frequency response with and without EFC-FB under pure real-time implementation compared to C-HiL implementation.

The abstract representation of the C-HiL setup is presented in Fig. 6.1. The EFC-

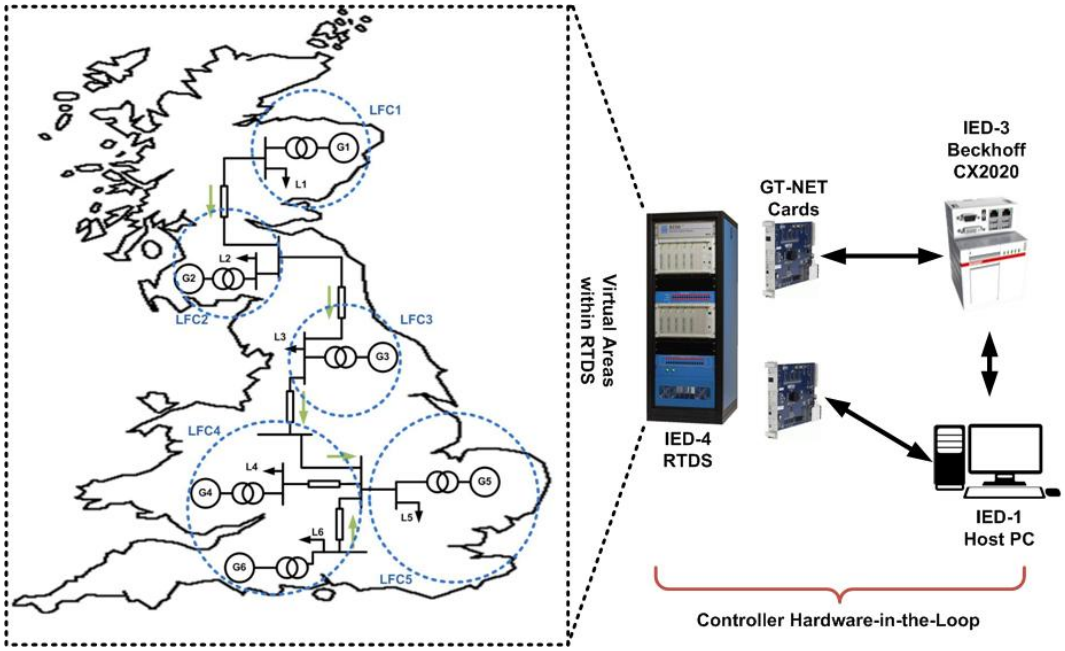

Figure 6.1: Abstract representation of C-HiL setup

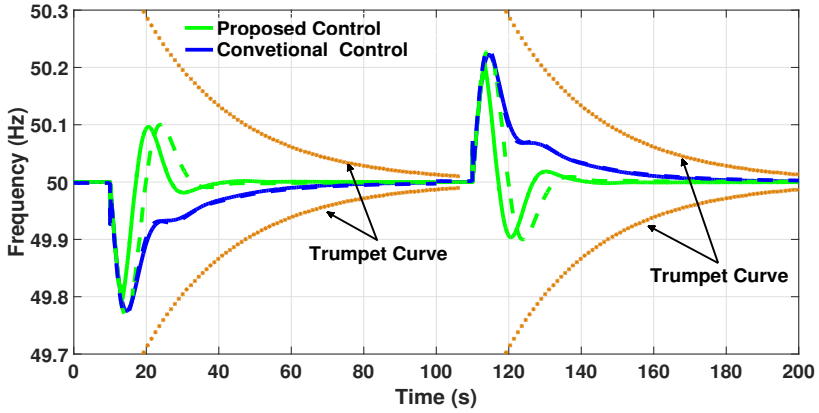

(a) Frequency; solid line represents pure simulation and dotted line represents C-HiL implementation.

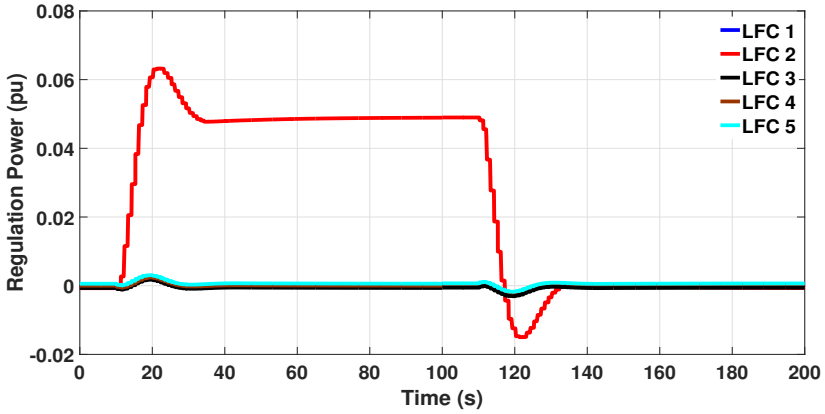

(b) Regulation power, C-HiL implementation.

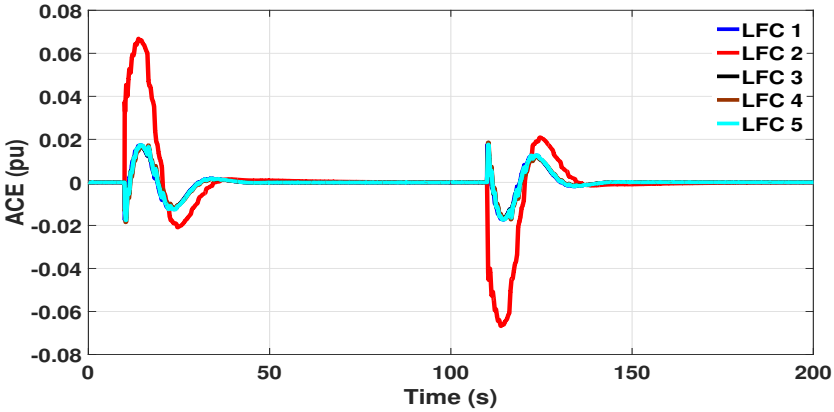

(c) Area control error (ACE), C-HiL implementation.

Figure 6.2: PoI-1: EFC-FB performance comparison, pure simulation vs C-HiL implementation.

Table 6.1: PoI-1: Test Metrics

Control and Implementation	T^{Rest} (s)	Δf^{ovr} (%)	f^{dev}_{max} (Hz)
Conventional LFC pure simulation	61.67	-	0.224
EFC-FB pure simulation	27.64	42.5	0.208
Conventional LFC C-HiL implementation	70.84	-	0.233
EFC-FB C-HiL implementation	31.41	43.2	0.231

FB is run at a time step of 10ms with the time constant of balance control loop's auxiliary controller chosen as $T_{I,aux} = 5s$, while all other parameters remain same as in Chapter 3. The system is subject to two disturbances in LFC 2, a loss of generation and a loss of load, with same magnitude as that of reference event. The performance will be assessed in terms of the three metrics defined in Chapter 5, frequency restoration time (T^{Rest}), relative frequency overshoot (Δf^{ovr}), and maximum frequency deviation (f^{dev}_{max}).

Upon running the simulation after the implementation, the EFC-FB did not perform as expected. The framework was unable to detect the location of the imbalance event, thereby rendering the control to be effectively same as the conventional load frequency control (LFC) framework. Upon an investigation of the implementation, it was found that a switch that was utilised in calculation of the extremum of rate of change of frequency was being reset. However, this implementation error was not noticed throughout the real-time simulation validation phase. A further investigation revealed that the small time-step implementation of the EFC-FB within the real-time simulations was masking the switch reset. A C-HiL implementation running at the intended time-step revealed the discrepancy. Although RTDS does allow for combined small and large time-step simulations, this is intended to be utilised for power electronic applications, where small time step refers to $2\mu s$ and large time-step refers to 50 μs. RTDS does not allow for multi-rate simulations for control applications where the intended large time-step is of the order of tens of milli-seconds. This is precisely the reason for undertaking C-HiL implementation where the control under test is prototyped. It allows for any implementation errors to be identified and resolved. The identified error was remedied for further testing.

The system frequency response subject to generation loss at t = 10s and a load loss at t = 110s is presented in Fig. 6.2 and the corresponding metrics in Table 6.1. The results for conventional LFC framework have been presented in addition to the EFC-FB for both, the pure simulation and C-HiL implementation. As can be observed from the results, there is a small difference in restoration time, with C-HiL implementation slower than pure simulation. More importantly, the overshoot is reduced in the C-HiL implementation. However, this is not to be observed as improvement in performance as the improvement in relative overshoot is due to a lower frequency nadir. The frequency nadir for EFC-FB with C-HiL implementation is lower than pure simulation for the presented disturbance. Although C-HiL implementation presents worse performance when compared to pure simulation implementation, the EFC-FB framework still presents improved performance compared to conventional LFC framework. The characterisation of frequency response is complete.

It can therefore be said that the objective of PoI has been successfully achieved. The exercise has lead to the identification in implementation errors, allowing for it to be resolved before its implementation with power hardware. Furthermore, the ability of EFC-FBs deployment in a distributed manner, prototyped within controllers, is proven.

6.2.2 PoI-2

PoI-2 can be reiterated as follows:

PoI-2: A detailed study on experimental validation of ancillary service provision capability of aggregators controlling a portfolio of highly distributed demand side devices has been undertaken by the author [1]. The study identifies that validation of any control relying on demand side aggregators for provision of time critical ancillary services, should incorporate the communication delays to demonstrate robustness. Furthermore, the results presented earlier in this thesis assumes a fixed communications delay. However, the communication delay referred to in here is the time it takes for a control command from the aggregator to reach the participating device and is highly dependent upon the communication architecture used by the potential demand side aggregator.

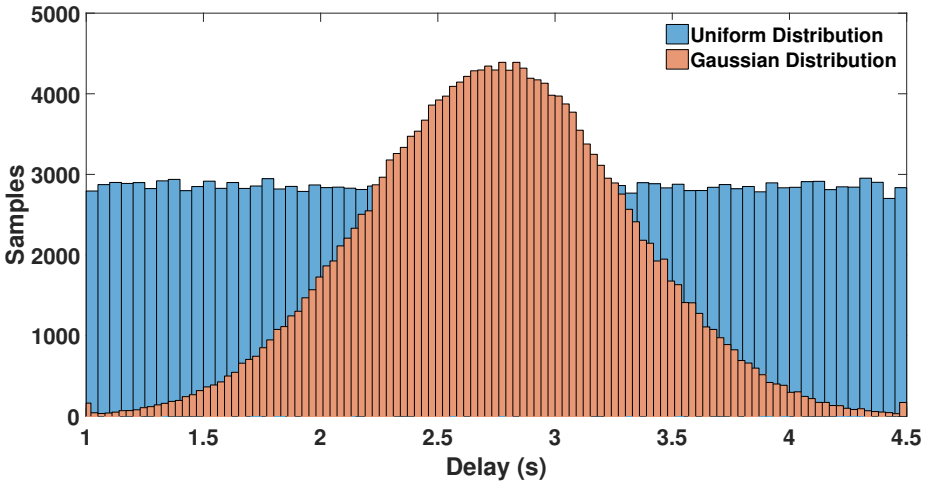

Figure 6.3: Time delay distribution utilised for PoI-2

Therefore, the second PoI has been formulated as the the characterisation of system frequency response with EFC-FB incorporating no communication delays compared to implementation incorporating realistic delays in C-HiL implementation. As this work does not consider any specific aggregator, the common communication architecture for aggregators defined in [2] will be utilised.

The performance of the communications networks that connects a control centre to the end devices for demand side applications has been analysed in [2] and the results show that the latency expected is between 1-4.5 seconds. The analysis presents an estimation of delay based on assumptions of technology and communications infrastructure. However, it does not provide a mean value for the delay nor a standard deviation. The variation in delay is mostly associated to the number of hops a packet will need to make in the neighbourhood area network before it reaches the device. For this work, two types of distributions will be considered as shown in Fig. 6.3, a uniform distribution and a Gaussian distribution. The probability distribution function for Gaussian distribution is given by

$$f(x) = \frac{1}{\sigma\sqrt{2\pi}} e^{-\frac{1}{2}\left(\frac{x-\mu}{\sigma^2}\right)^2} \tag{6.1}$$

where the mean value μ has been chosen as 2.75s (average of minimum and maximum latency) with a standard deviation of σ of 0.3s. The probability density function for

uniform distribution is given by

$$f(x) = \begin{cases} 0 & x \leq \mu - \frac{\sigma}{2} \\ \frac{1}{\sigma} & \mu - \frac{\sigma}{2} < x < \mu + \frac{\sigma}{2} \\ 0 & \mu + \frac{\sigma}{2} \leq x \end{cases} \tag{6.2}$$

when generating random numbers over a specified boundary (the delay range in this case), it is necessary to normalize the distributions such that each differential area is equally populated. In addition, random selection from uniform distributions are not

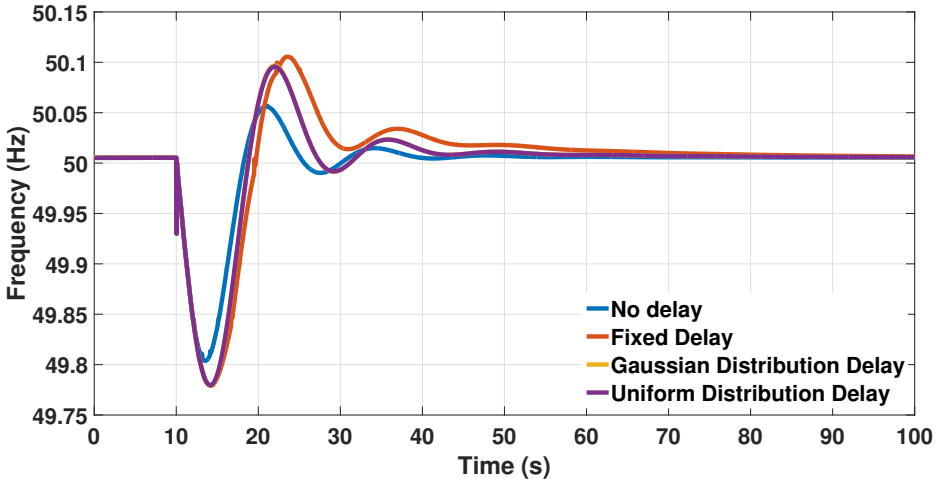

(a) Frequency.

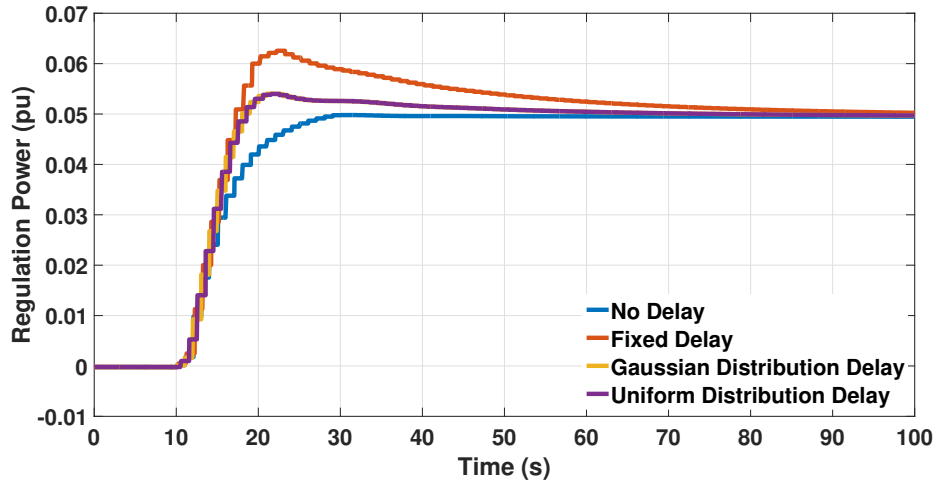

(b) Regulation power.

Figure 6.4: PoI-2: EFC-FB performance comparison with delays.

perfectly uniform.

Table 6.2: PoI-2: Test Metrics

Delay	T^{Rest}	Δf^{ovr}	f^{dev}_{max}
No delay	24.16	28.7	0.195
Fixed delay	59.86	47	0.23
Gaussian distribution delay	42.37	44	0.22
Uniform distribution delay	42.3	43.6	0.22

The parameters of the control except for the delays remain same as in the previous study. The response of the system subject to reference imbalance with EFC-FB incorporating different delays is presented in Fig. 6.4 and test metrics in Table 6.2. The value of fixed delay utilised is 3s. As can be observed, there is not much difference in performance when two different distributions of delay are utilised. With a fixed delay the frequency presents a slightly higher overshoot and restoration time. Communications delay plays an important role in selection of control parameters. To explain this further, consider the frequency responses presented in Fig. 6.5. In addition to frequency response with no delay and Gaussian distribution delay, two frequency responses are presented. The frequency response in red corresponds to a fixed delay of 5.5s with $T_{I,aux} = 5s$. The frequency response in green corresponds to Gaussian distribution

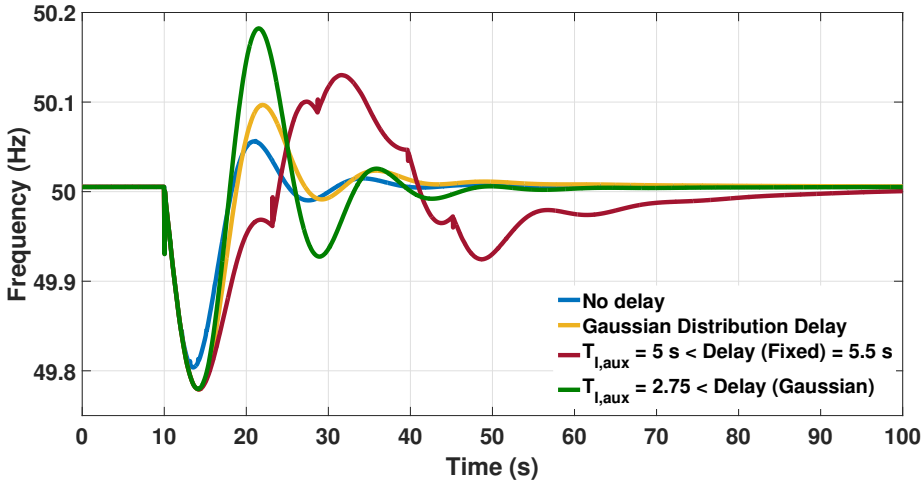

Figure 6.5: PoI-2: Further analysis of ELFC performance with delays.

delay (as presented earlier) with $T_{I,aux} = 2.75s$. In both cases, the value of $T_{I,aux}$ is less than the delay and the frequency response of the system deteriorates. Ignoring communications delay can lead to selection of parameters that can risk the stability of the system. Therefore, for the proposed control, the value of $T_{I,aux}$ should always be chosen greater than or equal to the worst case delay expected. As has been shown in Fig. 6.4a, the response of the system incorporating delays characterised for demand side applications is stable, with slightly lower frequency zenith but not much different restoration time.

In a real world scenario, fixed delay is unlikely to present itself due to the nature of communications network. In presence of fixed and varying delay, the performance of the proposed framework is verified. It can therefore be said that, the response of the system with EFC-FB incorporating different delays has been characterised, fulfilling the objective of PoI-2.

6.2.3 PoI-3

PoI-3 can be reiterated as:

PoI-3: The performance improvement of EFC-FB over present day LFC framework has been achieved by means of incorporation of balance control loop (BCL) that relies on area disturbance observer for a faster disturbance detection. The disturbance detection utilizes rate of change of frequency (RoCoF), that is regarded as a very noisy measurement. Any control that relies on RoCoF should therefore be validated by means of real measurements enabled by power hardware-in-the-loop implementation. Therefore, the final PoI is to validate the disturbance detection function of the proposed control in P-HiL implementation.

The P-HiL setup incorporating the reference power system is complex and therefore, before the PoI-3 is investigated further, the P-HiL setup will be presented in detail in the following section.

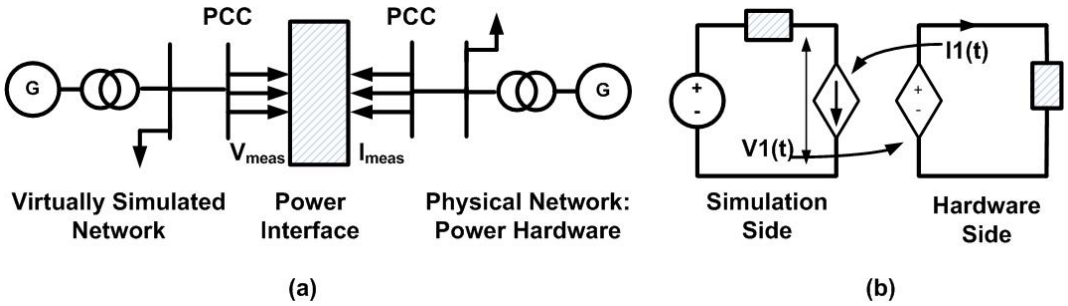

Figure 6.6: Example P-HiL setup

6.3 The P-HiL Setup

6.3.1 Components of the P-HiL Setup

An example representation of a P-HiL setup is presented in Fig. 6.6a. As can be observed from the figure, a P-HiL implementation comprises a virtually simulated network implemented within a digital real-time simulator (DRTS), a hardware component referred to as the hardware under test (HuT), and the power interface used for interconnecting both the subsystems [3]. The HuT connected to the simulation can represent a generation or a load component depending upon the direction of power flow at the chosen point of common coupling (PCC). The power interface hosts an interface algorithm allowing interconnection of the two subsystems. Different interface algorithms have been described in the literature [4-7]. For the purpose of this work, the voltage ideal transformer method (ITM) [4] where the voltage from the software side is represented on the hardware side using a voltage source and the currents from the hardware side are fed back using a current source on the simulation side (as shown in Fig. 6.6b), has been selected due to its straightforward implementation and good stability performance. T

In this section, the different components of the P-HiL setup are briefly described. First the simulation model of the GB reference power system is described establishing the PCC, followed by the presentation of the characteristics of the power interface used for the interconnection of the simulated system with the hardware, and finally the HuT utilised is detailed.

Great Britain Power System

A single line diagram of the reduced five-area GB power system is shown in Fig. 6.7. The bus wise generation, bus wise active and reactive power load, inter-area power flows have been presented in Tables 6.3 - 6.7. As can be observed from Fig. 6.7, the

Table 6.3: Bus wise Generation (MVA)

G_1	G_2	G_3	G_4	G_5	G_6
11500	20500	9660	16000	5500	500

Table 6.4: Bus wise Load: Active (MW)

L_1	L_2	L_3	L_4	L_5	L_6
8486	12548	8398	26852	2000	100

Table 6.5: Bus wise Load: Reactive (MVAR)

L_1	L_2	L_3	L_4	L_5	L_6
4109	6077	4067	13005	1041	500

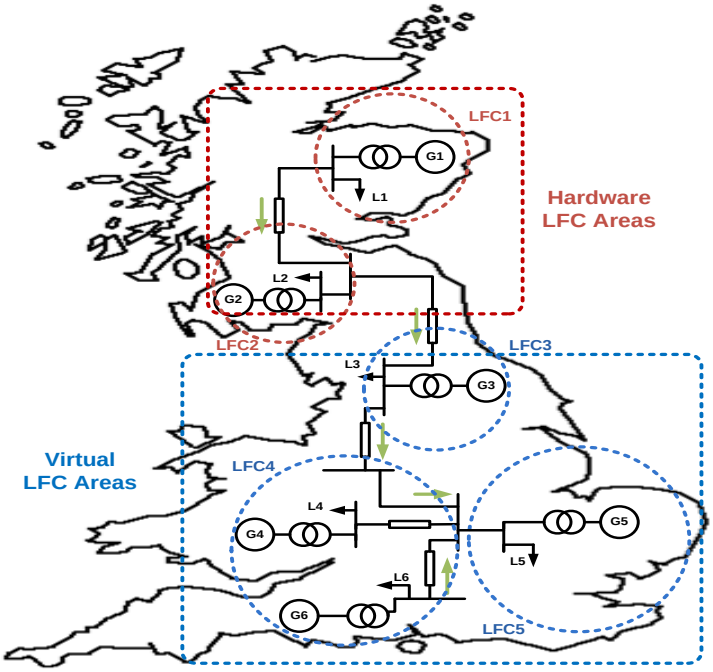

Figure 6.7: Five area GB reference power system.

Table 6.6: Inter-Area Power Flow: Active (MW)

$P_{LFC_1-LFC_2}$	$P_{LFC_2-LFC_3}$	$P_{LFC_3-LFC_4}$	$P_{LFC_4-LFC_5}$
2097	8900	9105	13080

Table 6.7: Inter-Area Power Flow: Reactive (MVAR)

$Q_{LFC_1-LFC_2}$	$Q_{LFC_2-LFC_3}$	$Q_{LFC_3-LFC_4}$	$Q_{LFC_4-LFC_5}$
1328	4257	5025	7088

HuT is to represent area 1 and 2 of the GB power system while the remaining areas will be part of the simulated network on the DRTS. As can be observed from Table 6.6 and 6.7, there is an active and reactive power flow from area 2 to area 3. Therefore, the PCC is between area 2 and 3, with the active and reactive power flow from area 2 to area 3 as 8900 MW and 4257 MVAR respectively.

Power Interface

The power interface is a 90kVA back-to-back converter unit with a switching frequency of 8 kHz responsible for amplifying the voltage received from the simulation (in this case with voltage ITM interface algorithm). The power interface amplifies and reproduces the voltages received from the simulation and therefore is controlled as a voltage source. At the same time, in the configuration used for this experiment, the power interface is also responsible for measuring the response of the HuT and sending it back to the DRTS for closing the loop with the simulation. Having analog-to-digital and digital-to-analog conversions at both ends, analog interface signals are exchanged between the power interface and the DRTS.

HuT

Components from the dynamic power system laboratory (DPSL) will constitute the HuT in this work. DPSL comprises a reconfigurable 125kVA, 400V three-phase AC power network with multiple controllable supplies and loads with flexible control systems and interfaces. The one line diagram of DPSL is presented in Fig. 6.8. The network is designed such that it can be split into three separate power islands (rep-

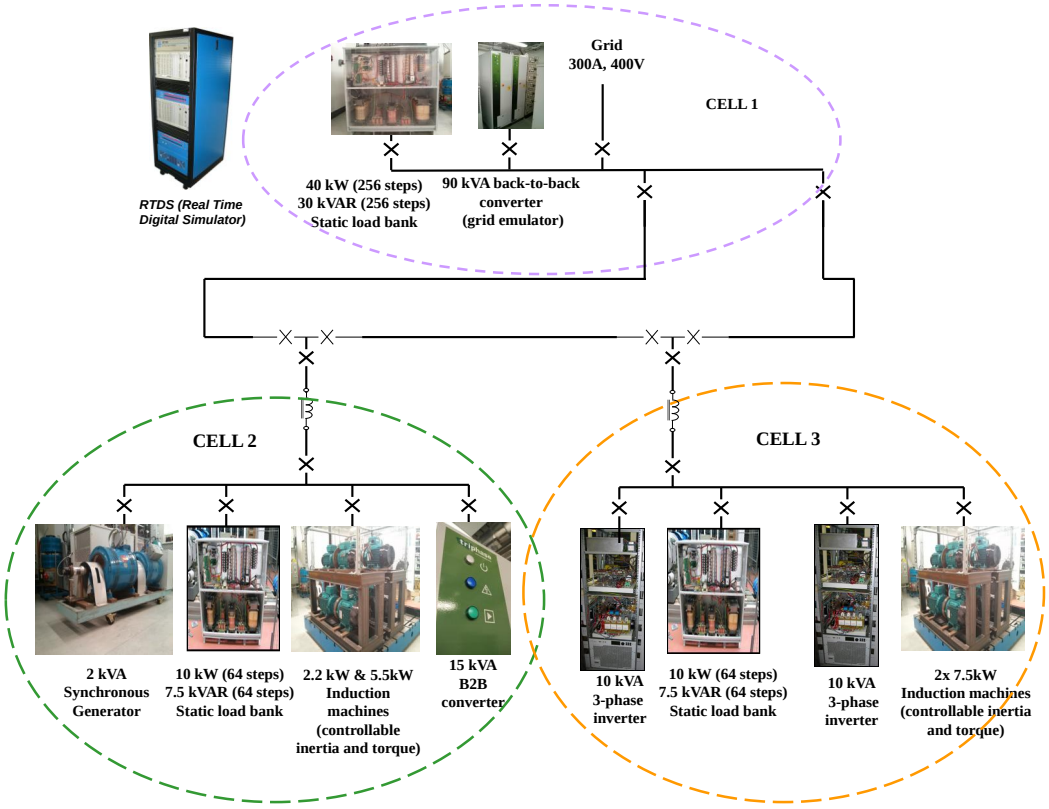

Figure 6.8: Dynamic Power Systems Laboratory Architecture

resented as cells in Fig. 6.8) under independent control, or connected together as an interconnected system.

The laboratory comprises two three-phase back-to-back converters (90kVA and 15kVA), two 10 kVA three-phase inverters, a 2kVA synchronous generator, and three static load banks. For the case under study,the power flow at PCC needs to be matched by the HuT, effectively emulating generation. Cell 2 and Cell 3 of the DPSL represent area 2 and area 1 respectively (as per the components identified in Chapter 5), while the 90 kVA back-to-back converter is used as the power interface. Since the laboratory equipment is relatively small compared to the required power transfers at the PCC, the response of the HuT (the measured currents at the hardware PCC) will be scaled up proportionally to match the test scenario. With the DPSL, the maximum power injection is limited by the capability of the two generation units within Cell 2 and 3,

i.e. 10kVA per cell. In order to represent the 8900MW and 4257MVAR from area 1 and 2, the hardware currents are scaled by means of a scaling factor. For this work the scaling factor is chosen as k=1x10^6.

6.3.2 Initialisation and Synchronisation of the P-HiL Setup

The incorporation of the five area GB reference power system within P-HiL setup entails the representation of a large portion of the test network by HuT. Such a P-HiL setup has not been reported in literature and presents challenges that need to be addressed. In the following sub-sections, first the challenge is defined followed by exploring the options available to address the challenge.

Challenge: A Paradoxical Scenario

The process of setting up a P-HiL simulation involves the following steps:

1. The power network within the DRTS is initialised, allowing for it to attain a steady state (referred to as initialisation in this work).

2. Interface signals from the initialised DRTS simulation are reproduced by the power interface.

3. The HuT response to the reproduced signals is measured and fed back to the DRTS by the power interface to complete the loop (referred to as synchronisation in this work).

For studies of synchronous power systems, the load and generation conditions along with the power transfer at selected points of interest are selected from known scenarios. This allows for testing under known stress conditions of the network or scenarios of interest (for example, a measured past pre-fault condition of the network, where a novel control algorithm can be tested in order to analyse if the performance of such controller can improve the behaviour compared to the former one). Therefore, when a P-HiL simulation is initialised and synchronised, it is important to ensure that the conditions at the different buses of the test network are comparable to that of a pure simulation.

In most P-HiL applications, the HuT is or represents a relatively small portion of the network compared to the grid emulation i.e., the rest of the system being simulated on the DRTS [8-10]. In such cases, the DRTS simulation can be initialised without the HuT, as the power network within the DRTS is usually a stiff grid whose voltage and frequency are not dependent upon the HuT to be interconnected. In a similar manner, the HuT is synchronised with DRTS simulation by means of a simple switch, closing the loop between HuT and DRTS. Operation of a switch always introduces transient; however, in cases where the simulated network is a stiff grid or the HuT is a small network component, this transient does not pose a risk to the stability of the system. It can therefore be said that the process of initialisation and synchronisation of P-HiL setup is relatively straightforward.

However, for the case under study, the HuT represents a significant portion of the test network. In such cases, the initialisation and synchronisation of P-HiL experiment presents a paradoxical scenario where the DRTS simulation cannot be initialised without the hardware currents, while the hardware currents cannot be produced without the DRTS simulation being initialised. To elaborate, as the HuT to be connected represents a large portion of generation of the test network, the DRTS simulation will fail to initialize due to the lack of generation. Without the DRTS simulation initialised, the power interface will not be capable of reproducing the interface signals and therefore the HuT response cannot be synchronised. On the other hand reproducing the interface signal during the initialisation of DRTS is risky as the signal might not be suitable for reproduction or may be over the safety limits of the power amplifier and HuT.

A number of studies have investigated the stability of P-HiL simulations [11-13], where the main findings are related to stability thresholds imposed by the interface algorithms used for the P-HiL implementation. Improvements to alleviate the identified stability limitations have been proposed in [14], [15]. However, these studies investigate the stability of a P-HiL setup, assuming that the initialisation of the P-HiL simulation sections, virtual and hardware, have been successfully completed independently and synchronisation by switch is feasible.

In the following sub-sections the options identified for initialisation and synchroni-

sation of P-HiL simulations, where the HuT represents a larger or significant portion of the test network such that the conventional approaches can no longer be employed, are presented. Through a discussion of the the advantages and disadvantages of each of the options, this sub-section aims to deduce the the best combination to be utilised.

Options for Initialisation of DRTS Simulation

As has been explained, the GB power system within the DRTS fails to initialize due to a lack generation. Therefore, to allow for the simulation to initialize, an auxiliary generation can be utilised, and the following four possible options have been identified. It should be noted that the options presented below are for more generic P-HiL setups and not limited to the case under study.

Detailed Simulation of HuT: A detailed model of the HuT can be developed as part of the network for initialising the DRTS simulation. In most cases, a detailed model would be the best option, however, developing a detailed model of the HuT can be an arduous task, and considering that the power flows at the PCC are known, much simpler solutions can be utilised.

AC Voltage Source: Readily available in every power system simulation tool, an AC voltage source can be utilised to initialize the test network for P-HiL simulation. However, as the AC voltage source acts as an infinite source, the power flow of the network at the PCC cannot be controlled. This would lead to, what can be referred to as, an unsuccessful initialisation as the state of the network is no longer the intended test scenario, required for comparison of results (with pure simulation results).

Synchronous Generator: A synchronous generator model can control the active power at its output terminals for emulating the required active power transfers at the PCC by means of a simple set-point. The reactive power of a synchronous generator is controlled by controlling the voltage at its terminal (controlling the excitation system). Either manual tuning of the voltage reference to the exciter or developing a simple PI control is required to attain the required reactive power flow at the PCC.

AC Controlled Current Source: For the emulation of power transfer behaviour at the PCC, a controlled current source allows for easiest implementation and high accuracy. This implementation will only require the measured voltage and the active, reactive power set points at the PCC for generating the current signals as:

$$I_d = \frac{P_{ref}V_d - Q_{ref}V_q}{V_d^2 + V_q^2} \tag{6.3}$$

$$I_q = \frac{P_{ref}V_q + Q_{ref}V_d}{V_d^2 + V_q^2} \tag{6.4}$$

where I_d is the direct axis current, I_q is the quadrature axis current, P_{ref} and Q_{ref} are the reference active and reactive powers to be injected at the PCC respectively, V_d is the direct axis voltage at PCC and V_q is the quadrature axis voltage at PCC. The direct and quadrature axis voltages required can be obtained with Park's transformation as:

$$\begin{bmatrix} V_d \\ V_q \\ V_0 \end{bmatrix} = \frac{2}{3} \begin{bmatrix} cos(\theta) & cos(\theta - 2\pi/3) & cos(\theta + 2\pi/3) \\ -sin(\theta) & -sin(\theta - 2\pi/3) & -sin(\theta + 2\pi/3) \\ 1/2 & 1/2 & 1/2 \end{bmatrix} \begin{bmatrix} V_a \\ V_b \\ V_c \end{bmatrix} \tag{6.5}$$

The three phase currents required for current controlled source can be obtained from the quadrature and direct currents using inverse Park's transformation as:

$$\begin{bmatrix} I_a \\ I_b \\ I_c \end{bmatrix} = \begin{bmatrix} cos(\theta) & -sin(\theta) & 1 \\ cos(\theta - 2\pi/3) & -sin(\theta - 2\pi/3) & 1 \\ cos(\theta + 2\pi/3) & -sin(\theta + 2\pi/3) & 1 \end{bmatrix} \begin{bmatrix} I_d \\ I_q \\ I_0 \end{bmatrix} \tag{6.6}$$

In this manner, the initialisation is straightforward and accurate when the power transfers at the PCC are known.

It is worthy to mention that the options discussed above are for the GB power system study, where the HuT represents a large portion of the test network, effectively emulating a generation. There might be a case when the HuT represents a large

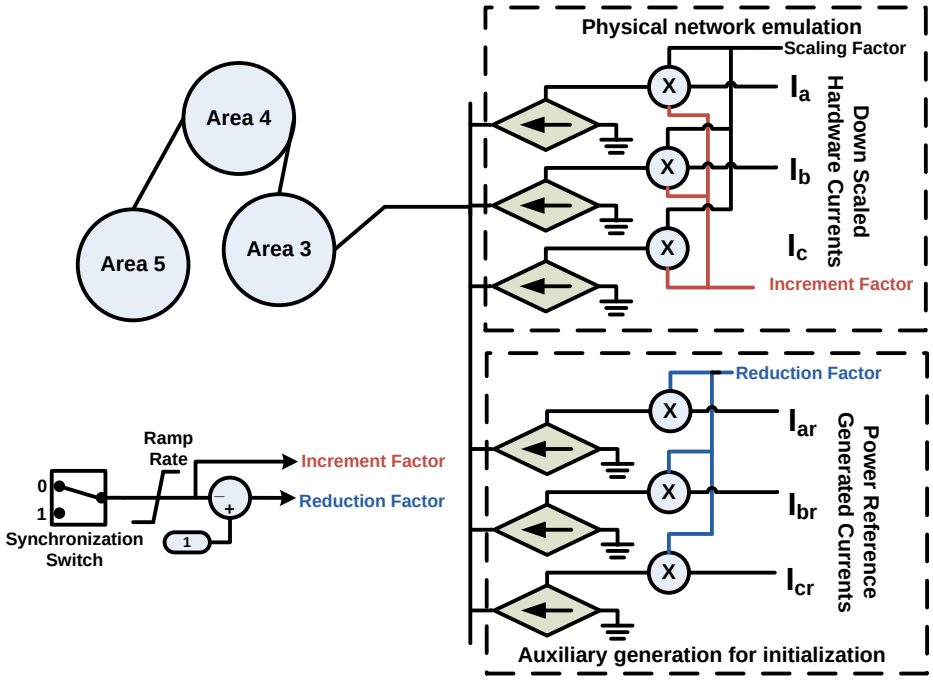

Figure 6.9: P-HiL initialisation and synchronisation.

portion of the test system and is an effective load. In such a scenario, although the P-HiL simulation might initialize, the frequency and voltage of the simulation might be beyond the normal bounds required for safe reproduction of interface signals by the power interface. Therefore, in a similar manner, options for initialisation would be required. Out of the four options discussed above, only one can be utilised for emulating an effective load, i.e., the current controlled source. By means of a simple sign change, emulation of a load is possible, making them an ideal solution for initialisation of any such P-HiL setup. A schematic of this configuration is shown in Fig. 6.9, where the five-area GB power system is divided into three-areas being simulated and the other two areas, area 1 and 2 are emulated by the current sources.

Options for Synchronisation with DRTS Simulation

During the process of synchronisation, the currents from the auxiliary generation utilised for initialisation need to be replaced by the hardware currents (measured response from HuT). It is essential to ensure that during the process of synchronisation the voltage and frequency of the network do not exceed the safety margins of the power

interface and HuT. In addition, when any voltage or frequency control algorithms are implemented within the network, it is often desired that the synchronisation of the HuT causes least possible change in system frequency and voltage in order not to cause any supplementary control actions due to the dynamics of synchronisation.

The synchronisation method to be utilised will depend upon the initialisation method selected. Therefore, in this sub-section, the synchronisation methods available for each of the initialisation method presented in previous sub-section will be discussed.

Detailed simulation of HuT: While a detailed model of HuT would be the best option for the purpose of initialisation of P-HiL, assuming an accurate enough model of HuT is available, for the purpose of synchronisation, a dispatching algorithm to reduce the generation and load of the emulated HuT would be required to avoid the frequency deviating to abnormal values when the HuT is connected. It can therefore be said that, utilising a detailed model of the HuT is not suitable for initialisation and synchronisation of P-HiL setups due to the requirement of developing dedicated HuT models and dispatch algorithms.

AC Voltage Source: Apart from the fact that the AC voltage source is not suitable for initialisation due to its response as an infinite machine, similarly, the power output of the voltage source cannot be controlled during synchronisation and the process can lead to an erroneous synchronisation.

Synchronous Generator: In order to attain a smooth transition from the emulated HuT (the synchronous generator) and the HuT, a complex control would be required (for governor and excitation system) to ensure least deviation in frequency and voltage during the process. Such a developed control would be a generic solution that can be reused, however, would be limited to scenarios where the HuT effectively emulated generation.

AC Controlled Current Source: If a controlled current source is utilised, the synchronisation can be achieved by means of the simple logic presented in Fig. 6.9. The

synchronisation process is begun by means of a synchronisation switch that inversely ramps up and down both controlled current sources. The ramp rate can be chosen such that it does not create any oscillations or transients on the system. Once the currents from the auxiliary generation are reduced to zero and the currents from the HuT are fully connected to the simulation, the system is synchronised.

From the above discussion, it can be deduced that for the purpose of initialisation and synchronisation of P-HiL setups, where the HuT represents a large portion of the test network, the most convenient option available is to utilize a controlled current source. A controlled current source offers the easiest implementation, is very accurate while at the same time a generic approach that can be utilised when the HuT emulates a generation or a load.

6.3.3 Accuracy of the P-HiL Setup

Once a P-HiL has been successfully initialised and synchronised, an important aspect of any P-HiL setup is to ensure its accuracy before any tests are undertaken. In any P-HiL setup, it can be observed that the power exchange at the physical PCC does not match the power exchange at the virtual PCC, i.e. although accurate power is being injected/drawn by the HuT at the physical PCC, the PCC within the DRTS simulation presents a different power factor. This behaviour can be attributed to the time delay of the entire P-HiL process: the processing time of the DRTS, the communication between DRTS and power interface, the power interface processing time for amplifying the signal and the feedback loop measurement and communication. This time delay presents itself as an additional phase difference between voltage and current. The added phase difference between voltage and current at the simulation PCC, affects the power factor of the HuT, leading to inaccurate active and reactive power exchanges compared to an ideal scenario.

The impact of time delay on the accuracy of simulations has been extensively evaluated and the need for compensating the delay emphasised in [16-18]. If these delays are not appropriately compensated, it is not possible to ensure the equality of the reference

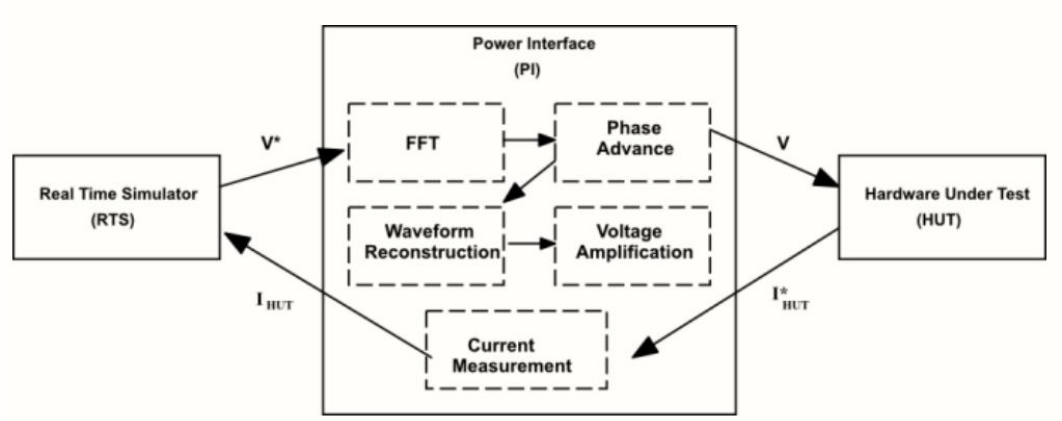

Figure 6.10: Time delay compensation method employed [22].

power and the injected power and therefore the fidelity of the simulation. A number of methods have been reported in literature to compensate for the delays encountered while closing the loop in a P-HiL setup [19-21]. For this work, a phase compensation method, as reported in [22], is utilised. The time delay of an AC signal is equivalent to a phase shift in the frequency domain, the method proposed to compensate for the time delay (as shown in Fig. 6.10) decomposes the signal from the DRTS with an FFT transforming the time domain signal into the frequency domain. In the frequency domain, additional phase is added to the fundamental and harmonics analysed to compensate for the time delay of the system. After the compensation takes place, the signal is reconstructed and can be accurately amplified by the power interface. For a specific implementation, this delay can be treated as approximately constant and deterministic, although this should be assessed on a case by case basis.

6.3.4 Initialisation and Synchronisation Results

A schematic of the P-HiL interconnection within RSCAD has been shown in Fig. 6.9. An auxiliary generation (the controlled current source in this case) is utilised to reproduce currents generated from the power reference i.e. 8900MW and 4257MVAR, initialising the real time simulation. Once the simulation has initialised and attained a steady state, the PCC voltages are reproduced using the power interface. The measured HuT currents should be equal (as much as possible) to the emulated HuT currents. In

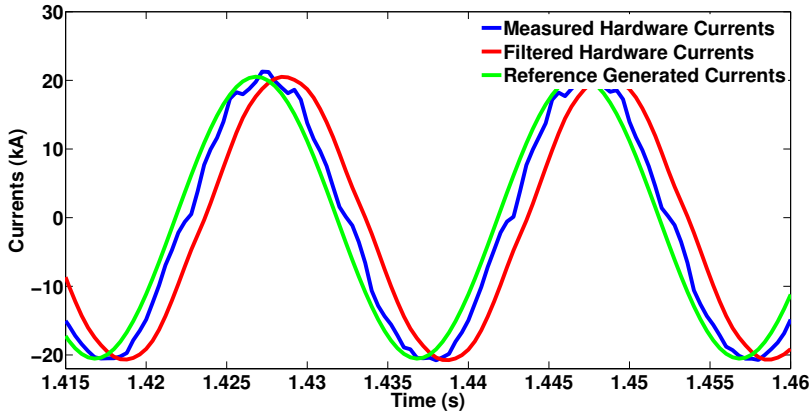

(a) Currents without compensation.

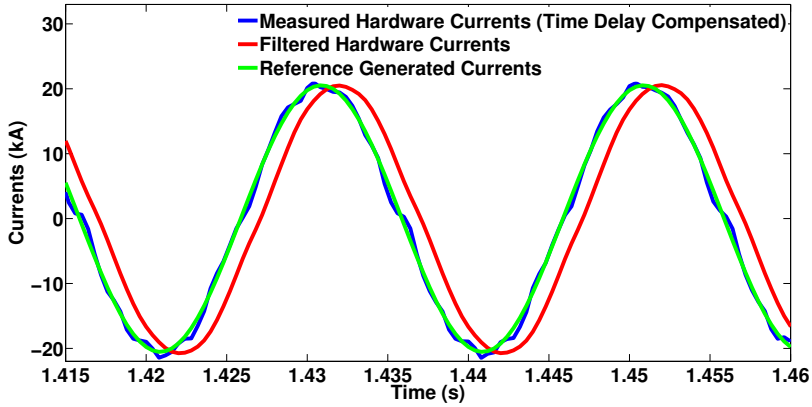

(b) Currents with time delay compensation.

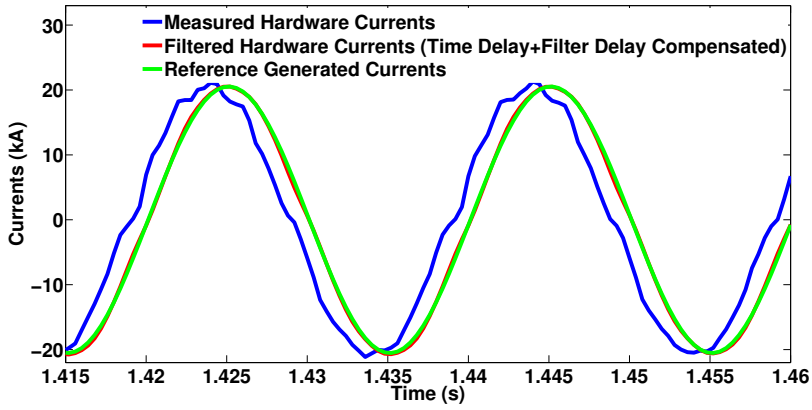

(c) Currents with time and filter delay compensation.

Figure 6.11: Time delay compensation

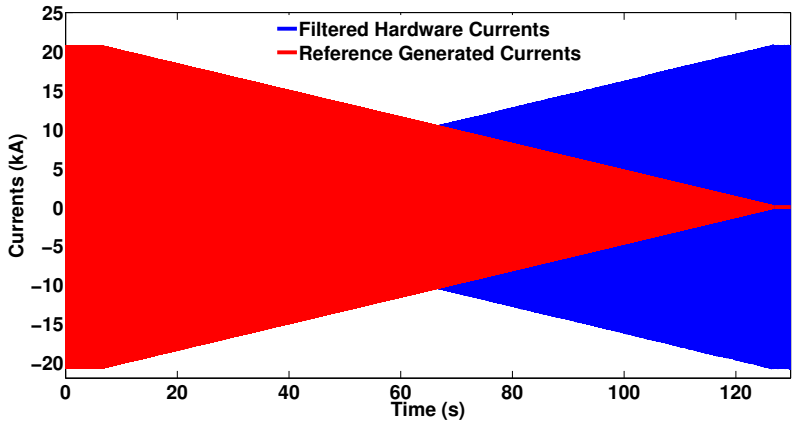

(a) Currents swapping during synchronisation.

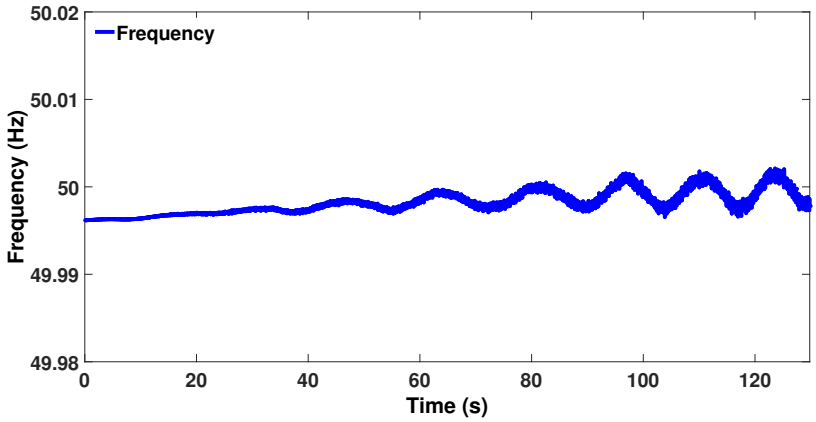

(b) Frequency at PCC during synchronisation.

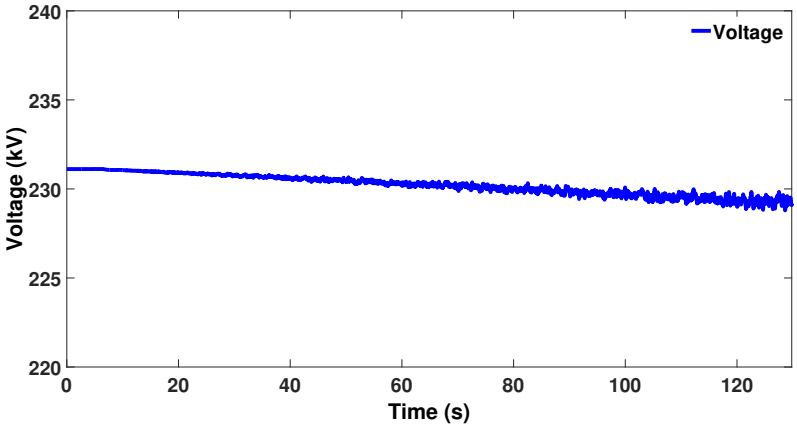

(c) Voltage at PCC during synchronisation.

Figure 6.12: Initialisation and synchronisation results for GB reference power system

this case, the currents are being generated by small scale power converters which produce a considerable number of harmonics. The amplitude of these harmonics when scaled up are not typical of transmission level harmonics. To mitigate this issue, the currents received at the DRTS are filtered by means of a low pass filter. The low pass filter cut off frequency is selected as 200Hz in order to reduce the impact of the harmonics, thereby alleviating the sensitivity of the simulation to oscillations. However, the low pass filter increases the time delay of the received signal. Therefore, time delay compensation is required not only to compensate for the delay characteristics of P-HiL setups, but more importantly in this case, the delay of the filter. This is because the selected cut-off frequency attains a much larger delay than the typical delay of P-HiL setups. The results of the time delay compensation are shown in Fig. 6.11a 6.11b and 6.11c.

Once the signals are accurate, the replacement process is initiated by means of the synchronisation switch. The currents are then ramped up and down simultaneously over a period of 120 seconds as shown in Fig. 6.12a. The frequency and voltage at PCC, during the process of synchronisation, are presented in Fig. 6.12b and 6.12c respectively. As can be observed from the two figures, although the HuT currents have been compensated for the time and filter delay and are approximately similar to the emulated currents (as shown in Fig. 6.11c), there is an obvious change in both voltage and frequency during the process of synchronisation. The change in frequency is less than 0.02% and the change in voltage is less than 0.05%. As has been mentioned earlier, the converters utilised produce considerable harmonics and therefore minor variations between the emulated and HuT currents do exist, causing the variation in voltage and frequency. Although the results tend to show an increasing oscillation in frequency, the frequency oscillations are due to the hardware coupling and do not increase as is evident from results of longer period of 300s available in [23]. The ramp rate utilised plays an important practical role in minimising such impacts during the process of synchronisation. Synchronising without a ramp rate, risks transients being introduced. The ramp rate is dependent upon the acceptable variation on voltage and frequency during the process of synchronisation. With the P-HiL simulation fully synchronised

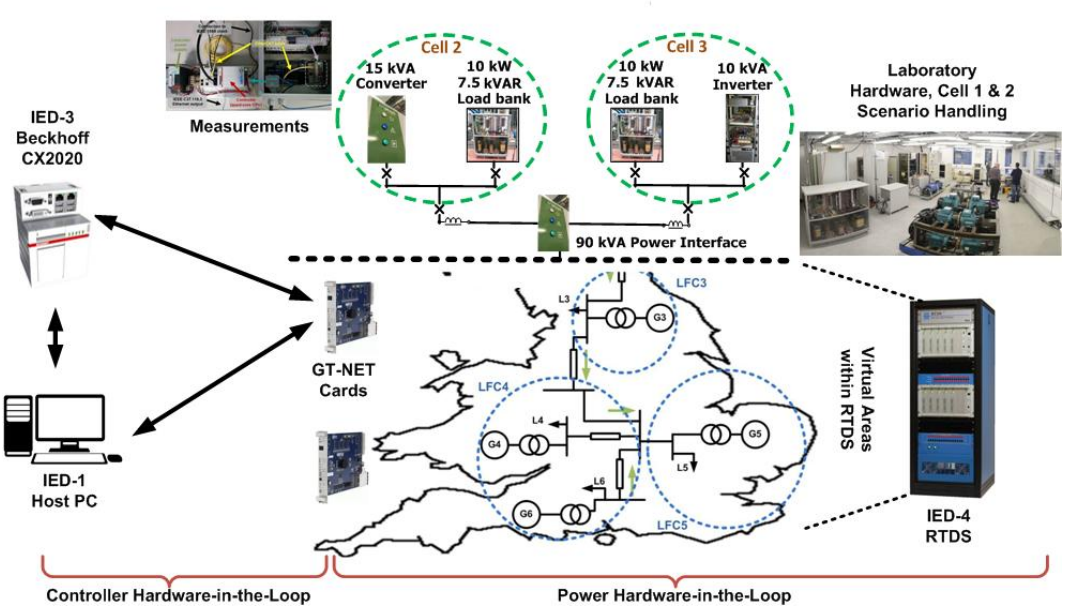

Figure 6.13: An abstract representation of control and power HiL setup

and the power transfers set as per the required scenario, the testing of, for example, new control algorithms in a more realistic environment is made possible.

6.4 Validation Results Continued

6.4.1 PoI-3

The abstract representation of the P-HiL implementation is presented in Fig. 6.13. Although the P-HiL setup was initialised and synchronised appropriately as presented in previous section, it was identified that the system was critically stable. The stability of a P-HiL setup where the voltages and currents are scaled is given by [17]:

$$L_{SW} < \frac{a^2}{b} L_{HW} \tag{6.7}$$

or

$$\frac{b}{a^2} \frac{L_{SW}}{L_{HW}} < 1 \tag{6.8}$$

with

$$a = \frac{V_{SW}}{V_{HW}} \tag{6.9}$$

$$b = \frac{I_{HuT_{full}}}{I_{HuT_{red}}} \tag{6.10}$$

where L_{SW} is the software side inductance, L_{HW} is the hardware side inductance, V_{SW}, V_{HW} are the phase nominal voltages of the software and hardware side respectively, $I_{HuT_{full}}$, $I_{HuT_{red}}$ are the nominal current of the full-scale HuT and the reduced-scale HuT respectively. For the study under consideration,

$$a = \frac{V_{SW}}{V_{HW}} = \frac{400kV}{400V} = 1 \times 10^3 \tag{6.11}$$

$$b = \frac{I_{HuT_{full}}}{I_{HuT_{red}}} = 1 \times 10^6 \tag{6.12}$$

$$\frac{b}{a^2} = 1 \tag{6.13}$$

$$\frac{L_{SW}}{L_{HW}} \simeq 1 \tag{6.14}$$

with the given values, as can be observed, the condition for stability is met, however, any small change can lead the system to instability. To allow for a safety margin, the value of $I_{HuT_{red}}$ is increased such that $b = 0.8$. As the currents from hardware units needed to be increased, this limits the spare power capacity that was reserved for reference imbalance event. For this reason, the value of imbalance event in this case is reduced to 800MW (maximum) represented by 1000W in hardware. This would suffice to achieve the objective of PoI-3, i.e., to test the ability of the control with real measurements.

The system is subject to two disturbances in LFC 2 (Cell 2 in hardware, Fig. 6.8), a loss of generation and a loss of load, with magnitudes of 800MW (1000kW in hardware) and 700MW (875W in hardware) respectively. The parameters of the control system remain same as in the previous study. The system frequency response subject to generation loss and load loss at $t = 10s$ are presented in Fig. 6.14 (superimposed). As can be observed, the EFC-FB was able to identify the imbalance evident from the restoration of frequency much faster than conventional LFC framework.

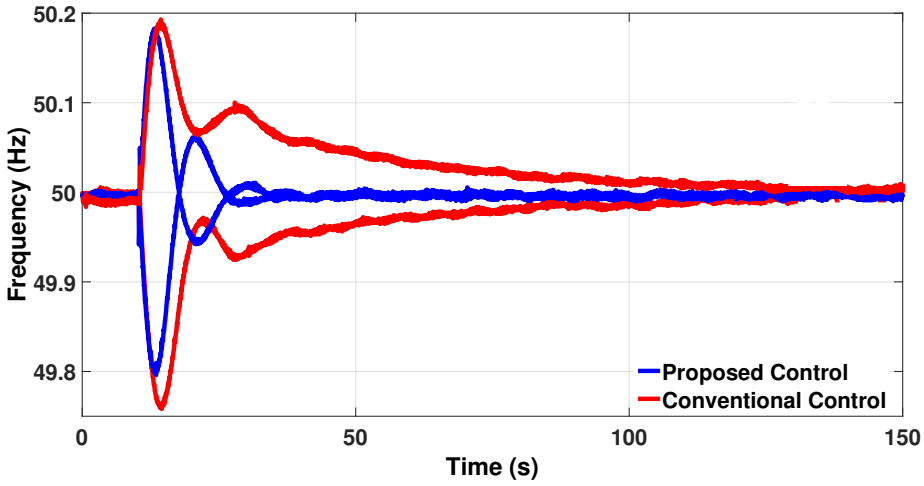

Figure 6.14: PoI-3: Frequency response in P-HiL implementation.

With the presented controller and power HiL implementation and validation, the following can be summarised:

- The discrete controller implementation enabled the further improvement of control implementation, with minor implementation bugs being realised through its discrete implementation, serving the purpose of prototype testing.
- The increased speed of frequency restoration under realistic communications delay has been demonstrated. With the incorporation of delays, the proposed control exhibits better frequency dynamics and restores frequency faster than the conventional framework.
- By the implementation of the control framework within the laboratory, the performance improvement of the proposed control over the conventional control has been demonstrated.

6.5 Conclusions

The analytical and experimental assessments in the work undertaken has demonstrated the aptness of the proposed control approach for dynamically changing power system of future. The experimental evaluation was an important step towards proving the

ability of the proposed controls to perform under real-world conditions. While the simulations already highlighted the benefits of these controls over state-of-the-art, it remained unclear whether the new approach would perform satisfactorily outside idealised simulated conditions. Therefore, the conducted experiments where imperative to highlight the real-world applicability of the proposed control. The resilience of the proposed controller to communications asynchronicity, finite measurement and control step resolution, various noise sources, parameter uncertainties, and other factors not explicitly incorporated in the mathematical model were tested in the process as well. The deployment of the control on dedicated controller hardware enabled rapid prototyping, allowing for an efficient iterative development process by feeding back experiences made under real conditions into the theoretical method.

With the development of the EFC and its validation in a laboratory environment, the ability of more decentralised and distributed operation of power system has been proven. Furthermore, the developed control, in essence works towards the objective of solving local problems locally. Beginning with the speculation of advantages of more local control, this exercise has proven some merits of prioritising of local response to a local imbalance, such as improved dynamic response, robust reserve activations and reducing the divergence from planned system conditions and hence minimising the operational implications of the disturbance. In addition, the developed controls support enhanced scalability in the future grid given the autonomy of the approaches.

REFERENCES

[1] M. H. Syed, G.M. Burt, R. D'Hulst, and J. Verbeeck,"Experimental Validation of Flexibility Provision by Highly Distributed Demand Portfolio", in *proceedings of the 2016 CIRED Workshop*, pp. 1-4, Helsinki, Finland, 2016.

[2] P. Dambrauskas, M. H. Syed, S. M. Blair, J. M. Irvine, I. F. Abdulhadi, G. M. Burt, and D. E. M. Bondy "Impact of realistic communications for fast-acting demand side management," *in CIRED - Open Access Proceedings Journal*, vol. 2017, no. 1, pp. 1813-1817, 10 2017.

[3] G. F. Lauss, M. O. Faruque, K. Schoder, C. Dufour, A. Viehweider, and J. Langston, "Characteristics and Design of Power Hardware-in-the-Loop Simulations for Electrical Power Systems", in *IEEE Trans. on Industrial Electronics*, vol. 63, no. 1, pp. 406-417, Jan. 2016.

[4] W. Ren, M. Steurer, and T. L. Baldwin, "Improve the Stability and the Accuracy of Power Hardware-in-the-Loop Simulation by Selecting Appropriate Interface Algorithms", in *IEEE Trans. on Industry Applications*, vol. 44, no. 4, pp. 1286-1294, July 2008.

[5] F. Lehfuss, G. Lauss, and T. Strasser, "Implementation of a multi-rating interface for Power-Hardware-in-the-Loop simulations", in *proceedings of 2012 38ˆth Annual Conference on IEEE Industrial Electronics Society (IECON)*, Montreal, QC, pp. 4777-4782, 2012.

[6] S. Lentijo, S. D'Arco, and A. Monti, "Comparing the Dynamic Performances of Power Hardware-in-the-Loop Interfaces", in *IEEE Trans. on Industrial Electronics*, vol. 57, no. 4, pp. 1195-1207, April 2010.

[7] E. Jong, R. de Graaff, P. Vaessen, P. Crolla, A. J. Roscoe, F. Lefuss, G. Lauss, P. Kotsampopoulos, and F. Gafaro, "European White Book on Real-Time Power Hardware in the Loop Testing", DERlab, 2012.

[8] J. Langston, K. Schoder, M. Steurer, O. Faruque, J. Hauer, F. Bogdan, R. Bravo, B. Mather, and F. Katiraei, "Power hardware-in-the-loop testing of a 500 kW photovoltaic array inverter", in *proceedings of 2012 38ˆth Annual Conference on IEEE Industrial Electronics Society (IECON)*, Montreal, QC, pp. 4797-4802, 2012.

[9] O. Naeckel, J. Langston, M. Steurer, F. Fleming, S. Paran, C. Edrington, and M. Noe, "Power Hardware-in-the-Loop Testing of an Air Coil Superconducting Fault Current Limiter Demonstrator", in *IEEE Trans. on Applied Superconductivity*, vol. 25, no. 3, pp. 1-7, June 2015.

[10] P. Kotsampopoulos, N. Hatziargyriou, B. Bletterie, G. Lauss, and T. Strasser, "Introduction of advanced testing procedures including PHIL for DG providing ancillary services", in *proceedings of the 39ˆth Annual Conference of the IEEE Industrial Electronics Society (IECON)*, Vienna, pp. 5398-5404, 2013.

[11] A. Viehweider, G. Lauss, and F. Lehfuss, "Stabilization of Power Hardware-in-the-Loop Simulations of Electric Energy Systems", Simulation Modelling Practice and Theory, vol.19, no.7, pp. 1699-1708, 2011.

[12] T. Hatakeyama, A. Riccobono, and A. Monti, "Stability and accuracy analysis of power hardware in the loop system with different interface algorithms", in *proceedings of the 2016 IEEE 17ˆth Workshop on Control and Modeling for Power Electronics (COMPEL)*, Trondheim, pp. 1-8, 2016.

[13] M. Dargahi, A. Ghosh, and G. Ledwich, "Stability synthesis of power hardware-in-the-loop (PHIL) simulation", in p*roceedings of the 2014 IEEE Power and Energy Society General Meeting - Conference & Exposition*, National Harbor, MD, pp. 1-5, 2014.

[14] E. Liegmann, A. Riccobono, and A. Monti, "Wideband identification of impedance to improve accuracy and stability of power-hardware-in-the-loop simulations", in *proceeding of the 2016 IEEE International Workshop on Applied Measurements for Power Systems (AMPS)*, Aachen, pp. 1-6, 2016.

[15] R. Brandl, ‘‘Operational Range of Several Interface Algorithms for Different Power Hardware-In-The-Loop Setups”,in *Energies*, 10, 1946, 2017.

[16] F. Huerta, R. L. Tello, and M. Prodanovic, “Real-Time Power-Hardwarein-the-Loop Implementation of Variable-Speed Wind Turbines”, in *IEEE Trans. on Industrial Electronics*, vol. 64, no. 3, pp. 1893–1904, 2017.

[17] I. D. Yoo, and A. M. Gole, “Compensating for interface equipment limitations to improve simulation accuracy of real-time power hardware in loop simulation”, in *IEEE Trans. on Power Delivery*, vol. 27, no. 3, pp. 1284–1291, 2012.

[18] W. Ren, “Accuracy evaluation of power hardware-in-the-loop (PHIL) simulation”, Ph.D. dissertation, The Florida State University, 2007.

[19] P. C. Kotsampopoulos, F. Lehfuss, G. F. Lauss, B. Bletterie, and N. D. Hatziargyriou, “The limitations of digital simulation and the advantages of PHIL testing in studying distributed generation provision of ancillary services”, in *IEEE Trans. on Industrial Electronics*, vol. 62, no. 9, pp. 5502–5515, 2015.

[20] P. Kotsampopoulos, V. Kleftakis, G. Messinis, and N. Hatziargyriou, “Design, development and operation of a PHIL environment for Distributed Energy Resources”, in *Proceedings of Industrial Electronics Conference (IECON)*, pp. 4765–4770, 2012.

[21] N. Ainsworth, A. Hariri, K. Prabakar, A. Pratt, and M. Baggu, “Modeling and compensation design for a power hardware-in-the-loop simulation of an AC distribution system”, in *proceedings of the NAPS 2016 - 48th North American Power Symposium*, 2016.

[22] E. Guillo-Sansano, A. J. Roscoe, and G. M. Burt, “Harmonic-by-harmonic time delay compensation method for PHIL simulation of low impedance power systems”, in *proceedings of the 2015 International Symposium on Smart Electric Distribution Systems and Technologies (EDST)*, Vienna, pp. 560-565, 2015.

[23] E. Guillo-Sansano, **M. H. Syed**, A. J. Roscoe, and G. M. Burt, "Initialization and Synchronization of Power Hardware-in-the-Loop Simulations: A Great Britain Network Case Study", in *Energies*, vol 11, no. 5, 1087, April 2018.

Chapter 7

Conclusions and Future Work

7.1 Summary

With the changes the power systems around the world are expected to undergo in the near future, the conventional approaches to frequency control ancillary service provision are being challenged. The need for new services to ensure security of supply has been established in literature. To this end, this thesis presents two novel frequency control approaches: (i) a secondary frequency control (SFC) referred to as fast balancing enhanced frequency control (EFC-FB), and (ii) a primary frequency control (PFC) referred to as responsibilising primary enhanced frequency control (EFC-RP). The proposed controls are enabled by effective event detection techniques developed. The performance of the proposed controls has been verified by real-time simulations conducted on a validated reduced dynamic model of the Great Britain (GB) power system. With the objective of appraising the proposed EFC-FB framework to technology readiness level (TRL) 5, this thesis further presents a novel methodology to facilitate laboratory validations of smart grid control solutions.

The following sections outline the major conclusions of this research and identify areas of research worth being taken forward as future work.

7.2 Conclusions

The contributions from the work undertaken throughout this thesis can be attributed to three distinct knowledge streams. The following three sub-sections present the contributions to each stream in detail.

7.2.1 Enhanced Frequency Control Approaches

Acknowledging the recently identified importance of locational information in addition to temporal information in effective provision of ancillary services, this thesis introduces the term "responsibilisation" that refers to the prioritisation of remedial control measures closer to source of an imbalance, thereby supporting the drive towards greater decentralisation of power systems. To this end, two responsibilising frequency control ancillary services were proposed. The two control approaches ensure the prioritisation of local response to a local imbalance, reducing the divergence from planned system conditions, thereby minimising the operational implications of any system imbalance event. In addition, they support enhanced scalability in the future grid given the relative autonomy of the approaches. Each of the following sub-sections will detail the conclusions of each proposed control.

Fast Balancing Enhanced Frequency Control

The incorporation of conventional Load Frequency Control (LFC) framework within a validated reduced dynamic model of GB grid, a first implementation of its kind, was a first step towards increased decentralisation and responsibilisation, where remedial control measures are taken closer to the location of the imbalance event, i.e. within the area of the disturbance as opposed to the current practice within GB grid where the response is from across the country. The GB grid, with conventional LFC framework incorporated, when subjected to reference imbalance event presented a satisfactory frequency response. As is well established, responsibilisation within conventional LFC framework is inherent, therefore the focus was directed towards improving the response speed.

An analysis of the conventional LFC framework response revealed the conflicting nature of the two objectives, the enhanced responsibilisation and improved response speed. Increasing the response speed of conventional LFC lead to degradation in responsibilisation. Further analysis identified limitations within the conventional LFC framework as a cause for the two objectives to project conflict. These limitations were identified as:

- The inability of the conventional LFC framework to ascertain definitive location of the imbalance event.
- The use of a common control effort for slower and faster acting resources.

To overcome the limitations identified, a novel EFC-FB is proposed. The proposed control incorporates a fast acting balance control loop (BCL), in addition to the secondary control loop (SCL). The BCL comprises an area disturbance observer, capable of fast, autonomous and definitive identification of imbalance event location. The control effort to fast acting resources is a combination of effort from BCL and SCL, while the control effort to slower acting resources is from SCL only, thereby decoupling the two. Addressing the limitations allows for unilateral activation of reserves only within the area where the imbalance event initiated even with faster response speeds. Furthermore, the definitive identification of imbalance location enables the use of direct power imbalance observed over area tie-lines to be utilised as control input, that is shown to avoid sympathetic activations at faster response speeds contrary to the conventionally utilised area control error.

The performance of the proposed control framework is verified by means of real-time simulations and small-signal analysis conducted on the reduced dynamic model of GB, before its implementation within the Dynamic Power Systems Laboratory (DPSL) for its appraisal to TRL 5. Controller hardware in the loop validation revealed issues in the implementation of the algorithm that were masked by small computational time step of real-time simulations. This highlights the importance of each stage of the validation chain and further reveals the limitation of pure simulation based approaches. These issues were addressed before the combined controller and power hardware in

the loop validation. The ability of the proposed framework to operate in real-world conditions, with actual measurements and communication delays, was proven, providing high degree of confidence in the credibility of the proposed control for real world implementation.

In essence it can be said that the proposed EFC-FB enables improved response speeds while at the same time not only ensuring effective, but also enhanced responsibilisation.

Responsibilising Primary Enhanced Frequency Control

Responsibilisation within PFC can be introduced by means of adapting the droop slopes of the LFC areas in real-time, if the location of the imbalance event can be detected within the timescale of PFC. The disturbance observer of the EFC-FB developed within this work could be utilised for the purpose of incorporating responsibilisation within PFC. The disturbance observer approach for event detection is much more robust compared to alternatives but still not appropriate to be utilised for PFC due to its centralised event detection as reported in Chapter 4.

Therefore, a novel decentralised responsibilising PFC has been proposed. The control achieves responsibilisation by means of fast and autonomous event detection and droop adaptation of LFC areas in real-time. The fast and autonomous event detection is achieved by means of calculating the transient phase offset (TPO) locally at resources participating in PFC, while the droop of LFC areas are adapted based on a droop curve proposed. The proposed approach is fully decentralised as it relies on local measurement only and requires no form of communication.

Real-time simulation results have shown that an event can effectively be identified within 100ms of its occurrence and the proposed droop curve enables effective responsibilisation. The linear droop curve proposed in this work serves as a proof of concept. More sophisticated droop curves can be designed to achieve more effective responsibilisation. This has not been explored within this work. The applicability and soundness of the proposed approach to be operated in conjunction with SFC has been demonstrated by means of small-signal analysis.

7.2.2 Methodology to Facilitate Laboratory Validation of Complex Smart Grid Control Solutions

The practical challenges that arise from the integration of control solutions within laboratory environments, for their validation, are identified. These practical challenges have been given little or no attention in the past, however, with increasing recognition of laboratory validations, this is the first attempt at reporting these challenges. The challenges identified were correlated to a lack of an integrated methodology. To address this issue of lack of an integrated methodology, an approach that utilizes SGAM as a tool to facilitate laboratory validations is proposed. The proposed methodology leads to a combined representation of control solutions and laboratory infrastructure, in other words a comprehensive validation environment, using the SGAM, facilitating the transition from the design of radical grid control solutions, to their rigorous validation.

The proposed SGAM modelling approach was utilised to develop the validation environment for the EFC framework. Through a qualitative assessment the competence of the proposed approach to: (i) entail efficiency in the process of control solution validation, (ii) incorporate a variety of non-monolithic validation setups and (iii) enhance repeatability and reproducibility of control solution validations, was established. This included the adoption of the approach in an independent smart grid laboratory (at Centre for Renewable Sources and Savings in Greece) to develop a tailored validation environment for the EFC-FB.

For the first time, two state-of-the-art smart grid laboratories were represented using SGAM. The representation of two state-of-the-art smart grid laboratories using SGAM presented an effective means to communicate research infrastructure features for the integration and validation of complex smart grid control solutions.

The conventional SGAM modelling approach is limited to representation of control solutions implemented within a single entity (for example, one DSO or TSO). This presents a limitation on the control solutions that can be represented using SGAM. This work further introduced a concept to represent a control solution implemented within more than one entity. This enables representation of distributed control solutions in SGAM broadening the conventional bounds of SGAM.

7.2.3 Extending the Boundaries of Real-Time Power Hardware-in-the-Loop Simulations

For the first time, the process of initialisation and synchronisation of a power hardware in the loop (P-HiL) setup, wherein the hardware under test (HuT) represents a significant portion of the network compared to the rest of the system being simulated within the digital real-time simulator (DRTS), has been demonstrated by means of implementation within the DPSL.

The initialisation and synchronisation of such setups present challenges such as the paradoxical scenario explained in detail in Chapter 6. This thesis presents a range of possible methodologies for improving the initialisation and synchronisation of such scenarios. The investigation of these alternatives has led to the identification of a recommended approach that uses current sources for initialisation and symmetrical ramping rates for synchronisation of the P-HiL simulation with the hardware under test.

The options available for initialisation and synchronisation of such P-HiL setups are discussed and the best practices drawn. Furthermore, an additional scenarios that would transgress from the traditional bounds of P-HiL techniques is identified. The resulting improved performance and extended range of feasible scenarios that can be studied have been validated by experimentation of frequency control scenarios for the GB system. This will allow for safer and more stable P-HiL simulations, and permit validation of a wider range of realistic simulations through P-HiL to the betterment of new controllers and power components.

7.3 Future Work

In this section, based on the findings and conclusions of the work undertaken, areas of future work have been identified and presented in the following sub-sections.

7.3.1 Enhanced Frequency Control Architecture for Future Power Systems

In this work, the two novel frequency control solutions for greater decentralisation and distributed operation of future power systems were developed. The following can be deduced:

- The two controls were developed independently.
- The traditional definitions used for frequency control are being challenged, the line between the primary frequency control and secondary frequency control is becoming more blurred.
- The TPO based method holds greater potential.

Therefore, the future work involves the development of a novel frequency control architecture that incorporates the TPO based disturbance detection for both frequency containment and restoration.

7.3.2 Refinement of Laboratory Validation Approach

The SGAM based modelling approach for laboratory validation of smart grid control solutions proposed in this work has proven to be advantageous. The methodology was adopted for laboratory validation of EFC framework proposed within this work by two independent laboratories. However, the methodology was confined to in-house developed control solution. The future work involves the use of the methodology for wide range of smart grid control solutions, in particular control solutions developed by third party, and to spread the use of the methodology to more laboratories across Europe. This will allow for feedback to be gathered and to identify the potential areas for further refinement of the proposed approach.

7.3.3 Improving Real-Time Simulations for Extending Laboratory Validations

The traditional P-HiL methods are being challenged by the need for expanding its envelope to validate larger power networks in larger P-HiL setups. An example of such is, the additional scenario identified within this thesis, of a power system incorporating high penetration of converter based generation and/or wide area monitoring control solutions. Such setups present a number of challenges in terms of the protection and stability of P-HiL. This again presents an excellent direction that is worthy of further exploration.

7.3.4 Monetisation of Developed Frequency Control Approaches

The monetisation and incorporation within the market of novel frequency support approaches such as those proposed in this work is an important aspect that remains to be investigated. Although it is intuitive that the change in market design is inevitable, driven by the need of the power system, it is important to understand how the responsibilising controls will be regulated to ensure fairness. It is assumed that responsibilisation would prevent wider system participation (as is its objective), thereby causing monetary hotspots in the network where participants stand to gain more profits than resources elsewhere in the network. An analysis of the impact of responsibilisation on market regulations and framework is an area that deserves more attention.

Appendices

Appendix A

Reduced Dynamic Model Parameters

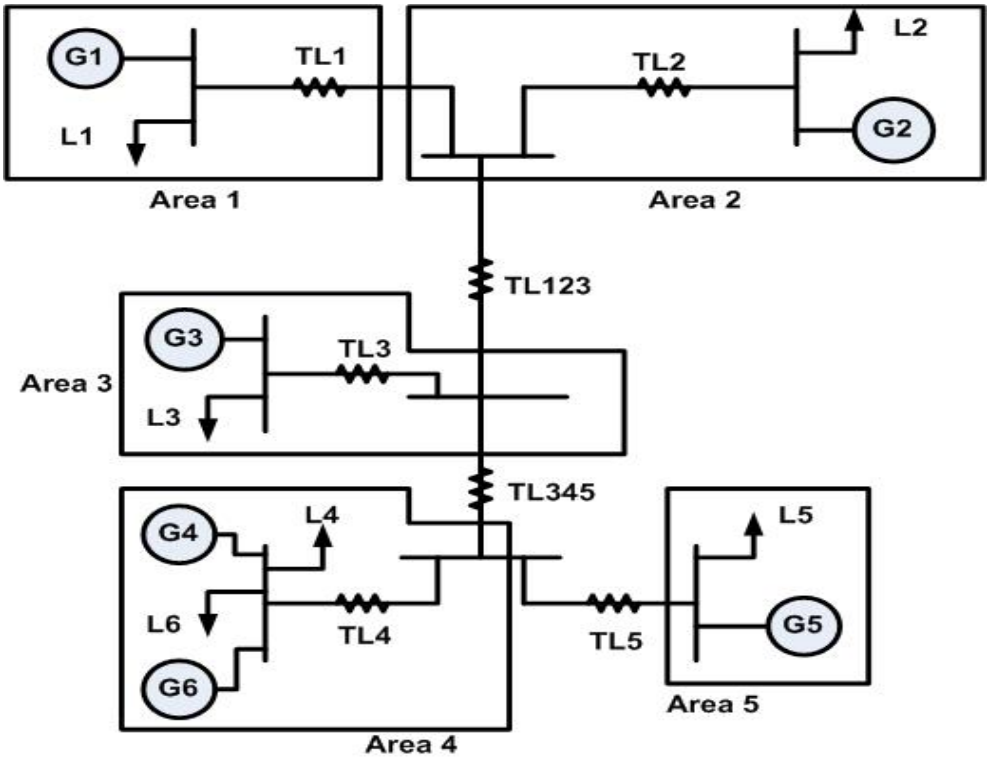

Figure A.1: Single line diagram of the reduced Great Britain model

The single line diagram of the reduced model of the Great Britain power system

used in this thesis is presented in Fig. A.1. The parameters of the model are presented in the following tables.The generator model generic initial values selected are shown in Table A.1 and Table A.2, the governor parameters in Table A.3, the excitation model parameters in Table A.4, the transformer model parameters in Table A.5. All the loads are connected in star and their parameters are shown in Table A.6 and Table A.7. The lines are modelled as pi-sections, the parameters of which are shown in Table A.8.

Table A.1: Generator Generic Parameters

Parameter	Value
f	50 Hz
V	13.8kV
X_d	1.0 p.u.
X_q	1.0 p.u.
X_d'	0.15 p.u.
X_q'	0.3 p.u.
X_d"	0.12 p.u.
X_q"	0.12 p.u.
T_{d0}'	3 sec
T_{q0}'	0.5 sec
T_{d0}"	0.02 sec
T_{q0}"	0.02 sec
X_l	0.1 p.u.
R_a	0.0015 p.u.

Table A.2: Specific Generator Parameters

	Area 1	Area 2	Area 3	Area 4	Area 5	Area 6
Generator Capacity (MVA)	11500	20500	9660	16000	5500	500
Inertia Constant (s)	4.12	4.12	4.68	4.68	4.68	4.68

Table A.3: Governor Model Parameters

Parameter	Value
R	7.6923
$T1$	4.8s
$T2$	0.4s
$T3$	0.1s
AT	1
Kt	2
$Vmax$	1p.u.
$Vmin$	0.31p.u.
$Dturb$	0
$Proc$	2
Pri	2

Table A.4: Excitation Model Parameters

Parameter	Value
T_b	20s
T_c	1.0s
T_{b1}	0
T_{c1}	0
T_a	0.02s
K_a	200
T_f	1s
K_f	0
K_i	4.54
I_{limit}'	4.4

Table A.5: Transformer Model Parameters

Parameter	Value
HV	400kV
LV	13.8kV
$pos.seq.R$	0p.u.
$pos.\ seq.X$	0.1p.u.
$zero\ seq.R$	0p.u.
$zero\ seq.X$	0.1p.u.
shunt cap.	0.0001p.u.

Table A.6: Load: Active (MW)

L_1	L_2	L_3	L_4	L_5	L_6
8486	12548	8398	26852	2000	100

Table A.7: Load: Reactive (MVAr)

L_1	L_2	L_3	L_4	L_5	L_6
4109	6077	4067	13005	1041	500

Table A.8: Line Parameters

Parameter	TL1	TL2	TL3	TL4	L5	L123	L345
Frequency (Hz)	50	50	50	50	50	50	50
pos. seq. R (ohms)	0.01	0.01	0.001	0.001	0.001	0.001	0.001
pos. seq. L (ohms)	0.15	0.5	1	0.1	0.1	1	0.1
pos. seq. C (Mohms)	0.55	0.2	1	0.08	0.08	0.55	0.08
zero. seq. R (ohms)	0.054	0.03	0.06	0.06	0.06	0.003	0.06
zero. seq. L (ohms)	0.015	0.06	0.18	0.3	0.3	0.0015	0.3
zero. seq. C (Mohms)	0.560	0.45	0.24	0.24	2.4	0.75	0.24